



Delft University of Technology

Delft screw injection pile tests factual report

Duffy, K.

Publication date

2024

Document Version

Final published version

Citation (APA)

Duffy, K. (2024). *Delft screw injection pile tests: factual report*. Delft University of Technology.

Important note

To cite this publication, please use the final published version (if applicable).
Please check the document version above.

Copyright

Other than for strictly personal use, it is not permitted to download, forward or distribute the text or part of it, without the consent of the author(s) and/or copyright holder(s), unless the work is under an open content license such as Creative Commons.

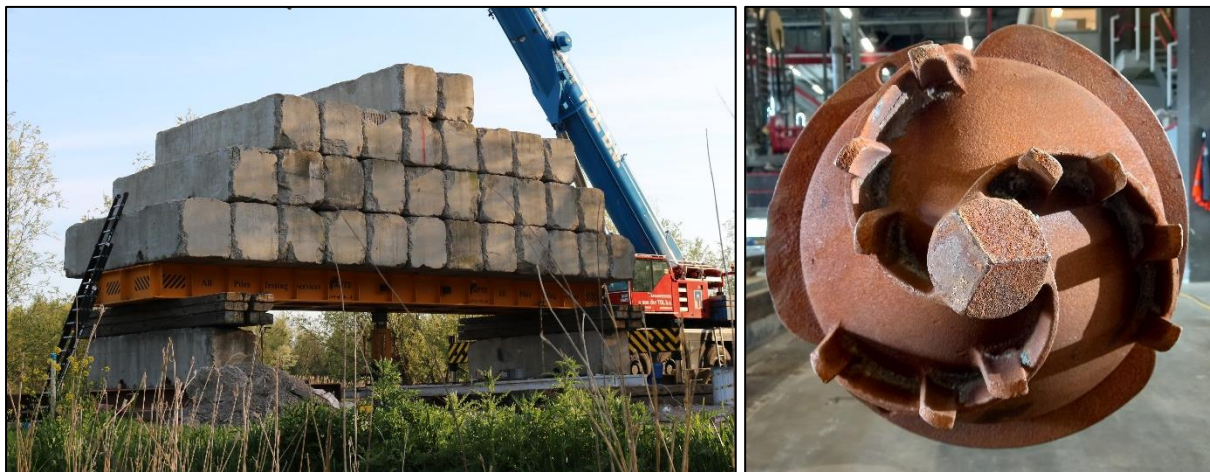
Takedown policy

Please contact us and provide details if you believe this document breaches copyrights.
We will remove access to the work immediately and investigate your claim.

*This work is downloaded from Delft University of Technology.
For technical reasons the number of authors shown on this cover page is limited to a maximum of 10.*

Delft Screw Injection Pile Tests

Factual Report



Revision 1

Prepared by: Kevin Duffy

Reviewed by: Dirk de Lange & Ken Gavin

24th November 2024

Table of Contents

1.	Introduction.....	5
1.1.	Project Background.....	5
2.	Ground Investigation	7
3.	Pile Fabrication & Installation.....	10
3.1.	Pile Fabrication and Installation.....	10
	SI pile (Fundex pile with grout injection).....	11
	SIc pile (Tubex pile with grout injection).....	12
	Installation Parameters	13
3.2.	Installation Observations.....	14
	Observations of outflowing grout.....	14
	Pile F1: Insufficient concrete	15
	Pile F2: Coarse aggregates at pile head.....	15
	Pile F3: Stuck casing	16
3.3.	Drilling rig data	17
3.4.	Grout data	19
4.	Pile Testing	21
4.1.	Test frame	21
4.2.	Strain Instrumentation.....	23
	SI piles.....	24
	SIc piles.....	25
4.3.	Test Procedure	27
4.4.	Sonic Integrity Testing.....	29
4.5.	Pile Extraction.....	29
5.	Test Results.....	32
5.1.	5 th April 2022: Pile T1	33
5.2.	7 th April 2022: Pile F1.....	42
5.3.	9 th April 2022: Pile T2.....	52
5.4.	12 th April 2022: Pile F2.....	62
5.5.	14 th April 2022: Pile T3	72
5.6.	20 th April 2022: Pile F3.....	82
5.7.	All Combined.....	91
6.	Data Interpretation	92
6.1.	Strain-to-force conversion	92

Theoretical stiffness.....	92
Measured stiffness.....	92
6.2. Load distribution	94
6.3. Mobilisation of base and shaft resistance.....	95
Unit shaft resistance	99
7. Data Quality & Lessons Learned.....	100
7.1. The benefits of instrumenting indoors	100
7.2. Strain distribution at the pile ends.....	101
7.3. Difficulties in sustaining a constant load.....	102
7.4. Impact of loading on levelling stations.....	103
7.5. Impact of loading on reference frame.....	104
References	106
Appendix A Site Investigation: CPTs.....	107
A.1 F1.....	107
A.2 F2.....	108
A.3 F3.....	109
A.4 T1.....	110
A.5 T2.....	111
A.6 T3.....	112
A.7 Interpolated CPTs.....	113
Appendix B Guidance Document for Pile Installation.....	114
Appendix C Prediction of Pile Behaviour.....	119
Appendix D General Specifications.....	121
D.1 Calibration Sheet: Load Cell.....	121
D.2 Calibration Sheet: Potentiometers	123
D.3 Leica DNA03.....	129
D.4 Fujikura JBS-00240D.....	130
D.5 Fibre Optic Data Logger: fibrisTerre fTB 5020.....	132
D.6 Pile Tip.....	133
SI piles (<i>Fundex</i> pile).....	133
SIc piles (<i>Tubex</i>).....	134
D.7 Concrete Mix & Delivery Tickets (<i>Betonbonnen</i>)	135
SI piles.....	135
SIc piles.....	139
Appendix E Measurements of Test Set-Up.....	141
E.1 Instrumentation.....	141

E.2	Test frame	143
E.3	Pile head	144
E.4	Reference point location.....	145
Appendix F	Load-Strain Response.....	147
	Pile T1.....	147
	Pile F1.....	148
	Pile T2.....	149
	Pile F2.....	150
	Pile T3.....	151
	Pile F3.....	152

1. Introduction

This report presents the execution and results of axial pile load tests on screw injection piles in the south of Delft in 2022. Two types of screw injection piles were tested: a screw injection pile with the steel casing removed (SI, *Fundex* pile) and a screw injection pile with the casing remaining in-situ (SIc, *Tubex* pile). The tests were carried out with the guidance of NPR 7201 (NPR 7201, 2017) and NEN 9997-1 (NEN, 2017), with each pile loaded under compression to a pile base displacement of 20%. During this process, strains were measured along the entire pile length, giving comprehensive insights into the pile base and shaft response.

This document provides a factual summary of the results for dissemination to the NPR 7201 advisory committee, with the primary aim of fully detailing of the test methodology and execution, along with the underlying dataset. Minimal interpretation of these results is presented in this report and has instead been published in the following publications:

- Duffy, K.J., Gavin K.G., Korff, M., de Lange, D.A. (2024) Base resistance of screw displacement piles in sand. *Journal of Geotechnical and Geoenvironmental Engineering*, 150(8), <https://doi-org.tudelft.idm.oclc.org/10.1061/JGGEFK.GTENG>
- Kevin Duffy (2025) *Axial capacity of piles in sand: A field investigation using distributed fibre optic sensing*. [Doctoral dissertation, Delft University of Technology]. (to be published)

The data from the tests is publicly available on the 4TU.ResearchData repository under doi: 10.4121/78720ecb-daf4-4676-b5f4-281e93e4388a (*Static load tests on screw injection piles with distributed fibre optic sensors in Delft*).

1.1. Project Background

The pile tests were supported by Rijkswaterstaat and forms part of the Improved Axial Capacity of Piles in Sand (InPAD) research project, supported by the Top Consortia for Knowledge and Innovation (TKI) and the following partners:

- Deltares
- Fugro
- Gemeente Rotterdam
- NVAF
- Port of Rotterdam
- Rijkswaterstaat
- TU Delft

The InPAD project began on October 1st 2019 and was focused on investigating a number of aspects of pile behaviour including, but not limited to:

- i. The impact of friction fatigue on the distribution of α_s values on displacement piles.
- ii. Determination of accurate pile base resistances that include the effect of residual loads and therefore allow consistent α_p factors.
- iii. Whether limiting q_c values are necessary for estimating shaft resistance.
- iv. If limiting values on the pile base resistance are necessary.
- v. Determine the design value of the cone penetration test (CPT) end resistance q_c (i.e. what averaging technique to adopt)?
- vi. What are the impacts of ageing on the capacity of piles?

Research into these questions was performed through a multi-faceted approach, including field testing, numerical modelling and centrifuge testing. Three full-scale test sites have been carried out as part of the InPAD project. This includes tests on vibro piles, tubular piles, driven precast piles and SIc piles at Amaliahaven (Duffy, Gavin, Korff, *et al.*, 2024), along with driven closed-ended pile tests on the premises of Deltares in Delft.

The site presented in this report has been performed at a location on TU Delft Campus. The field tests target certain sub-questions related to screw injection piles. In particular, the degree of soil displacement during installation is not clearly understood along with the corresponding effect on the ultimate capacity of the piles. Furthermore, how installation parameters, such as grout injection and the extraction of the casing, influence the pile response is also uncertain, particularly for full-scale piles.

The roles and responsibilities of all parties involved with the construction and execution of the pile test programme are included in the **Table 1.1** along with the key dates of the test programme in **Table 1.2**. The representatives of the national pile test committee NPR 7201 for the screw injection pile test at Delft are Jan van Dalen, Henk Brassinga and Rob van Dorp.

Table 1.1: Parties involved during the pile testing and their respective roles

Party	Role(s)
APTS (BMNED + IFCO)	Test execution
BMNED	Site investigation
Deltares	Project management, execution & interpretation of pile tests
Funderingstechnieken Verstraeten B.V.	Installation of piles
NVAF	Assessment of pile installation protocol
Rijkswaterstaat	Primary sponsor
TU Delft	Planning, execution & interpretation of pile tests

Table 1.2: Timeline of the pile test programme

Event		Date
Site investigation		December 2021
Pile installation		February 2022
Pile tests	T1	5th April 2022
	F1	7th April 2022
	T2	9th April 2022
	F2	12th April 2022
	T3	14th April 2022
	F3	20th April 2022
Cutting of pile heads		April 2022

2. Ground Investigation

The test site was a greenfield site owned by TU Delft (Figure 2.1), next to a showcase location for flood defence systems called Flood Proof Holland. Prior to load testing, no other land use was recorded at the pile test site. The site is also located close to the Deltares campus where tests were performed on three driven precast piles in 2021 as part of the InPAD project.

The six test piles were installed on a north-west to south-east axis, alternating between SI and SIc piles. These piles were spaced four metres apart from one another (Figure 2.2). A minimum of three CPTs were executed within two metres of each pile (Figure 2.3; Appendix A) to a depth of NAP - 32.25m (surface level \approx NAP -2.25m). Seven of the nineteen CPTs also include u_2 porewater pressure measurements. All CPTs have been executed according to ISO 22476-1 Application Class 3, consisting of inclinometer measurements in two directions and all with a cone tip area of 15 cm² and friction sleeve area of 225 cm². No post-installation CPTs were made.



Figure 2.1: Location of the 2020/21 precast pile test site on the Deltares campus along with the SI pile test described in this report

The surface of the site consists of a 1m bed of made ground of well-compacted gravel and cobbles (in Dutch: *repak*). This is with the exception of the northernmost pile, T1, where the made ground was also overlain by a bed of soft clay fill–soil which was drained and overlain with rubble during preparation of the test site. Below the made ground clay, was a layer of very soft highly organic clay from NAP -3m to NAP -10m, followed by a layer of firm clay with a sand bed to NAP -18m. The load-bearing layer is found beneath the firm clay, consisting of coarse sand with cone resistances from 10 to 20 MPa. This sand layer forms part of the Pleistocene-era Kreftenheye Formation, found across much of North and South Holland.

No boreholes were performed at the pile test site, although boreholes to 10m depth have been performed across the Flood Proof Holland terrain. Oedometer, triaxial, particle size distribution and direct simple shear tests were performed on these samples. In addition, the subsurface stratigraphy and geological history is almost identical to the precast pile test site at Deltares. From this site, one borehole has been carried out and samples remain in storage for particle morphology and mineralogy tests.



Figure 2.2: Site plan including the executed site investigation

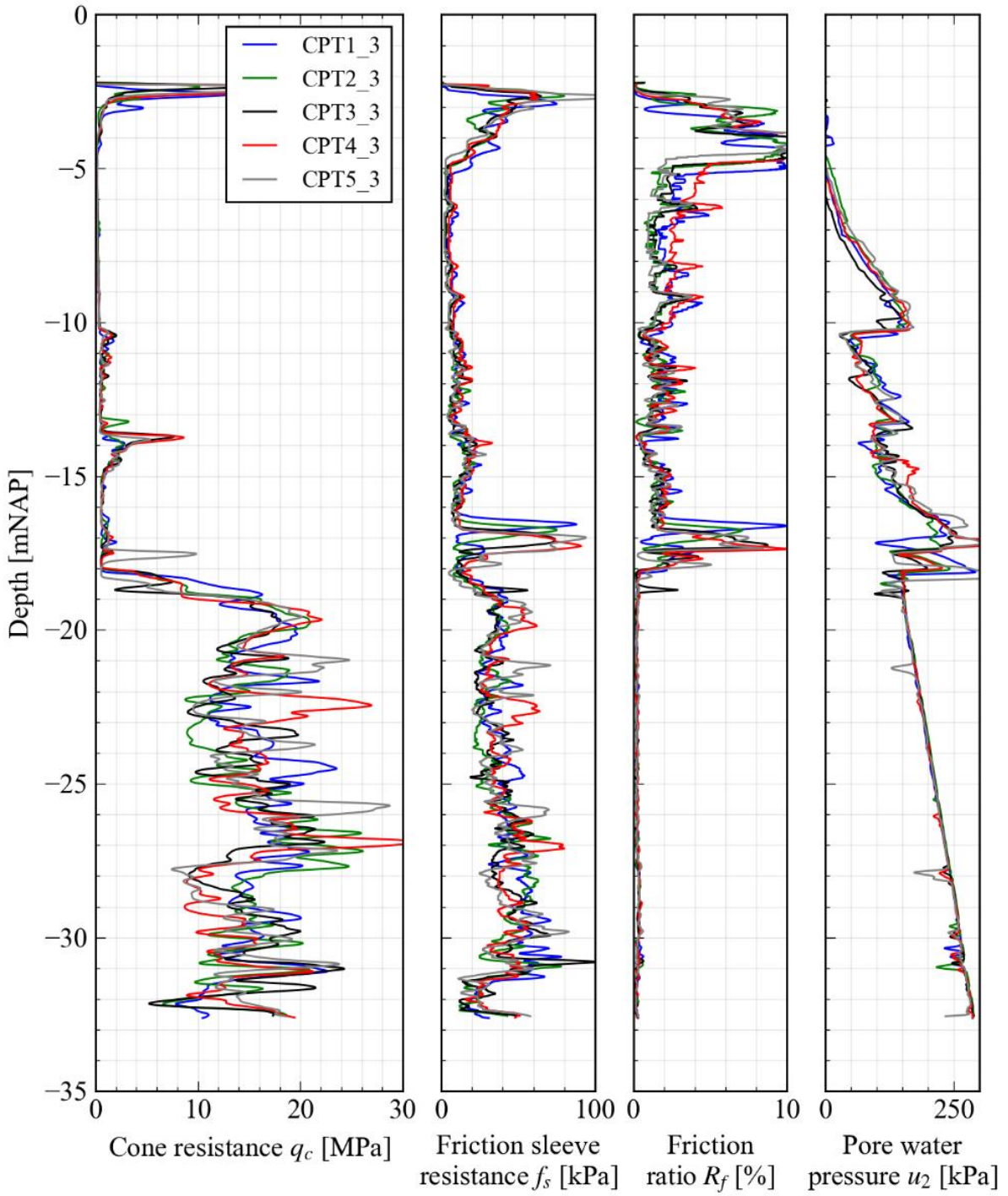


Figure 2.3: CPTs executed along the centreline of the pile test site

3. Pile Fabrication & Installation

Six piles were tested at the site: three SI piles (“Fundex” piles) and three SIc piles (“Tubex” piles). The geometries of these piles along with other relevant information are listed in **Table 3.1**.

Table 3.1: Pile geometries, installation data & specifications

	SI (Fundex)			SIc (Tubex)		
	F1	F2	F3	T1	T2	T3
Embedded pile length [m]	19.97	19.23	19.99	19.90	20.31	20.88
Ground elevation [m +NAP]	-2.25					
Pile toe elevation [m +NAP]*	-22.02	-21.28	-22.04	-22.15	-22.56	-23.13
Penetration into sand [-]	$8.7D_{eq}$	$5.5D_{eq}$	$8.4D_{eq}$	$8.4D_{eq}$	$8.2D_{eq}$	$9.8D_{eq}$
(x, y) coordinates †	(86447.2, 444560.0)	(86449.1, 444552.2)	(86451.1, 444544.4)	(86446.4, 444563.8)	(86448.2, 444556.1)	(86450.1, 444548.4)
Inner diameter – steel casing [m]	0.315			0.357		
Outer diameter – steel casing [m]	0.355 (casing) 0.380 (casing tip/ <i>boorkron</i>)			0.382		
Maximum diameter – screw tip [m]	0.470			0.470		
$q_{c,avg, Koppejan}$ [MPa]‡	10.0	8.9	9.4	9.6	9.2	12.1
$q_{c,avg, De Boorder}$ [MPa]‡	11.9	13.3	12.4	11.3	11.3	14.8

3.1. Pile Fabrication and Installation

The primary goal of installation was to replicate a set of screw injection piles resembling those installed in practice, whilst assuring sufficient quality to act as a test pile. As a result, no intentional variation in the installation parameters was planned prior to installation. Establishing parameters redolent of industry practice was carried out by the NVAF (*Nederlandse Vereniging Aannemers Funderingswerken*) who made a guidance document based on typical practice in the Dutch industry (Appendix B, in Dutch).

All six piles were designed and manufactured by Funderingstechnieken Verstraeten B.V., Oostburg. Both pile types have near-identical screw tips (see Appendix D.6, Appendix D.6 and **Figure 3.1**), with three grout injection outlets facing transversally from the pile. The purpose of this screw tip is to mix the soil and grout and provide a strong grout body along the pile, whilst reducing the installation resistance. Both piles used the same grout mix: Webertec GM42 CEM III/B (with limestone filler) with a target water-cement factor of 1.5. Water from an adjacent canal was used.

All piles were installed using a Fundex F3500 drilling rig and a Fundex-made rotary head (*boormotor*) on the 31st of January and 1st of February 2022.

* The pile toe is deemed as the widest point of the screw tip, i.e. the diameter of the screw flange

† Based on EPSG:28992: Amersfoort / RD New datum

‡ $q_{c,avg}$ has been calculated based on the average of $q_{c,avg}$ obtained from each CPT within two metres of the pile, executed before pile installation



Figure 3.1: Screw tip of the SIc piles. The same tip was also used for the SI piles

SI pile (Fundex pile with grout injection)

The SI pile was constructed using a reusable steel casing, measuring 320 mm in inner diameter and 380 mm in outer diameter (at the casing tip; *boorkron*). The steel casing is mated to a sacrificial pile tip using interlocking teeth. A reusable steel conduit was also used for each pile to transport grout to the pile tip.

To resist the bending moments expected in the upper clay layer whilst avoiding the use of a highly congested reinforcement cage, a HEB 160 profile, 21m in length, was used as reinforcing. To provide additional strength against any bending applied perpendicular to the web, two reinforcing bars were placed on either side of the web across the upper six metres of the HEB profile. A steel tube 21mm in outer diameter was welded along the centre of the web, used to house a telltale for use during pile testing (**Figure 3.2**).

The concrete mix for the SI piles used a smaller maximum aggregate size ($D_{max} = 8\text{mm}$) compared to the SIc piles ($D_{max} = 16\text{mm}$) to minimise the congestion of aggregate in the pile reinforcement. The full concrete mix is provided in Appendix D.7.

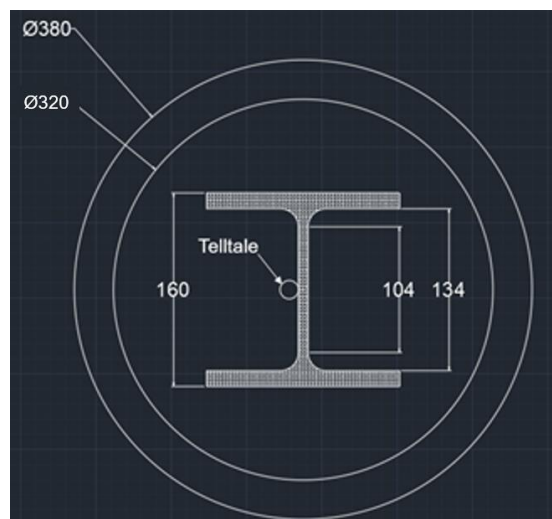


Figure 3.2: SI pile reinforcing drawn to scale, with reference to the inner diameter of the casing (315 mm) and the casing tip (*boorkron*; 380 mm)

The installation procedure for the test site is outlined below and schematised in **Figure 3.3**:

1. **Prior to installation:** Sacrificial screw tip placed at the location, coated with a lubricant and then mated with the casing.
2. **Commencement of installation:** grout injection applied along with rig pulldown and torque.
3. **0.25m prior to installation depth:** grout injection stopped. Penetration continued to target depth.
4. **Target depth reached:** drilling rig and drilling motor remaining on pile head.
5. **Reinforcement placement:** Reinforcement placed in pile, resting on the pile base.
6. **Concrete placement:** concrete poured directly from a skip at the pile head, partially filling the casing.
7. **Tube withdrawal:** Tube withdrawn using a clockwise and anti-clockwise motion. Concrete topped up every two or three times from the top of the casing.

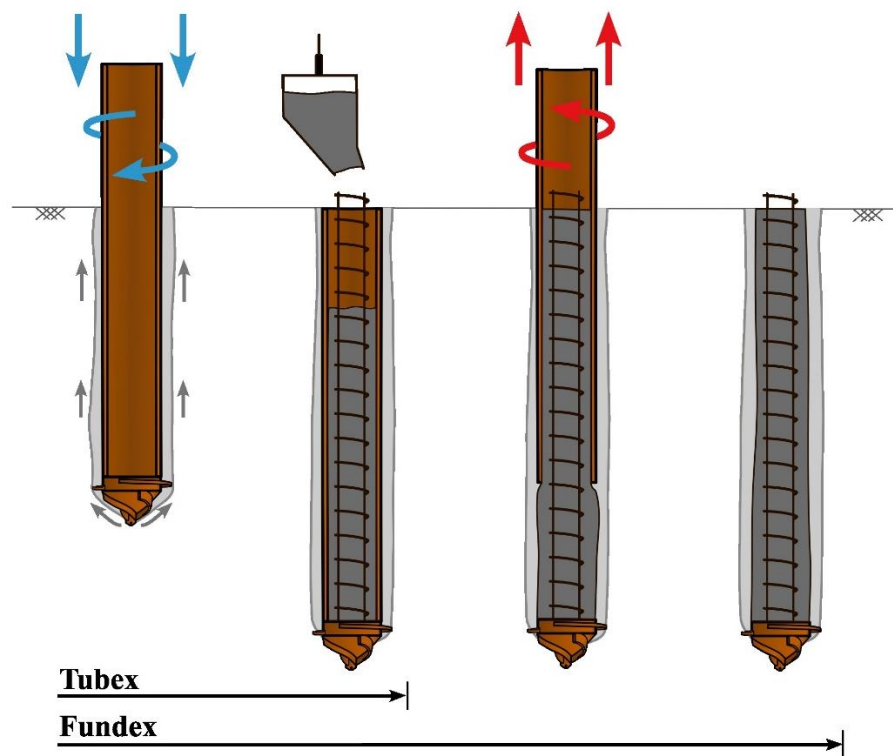


Figure 3.3: Installation procedure of the SI (Fundex) and SIc (Tubex) piles. Note: the casing dimensions is different for both piles and no reinforcing was placed in the SIc piles

SIc pile (Tubex pile with grout injection)

The SIc pile was constructed using a sacrificial steel casing, measuring 357 mm in inner diameter and 382 mm in outer diameter. A screw tip was welded to the bottom and had the same shape as the SI piles. A sacrificial fluidisation conduit, 48 mm in outer diameter, was also placed within the pile and connected directly to the screw tip. All components of the sacrificial casing are fabricated from S355 steel, weighing approximately three tonnes.

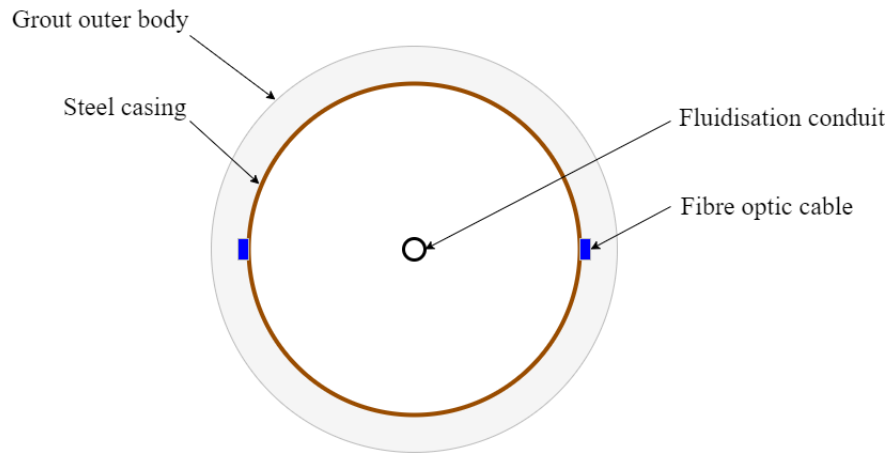


Figure 3.4: Cross-section of the SIc piles (not drawn to scale) including instrumentation. The fluidisation conduit was used to house a telltale during pile testing

The installation procedure for the test site is outlined below and shown in **Figure 3.3:**

1. **Commencement of installation:** grout injection applied along with rig pulldown and torque.
2. **0.25m prior to installation depth:** grout injection stopped. Penetration continued to target depth.
3. **Target depth reached:** drilling rig moved to next location. Empty tube awaiting concrete.
4. **Concrete placement:** concrete poured directly from a skip at the pile head.
5. **Flushing of fluidisation conduit:** conduit flushed out with water to allow placement of telltale during pile testing.

Installation Parameters

During installation, the following measurements were recorded with respect to time and penetration depth in the drilling rig:

- Pile torque
- Rotational direction and velocity (revolutions per minute)
- Grout pressure
- Grout flow rate
- Penetration depth
- Pulldown force (pullup force not measured)
- Oil pressure

Guideline installation parameters based on typical practice were established by the NVAF, shown in Table 3.2. Further details are provided in the report *Advies Uitvoeringsparameter Schroefinjectiepalen*.

Table 3.2: Key installation parameters for the installation of the SI and SIc piles. The NVAF protocol is provided in [blue](#)

	Unit	SI	SIc
Flow rate	L/min	75 (55-100)	
Flow rate last 0.25 m	L/min	0	75 (55-100)
Penetration rate (Holocene)	m/min	2.5	

Penetration rate (Pleistocene)	m/min	0.25-1	
Torque	kNm	Less than rig capacity (No specification)	
Pull-down	tonnes	Greater than buoyancy force acting on the tube (=4 tonnes) and to enough to maintain the required penetration rate	
Grout type	-	Webertec GM42 CEM III/B (with limestone filler)	
Grout: water-mix factor	-	1.5 (1.0-2.0)	
Concrete	-	C45/55 CEM III/B F4 ($D_{max} = 16$ mm)	C45/55 CEM III/B F4 ($D_{max} = 8$ mm)
Other specifications			
<ul style="list-style-type: none"> At no point may the casing be pulled upwards during installation Both clockwise and anti-clockwise rotation of the screw tip is not preferred but permitted if risk of a stuck auxiliary tube 			

3.2. Installation Observations

The SIc piles were installed on the 31st January 2022 (in the order T1, T2 then T3) and the SI piles the day after (F1, F2 then F3). Some general observations of the pile installation are written below.

Observations of outflowing grout

Almost immediately upon penetration of pile T1, the first pile to be installed, no grout outflow was observed (**Table 3.3**). For subsequent piles, some adjustments were made to the installation parameters to improve the outcoming grout flow and ensure a complete grout shell around the entire length of the pile. These changes included an increase in flow rate across both pile types along with a reduced penetration rate in the upper clay layer for the SIc piles. This did not have a clear effect on the grout outflow rate.

Table 3.3: Qualitative assessment of grout flow during pile installation

	F1	F2	F3	T1	T2	T3
Made ground	Heavy flow	Heavy flow	Heavy flow	Heavy flow	Heavy flow	Heavy flow
First clay	No flow	No flow	No flow	No flow	No flow	No flow
First sand	Heavy flow	For first 2m of layer: slow to medium flow	Medium flow for first 2m, to light flow for remainder of layer	No flow	No flow	No flow
Second clay	Heavy flow	No flow to light flow	No flow	No flow	No flow	No flow
Second sand	Heavy flow	Heavy flow	No flow	Very small flow initially but then stops	No flow	At -18.0mNAP: Slow mass of grout flow coming out, stops by 18.5mNAP

Pile F1: Insufficient concrete

An insufficient amount of concrete was ordered for pile F1, the first of the three SI piles. This resulted in the concrete body of the pile only being formed up to 60cm below surface level. This has been accounted for during the construction of the pile cap (Section 4.1).

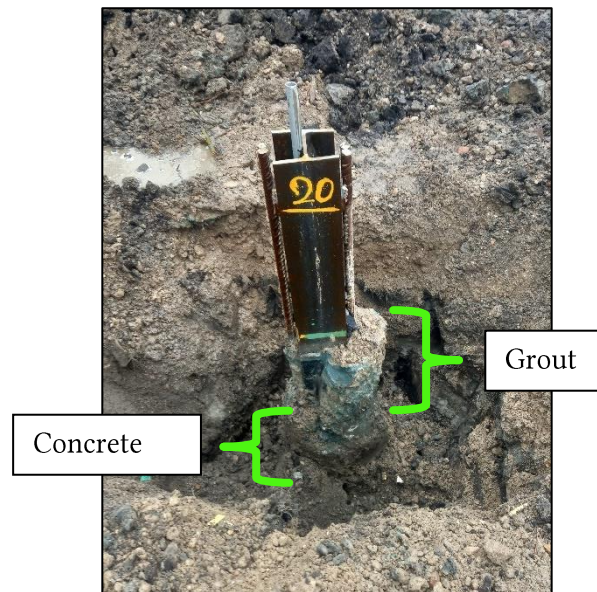


Figure 3.5: Pile head of F1 after installation

Pile F2: Coarse aggregates at pile head

A large number of concrete aggregates was observed around the head of pile F2 following installation (**Figure 3.6**), suggesting some segregation of concrete aggregates within the concrete mix. This was not observed for piles F1 and F3, however, the strain measurements (Section 5) and the sonic integrity tests (Section 4.4) do not suggest significant differences between the three piles. As a result, the degree of segregation is believed to be relatively minor.



Figure 3.6: Pile F2 following installation, showing the coarse aggregates surrounding the pile

Pile F3: Stuck casing

Pile F3, the last pile to be installed, encountered difficulties during the withdrawal of the auxiliary tube. After the reinforcing and concrete was placed in the pile, withdrawal of the casing commenced using anti-clockwise and clockwise rotations of the auxiliary tube in combination with a pull-up force. After five metres of extraction, it was observed by the drillmaster that the reinforcing was also being pulled up upwards with the pile, possibly caused by cohesive or arching forces through the concrete between the reinforcing and the auxiliary tube.

To prevent the reinforcing from being brought upwards with the pile, the auxiliary tube was rotated in both directions at the same installation depth and brought upwards and downwards by roughly two metres, however this had no effect on the upward movement of the reinforcing and it was decided to leave the auxiliary tube in place. In doing this, the auxiliary tube was re-installed to approximately five centimetres above the sacrificial steel tip (to prevent the reinteraction with the tip) and the casing was cut above surface level. No measurements were recorded by the drilling rig during this process, a process which lasted roughly three hours.

Video timelapses of the installation also suggest that the forces exerted by the drilling rig had a significant effect on the surrounding soil.

Following installation significant inclination in the reinforcing at the surface was also observed (**Figure 3.7**).

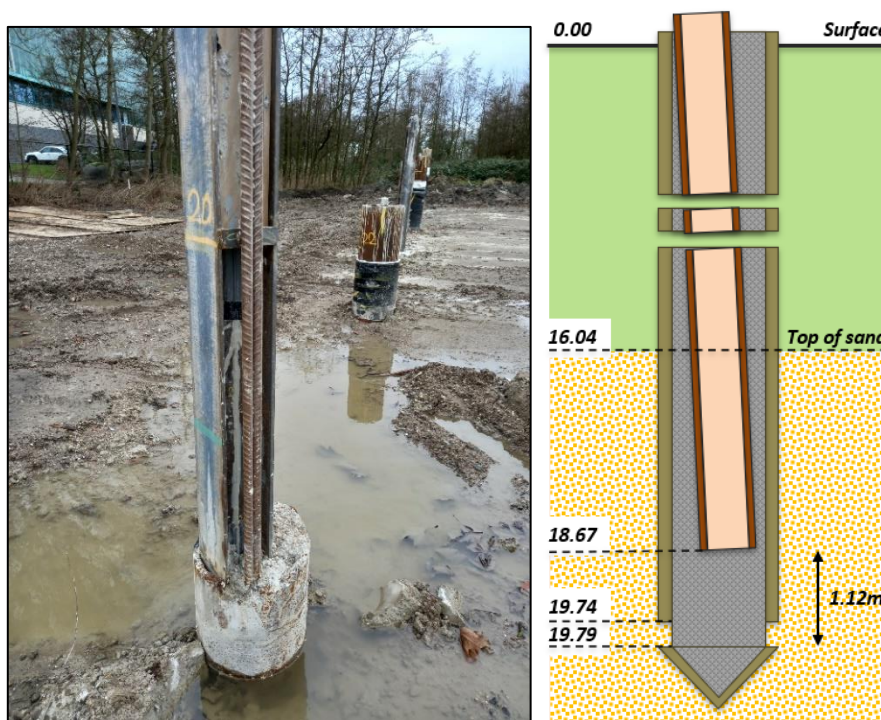
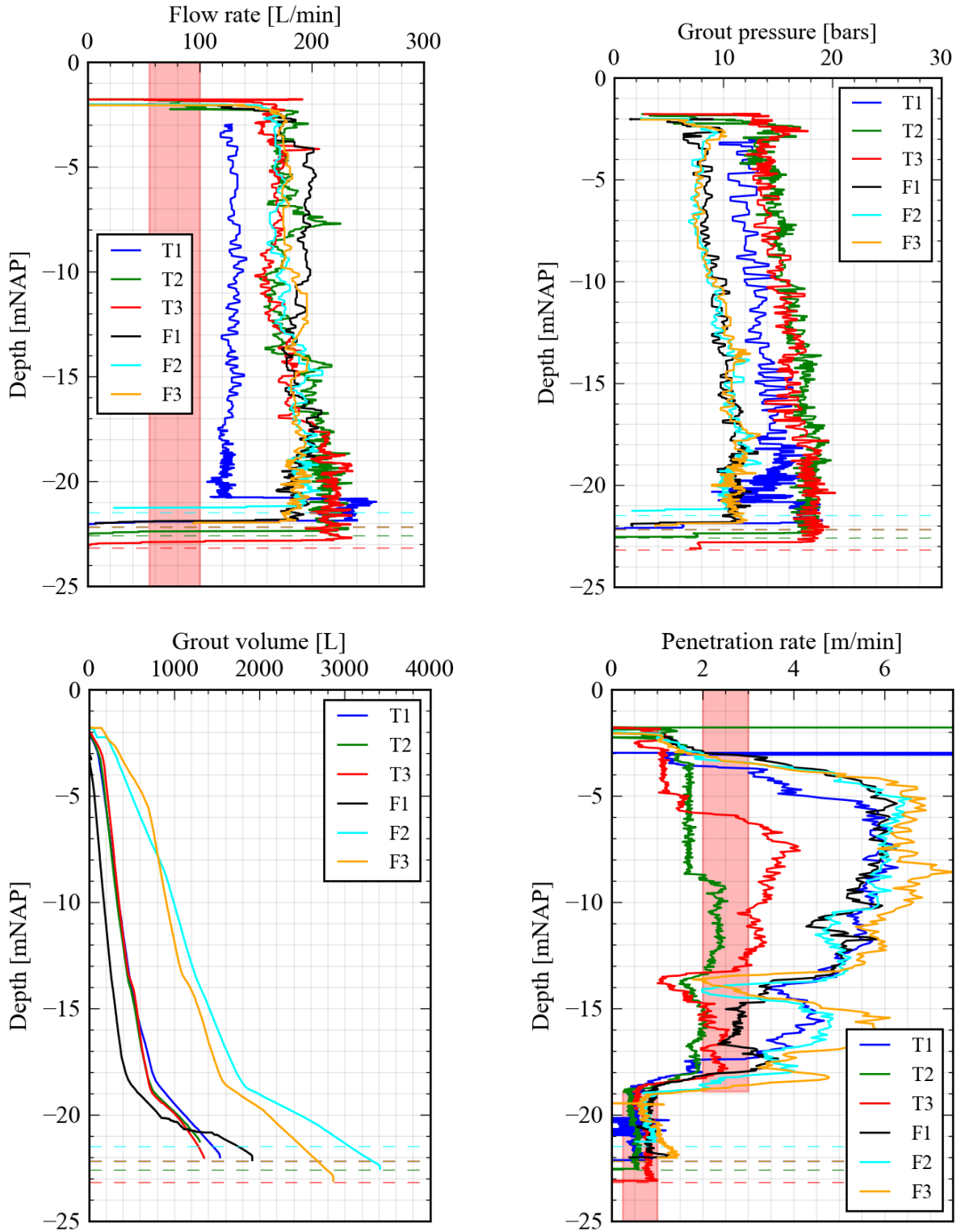


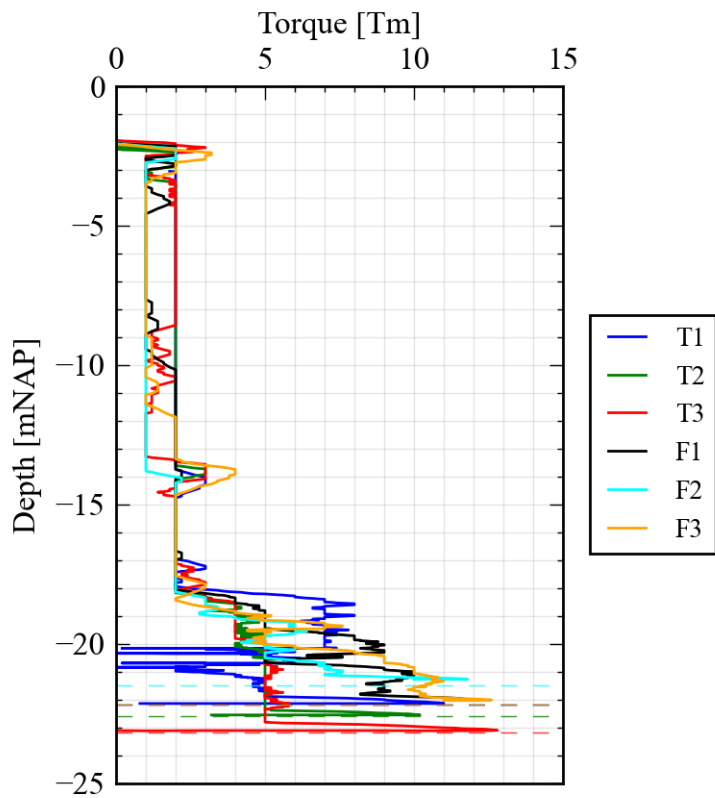
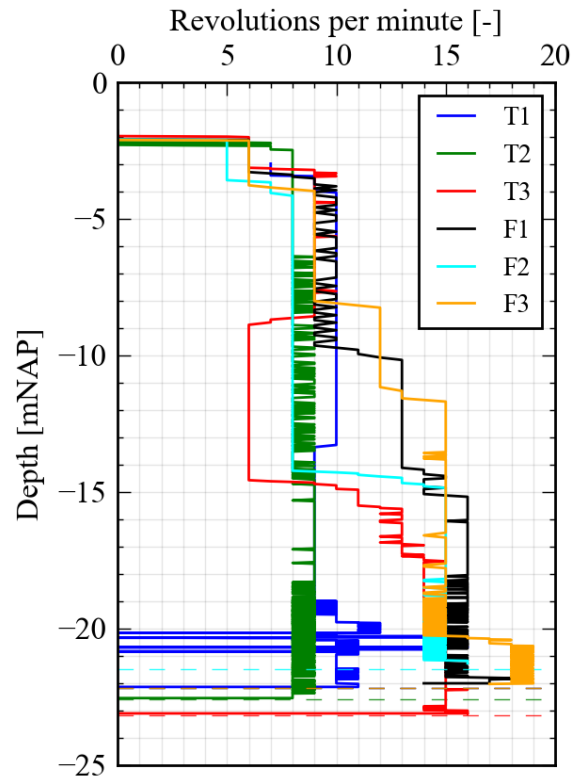
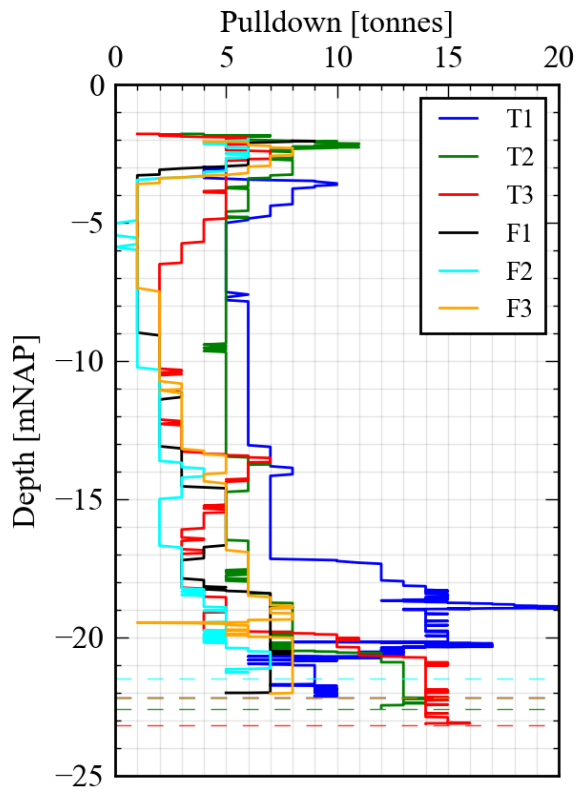
Figure 3.7: Inclination in reinforcing with respect to the stuck casing of pile F3

3.3. Drilling rig data

Provided below is the data collected from the drilling rig during pile installation. The elevation of the pile tip is indicated by a dashed line.

Note that systematic differences between the pressure between the Fundex and Tubex piles are caused by the differences in the non-return valve at the pile tip.





3.4. Grout data

In total, 35 grout samples were collected, 19 directly from the grout mixing plant (incoming grout) and 16 coming from the annular space around the pile (outcoming grout). The outcoming grout was collected from a trench dug adjacent to the pile (**Figure 3.8**), a trench which was periodically emptied if overflowing with grout.



Figure 3.8: Trench in front of pile to collect outflowing grout

A large degree of variation in the incoming water-mix factor was exhibited, with an average WMF of 1.44 and coefficient of variation of 46% (**Figure 3.9**). Some of the variation can partly be attributed to the sampling regime: samples could only be taken at the grout mixing tank which was a highly dynamic environment and made it difficult to take representative samples.

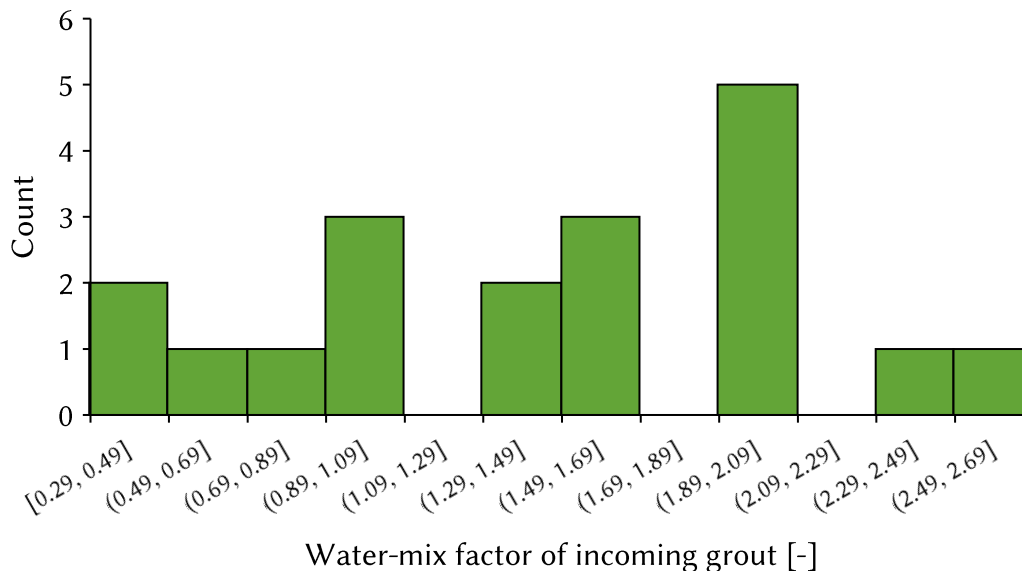


Figure 3.9: Water-mix factor of incoming grout

To convert measured unit weights to a percentage sand in the outcoming grout, a constant WMF in the outcoming grout was taken by assuming an outcoming WMF equal to the average incoming WMF. In the lower Pleistocene sand layer, the outcoming grout had an average sand content of 19% by mass when considering both sieve tests and unit weight measurements (**Figure 3.10**). Low grout outflow

rates around the pile meant it was difficult to take a representative sample—although the results of the samples taken are generally relatively in agreement with one another.

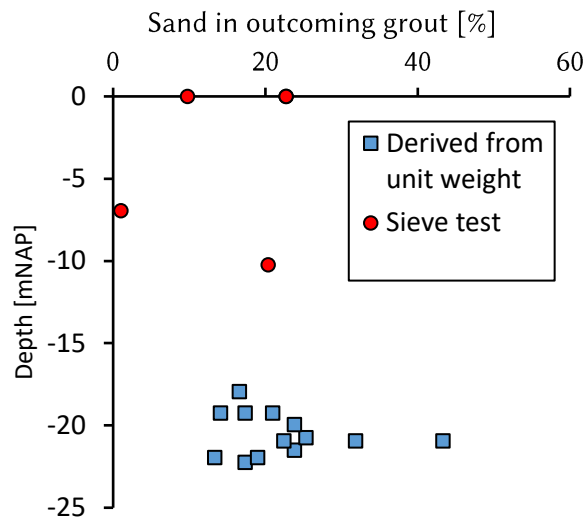


Figure 3.10: Percentage sand over depth for samples taken when the pile tip was at a certain depth

4. Pile Testing

4.1. Test frame

The test frame was a deadweight system provided by APTS, consisting of a 12 m long steel frame and concrete blocks (**Figure 4.1**). Each block weighed approximately ten tonnes, with the steel frame weighing twelve to thirteen tonnes. At each footing, a series of wooden and steel dragline mats are placed to spread the load, with each footing 33 m² in plan area.

A pile cap of shrink-free mortar was constructed for the SI piles with approximately 5cm of cover between the top of the reinforcing and the surface of pile head. The pile cap extended just below the pile surface and had a diameter 470 mm for all piles.

A steel transition piece between the pile and the hydraulic jack facilitated the measurement of the telltale and the passage of the fibre optic cables. Between the top of the pile and the transition piece, a soft lead plate was also placed to minimise any localised cracking of the pile head during loading. A telltale, 1cm in diameter, was placed in the reservation tube of each pile, running the entire length of the pile from pile head to near the screw tip. By measuring the displacement between the top of the telltale and the top of the pile, the elastic shortening of the pile could be deduced.

One hydraulic jack (Enerpac CLR 60010 jack; Enerpac ZE5840LW-R pump) provided the load on the pile during the test and the oil pressure was recorded every 13 seconds during the test. On top of the jack, one load cell was placed (Belotti CRR 225; Appendix D.1), also recording at a frequency of 13 seconds.

Displacement of the pile head was measured using four potentiometers (Novotechnik LWH 150, Appendix D.2). These were fixed to the transition piece and measured relative to a wooden reference frame resting on two supports approximately 5.5m from the piles' central axes. Displacement measurements were made every 13 seconds. Additional potentiometers were used in the case of breakage or as supplemental measurements (ELAP PLS potentiometers).

The displacement measurements were also cross-checked using two different levelling stations, both with an accuracy of 0.3 mm (Leica DNA03, see Appendix D.3). One levelling station automatically logged every five seconds, and the other was checked manually every five minutes. Both levelling stations measured with respect to a reference point, the location of which was different for each pile test (Appendix E.4). Changes in the reference frame or settlement at the test frame footings was also monitored using the manual levelling station.

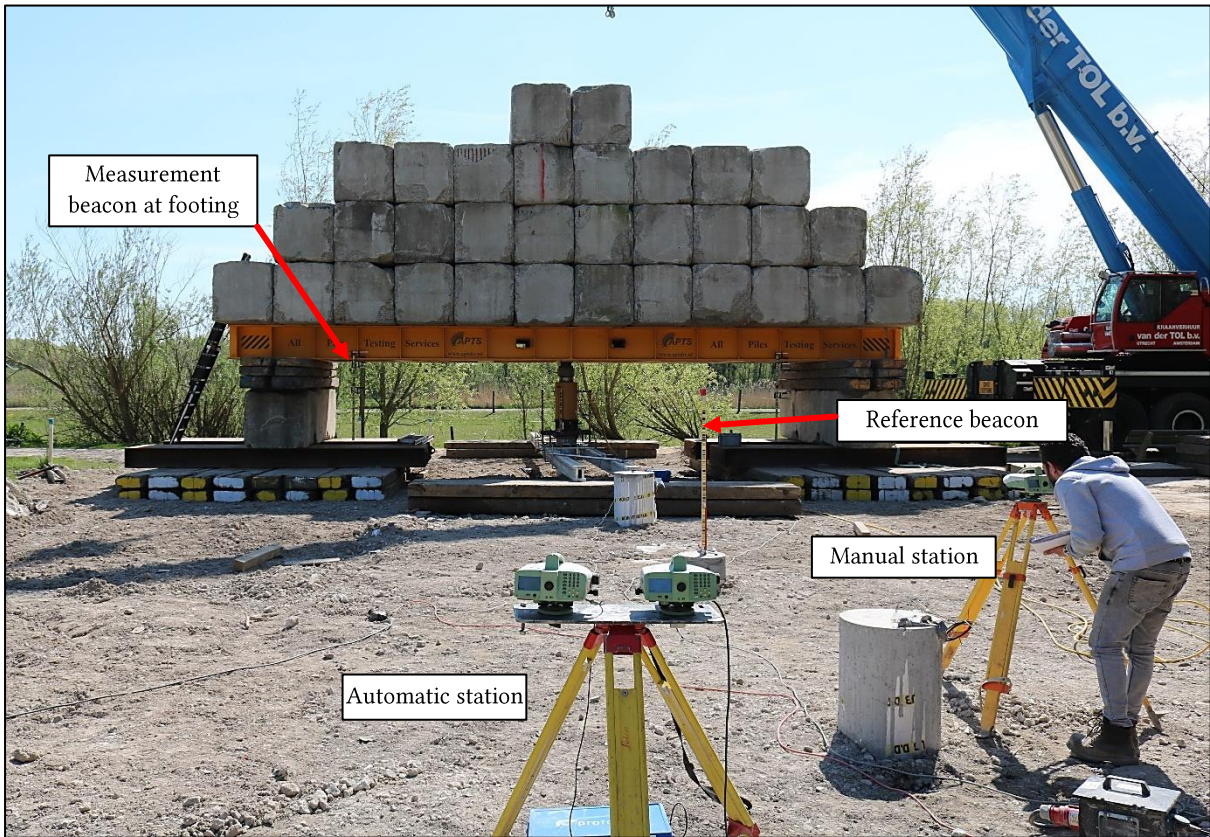
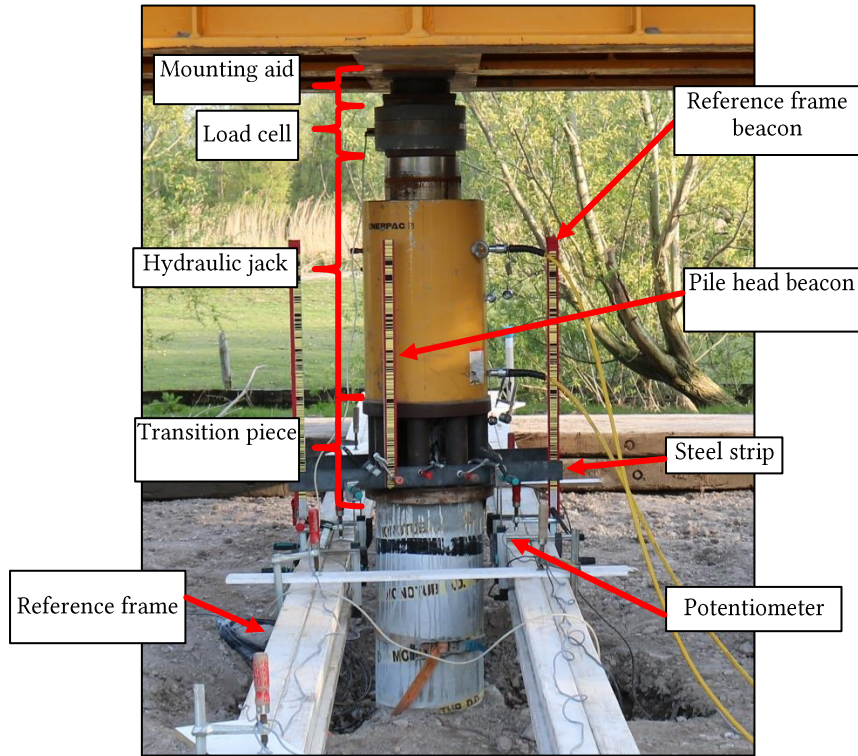


Figure 4.1: Levelling stations at the test site, with one instrument of the automatic station focused on the pile head and another instrument at the reference point

4.2. Strain Instrumentation

All piles were instrumented along their entire length with a steel-reinforced fibre optic cable (Fujikura JBS-00240D provided by ONSFiber; Figure 4.2) for the purposes of measuring mechanical strain. The cable consists of two colour-coded optical fibres lying adjacent to one another and encased in a polyethylene sheath.

The FO cables were interrogated using the fibrisTerre fTB 5020 data logger, which provided a distributed strain profile along the entire fibre optic cable (including connecting cables) using Brillouin Optical Frequency Domain Analysis (BOFDA). Measurements were recorded every ninety seconds and with a spatial resolution of 20 cm (5cm using fibrisTerre’s proprietary enhanced spatial resolution function) and an accuracy of 2 $\mu\epsilon$. To facilitate the BOFDA measurements, the fibre optic cables must be arranged in a looped configuration, either using optical fibres within the same cable, or passing a cable from one side of the pile to another.

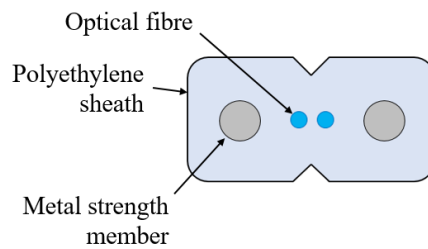


Figure 4.2: Fujikura JBS-00240D (2.8×1.6 mm; not drawn to scale) optical fibre cable

For both the SI and SIc piles, the cables were glued to the steel surfaces of the H-beam reinforcing and tube respectively. This process was carried out indoors at room temperature to avoid rust or contaminants affecting the glue-plastic-steel bonds. The steel surfaces were prepared using a scouring tool to remove rust, followed by degreasing and a final cleaning with compressed air. A two-component epoxy was used, Araldite 2015-1, because of its (i.) relatively slow curing time compared to cyanoacrylate, allowing time for any adjustments to be made (ii.) high viscosity for gluing on inclined surfaces and (iii.) high strength after curing. All glued surfaces were allowed to cure for at least twelve hours before the pile was rotated or moved.

All cables were mechanically spliced to an outdoor patch cable running to the measurement cabin for pile testing and the quality of the fibre optic network was assessed using an OTDR device, with all piles satisfying the intensity loss criterion of <0.5 dB, with the exception of Pile F3 due to pile installation issues (see Section 5.6).

Strain measurements were also made before and after pile testing (**Table 4.1**), although no reference measurement was made prior to installation and nor has temperature compensation been applied between measurement times.

Table 4.1: Dates of strain measurements

	Before test	During test	After test	Comments
F1	06/04/22	07/04/22	Connectors broken	
F2	09/04/22	12/04/22	22/04/22	
F3		20/04/22	22/04/22	Fibre A broken. Only Fibre B & Fibre C interrogated
T1		05/04/22	22/04/22	
T2	07/04/22	09/04/22	Connectors broken	
T3	12/04/22	14/04/22	22/04/22	

The instrumentation procedure specific to each pile type are specified below.

SI piles

The SI piles were instrumented on the reinforcing along three axes, labelled A, B and C (**Figure 4.3**). Using the two optical fibres in each cable, a connection was made at the bottom of the pile and placed in a protective cassette (**Figure 4.4**). As a result, six strain profiles could be obtained, i.e. two on each of the three axes. An advantage of the configuration was its redundancy in the event of fibre breakage, allowing for a continuous loop to be formed across the remaining measurement axes in the event one or more of the axes broke.

Each axis was instrumented separately. First the cable was pulled taut along the length of the entire pile and taped at intervals of approximately 2-3 m. Epoxy was then placed over the cable itself and shaped/streamlined using a scraper. At the pile head, the ends of the cables were placed under a removable wooden box (**Figure 4.5**). Following installation, the box was removed and the ends of the cables were spliced together, with a connector placed on measurement line A1 and C3.

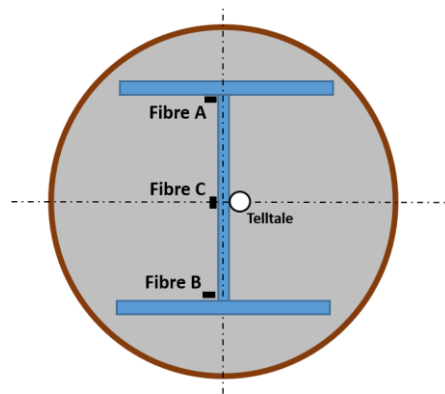


Figure 4.3: Cross section of the SI pile, indicating the instrumentation



Figure 4.4: Protective cassette at the bottom of the reinforcing of the SI piles. The lowermost measurement was therefore roughly one pile diameter from the base of the reinforcing

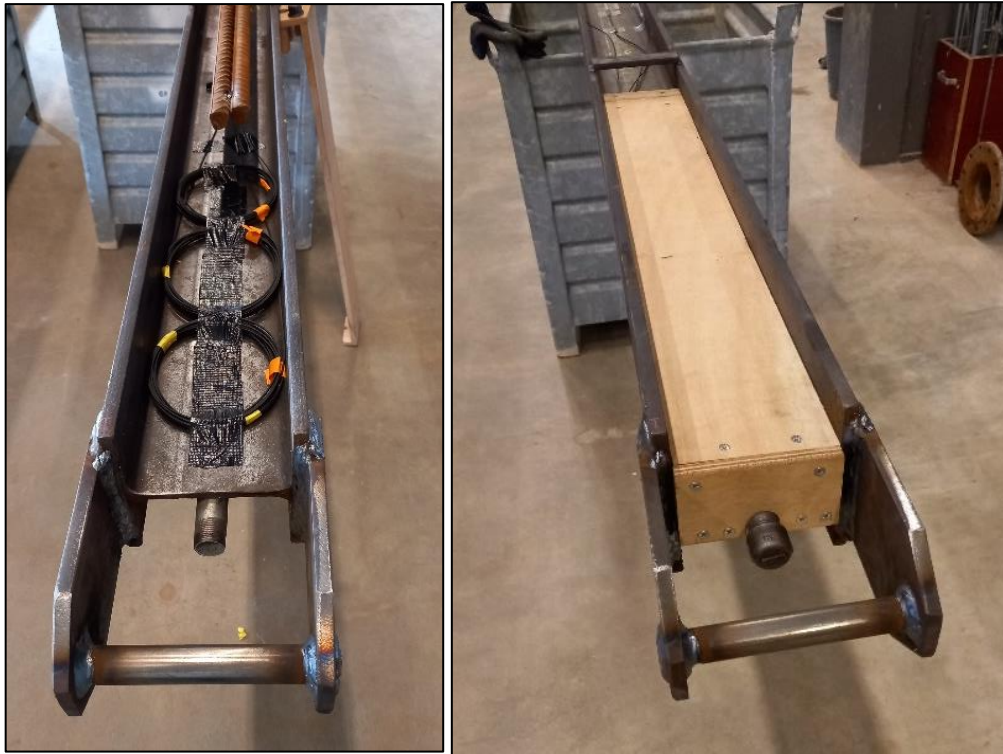


Figure 4.5: Top of the SI pile reinforcing, with and without the protective wooden box

SIc piles

One fibre optic cable was instrumented on the SIc pile in pre-formed axially opposing grooves on the outside of the pile (Figure 4.6). The grooves were roughly parabolic in shape, 5mm at their deepest point. At the bottom of the pile, the groove looped around the tube, transitioning from one side to the other (**Figure 4.7**), allowing for a continuous strain distribution to be obtained on axially opposing sides of the pile. The lowermost measurement was approximately 35 cm above the pile base.

The connecting ends of the fibre optic cable were then taped close to the pile head and covered using protective layers of foam and rubber (**Figure 4.8**).



Figure 4.6: Fibre optic cable within the prepared groove of the SIc pile



Figure 4.7: Grooves prepared at pile tips, showing the glued-in-placed FO cable transitioning from one side to another. Two grooves were created at the pile tip, although only one groove was ultimately used. The distance to the last possible FO reading is shown



Figure 4.8: Protecting the loose fibre optic cables at the pile heads using foam and rubber mats

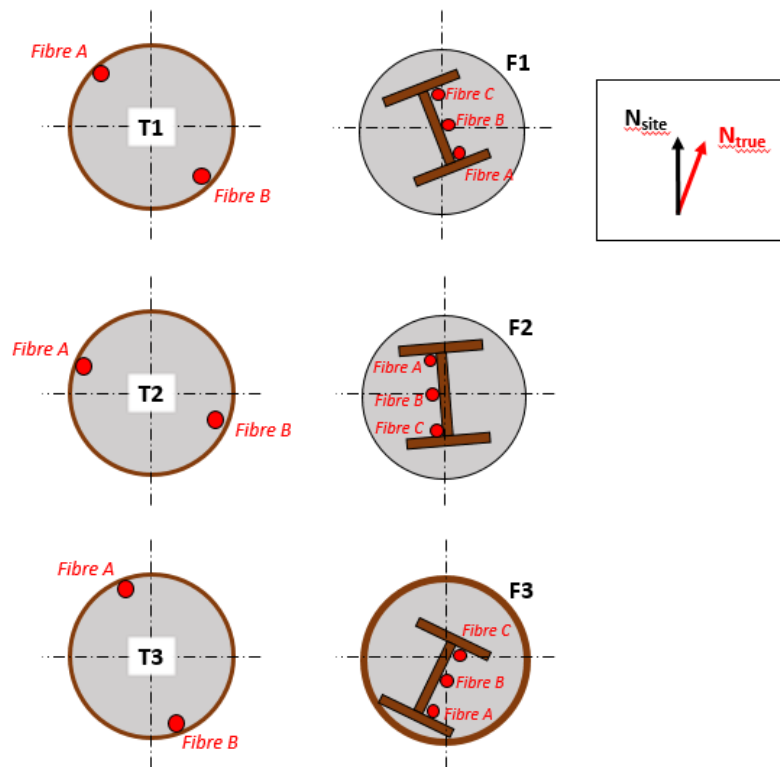


Figure 4.9: Orientation of the fibre optic cables after installation

4.3. Test Procedure

Pile testing was performed with the guidance of NPR 7201 (2017), albeit with the omission of the unload/reload cycles following each load step. The target capacity was estimated based on the current NEN 9997-1 pile design method, in addition to the design method developed for SIC piles from the InPAD test programme at Amaliahaven (see Appendix B for calculation details). This was adjusted during the test programme depending on the results of previous tests.

The pile was first loaded to 5% of the target load, allowing for verification of the measurement equipment. Load steps equal to one-eighth of the target load were prescribed, with each load holding period lasting at least thirty minutes when the load was less than 50% of the target load, to at least one hour for load steps greater than 50% of the target load (i.e. beyond Step 4).

During each load step, the creep parameter (*kruipmaat*) over the last fifteen minutes of each load holding period was assessed according to the following formula:

$$k = \frac{u_2 - u_1}{\log t_2 - \log t_1}$$

where: u_1 and u_2 is the settlement (in millimetres) of the pile head at time t_1 and t_2 (in minutes) respectively. The decision to conclude or extend the load step was then determined based on the decision tree outlined in **Table 4.2**.

Table 4.2: Decision tree for the termination or extension of each load step. Minimum step duration must be met (>30 min up to and including Step 4; >60 min Step 5 and higher)

$k < 0.75$ mm	Increase load by full step
$0.75 \text{ mm} < k < 2$ mm	Increase load by half step
$k > 2$ mm (and decreasing or stable)	Increase load by quarter step
$k > 2$ mm (and increasing)	Increase step duration by max. 60 min. After this, increase by a quarter step

The primary pile test concluded if the settlement of the pile base (calculated by subtracting the elastic shortening s_{el} of the pile from the settlement at the pile top s_0) exceeded 20% of the equivalent pile diameter D_{eq} (=94 mm for all piles). During the test itself, the elastic settlement was determined based on the theoretical elastic shortening and the telltale measurements.

Once the failure criterion was attained, a “relaxation phase” was carried out by stopping the hydraulic pumping system and letting the pile displace under the gradually decreasing load until an equilibrium was attained. This step lasted up to thirty minutes or until an asymptotic trend became clear in the settlement readings.

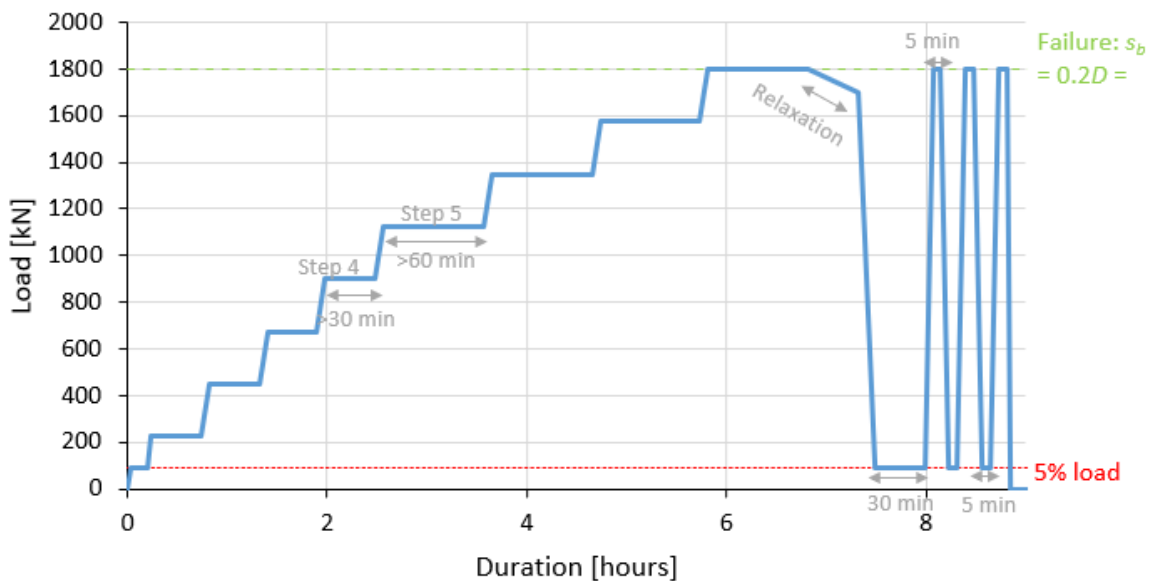


Figure 4.10: Schematic of the load test procedure. Note: the number of steps and duration may vary depending on the creep criteria

Following the completion of the main test, the load was reduced to the 5% load over a period of 10 minutes, with load held at 5% load for 30 minutes. Subsequently, up to three unload/reload cycles to the failure load were carried out to investigate the effect of cyclical loading on the shaft friction of the pile. To facilitate strain measurements at the peaks and troughs of the load cycles, the load was held for five minutes.

4.4. Sonic Integrity Testing

Sonic integrity tests (SIT) were performed on all piles (**Figure 4.11**), except for pile T3 which was being load tested on the day of the SIT tests. The two SIc piles exhibit some return noise across much of their lengths. After a depth of approximately 16m, the velocity reduces rapidly and any reflection at the pile toe is not clear. For the SI piles, the same reduction of wave velocity occurs after 16m and even more noise in the measurements was exhibited. No significant variation is shown in pile F3 compared to the other SI piles despite the stuck casing.

Overall, it is difficult to interpret the quality of the piles from the SIT tests. This may be large in part due to the composition of the piles themselves: with the large amount of steel present through the casing of the SIc piles and the H-beam reinforcing of the SI piles. In both instances, the large amount of steel can lead to signal damping and reflection, making it difficult to distinguish between discontinuities across the pile length.

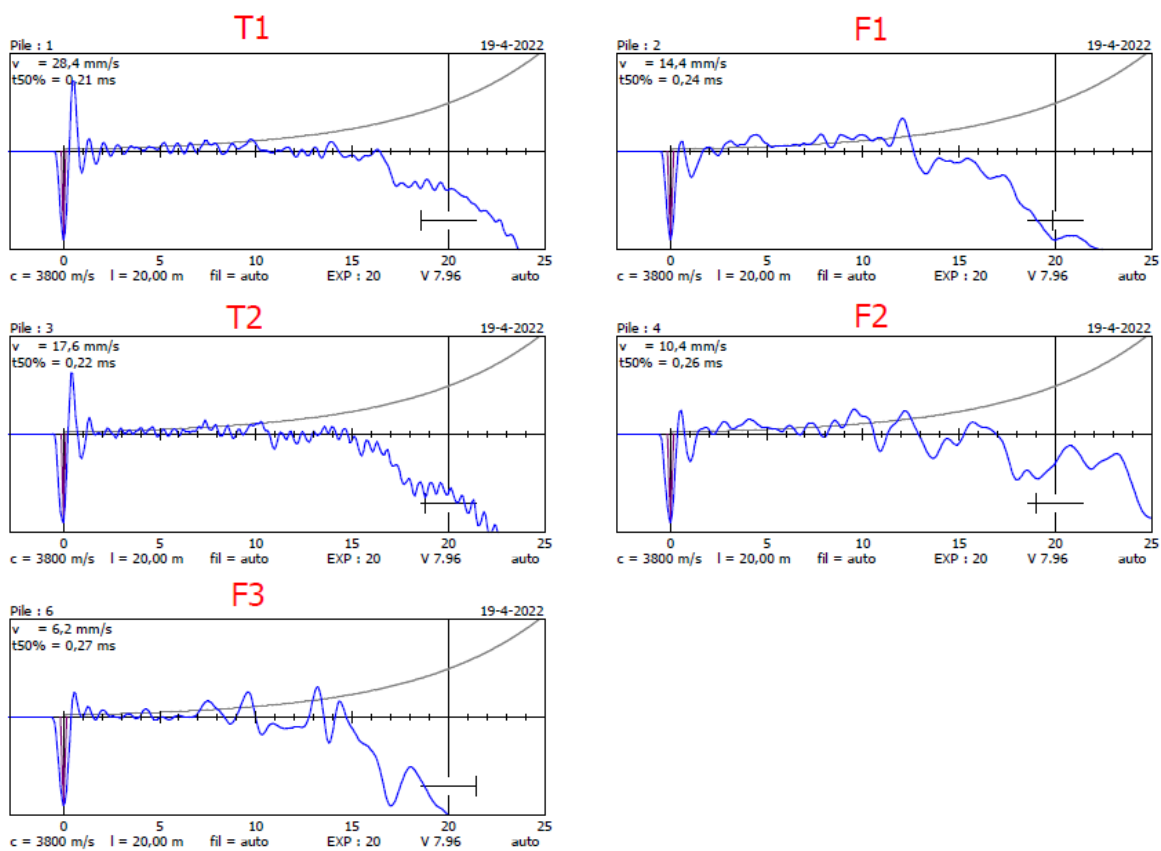


Figure 4.11: Selected blows from the sonic integrity tests. Signal amplification has been applied to the presented readings

4.5. Pile Extraction

Because of environmental, financial and technical considerations, the piles were not extracted after testing. Nonetheless, the upper three metres of all six piles was sawn off to return the site back to the proprietor.

No evidence of any grout was present along the top of SIc piles (e.g. **Figure 4.12**). For the SI piles, an 0.5-2cm thick light grey layer, with little to no aggregates, was present around the upper parts of piles F1 and F2 (**Figure 4.13**). Given the low amount of aggregates in this region, the layer is likely to be the grout shell and was firmly bonded with the concrete core.

On pile F3 (with the lost casing), a thin film of grout less than 0.5 cm in thickness was present in some spots (**Figure 4.14**), although this grout layer was easily removable with light force. Unlike the tube of the SIC piles, much of the corroded layer of the casing was absent, possibly because of abrasion during the attempted extraction of the casing.



Figure 4.12: Head of pile T1 after extraction. No clear evidence of grout was present at the head of any of the SIC piles

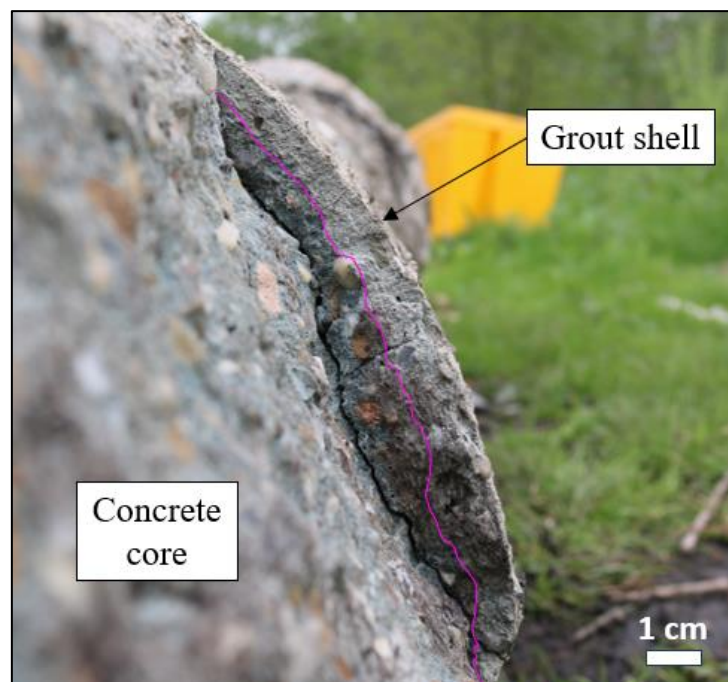


Figure 4.13: Close up of the circumference of pile F1, showing a small 1 cm layer of grout on the surface of the pile



Figure 4.14: Close-up of the head of pile F3, with one of the broken pieces placed on top of the pile

5. Test Results

In this chapter, the results from each load test are provided in chronological order. Data processing, analysis and visualisation was primarily carried out using the Python programming language, including the apriori prediction of pile capacity and the CPT averaging methods. Microsoft Excel has also been used for specific tasks and all data is available in .csv format.

Note that compressive strain and downward displacement of the pile are indicated as positive quantities. Details of geometrical measurements, such as the distance between the test frame footings and the pile, are included in Appendix E.

Several general comments are included below:

- The potentiometers and the two reference frame beams have been labelled with respect to site North (**Figure 4.9**).
- Occasional power shutdowns occurred due to the overloading of the generator by the hydraulic jack, creating small measurement gaps in the Leica levelling station readings. This usually occurred when approaching a new load step, i.e. when high demand was placed on the local power system.
- Displacement readings at the pile head are taken from the potentiometers by default, with the exception of pile T1 where the Leica levelling station was used because of a corrupted storage card.
- The reference point was changed several times across the load test programme (Appendix E.4) to ensure an appropriate line-of-sight.
- Displacement measurements have been corrected for based on the reference point, with the assumption that there was no movement in the reference point itself.
- No correction has been made for movement in the reference frame because of the lower frequency of the reference frame measurements compared to the pile head displacement measurements.
- Corrections have been made for any particularities e.g. readjustment of potentiometer readings

5.1. 5th April 2022: Pile T1

Pile T1 was tested on the 5th of April, the first of all piles to be tested. Weather conditions throughout the test were wet, with a moderate breeze reducing to a light breeze over the course of the test.

The start of the test was delayed by two hours due to difficulties with setting up equipment. The test then concluded just before $0.1D$ instead of the target base displacement of $0.2D$ because of concerns regarding the stability of the test frame. Three load cycles were performed at the end of the test, although the failure load could not be reached again.

After the test, the memory card of the potentiometers was found to be corrupted and the potentiometer data was irretrievable. Potentiometer data recorded manually during the test is available, albeit at a frequency of every five minutes. As a result, the measurements used for monitoring the head displacement of pile T1 are the automatic Leica measurements.

Table 5.1: Remarks during the test on pile T1

Relevant period		Remark
Time	Step	
	refSLT to Step 3	Measurement frequency of the potentiometers was incorrectly set at three minutes. Re-adjusted to five seconds
	End Step 5	Potentiometer on the telltale got jammed within the transition piece. Lowered 25mm to prevent the problem occurring again. Data has been adjusted to account for this by assuming linear-elastic response of the pile over these loads.
	1900kN	Half step was included at the end of step because creep was around 1.2 mm. Creep < 0.75mm in subsequent step.
23:46	2475kN	Full step to 2475kN was taken due to time and recalculation of pile capacity, creep = 1.75mm
23:50	2475kN	Concern with the ultimate capacity of the test frame due to gap occurring between the frame and footing.
00:08	Step 15	No relaxation phase included due to time constraints.
00:37	Reload(1)	Pump could not reach to 2670kN due to rapid settlement of pile
00:55	Unload(1)	Had to stop potentiometers due to lack of clearance. Leica system continued running
Entire test		Original potentiometer readings on the pile head were missing due to corrupted memory card.

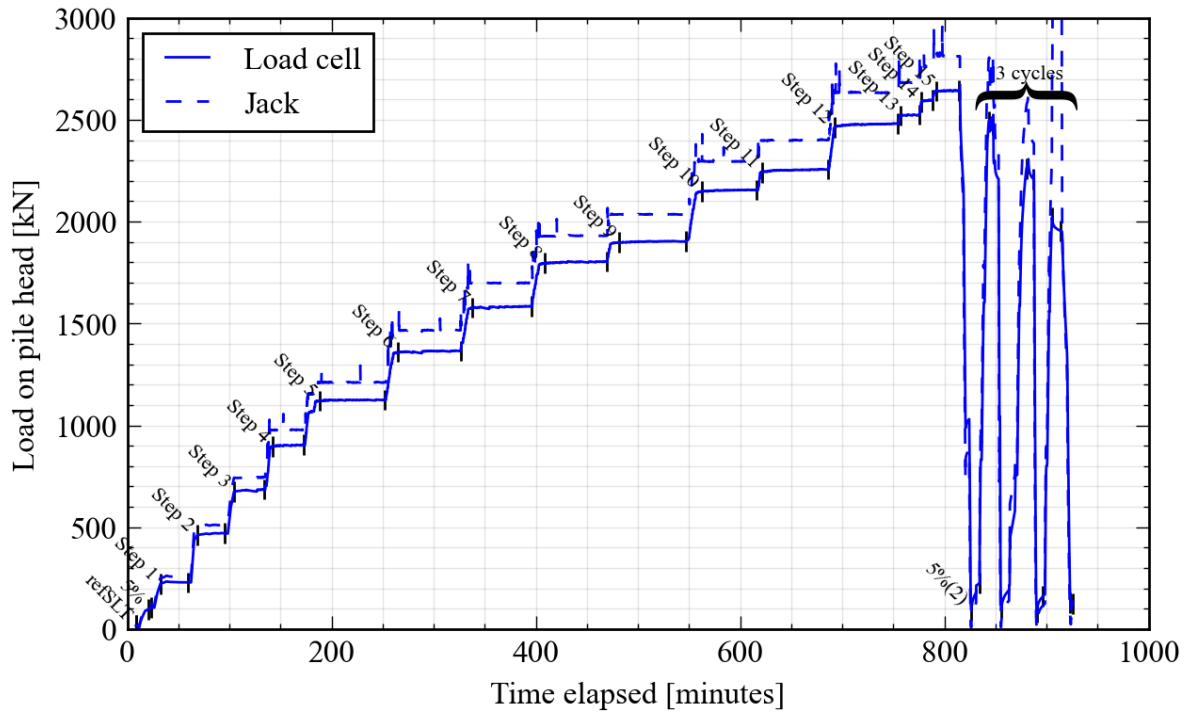


Figure 5.1: Plot of load exerted on pile head against the time elapsed for T1. The load given by the jack have been derived from the measured hydraulic pressure

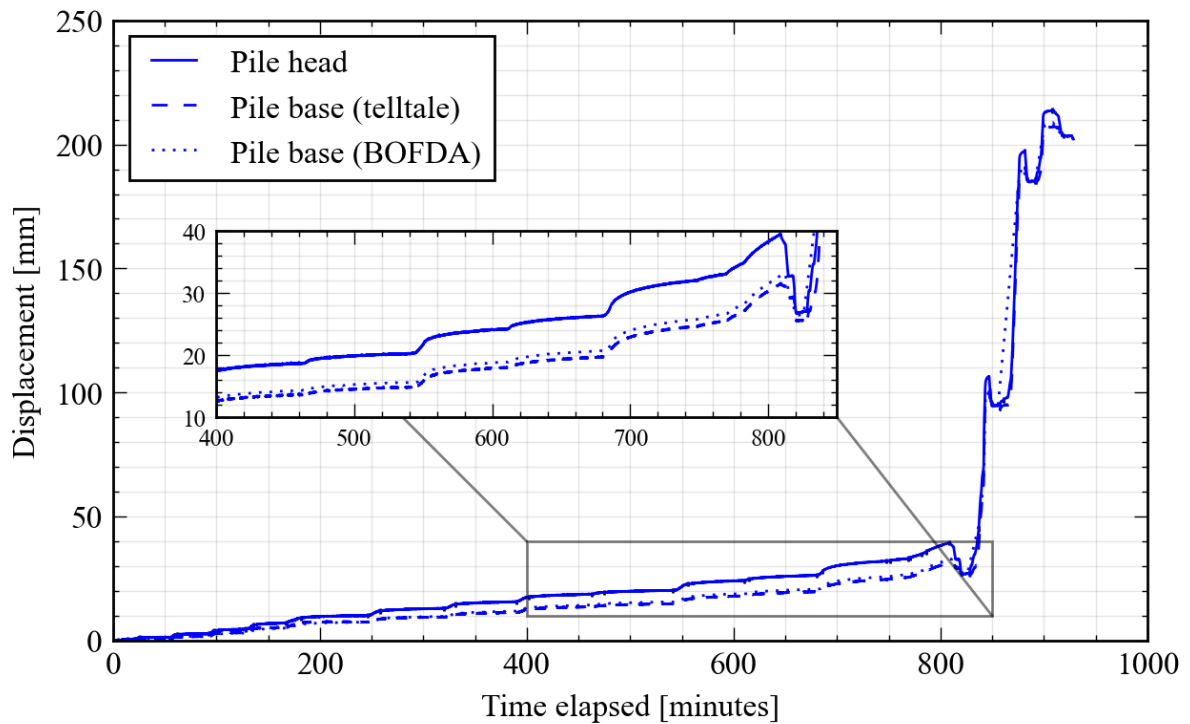


Figure 5.2: Plot of measured displacement at the pile head against the time elapsed for T1. The levelling station measurements have been used

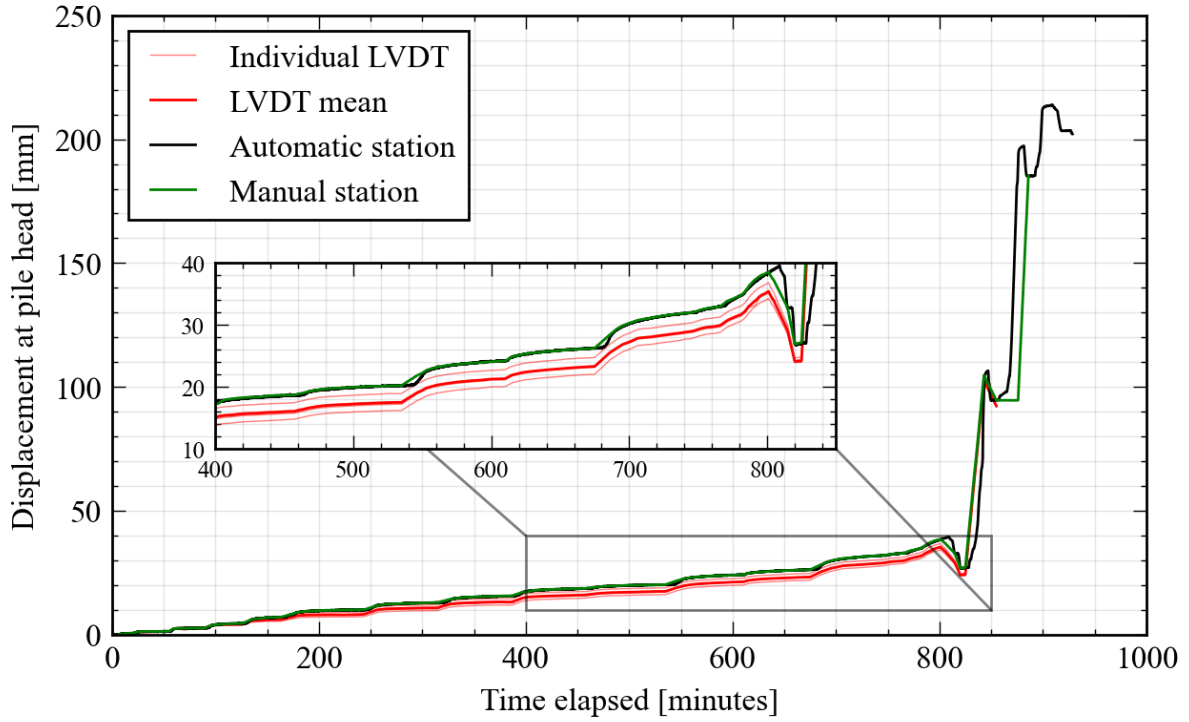


Figure 5.3: All pile head displacement readings for pile T1

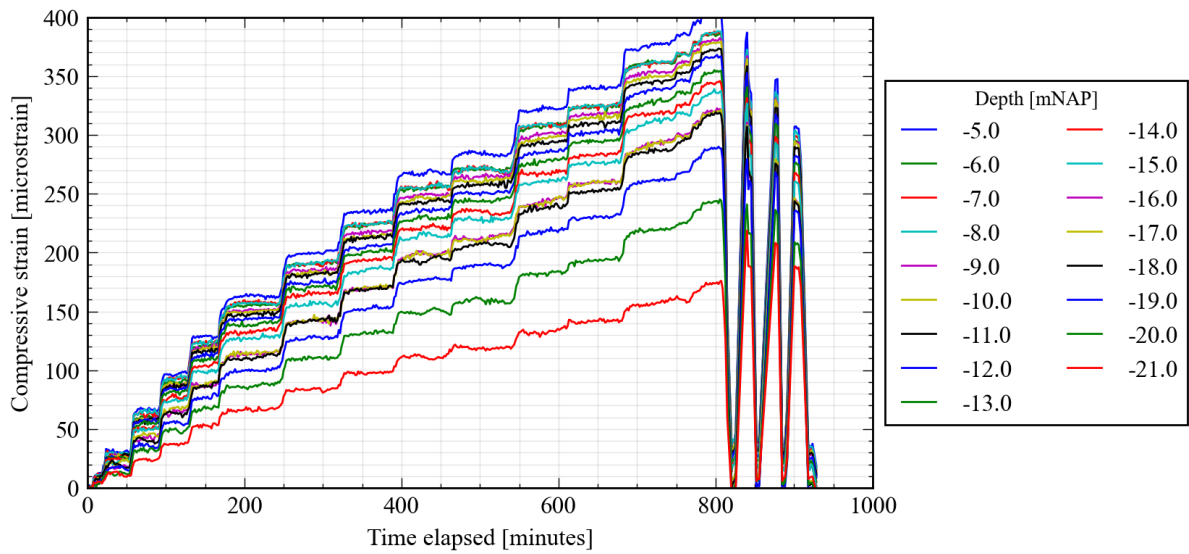


Figure 5.4: Plot of average strain along all measurement axes versus time for selected BOFDA increments for T1

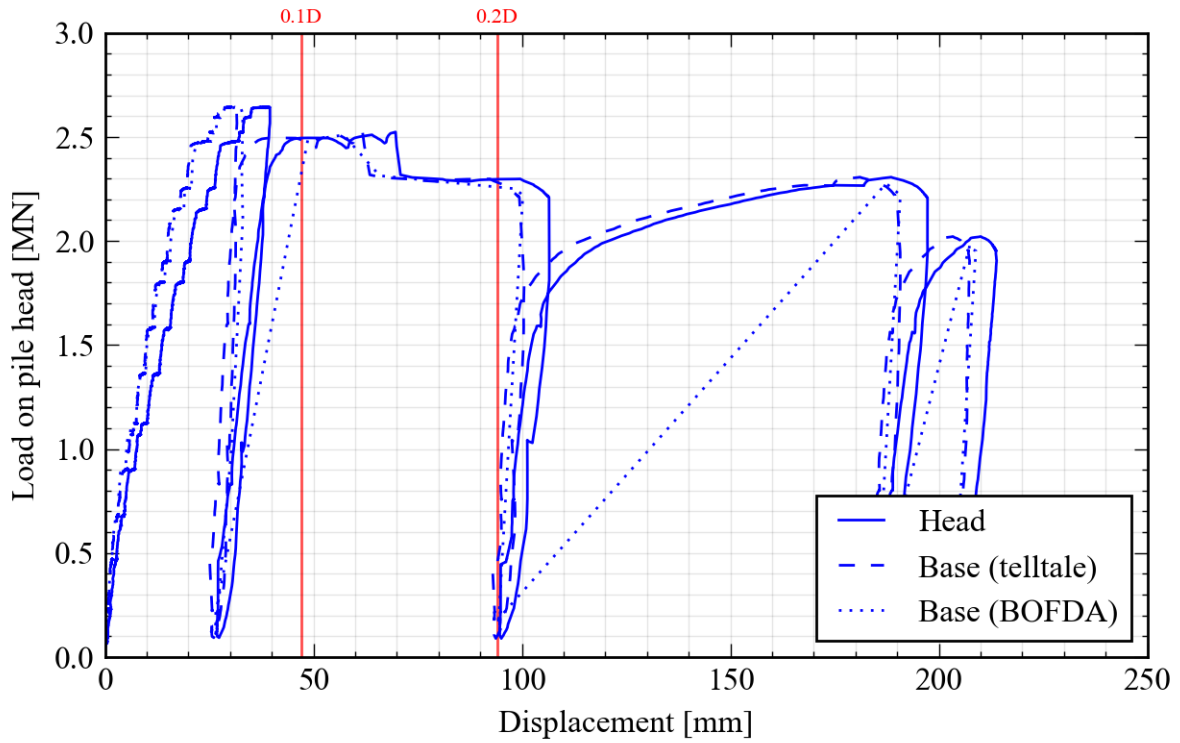


Figure 5.5: Plot of load versus displacement for T1

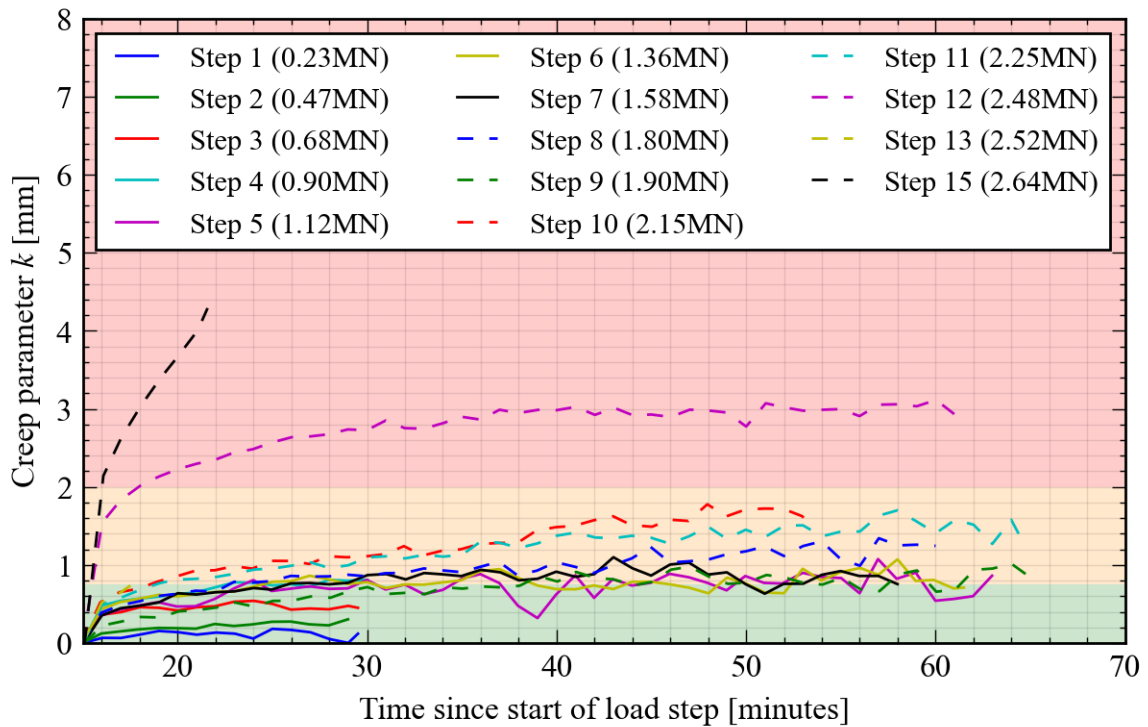


Figure 5.6: Creep parameter versus time across selected load steps for T1. The thresholds for increasing the step size/duration are also indicated

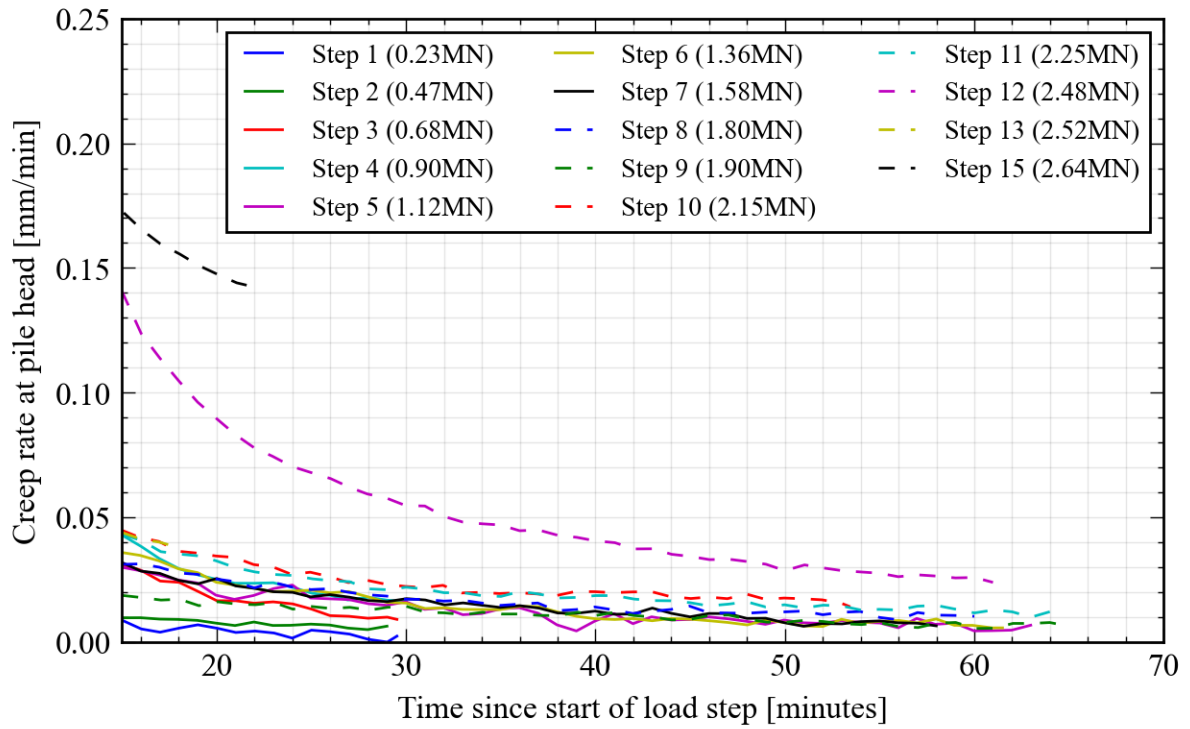


Figure 5.7: Creep rate versus time across selected loading steps for T1

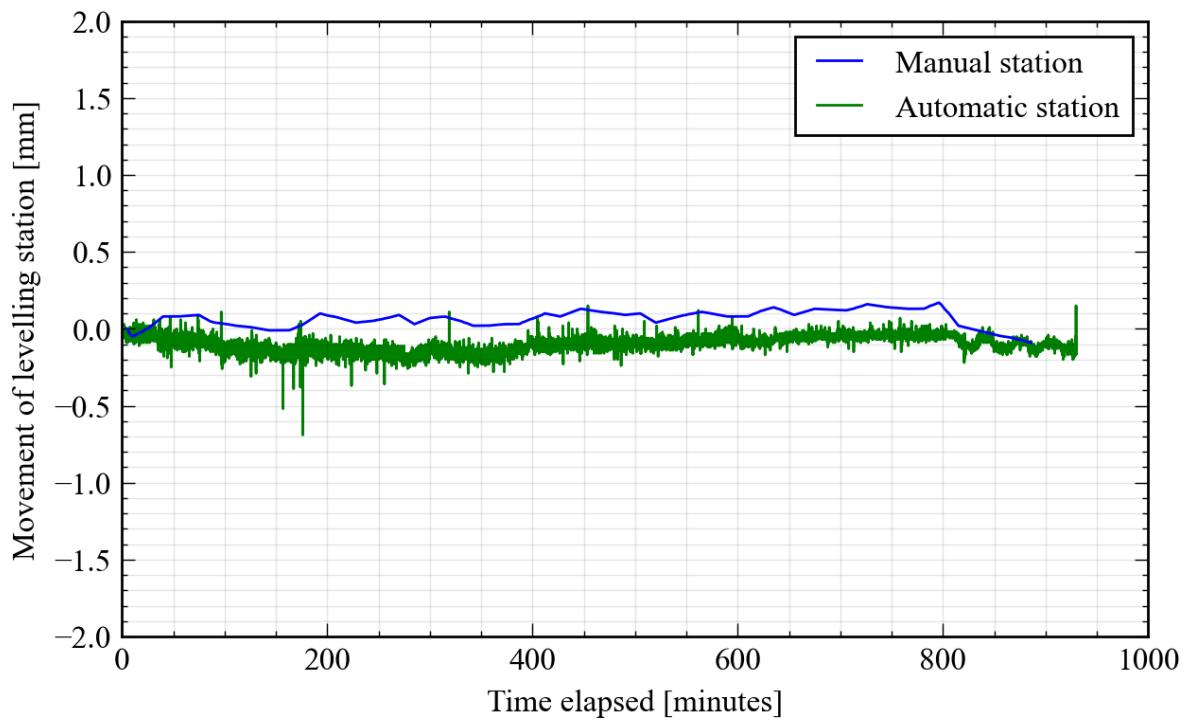


Figure 5.8: Movement of the levelling stations for pile T1, assuming a fixed reference point. Positive sign indicates upward movement

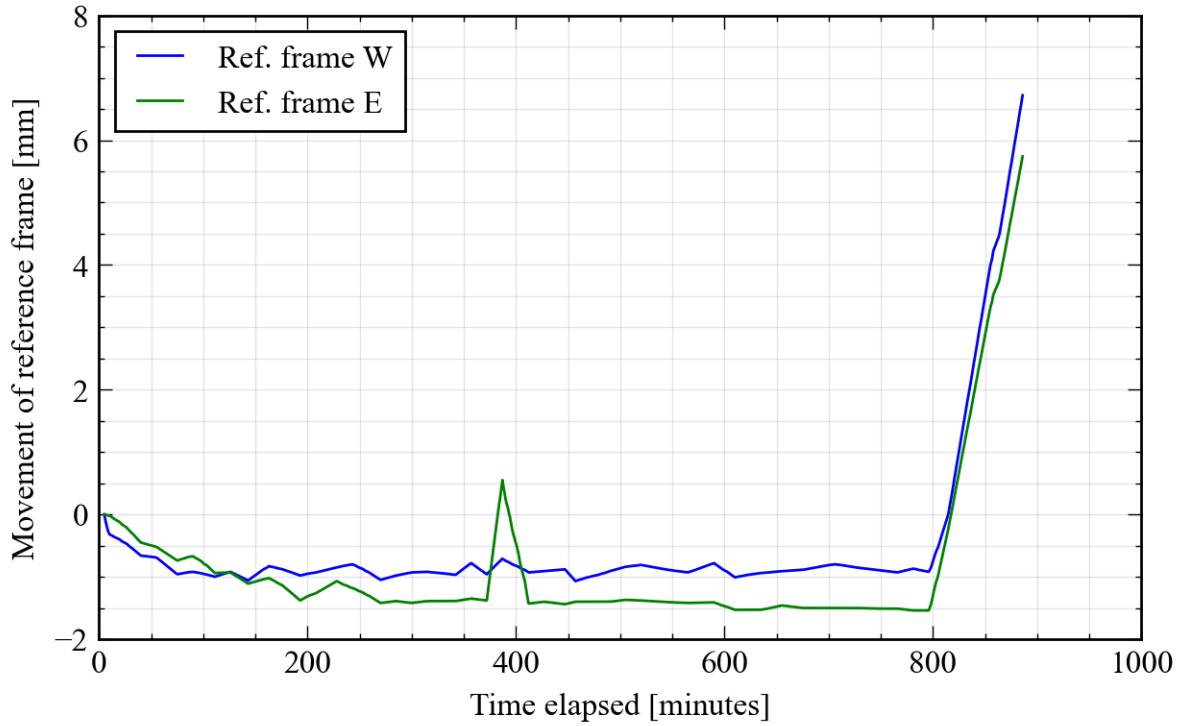


Figure 5.9: Measurements of the reference frame during the test on pile T1. Positive sign indicates upward movement

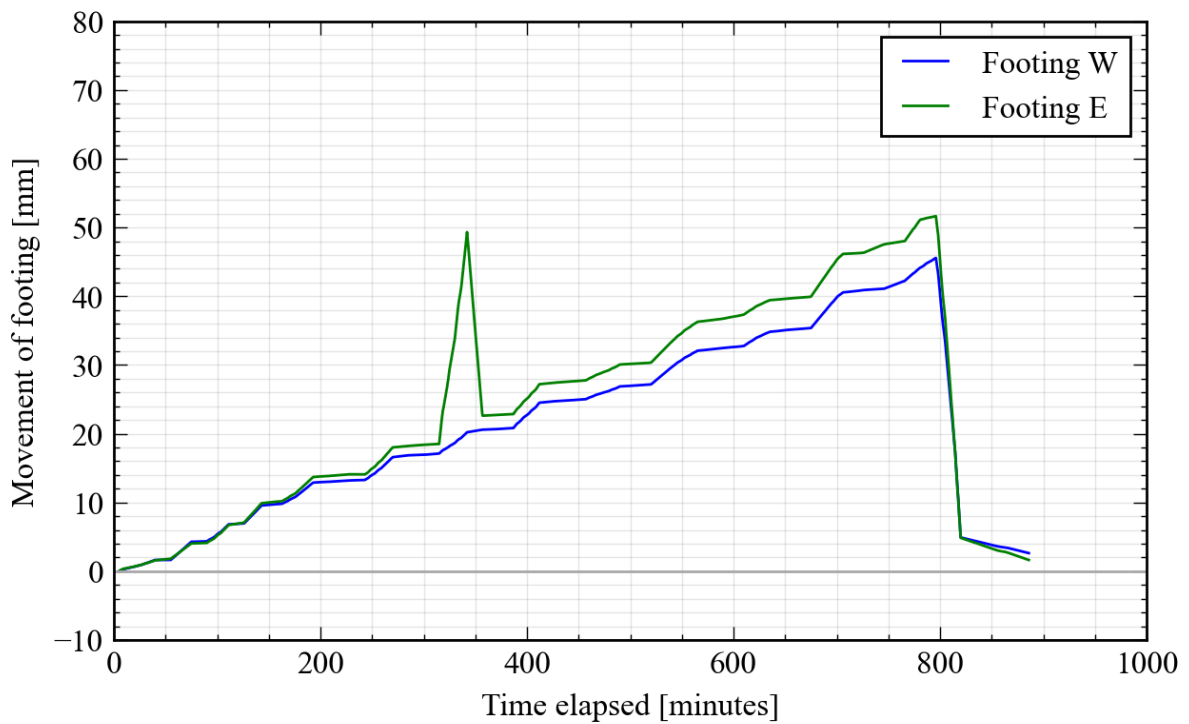


Figure 5.10: Measurements of the test frame footings during the test on pile T1. Positive sign indicates upward movement

Table 5.2: List of load steps and corresponding durations in pile test T1

Step	Start	End	Duration (HH:MM)	Average Load [kN]
refSLT	05/04/2022 10:40	05/04/2022 10:45	00:05	17
5%	05/04/2022 10:54	05/04/2022 11:00	00:06	104
Step 1	05/04/2022 11:06	05/04/2022 11:36	00:30	230
Step 2	05/04/2022 11:42	05/04/2022 12:12	00:30	468
Step 3	05/04/2022 12:18	05/04/2022 12:48	00:30	680
Step 4	05/04/2022 12:56	05/04/2022 13:27	00:31	901
Step 5	05/04/2022 13:42	05/04/2022 14:46	01:04	1124
Step 6	05/04/2022 14:58	05/04/2022 16:00	01:02	1363
Step 7	05/04/2022 16:11	05/04/2022 17:10	00:59	1581
Step 8	05/04/2022 17:22	05/04/2022 18:23	01:01	1801
Step 9	05/04/2022 18:35	05/04/2022 19:41	01:06	1902
Step 10	05/04/2022 19:56	05/04/2022 20:50	00:54	2154
Step 11	05/04/2022 20:55	05/04/2022 22:00	01:05	2253
Step 12	05/04/2022 22:06	05/04/2022 23:08	01:02	2477
Step 13	05/04/2022 23:11	05/04/2022 23:29	00:18	2523
Step 14	05/04/2022 23:31	05/04/2022 23:42	00:11	2594
Step 15	05/04/2022 23:46	06/04/2022 00:08	00:22	2642
5%(2)	06/04/2022 00:20	06/04/2022 00:28	00:08	177
Reload(1)	06/04/2022 00:37	06/04/2022 00:41	00:04	2484
Unload(1)	06/04/2022 00:49	06/04/2022 01:01	00:12	216
Reload(2)	06/04/2022 01:14	06/04/2022 01:21	00:07	2244
Unload(2)	06/04/2022 01:24	06/04/2022 01:31	00:07	138
Reload(3)	06/04/2022 01:39	06/04/2022 01:48	00:09	1969
Unload(3)	06/04/2022 01:57	06/04/2022 01:59	00:02	113

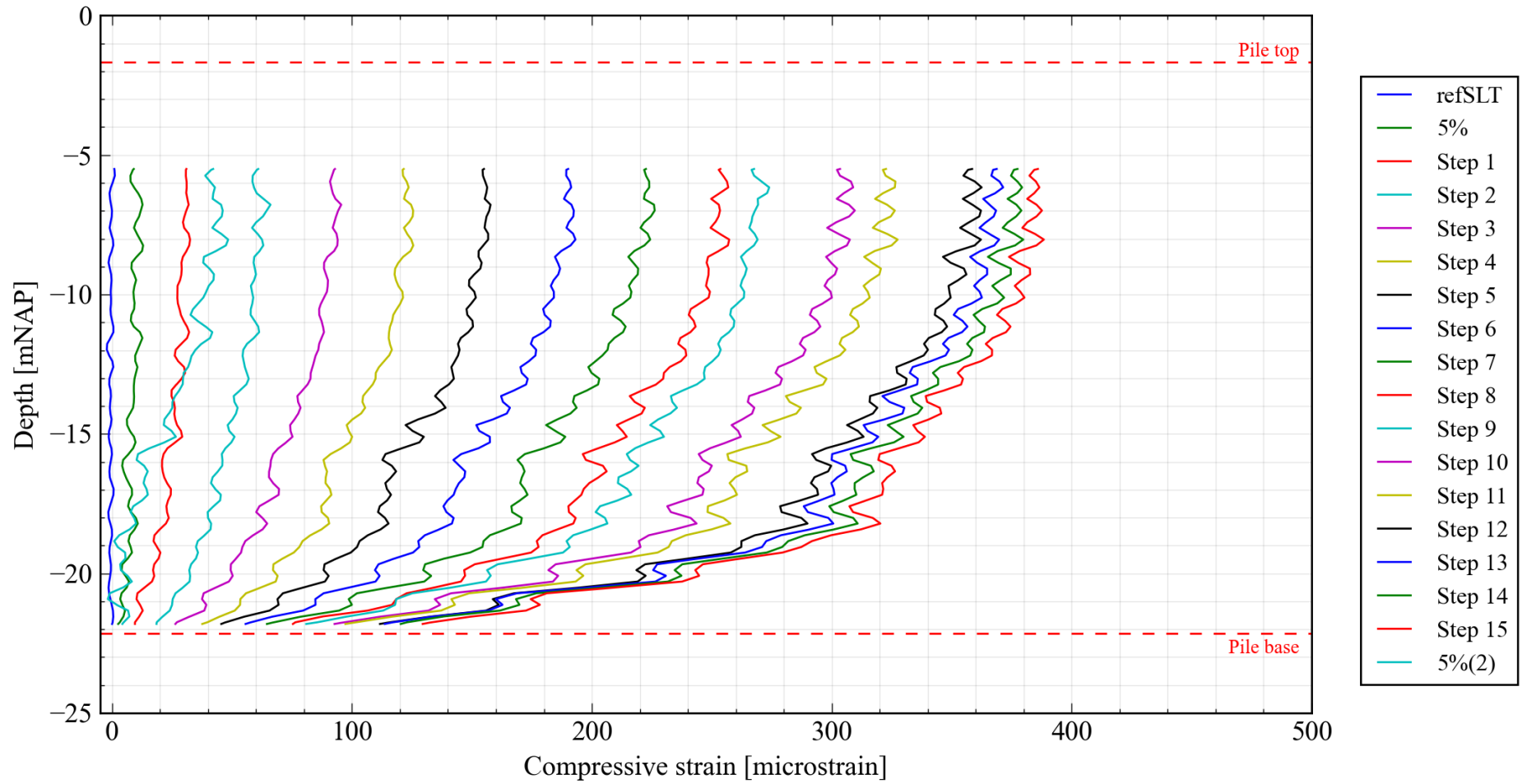


Figure 5.11: Average strain measurements in pile T1 at the end of each load step

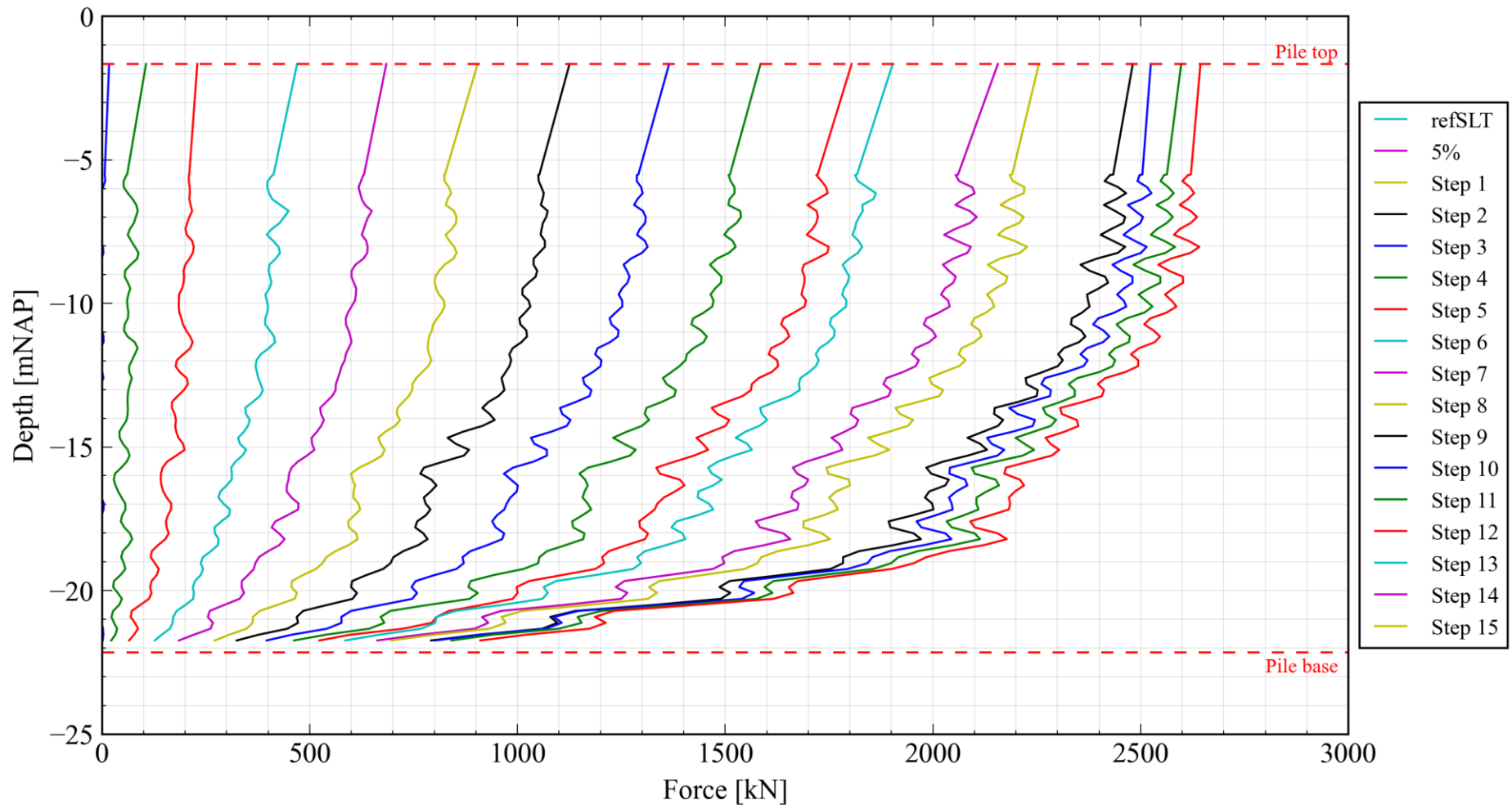


Figure 5.12: Normal force measurements in pile T1 at the end of each load step, including the load measured by the load cell. For more details on strain-to-force conversion, see Section 6.1

5.2. 7th April 2022: Pile F1

Pile F1 was tested on the 7th of April, the second of all piles to be tested. The start of the test was delayed due to difficulties with setting up equipment and existing problems with the storage capacity of the potentiometers. To accommodate for the larger than expected capacity of pile T1, the number of blocks on the test frame was increased from 2900 kN to 3200kN.

Weather conditions at the start of the test were very windy and wet and had a visible effect on the beacons used for the levelling station. To minimise the effect of wind on the reference beacon, the beacon was placed on the leg of a crane 15.6m away from the pile (see Appendix E.4). There were occasional showers throughout the evening, with the wind strength reducing to near zero over the same period.

Two potentiometers (**Figure 5.13**) were added at the pile head as a backup to the existing potentiometers. These were placed at the NW and SE side of the pile and used a separate data logger to that of the existing potentiometers. The additional potentiometers were removed during Step 12 due to insufficient stroke available.

Three short half-steps were implemented for Step 7, Step 9 and Step 11. These allowed for the failure load to be approached carefully, whilst finishing the test within a feasible time range due to the late start. The load was increased by one full increment if the creep rate of the pile was still relatively minimal and the failure criterion of the pile was not expected in that period.

The test concluded after the second unload/reload cycle at 01:55 due to insufficient stroke remaining in the jack. Significant inclination at the pile head could be visibly seen towards the end of the test, with comparatively low displacements exhibited by PM SE and a minor degree of cracking at the north-western side of the pile (**Figure 5.14**). This was partially restrained by the cardboard mould surrounding the pile cap and so it is believed this crack was just superficial in nature.

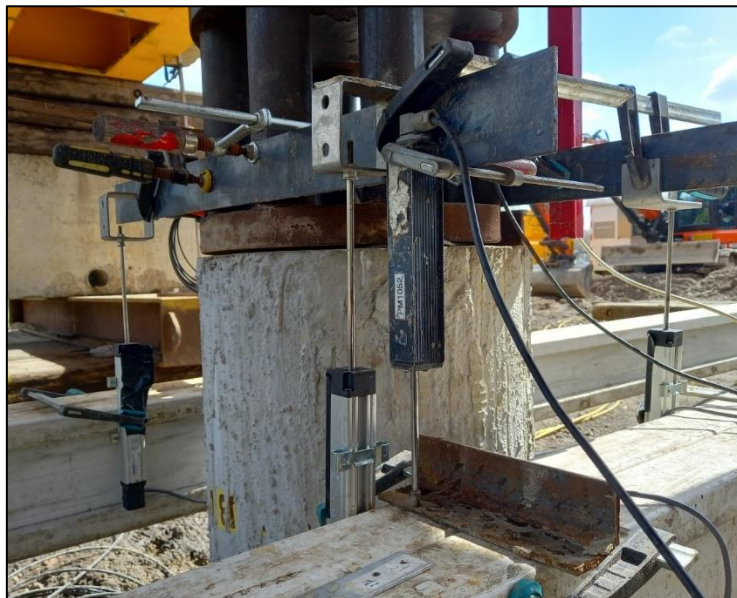


Figure 5.13: Position of additional potentiometer at the north-western side of pile, placed in the opposite direction of the normal potentiometers



Figure 5.14: Cracking in the head of pile F1 on the surface of the pile head, at its north-western side

Table 5.3: Particularities associated with the test on pile F1

Relevant period		Remark
Time	Step	
14:26	5%	PM NW was found not to be responding and was reconfigured. During data processing, the reading from PM NW at 14:26 was set as the average of remaining three potentiometers
23:30	Step 12	Additional potentiometers removed due to lack of available stroke
23:50	Relaxation	Data logger for the potentiometers was paused for three minutes in order to collect the readings
	Unload(1)	Potentiometers re-adjusted to allow for additional stroke

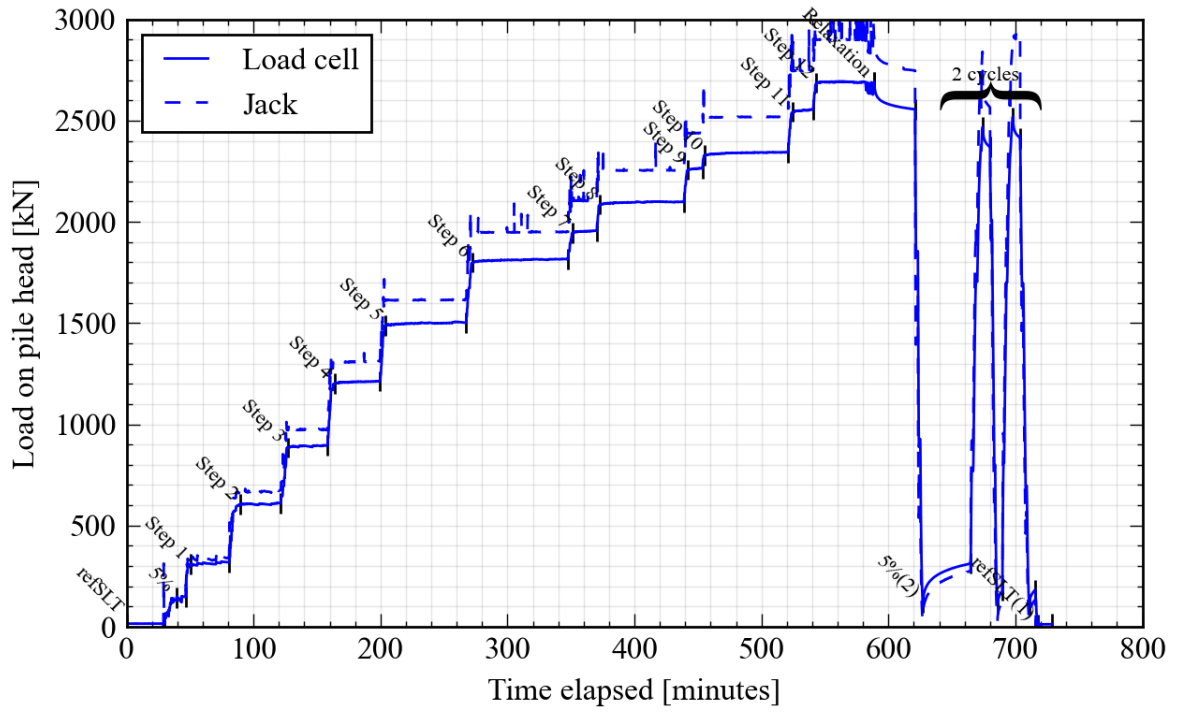


Figure 5.15: Plot of load exerted on pile head against the time elapsed for F1

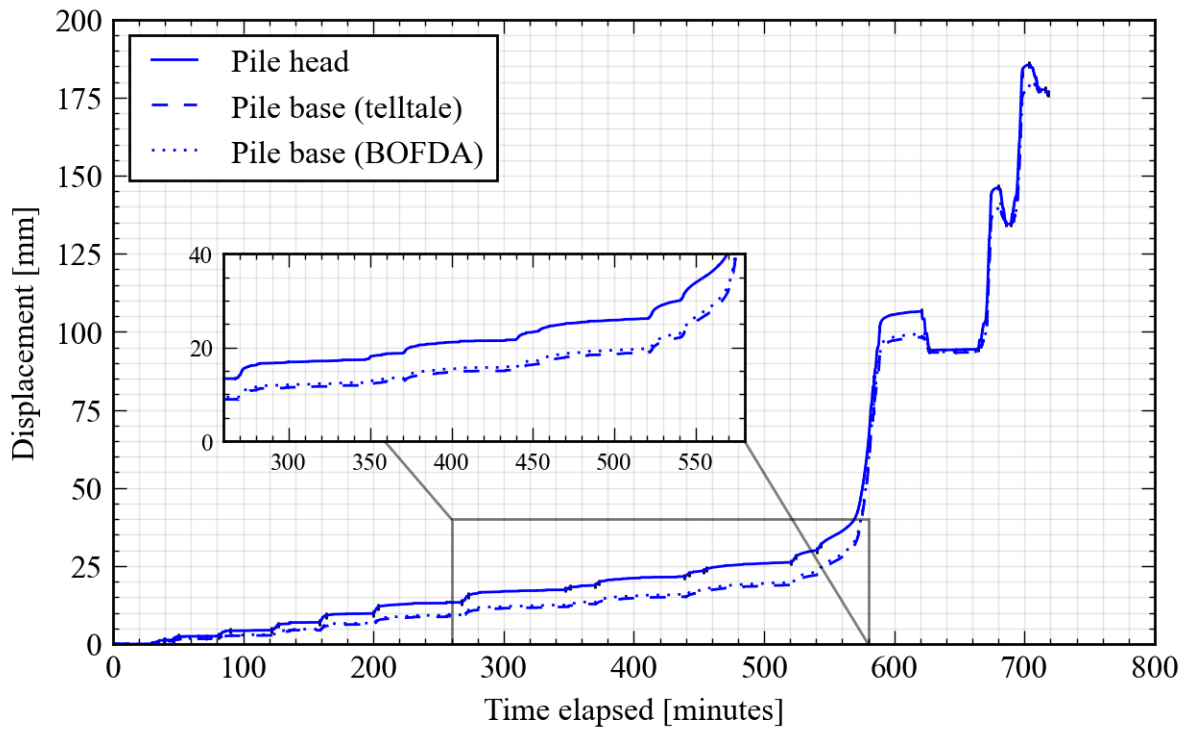


Figure 5.16: Plot of displacement against the time elapsed for F1

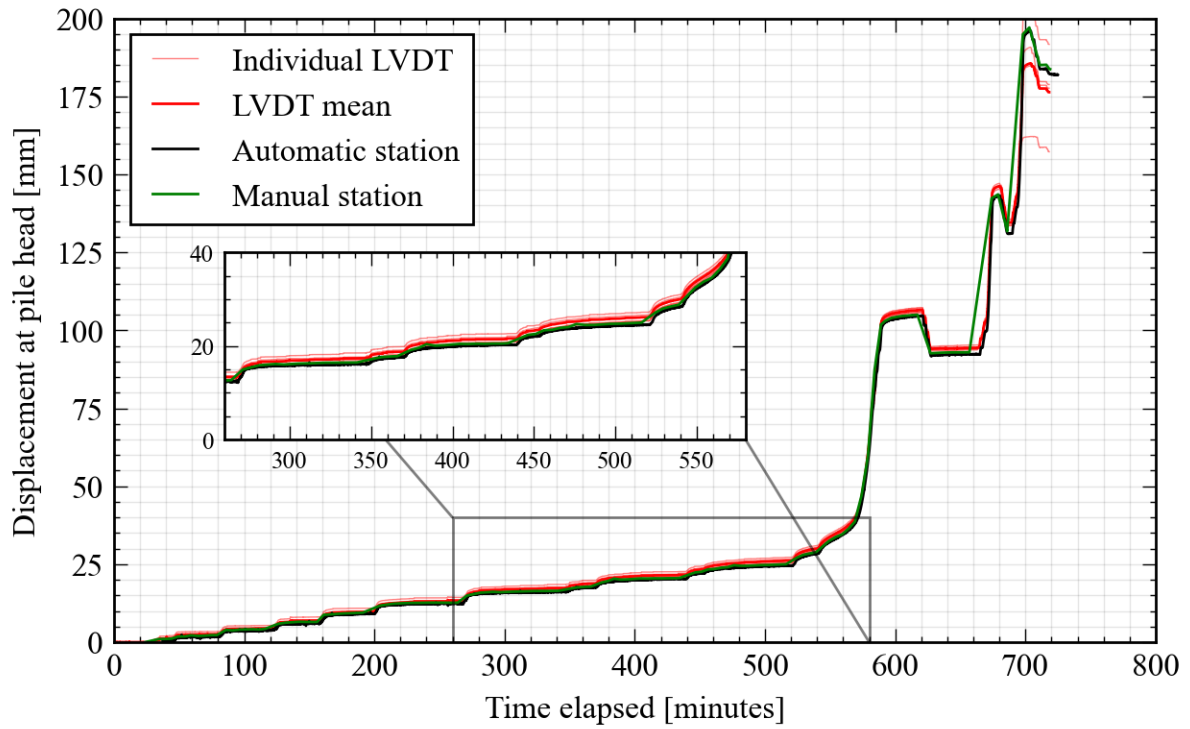


Figure 5.17: All settlement at pile head readings for pile F1

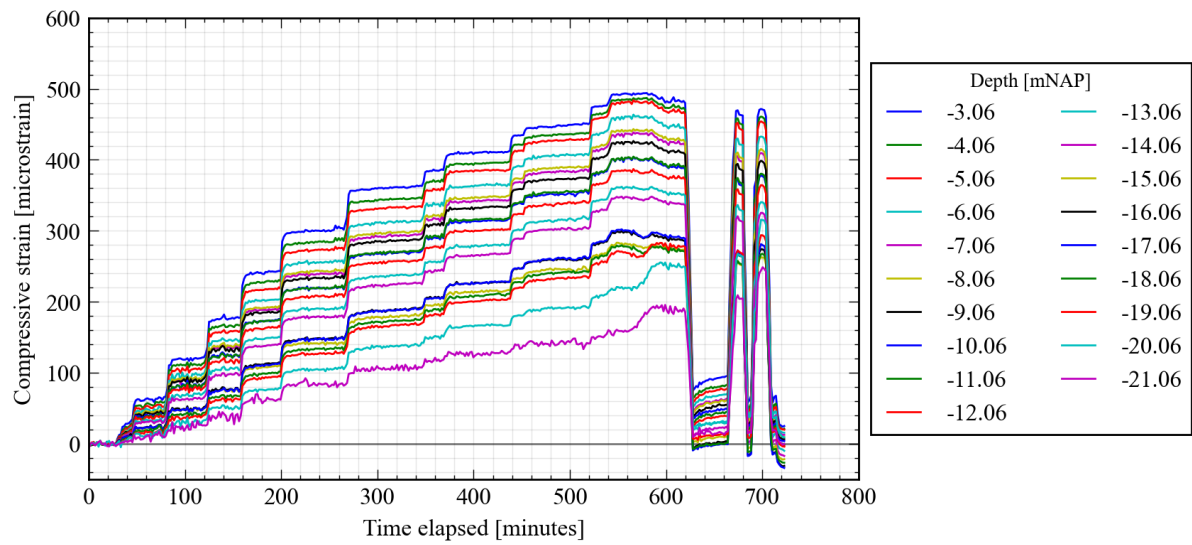


Figure 5.18: Plot of strain versus time for selected BOFDA increments for pile F1

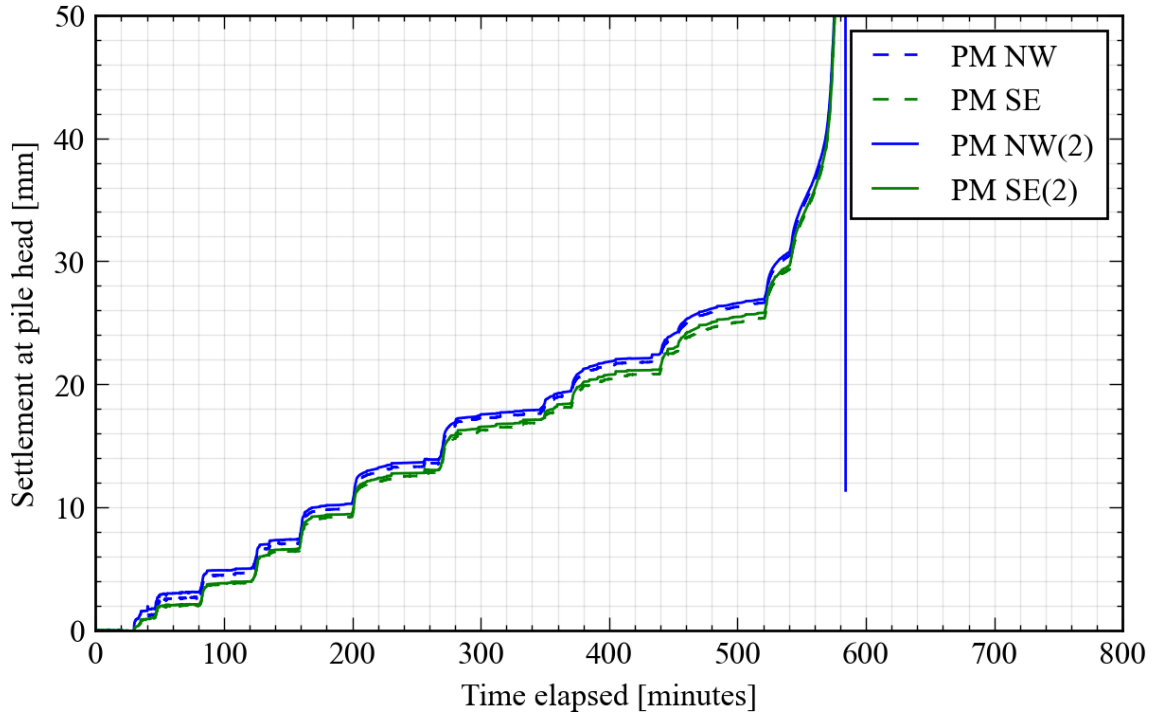


Figure 5.19: Comparison of the original potentiometers PM NW and PM SE to the additional potentiometers PM NW(2) and PM SE(2) used for pile F1. Good agreement between the potentiometers was exhibited

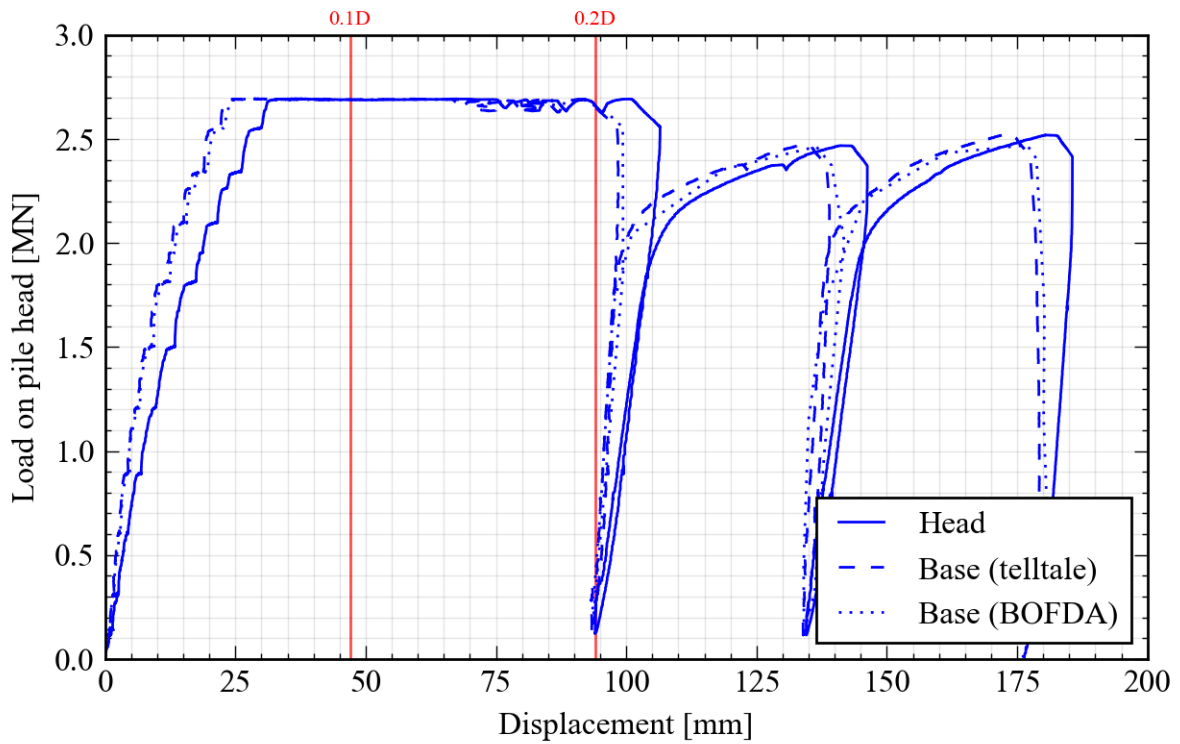


Figure 5.20: Plot of load versus displacement for F1

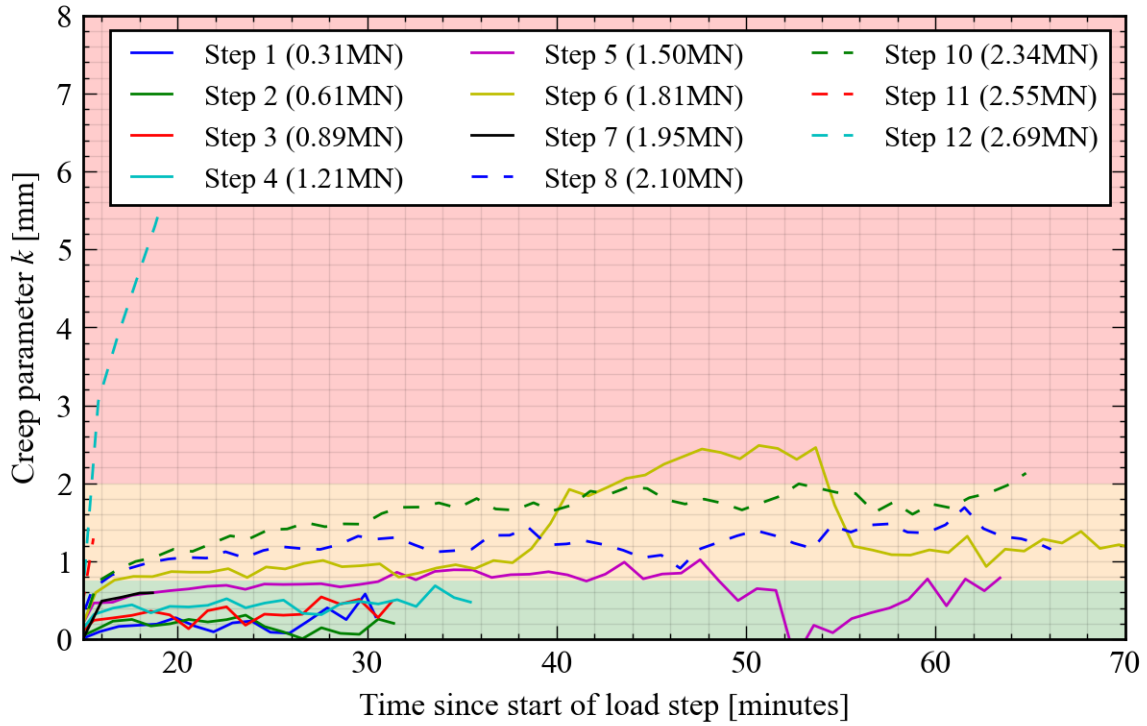


Figure 5.21: Creep parameter versus time across selected load steps for F1. The thresholds for increasing the step size/duration are also indicated

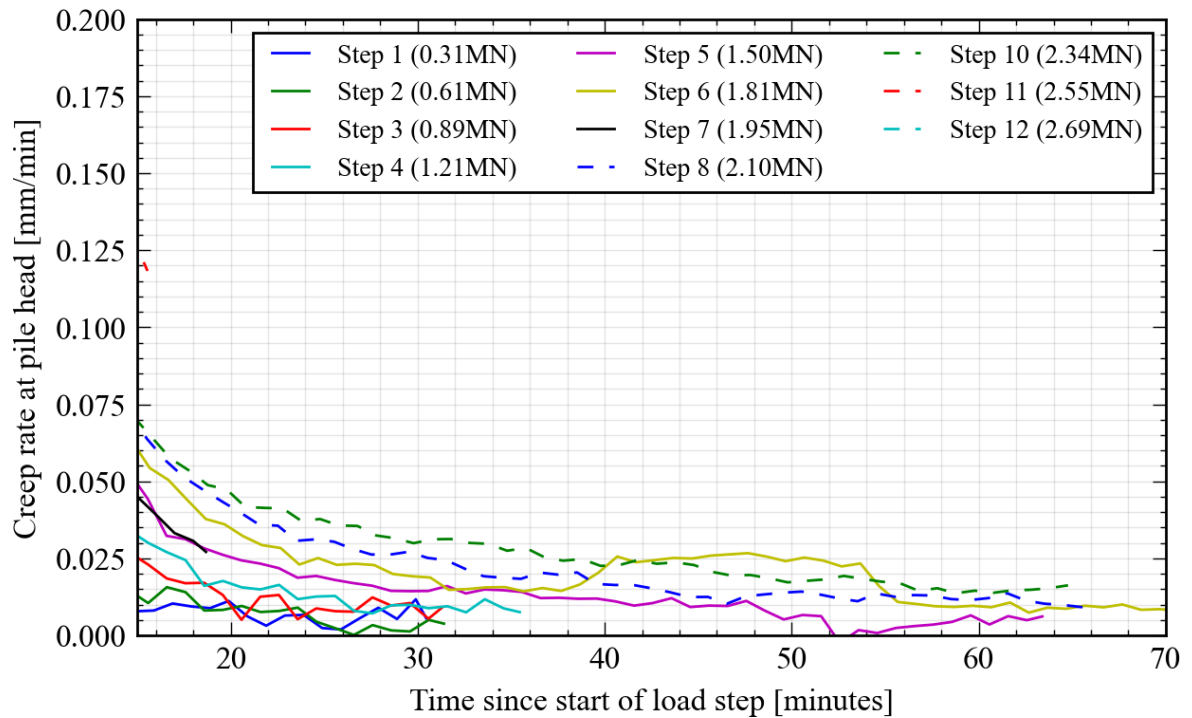


Figure 5.22: Creep rate versus time across selected loading steps for F1

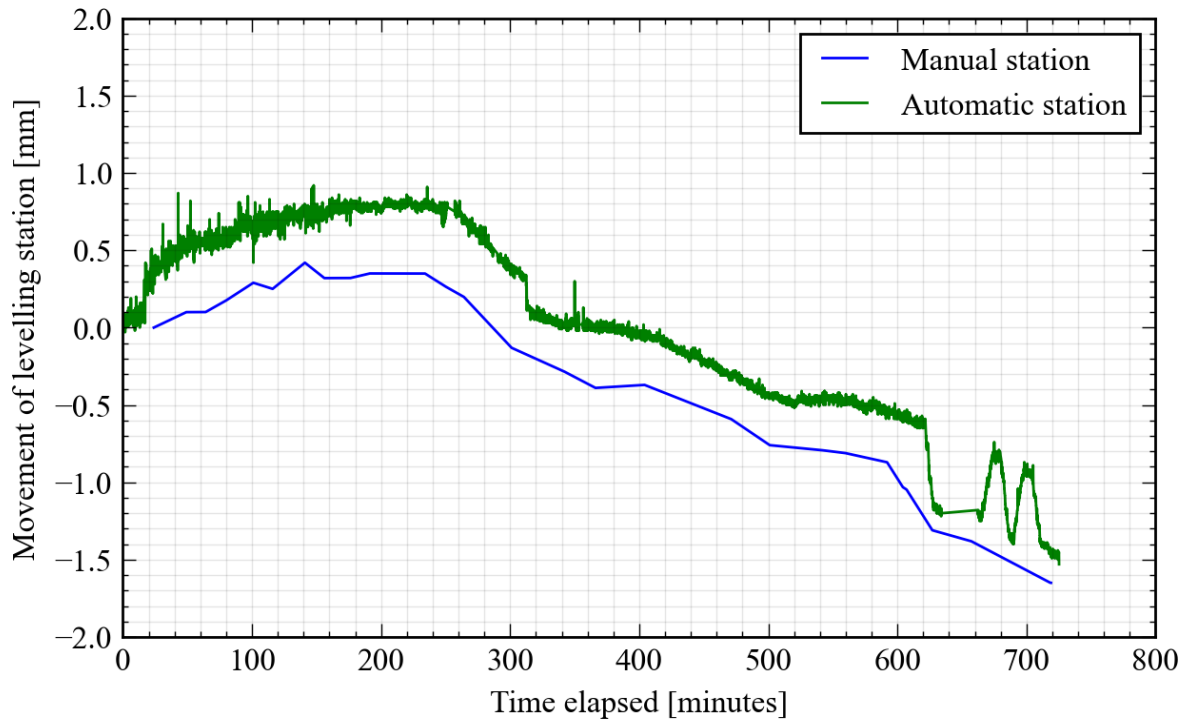


Figure 5.23: Movement of the levelling stations for pile F1, assuming a fixed reference point. Positive sign indicates upward movement

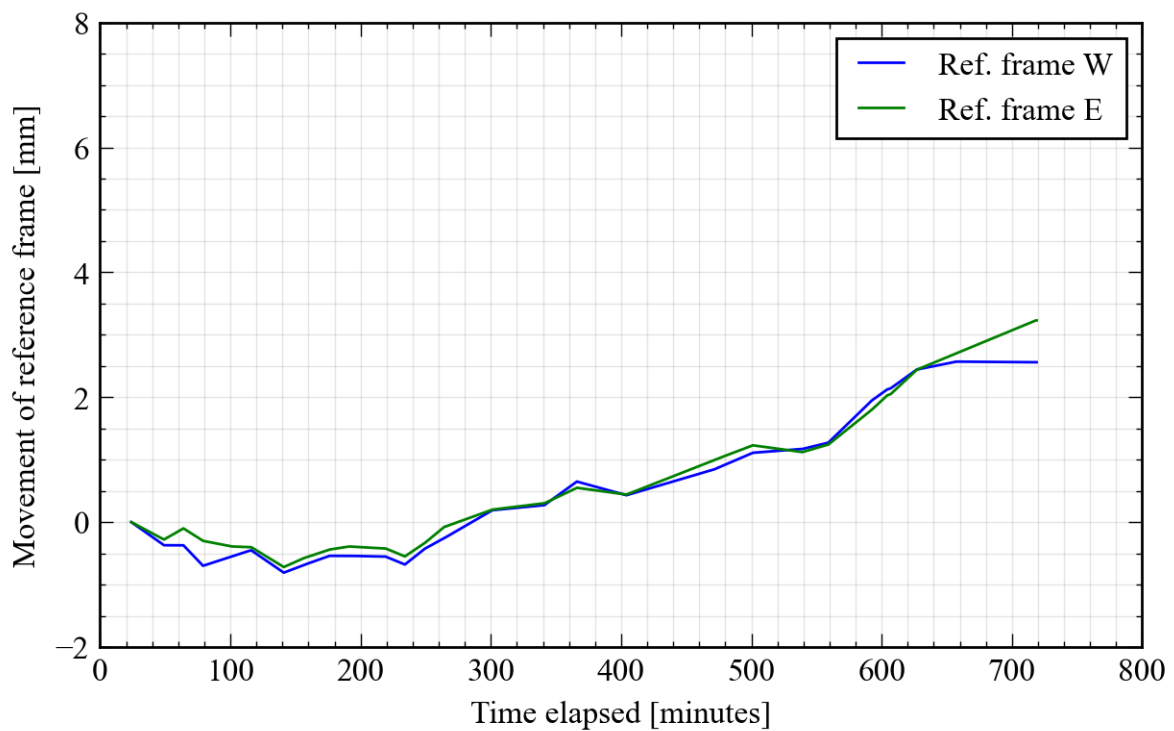


Figure 5.24: Measurements of the reference frame during the test on pile F1

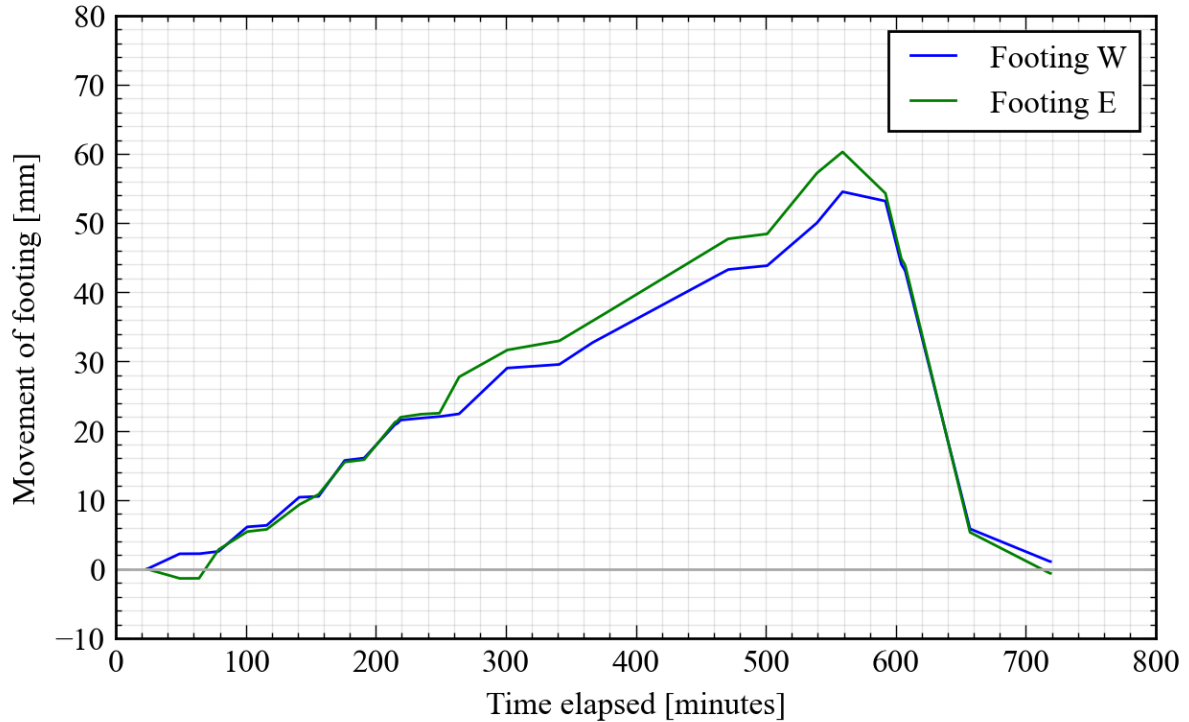


Figure 5.25: Measurements of the test frame footings during the test on pile F1. Positive sign indicates upward movement

Table 5.4: List of load steps and corresponding durations in pile test F1

Step	Start	End	Duration (HH:MM)	Average Load [kN]
refSLT	07/04/2022 13:46:00	07/04/2022 14:15:44	00:29	16
5%	07/04/2022 14:25:19	07/04/2022 14:32:30	00:07	143
Step 1	07/04/2022 14:36:12	07/04/2022 15:07:06	00:30	313
Step 2	07/04/2022 15:15:49	07/04/2022 15:47:37	00:31	607
Step 3	07/04/2022 15:52:50	07/04/2022 16:24:23	00:31	892
Step 4	07/04/2022 16:29:49	07/04/2022 17:05:43	00:35	1209
Step 5	07/04/2022 17:09:51	07/04/2022 18:13:38	01:03	1499
Step 6	07/04/2022 18:18:39	07/04/2022 19:33:44	01:15	1812
Step 7	07/04/2022 19:37:00	07/04/2022 19:56:21	00:19	1953
Step 8	07/04/2022 19:58:57	07/04/2022 21:05:07	01:06	2096
Step 9	07/04/2022 21:08:23	07/04/2022 21:19:42	00:11	2262
Step 10	07/04/2022 21:21:26	07/04/2022 22:26:58	01:05	2340
Step 11	07/04/2022 22:30:39	07/04/2022 22:46:45	00:16	2550
Step 12	07/04/2022 22:49:22	07/04/2022 23:34:50	00:45	2686
Relaxation	07/04/2022 23:34:50	08/04/2022 00:07:02	00:32	2580
5%(2)	08/04/2022 00:13:08	08/04/2022 00:50:45	00:37	267
Reload(1)	08/04/2022 01:00:21	08/04/2022 01:06:00	00:05	2394
Unload(1)	08/04/2022 01:12:06	08/04/2022 01:15:48	00:03	156
Reload(2)	08/04/2022 01:24:04	08/04/2022 01:29:44	00:05	2439
Unload(2)	08/04/2022 01:36:55	08/04/2022 01:41:42	00:04	160
refSLT(1)	08/04/2022 01:43:27	08/04/2022 01:54:59	00:11	12

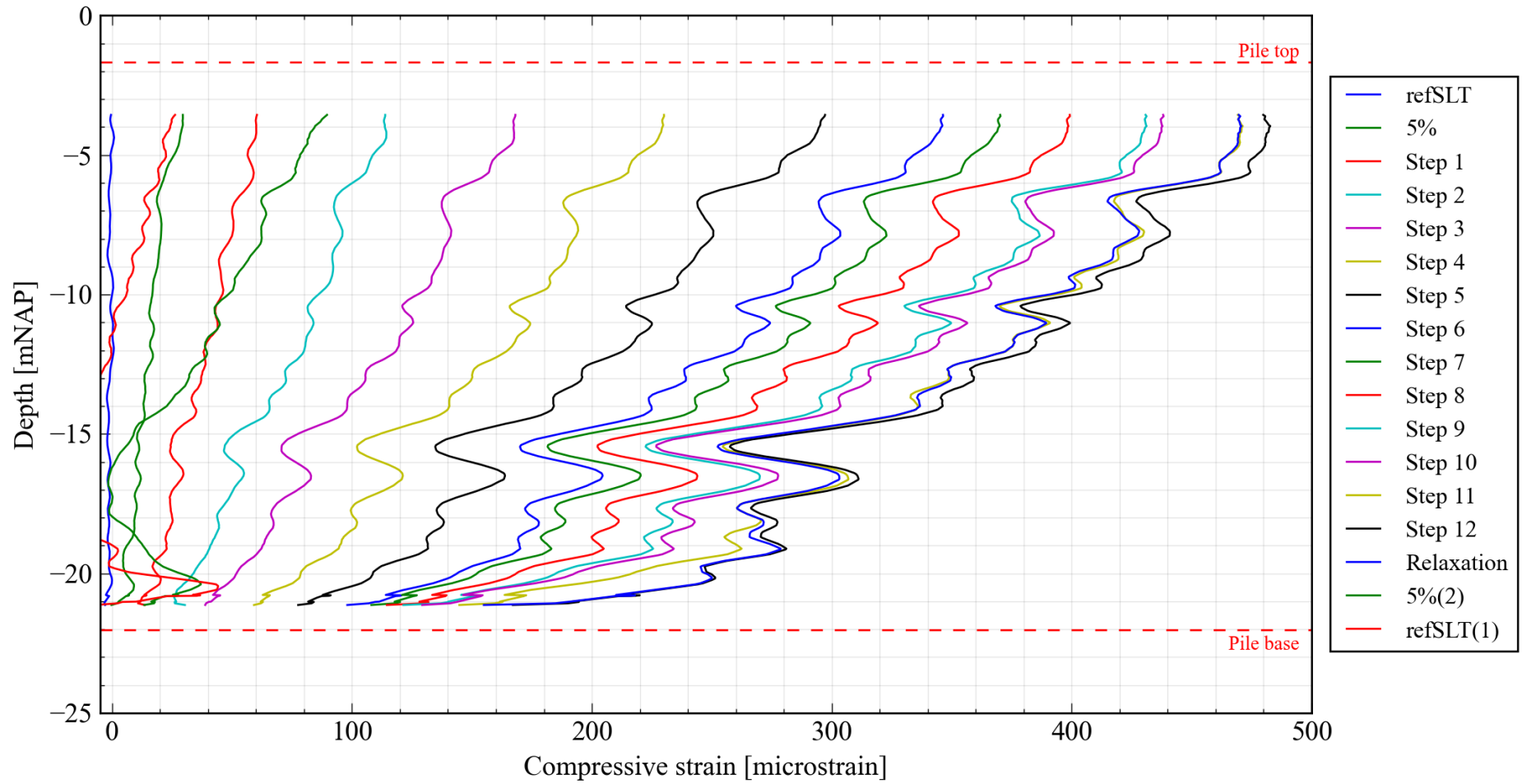


Figure 5.26: Strain measurements in pile F1 over the course of the load test

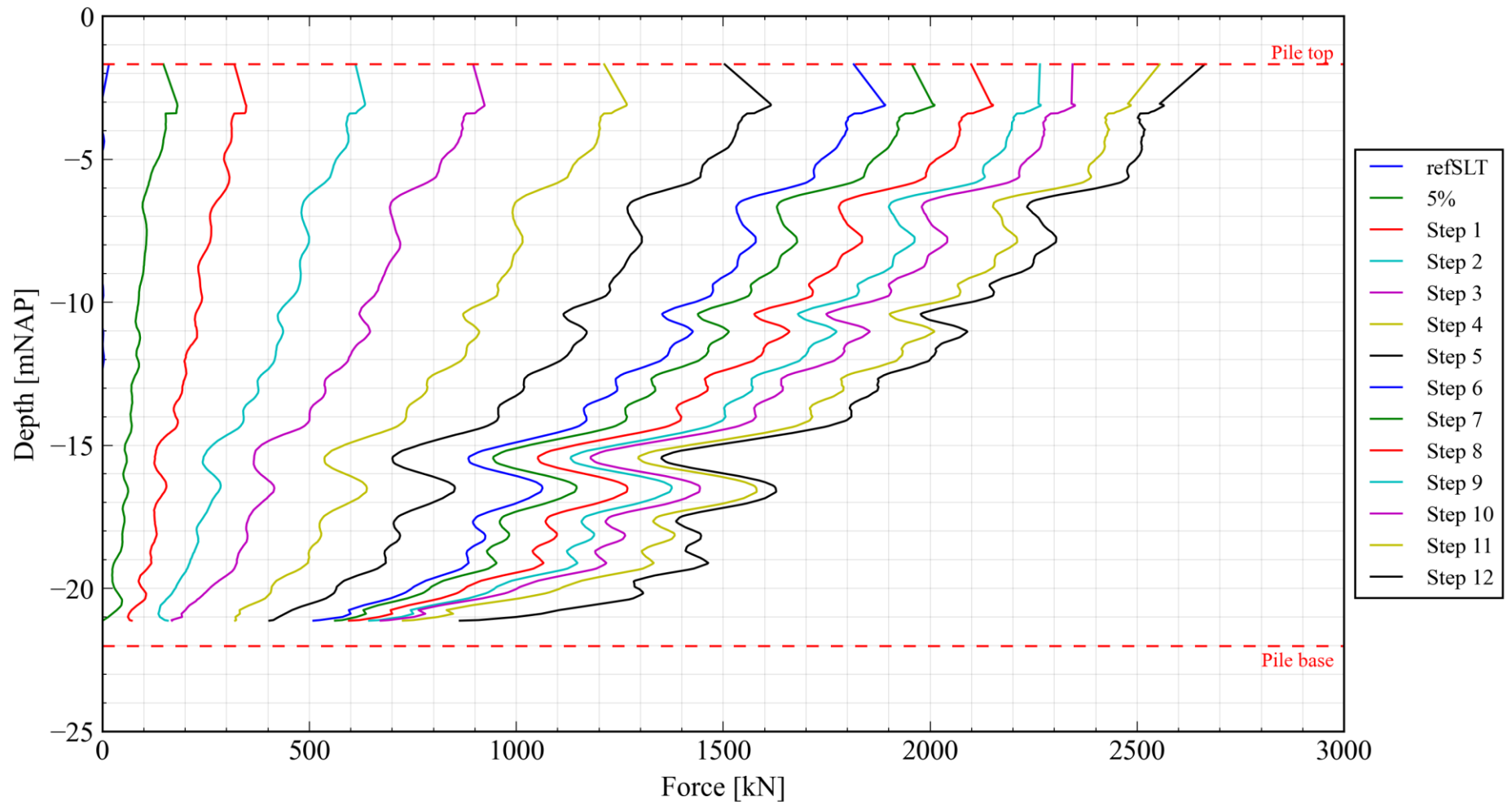


Figure 5.27: Normal force measurements in pile F1 at the end of each load step, including the load measured by the load cell. For more details on strain-to-force conversion, see Section 6.1

5.3. 9th April 2022: Pile T2

Pile T2 was tested on the 9th of April, the third of all piles to be tested. Weather conditions were sunny and calm, but relatively cold, with a couple of showers over the course of the day.

In contrast to previous tests, the telltale potentiometer was placed upside-down with the tip placed underneath the topside of the transition piece (**Figure 5.28**). This was done because the potentiometer tip could not be placed directly on the pile head itself because of the lead plate getting in the way and potentially affecting the readings during the test.

Before the start of the test, PM SE found not to working because of an issue with its internal parts. This was replaced by another potentiometer, albeit one with a smaller stroke. An additional potentiometer (PM NW(2)) was also used as a supplementary measurement.

Failure of the pile occurred very suddenly, with the jack struggling to follow the rapidly displacing pile. Once a stable condition was reached, the pile was unloaded back to 5%. After this point, full unload/reload cycles were attempted to the failure capacity but this capacity could not be reached again. The potentiometers at the pile head were removed during these cycles because of the lack of clearance available between the steel strip and the reference frame, although the levelling stations continued to record during this period.

Based on the interpretation of the load distributions (**Figure 5.41**, Section 6.2), it was later found that structural failure in the grout shell in the lower sand layer, manifesting in a loss of load transfer to the lower sand layer during subsequent reloading cycles.

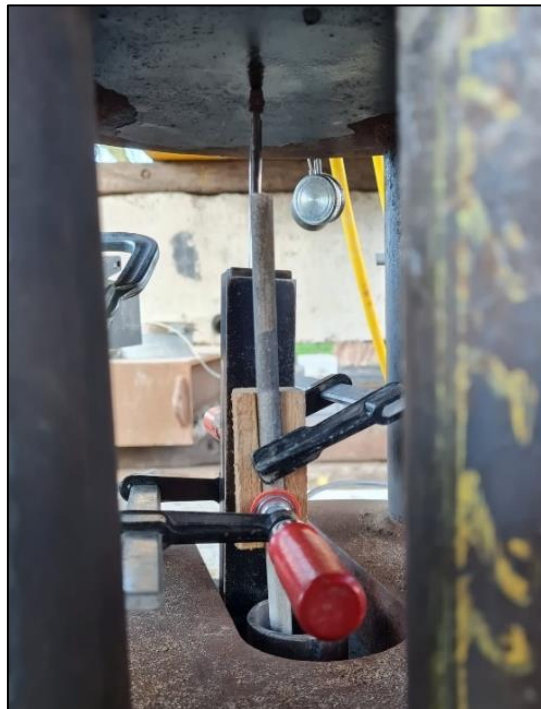


Figure 5.28: Placement of the telltale potentiometer for pile T2. The platen is touching the top side of the transition piece



Figure 5.29: Northern-western side of pile T2, with additional potentiometers on the south-eastern side (left) and north-western sides (right)

Table 5.5: Particularities associated with the test on pile F1

Relevant period		Remark
Time	Step	
	Step 3 -> Step 4	Laptop crashed during loading to Step 4. Further loading paused whilst laptop rebooted.
19:54	5%(2)	Potentiometers removed to due to insufficient room available to allow for displacement during unload/reload cycles
20:10	5%(2)	Settlement beacon on the pile readjusted by 10cm prior to unload/reload cycles

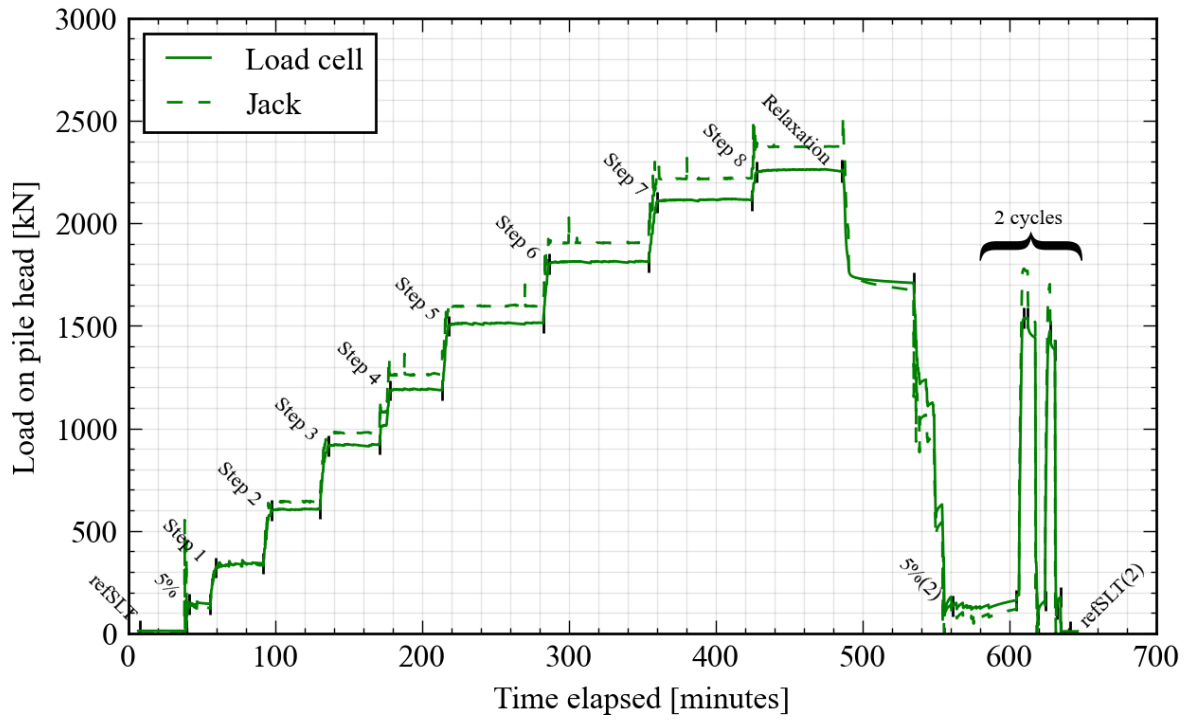


Figure 5.30: Plot of load exerted on pile head against the time elapsed for T2

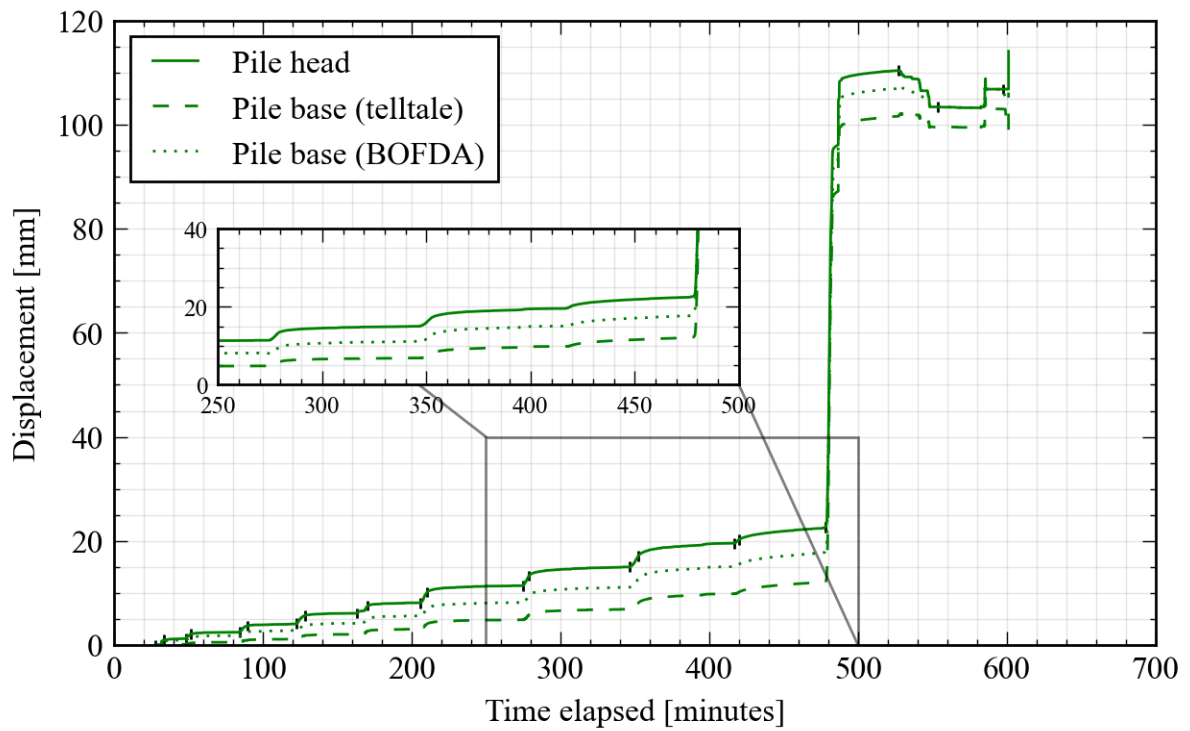


Figure 5.31: Plot of settlement measured at the pile head against the time elapsed for T2

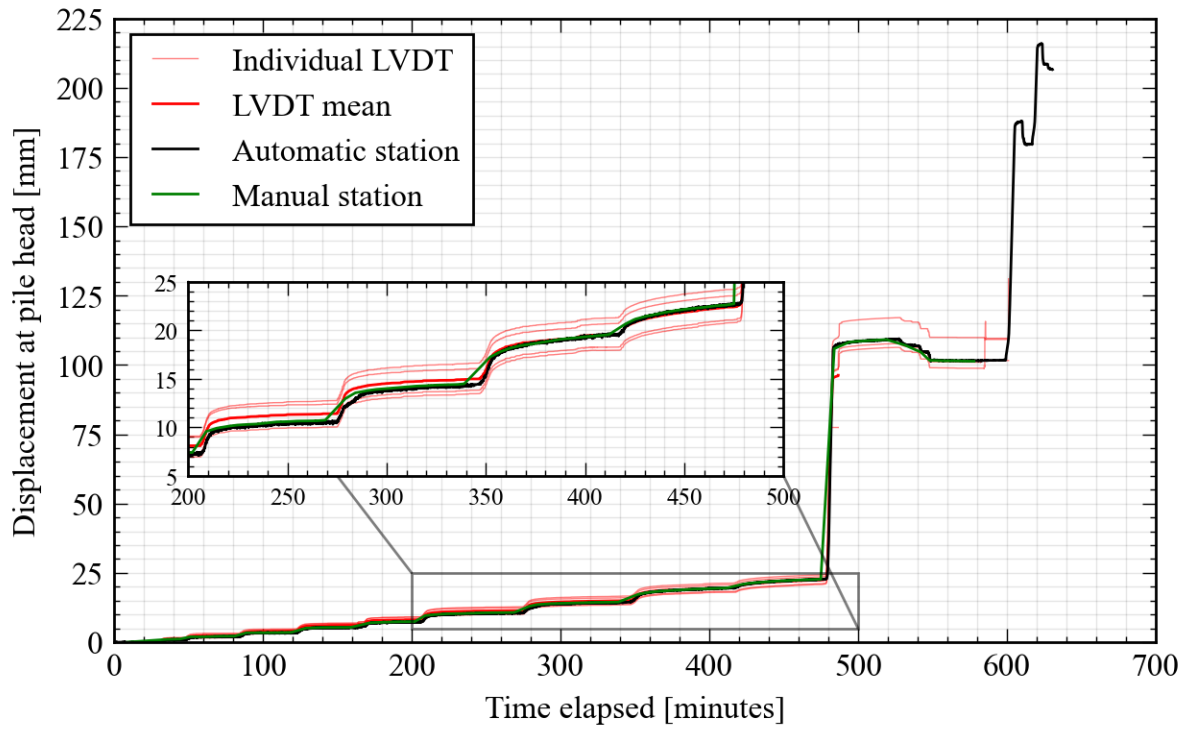


Figure 5.32: All settlement at pile head readings for pile T2

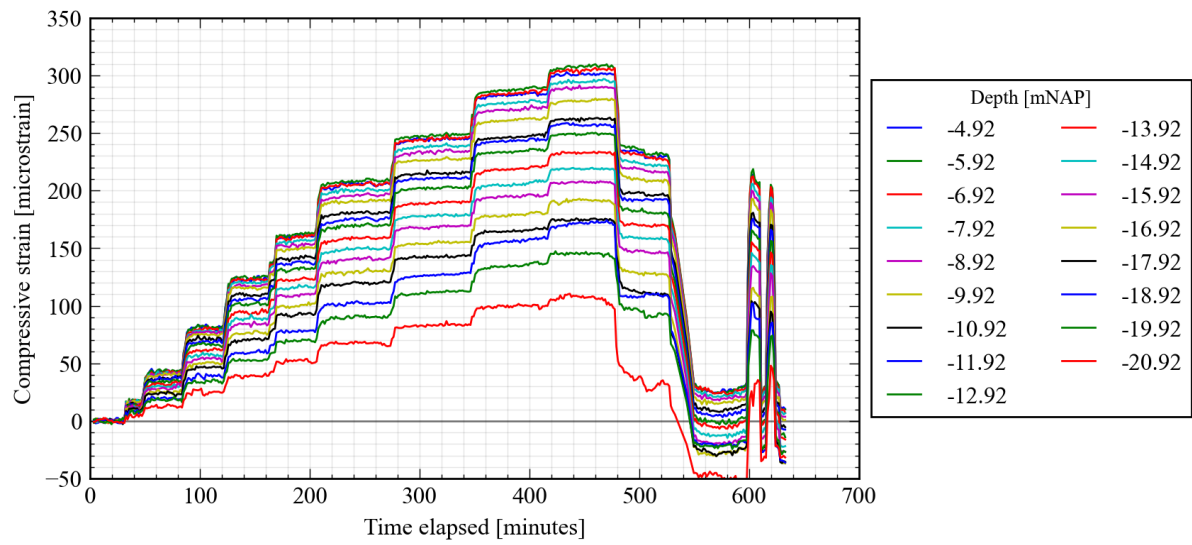


Figure 5.33: Plot of strain versus time for selected BOFDA increments for T2

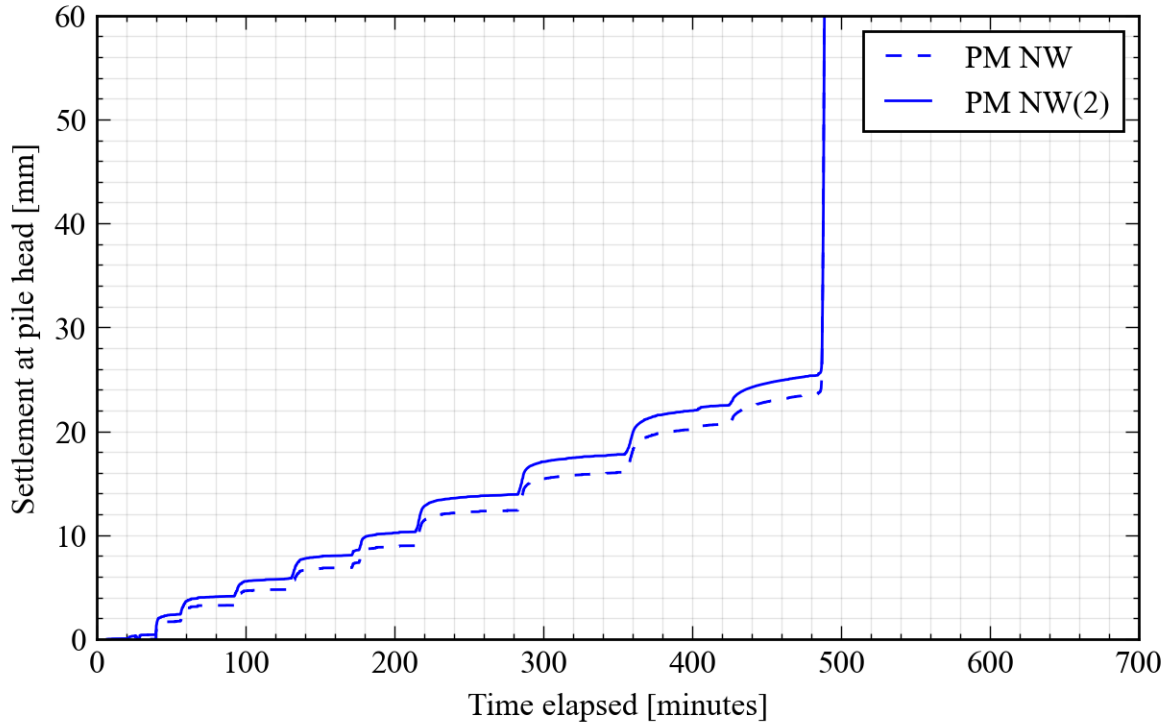


Figure 5.34: Comparison of the original potentiometer PM NW to the additional potentiometer PM NW(2) for pile T2

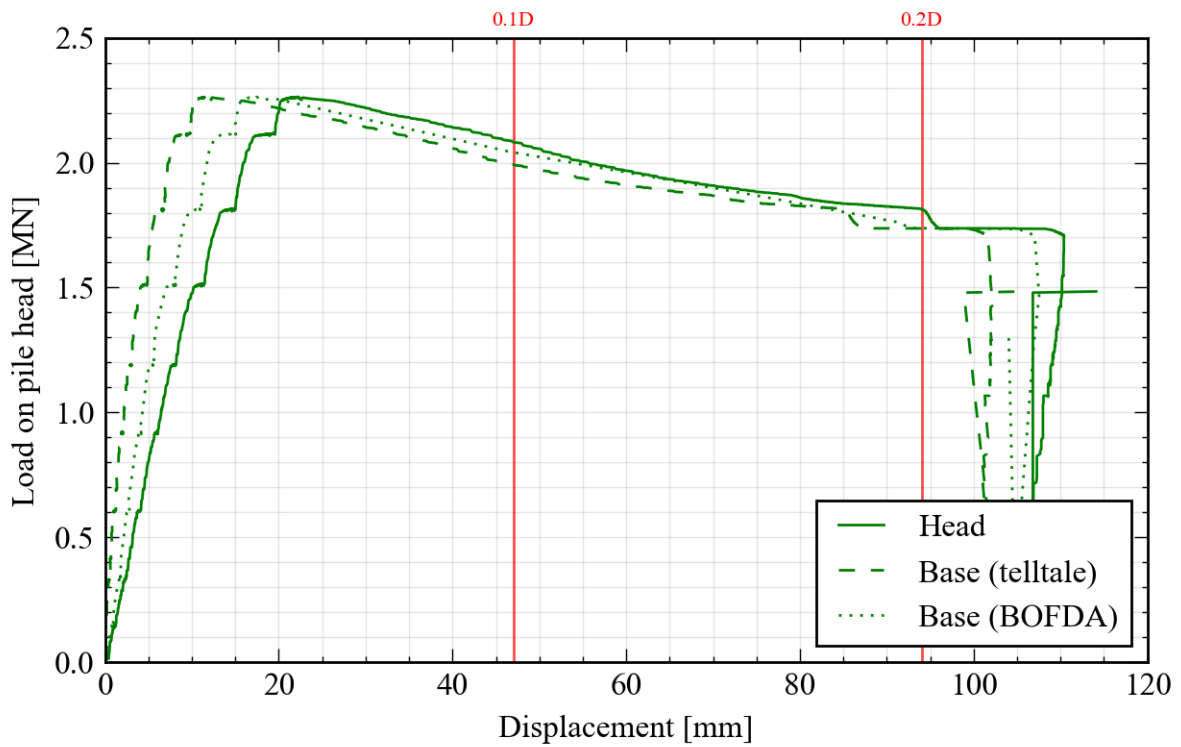


Figure 5.35: Plot of load versus settlement at pile head for T2

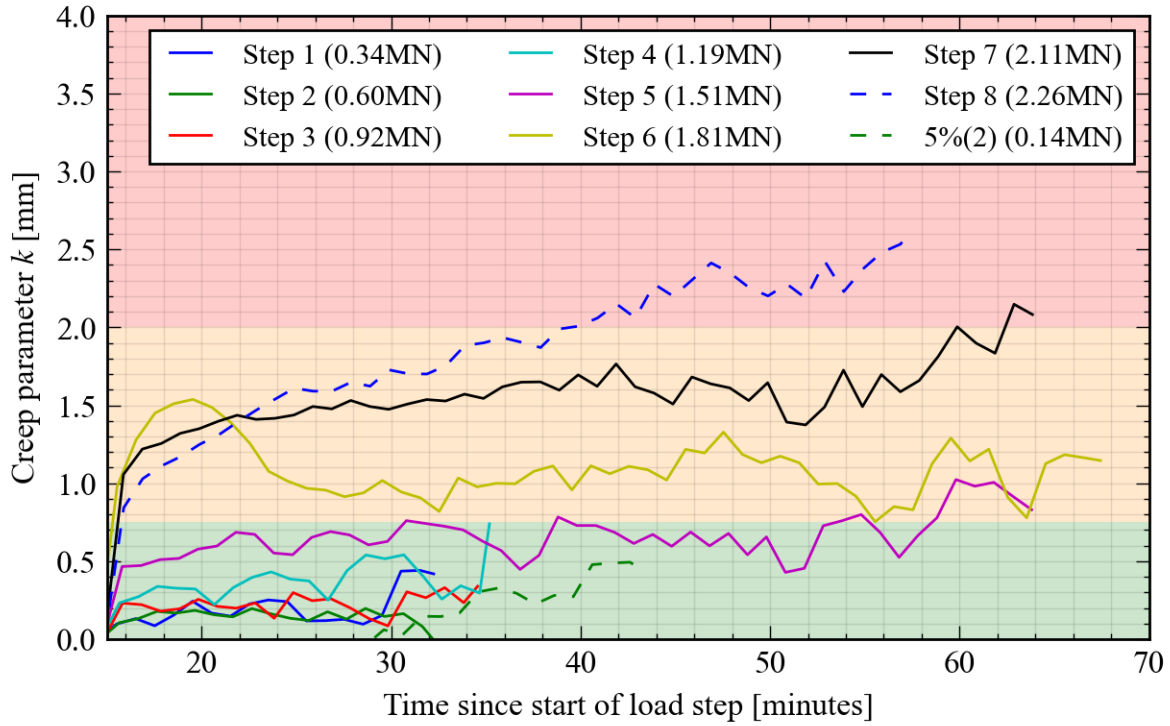


Figure 5.36: Creep parameter versus time across selected load steps for T2. The thresholds for increasing the step size/duration are also indicated

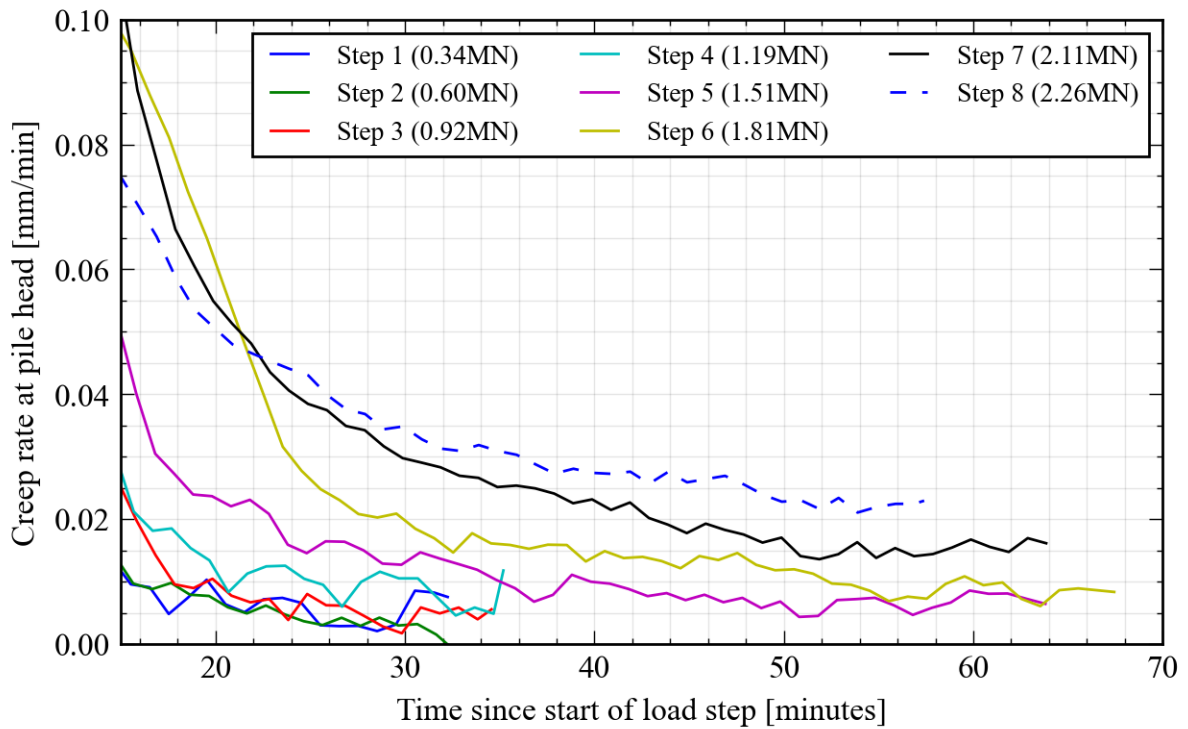


Figure 5.37: Creep rate versus time across selected loading steps for T2

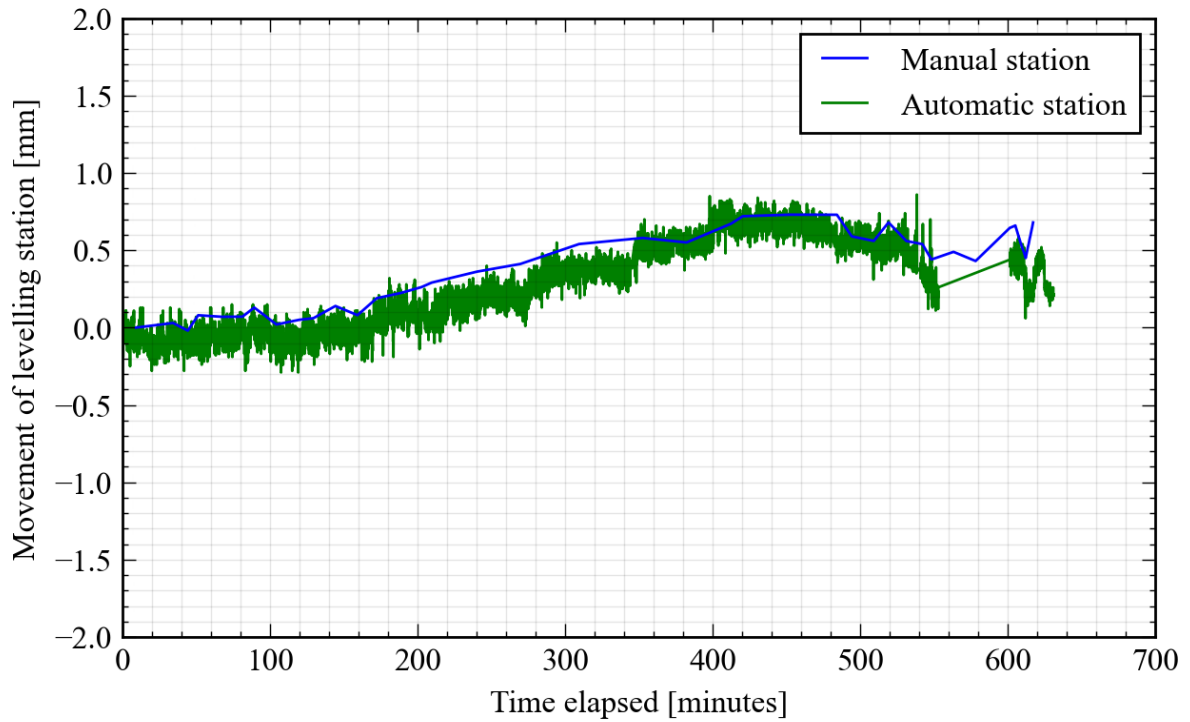


Figure 5.38: Movement of the levelling stations for pile T2, assuming a fixed reference point. Positive sign indicates upward movement

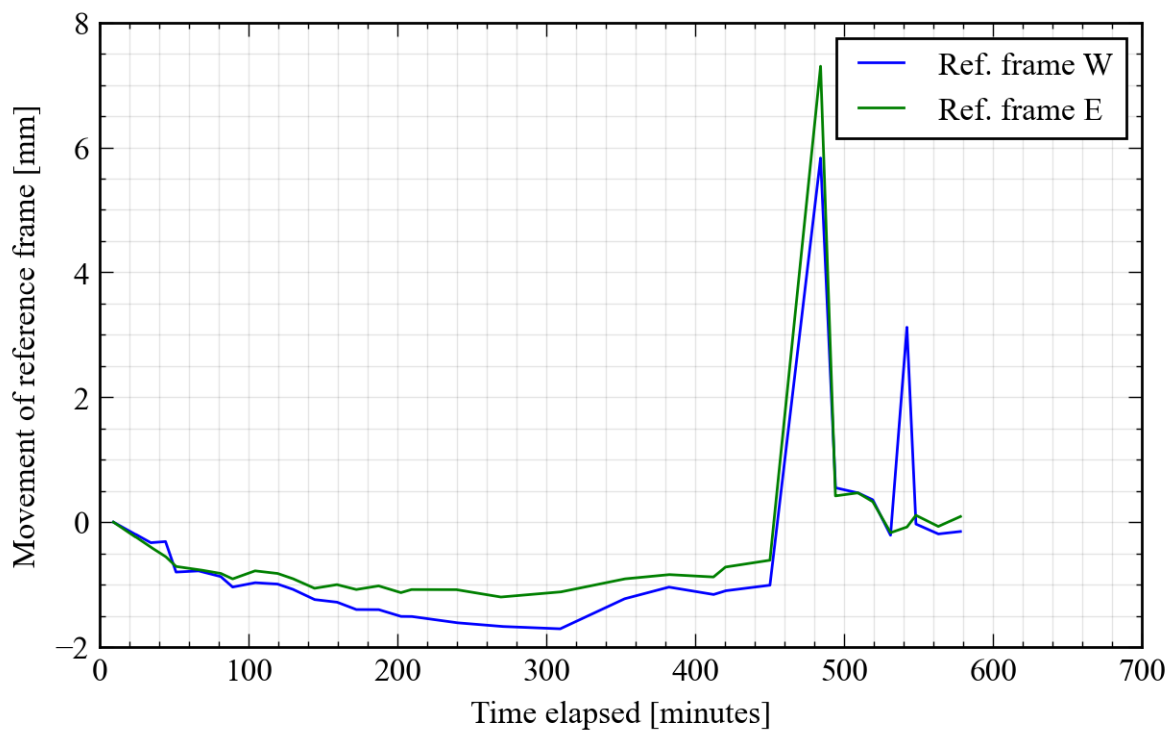


Figure 5.39: Measurements of the reference frame during the test on pile T2. The abrupt peak in the measurements corresponds to the sudden failure of the pile during Step 8

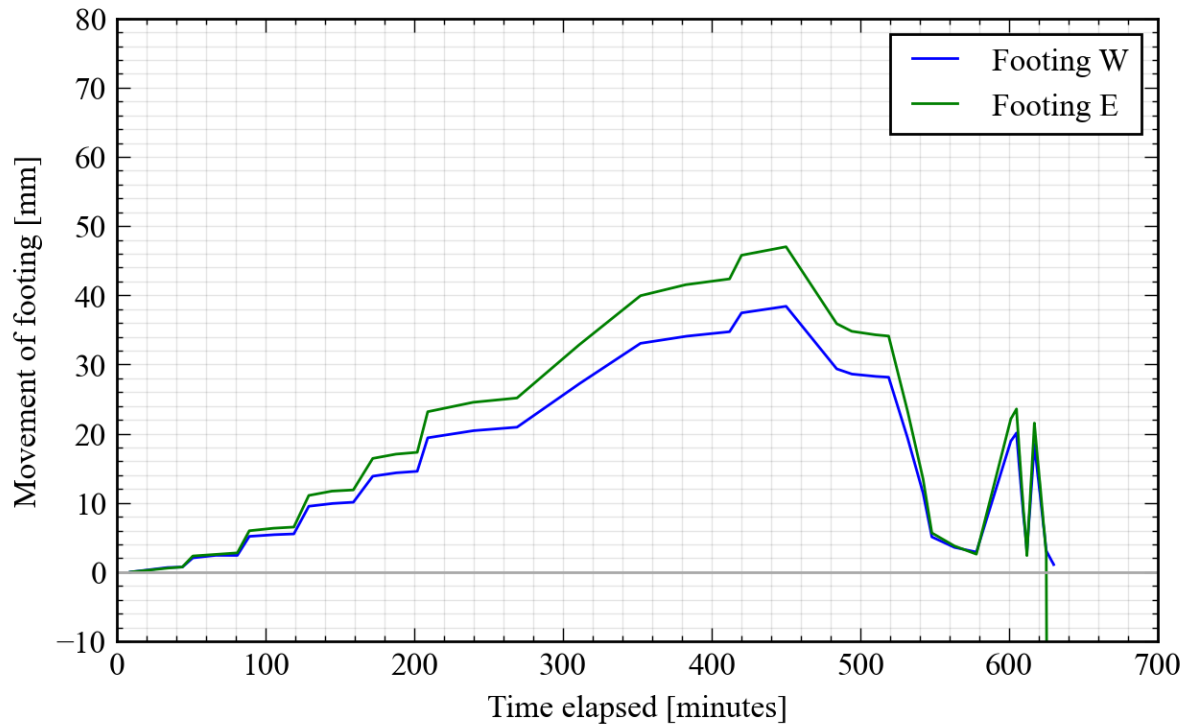


Figure 5.40: Measurements of the test frame footings during the test on pile T2. Positive sign indicates upward movement

Table 5.6: List of load steps and corresponding durations in pile test T2

Step	Start	End	Duration (HH:MM)	Average Load [kN]
refSLT	09/04/2022 10:16:00	09/04/2022 10:47:38	00:31	13
5%	09/04/2022 10:49:49	09/04/2022 11:04:14	00:14	145
Step 1	09/04/2022 11:07:57	09/04/2022 11:40:26	00:32	337
Step 2	09/04/2022 11:45:42	09/04/2022 12:18:53	00:33	605
Step 3	09/04/2022 12:24:20	09/04/2022 12:59:27	00:35	918
Step 4	09/04/2022 13:06:39	09/04/2022 13:42:01	00:35	1189
Step 5	09/04/2022 13:46:23	09/04/2022 14:50:59	01:04	1511
Step 6	09/04/2022 14:54:55	09/04/2022 16:02:47	01:07	1812
Step 7	09/04/2022 16:08:15	09/04/2022 17:12:56	01:04	2114
Step 8	09/04/2022 17:16:13	09/04/2022 18:14:01	00:57	2259
Relaxation	09/04/2022 18:14:15	09/04/2022 19:03:07	00:48	1752
5%(2)	09/04/2022 19:29:46	09/04/2022 20:13:18	00:43	138
Reload(1)	09/04/2022 20:18:29	09/04/2022 20:20:52	00:02	1537
Unload(1)	09/04/2022 20:27:47	09/04/2022 20:32:46	00:04	138
Reload(2)	09/04/2022 20:36:01	09/04/2022 20:39:28	00:03	1403
Unload(2)	09/04/2022 20:40:33	09/04/2022 20:43:08	00:02	162
refSLT(2)	09/04/2022 20:43:34	09/04/2022 20:50:00	00:06	10

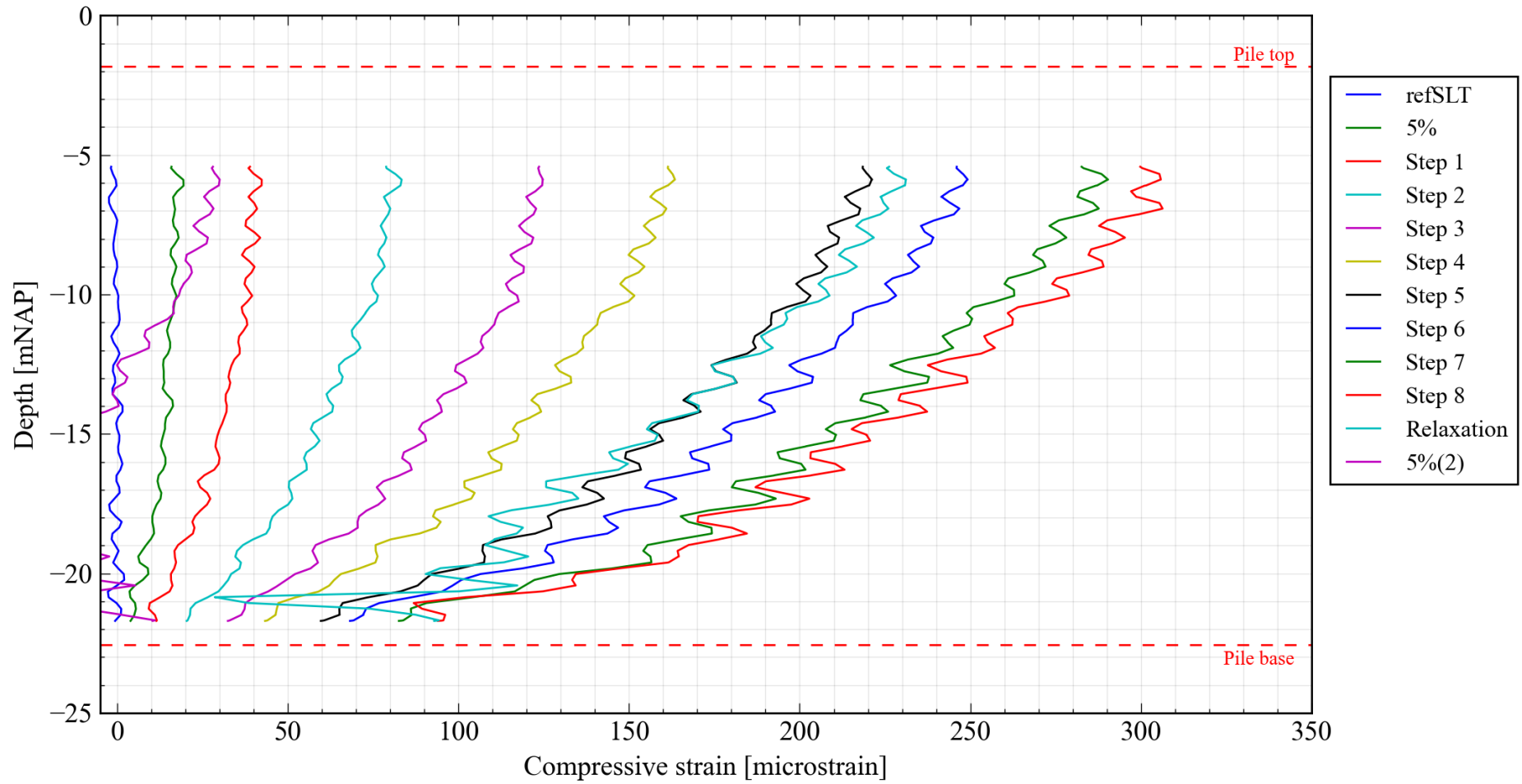


Figure 5.41: Strain measurements in pile T2 over the course of the load test. Noisy strain readings are evident in the lower sand layer (NAP -17m onwards) at the end of the Relaxation load step

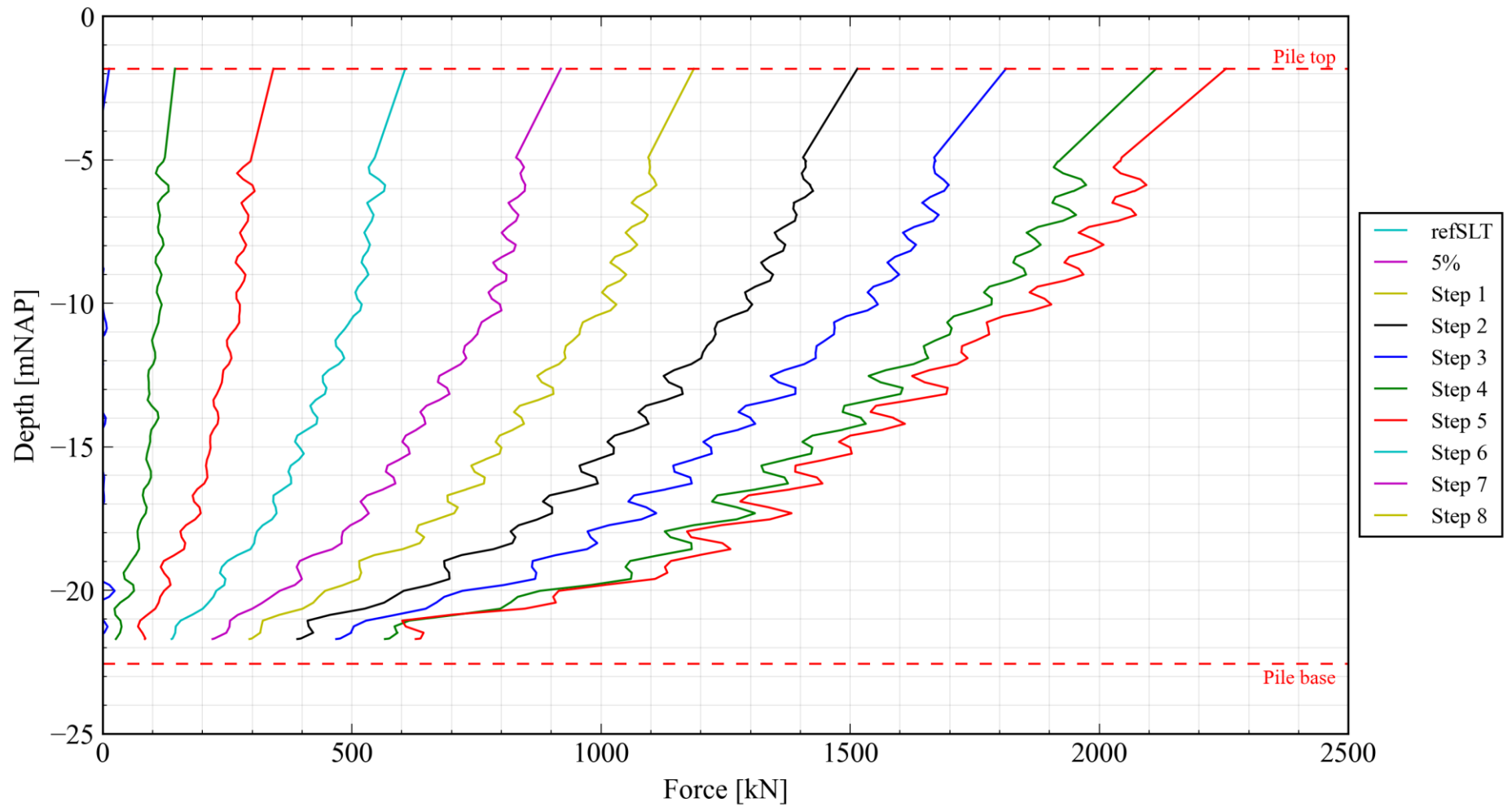


Figure 5.42: Normal force measurements in pile T2 at the end of each load step, including the load measured by the load cell. For more details on strain-to-force conversion, see Section 6.1

5.4. 12th April 2022: Pile F2

Pile F2 was tested on the 12th of April, the fourth of all piles to be tested. Weather conditions throughout the test were sunny with a slight breeze.

The pile was excavated to below a 25cm thick grout shell at the ground surface. This grout shell was relatively inconsistent in diameter, with the eastern side of the pile having a grout thickness of 30cm and the western side of just 5cm with respect to the pile's cross-section. Below this shell, little to no grout was present (Section 4.4). During the latter end of the load test (likely during the unload/reload cycles), this grout shell broke.

Similar to the test on pile T2, the telltale potentiometer was placed upside-down with the tip placed underneath the topside of the transition piece (**Figure 5.28**). This was due to the lack of space for the platen on the upper surface of the pile head.

Bending in the pile was observed in the fibre optic readings and potentiometers at the start of the test and so from Step 2, the increase in load was approached more slowly to avoid any excessive bending or damage to the pile.



Figure 5.43: Pile F2 prior to testing. Note the grout shell at the base of the pile cap



Figure 5.44: Placement of the telltale PM for pile F2. The platen is touching the top side of the transition piece

Table 5.7: Particularities associated with the test on pile F1

Relevant period		Remark
Time	Step	
	Step 1	Data gap in fibre optic measurements in order to reduce fibre attenuation
23:10	5%(2)	Potentiometers re-adjusted to allow for additional stroke

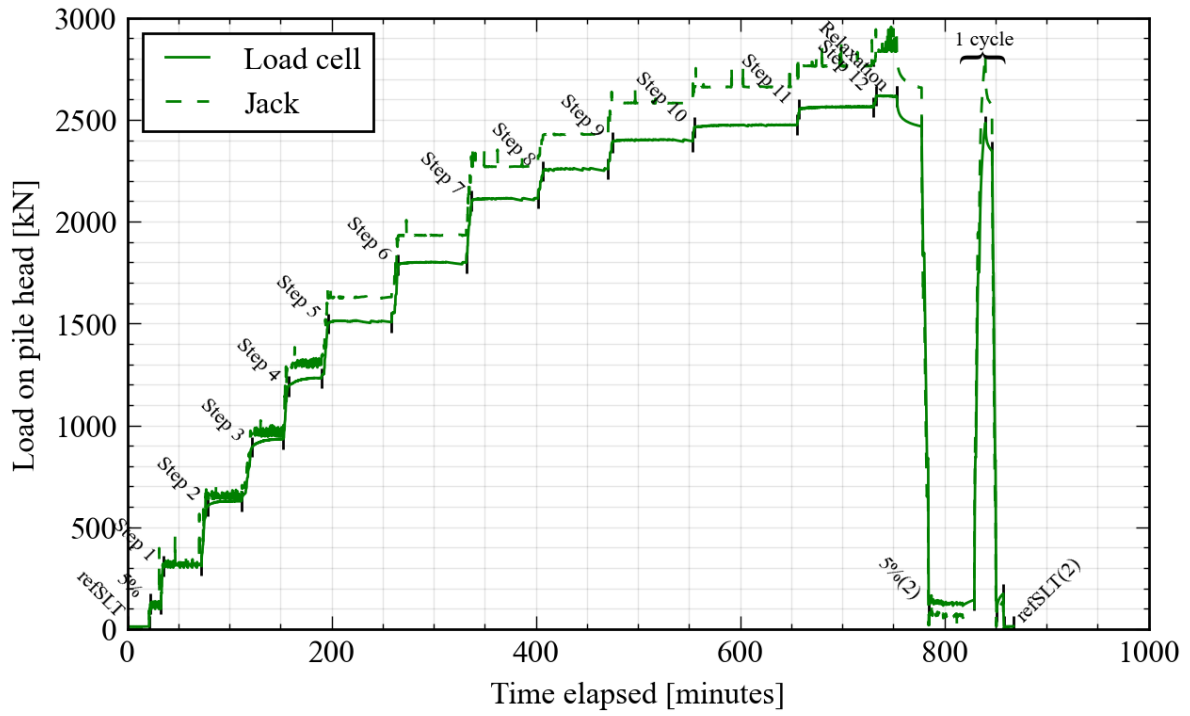


Figure 5.45: Plot of load exerted on pile head against the time elapsed for F2

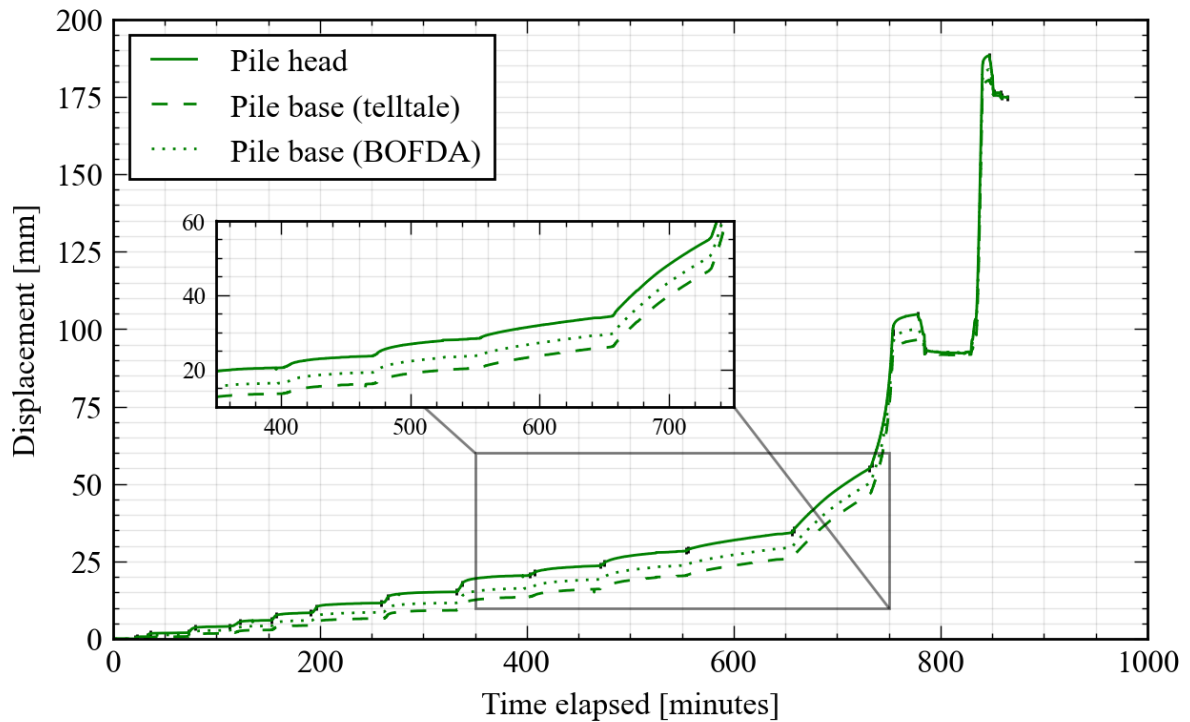


Figure 5.46: Plot of displacement measured at the pile head against the time elapsed for F2

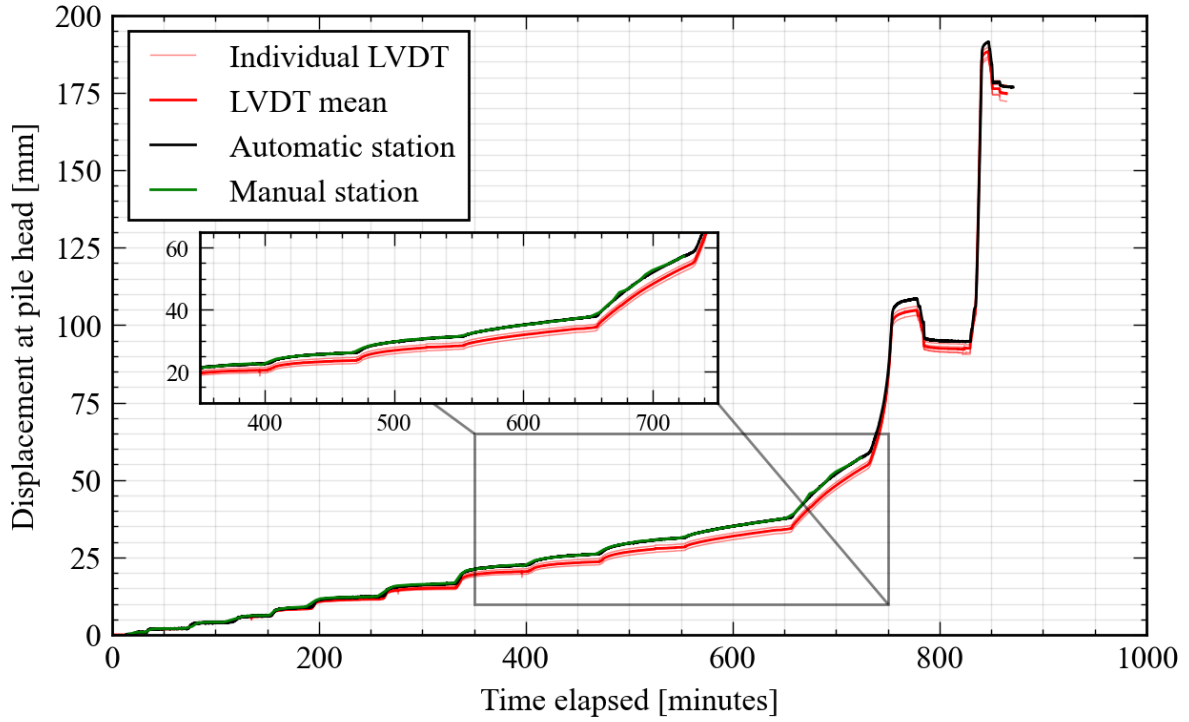


Figure 5.47: All pile head displacement readings for pile F2

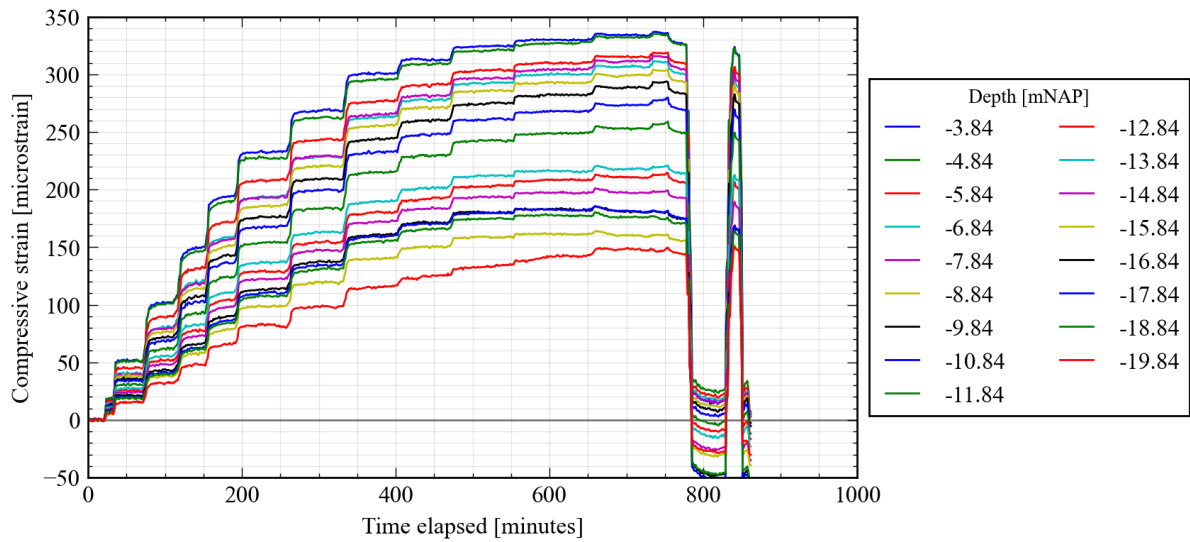


Figure 5.48: Plot of strain versus time for selected BOFDA increments for F2

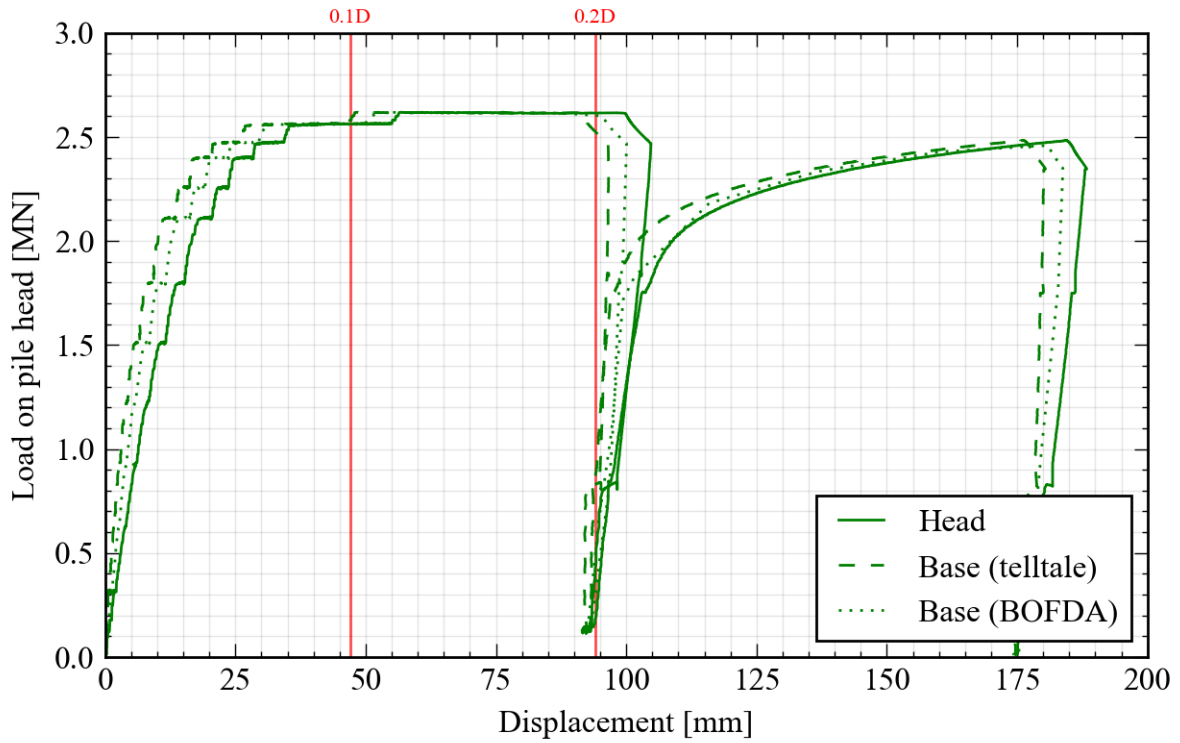


Figure 5.49: Plot of load versus displacement at pile head for F2

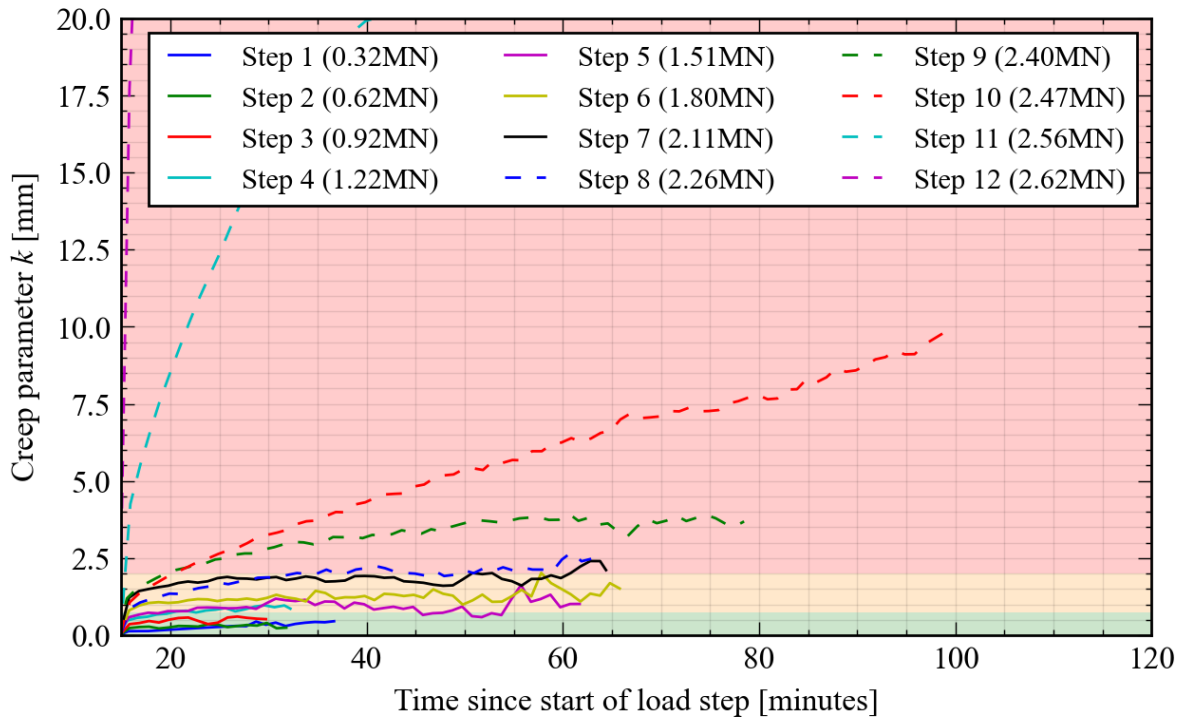


Figure 5.50: Creep parameter versus time across selected load steps for F2. The thresholds for increasing the step size/duration are also indicated

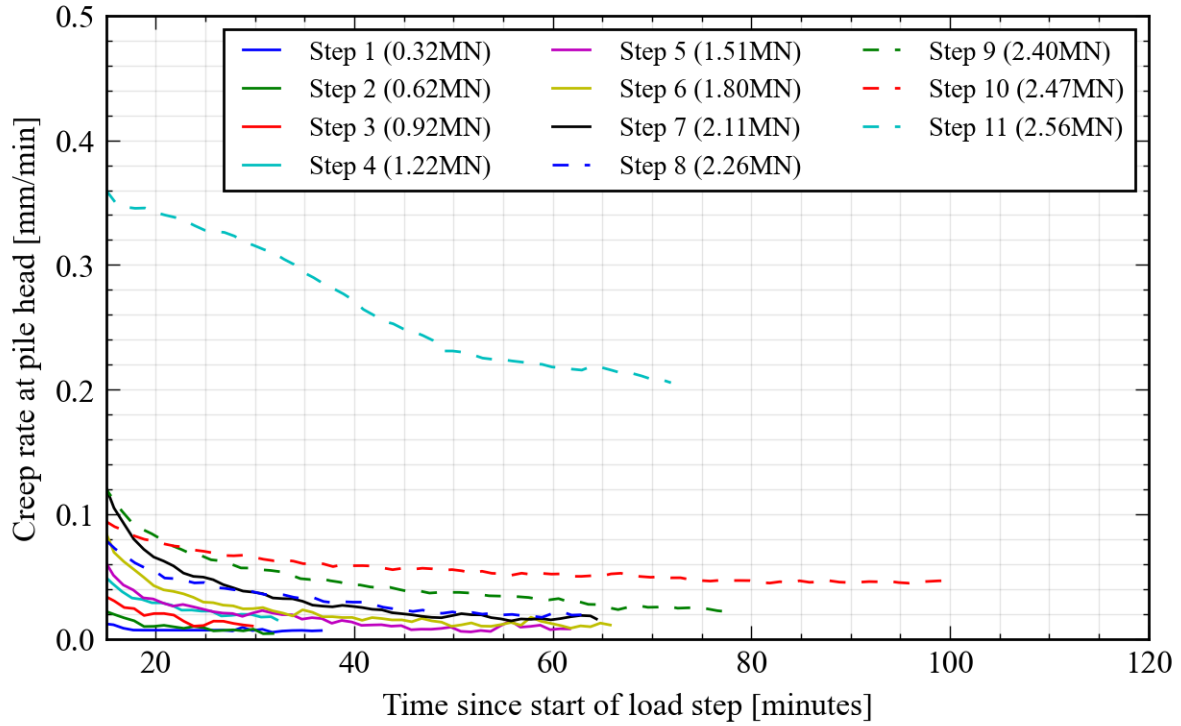


Figure 5.51: Creep rate versus time across selected loading steps for F2. Step 12 has not been plotted due to high creep rate

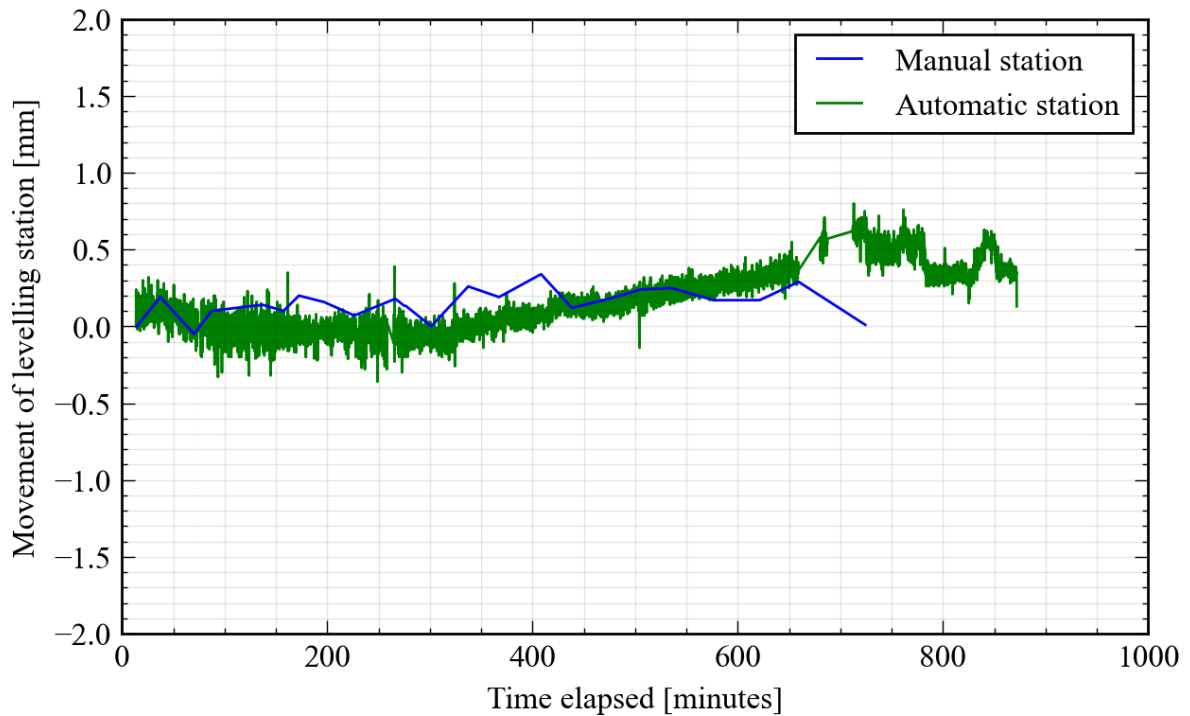


Figure 5.52: Movement of the levelling stations for pile F2, assuming a fixed reference point. Positive sign indicates upward movement

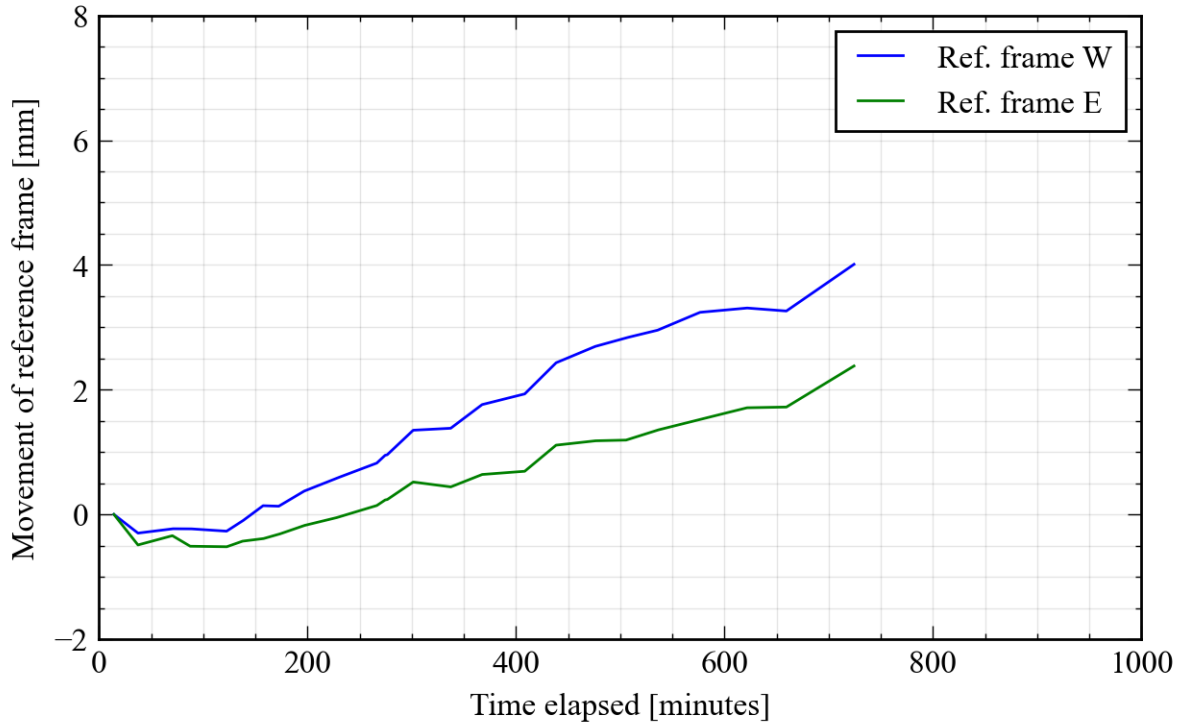


Figure 5.53: Measurements of the reference frame during the test on pile F2

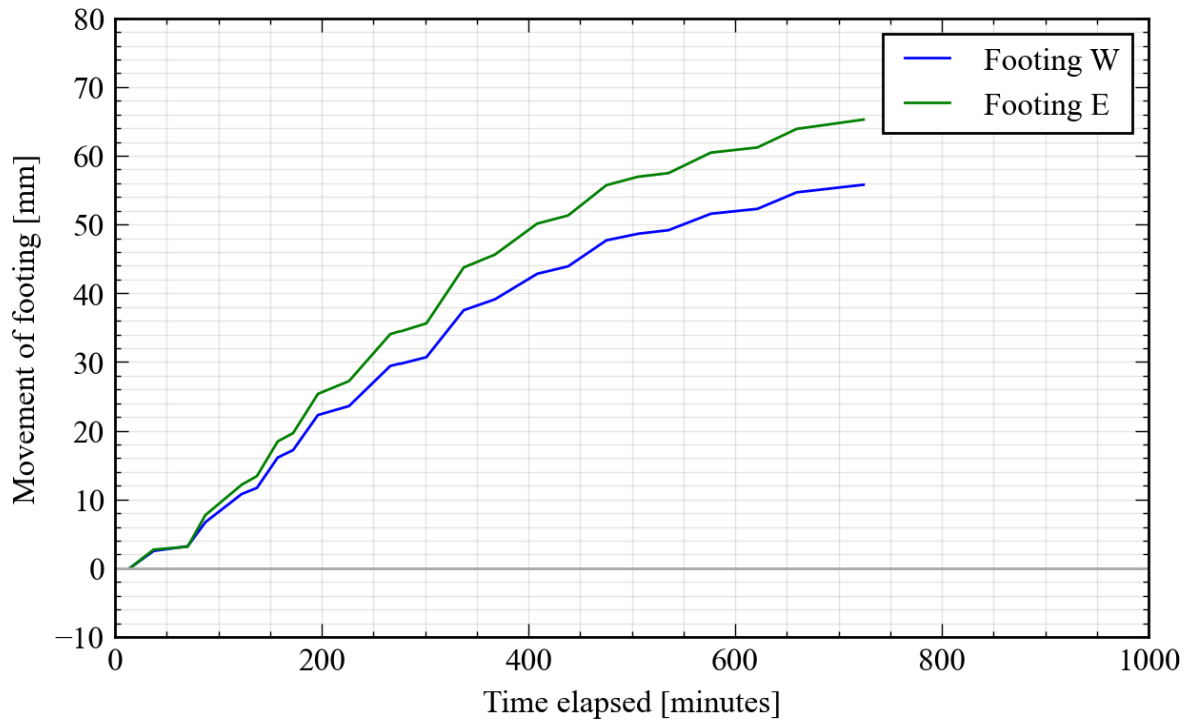


Figure 5.54: Measurements of the test frame footings during the test on pile F2. Positive sign indicates upward movement

Table 5.8: List of load steps and corresponding durations in pile test F2

Step	Start	End	Duration (HH:MM)	Average Load [kN]
refSLT	12/04/2022 09:30:00	12/04/2022 09:52:28	00:22	13
5%	12/04/2022 09:53:46	12/04/2022 10:04:08	00:10	128
Step 1	12/04/2022 10:06:31	12/04/2022 10:43:52	00:37	316
Step 2	12/04/2022 10:50:20	12/04/2022 11:22:57	00:32	625
Step 3	12/04/2022 11:33:20	12/04/2022 12:03:48	00:30	924
Step 4	12/04/2022 12:08:46	12/04/2022 12:41:13	00:32	1223
Step 5	12/04/2022 12:47:31	12/04/2022 13:49:56	01:02	1510
Step 6	12/04/2022 13:56:24	12/04/2022 15:02:59	01:06	1798
Step 7	12/04/2022 15:08:24	12/04/2022 16:13:12	01:04	2112
Step 8	12/04/2022 16:18:11	12/04/2022 17:21:57	01:03	2257
Step 9	12/04/2022 17:25:50	12/04/2022 18:44:46	01:18	2400
Step 10	12/04/2022 18:46:16	12/04/2022 20:26:59	01:40	2473
Step 11	12/04/2022 20:29:09	12/04/2022 21:41:57	01:12	2562
Step 12	12/04/2022 21:44:20	12/04/2022 22:04:24	00:20	2617
Relaxation	12/04/2022 22:04:24	12/04/2022 22:28:51	00:24	2495
5%(2)	12/04/2022 22:36:12	12/04/2022 23:20:31	00:44	130
Reload(1)	12/04/2022 23:30:52	12/04/2022 23:38:00	00:07	2384
Unload(1)	12/04/2022 23:42:19	12/04/2022 23:48:47	00:06	149
refSLT(2)	12/04/2022 23:49:26	12/04/2022 23:58:57	00:09	14

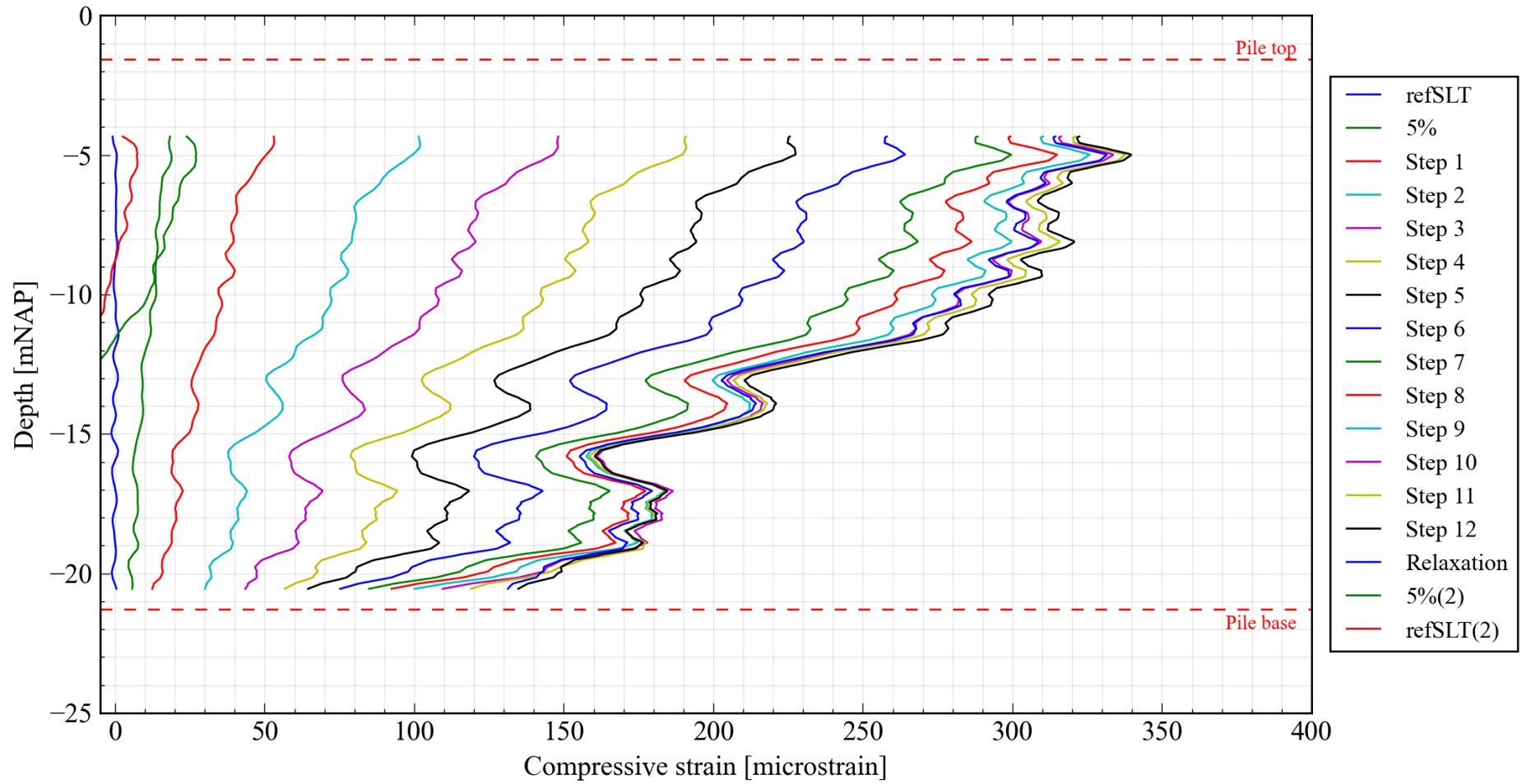


Figure 5.55: Strain measurements in pile F2 over the course of the load test

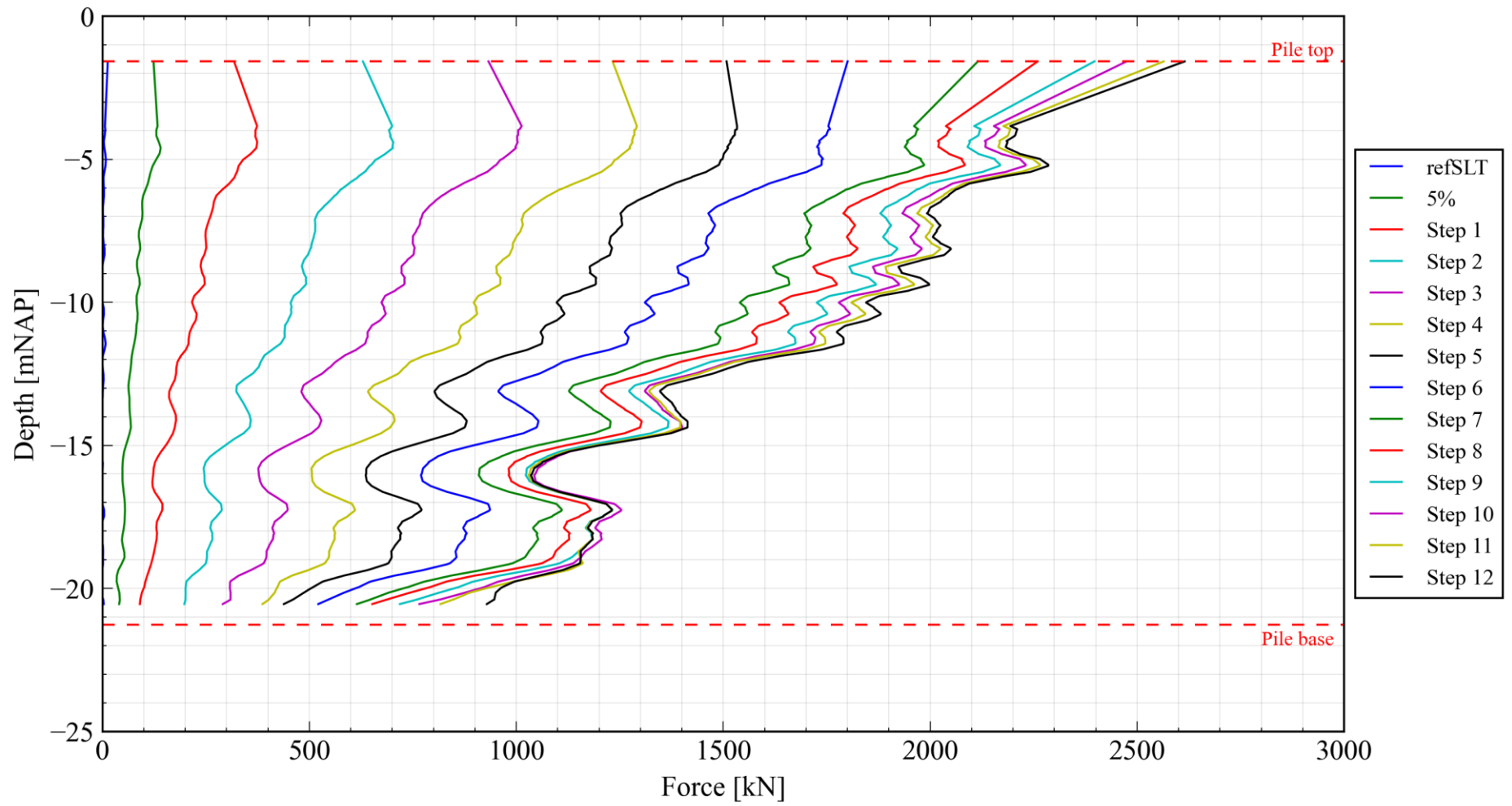


Figure 5.56: Normal force measurements in pile F2 at the end of each load step, including the load measured by the load cell. For more details on strain-to-force conversion, see Section 6.1

5.5. 14th April 2022: Pile T3

Pile T3 was tested on the 14th of April, the fifth of all piles to be tested. Weather conditions throughout the test were warm and sunny with little to no breeze in the morning, increasing to a slight breeze later in the afternoon.

Prior to load testing, it was realised that internal issues relating to PM_SE was leading to noisy measurements. An additional sensor PM_SE(2) was placed as a back-up to this sensor (**Figure 5.57**). Furthermore, all potentiometers with the exception of PM_SE(2) were not automatically logging until midway through step 1. Manual readings of these potentiometers were recorded every five minutes as per testing protocol.

Slightly larger load steps of 350 kN were used because of the pile's longer embedment depth compared to other piles. Noticeably higher creep rates were exhibited in the pile relatively early on in the test, although in anticipation of a higher load, full steps were continued. With the creep continuing to pick up, the step sizes were reduced after Step 5 and plunging failure eventually occurred during Step 6, at a much lower load (1827 kN) than predicted. A later interpretation of the load distributions (**Figure 5.70**, Section 6.2) showed that the grout shell in the lower sand layer failed, manifesting in a loss of load transfer to the lower sand layer during subsequent reloading cycles.

For the second load cycle, Reload 2, it was not clear if there would be sufficient stroke left on the hydraulic jack for another full unload/reload cycle. Therefore instead of the conventional loading cycles, the pile was reloaded to just under the attained maximum load and loaded incrementally, with each increment duration corresponding to at least measurement duration of the FO data logger. A higher load than that obtained in the main test was reached.

A load of 1000kN was left on the pile over the weekend to minimise settlement of the test frame. The strain in the pile was measured for five minutes after reloading and stopped thereafter.

Table 5.9: Particularities associated with the test on pile F1

Relevant period		Remark
Time	Step	
09:45	Step 1	Potentiometers start logging
13:36	Step 5	PM_SE(2) adjusted
16:36	Reload(2)	PM_SE(2) removed



Figure 5.57: Back-up sensor PM_SE(2)

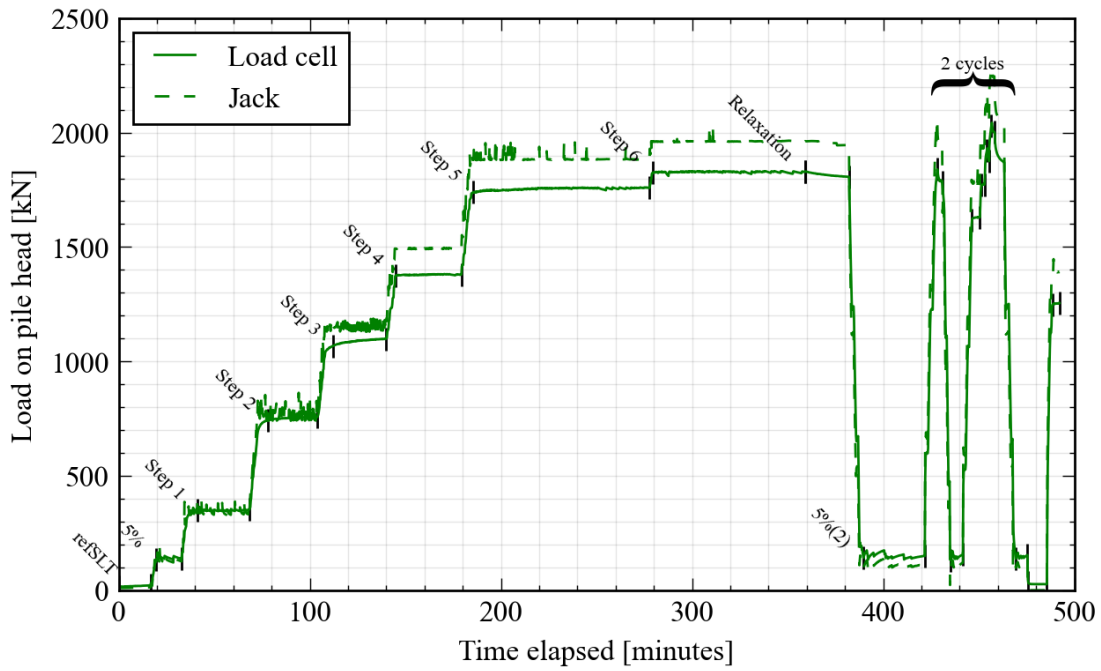


Figure 5.58: Plot of load exerted on pile head against the time elapsed for T3

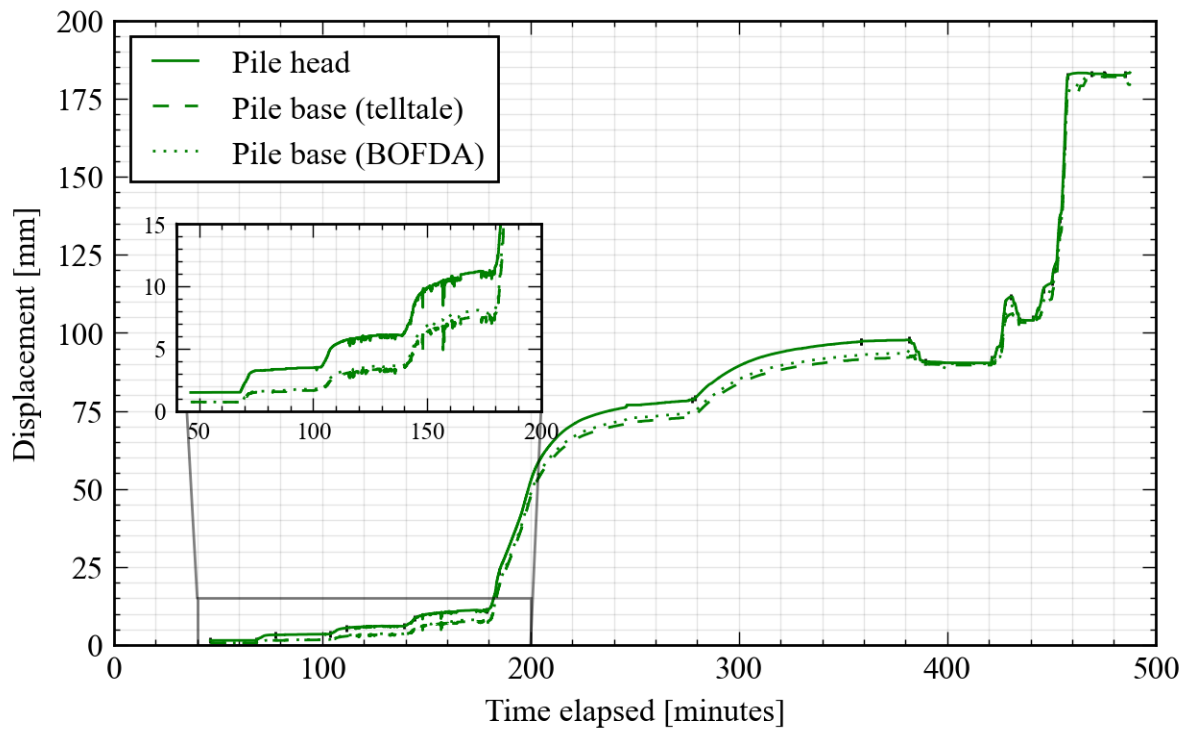


Figure 5.59: Plot of settlement measured at the pile head against the time elapsed for T3

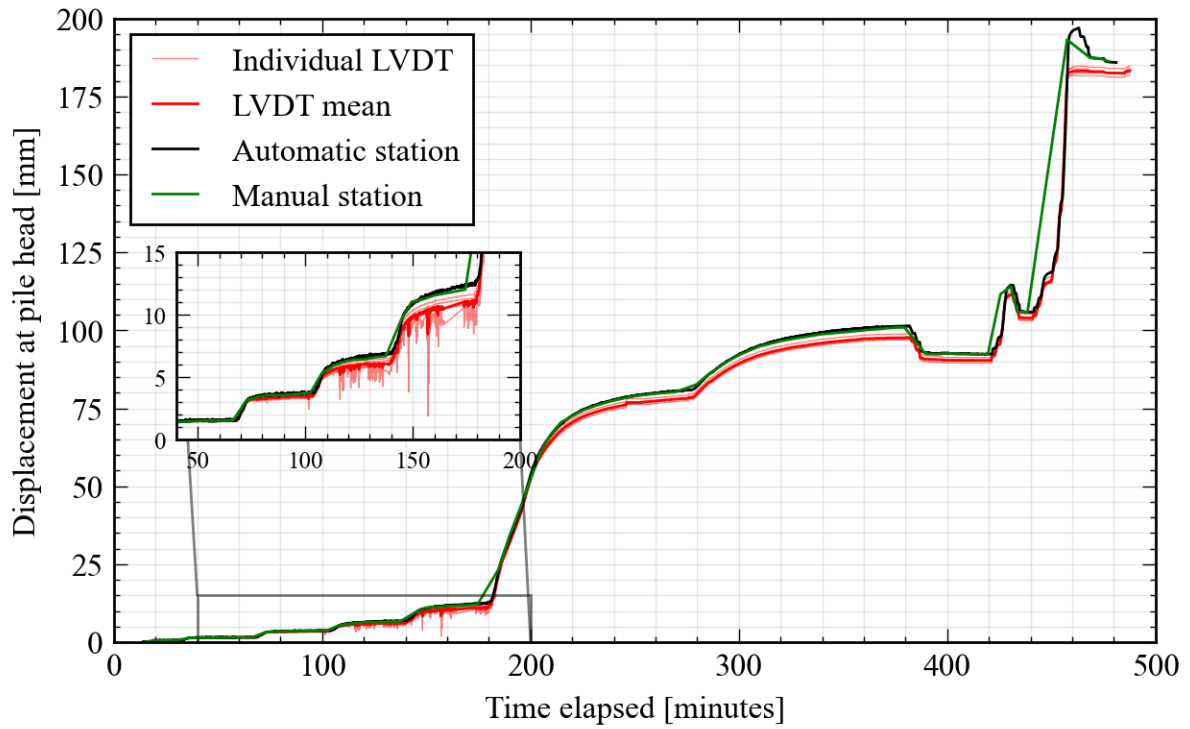


Figure 5.60: All settlement at pile head readings for pile T3

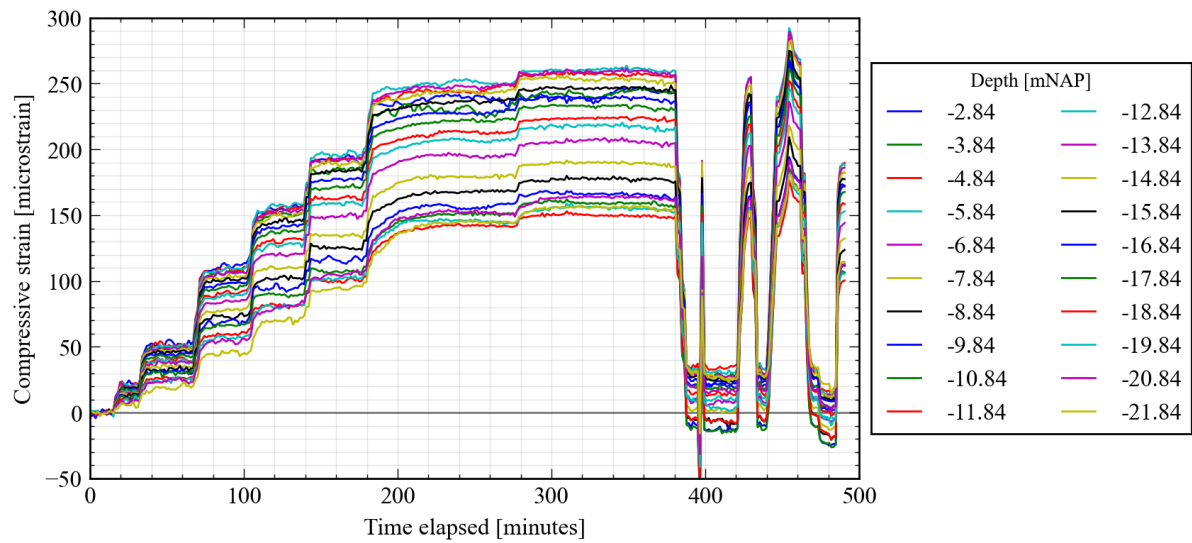


Figure 5.61: Plot of strain versus time for selected BOFDA increments for T3

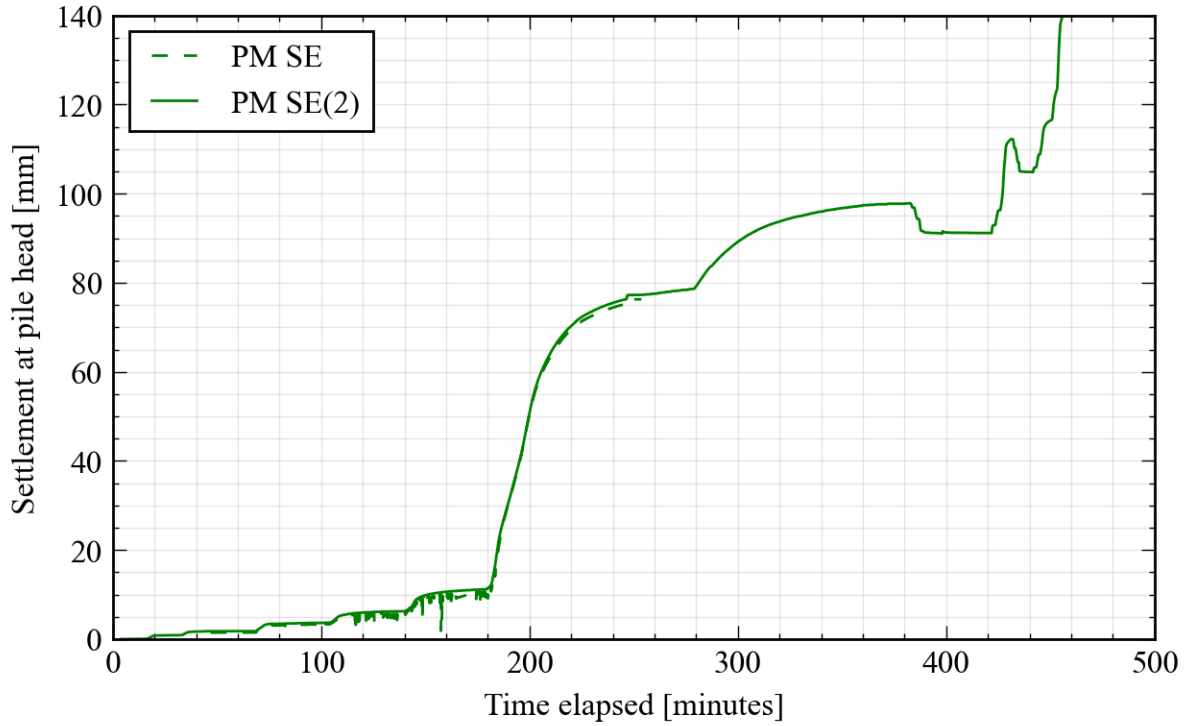


Figure 5.62: Additional potentiometer readings for pile T3

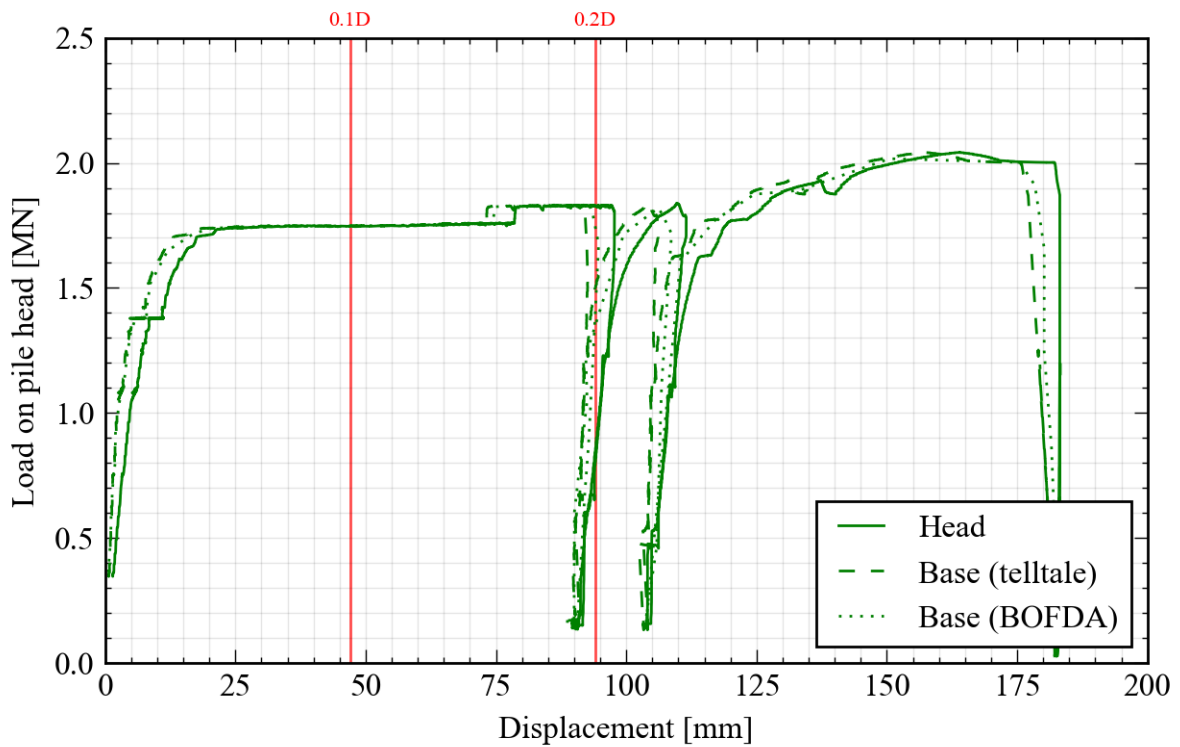


Figure 5.63: Plot of load versus displacement for T3

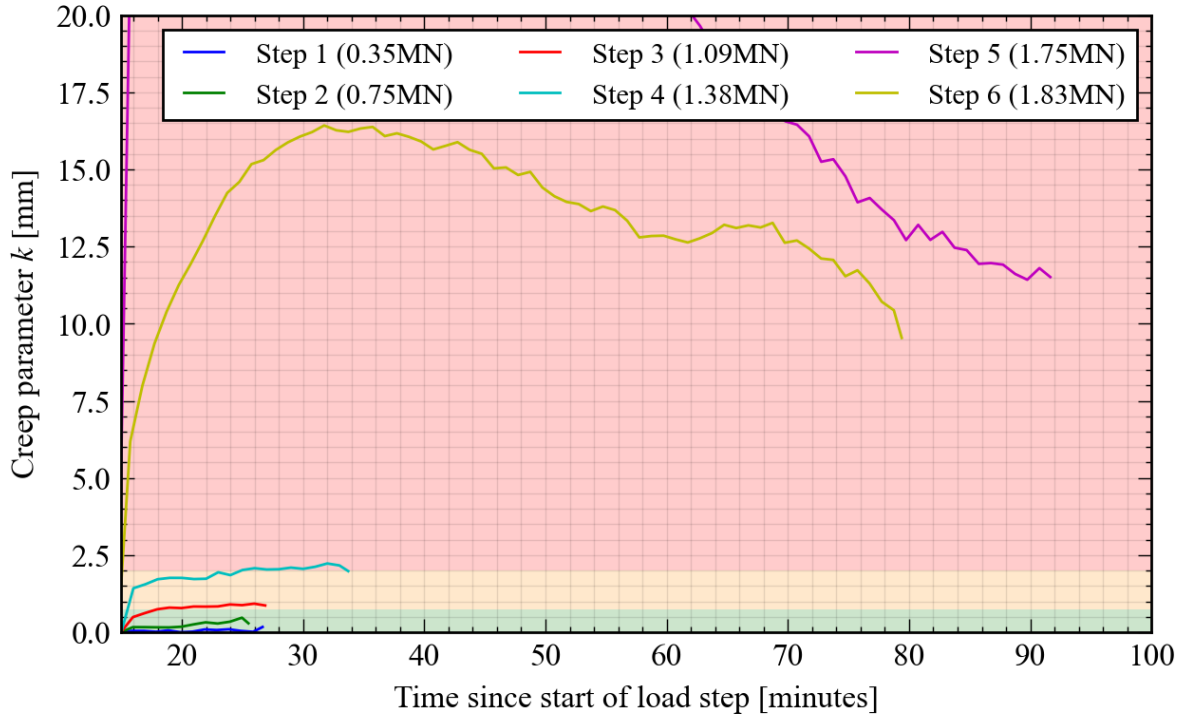


Figure 5.64: Creep parameter versus time across selected load steps for T3. The thresholds for increasing the step size/duration are also indicated

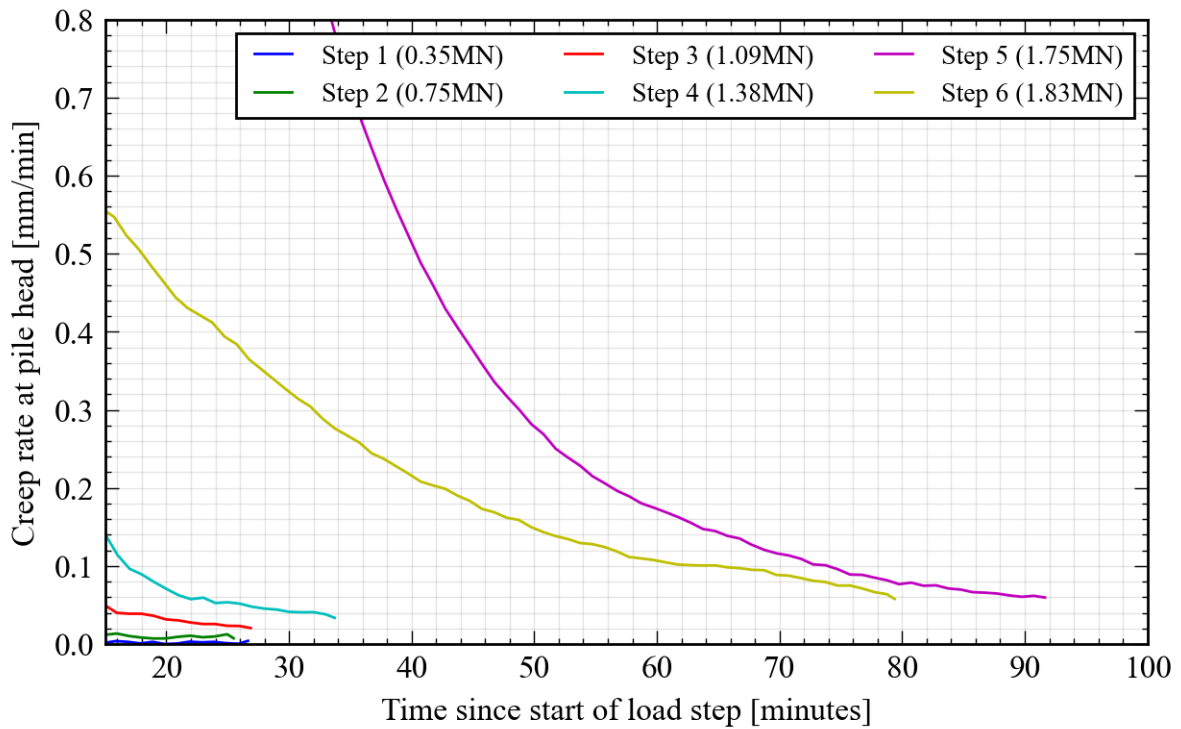


Figure 5.65: Creep rate versus time across selected loading steps for T3

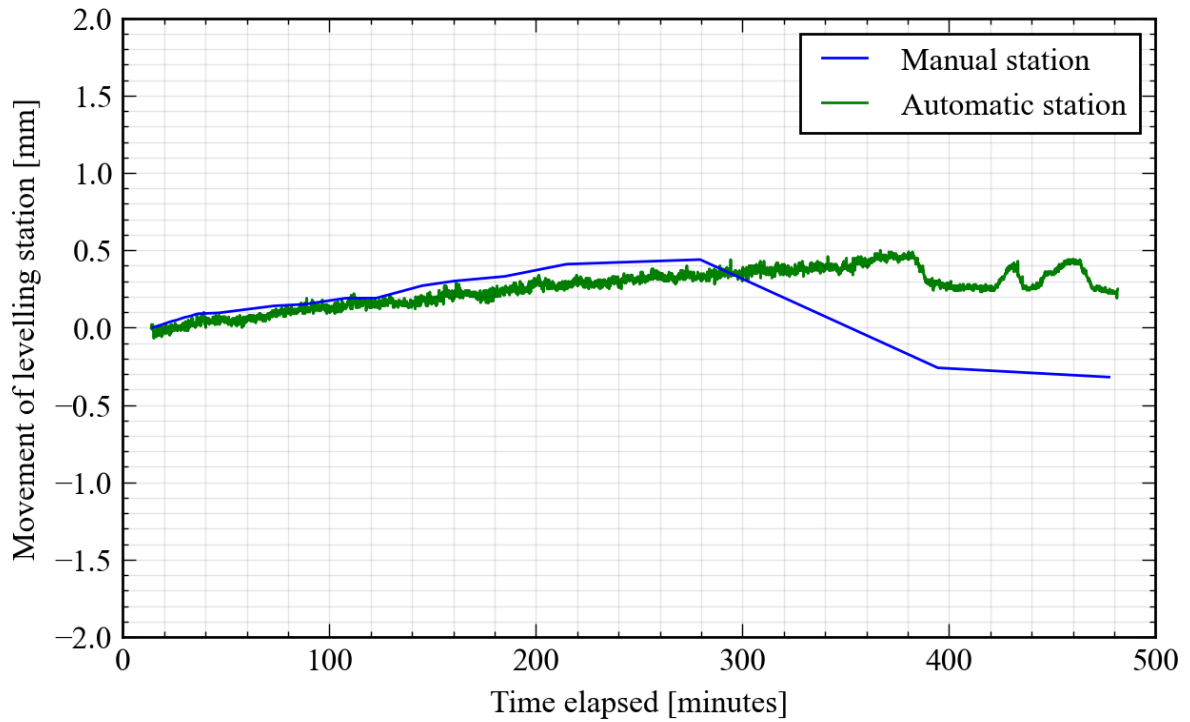


Figure 5.66: Movement of the levelling stations for pile T3, assuming a fixed reference point. Positive sign indicates upward movement

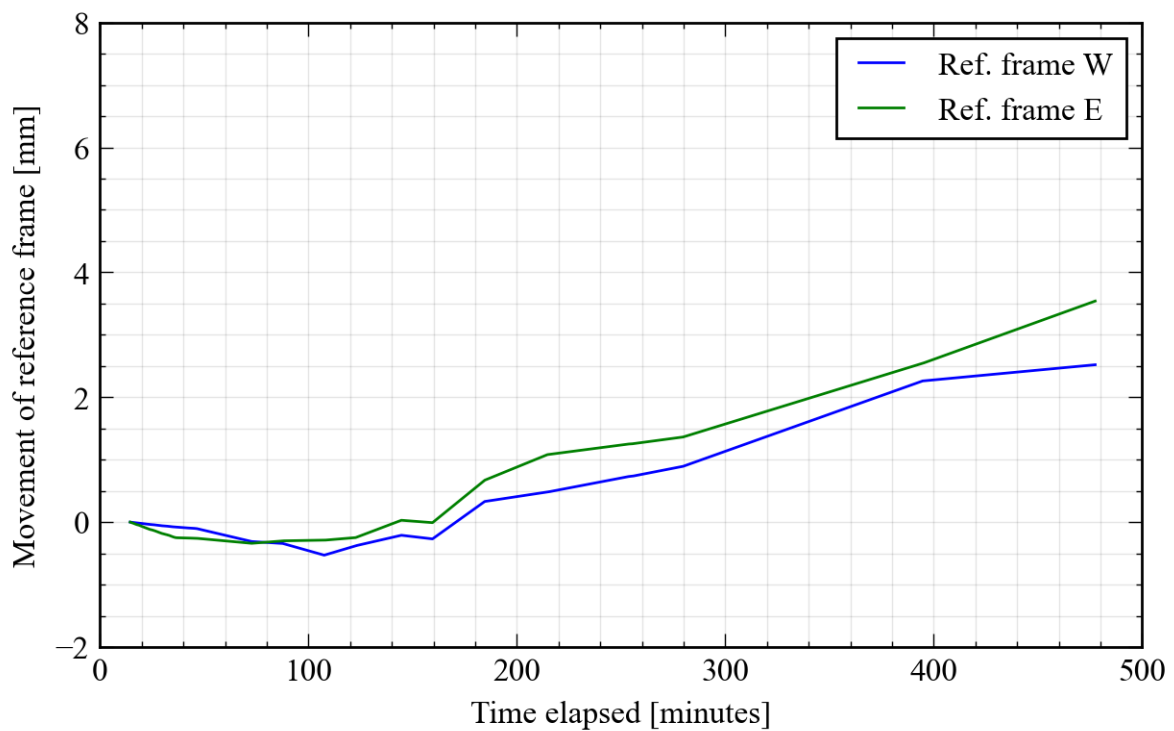


Figure 5.67: Measurements of the reference frame during the test on pile T3

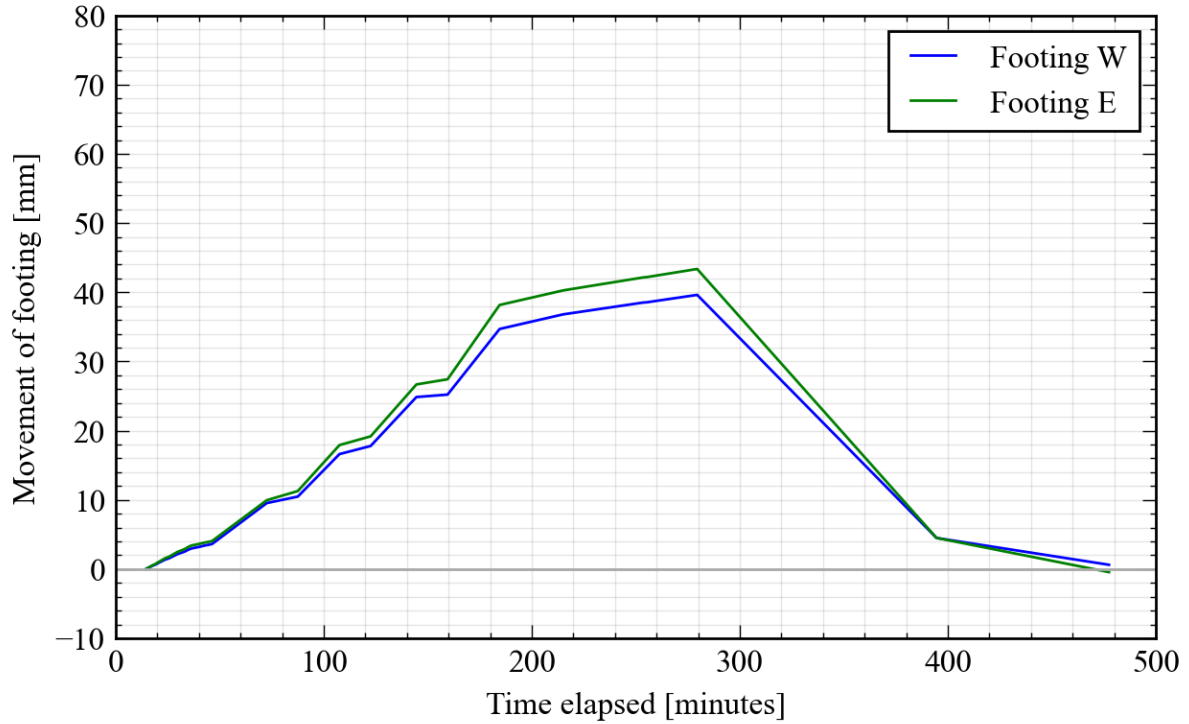


Figure 5.68: Measurements of the test frame footings during the test on pile T3. Positive sign indicates upward movement

Table 5.10: List of load steps and corresponding durations in pile test T3

Step	Start	End	Duration (HH:MM)	Average Load [kN]
refSLT	14/04/2022 09:00:30	14/04/2022 09:16:46	00:16	20
5%	14/04/2022 09:19:48	14/04/2022 09:33:01	00:13	142
Step 1	14/04/2022 09:41:15	14/04/2022 10:08:33	00:27	350
Step 2	14/04/2022 10:18:05	14/04/2022 10:44:03	00:25	752
Step 3	14/04/2022 10:52:04	14/04/2022 11:19:48	00:27	1088
Step 4	14/04/2022 11:25:00	14/04/2022 11:59:26	00:34	1379
Step 5	14/04/2022 12:05:30	14/04/2022 13:37:47	01:32	1754
Step 6	14/04/2022 13:39:31	14/04/2022 14:59:18	01:19	1827
Relaxation	14/04/2022 14:59:18	14/04/2022 15:22:14	00:22	1816
5%(2)	14/04/2022 15:29:49	14/04/2022 16:01:53	00:32	151
Reload(1)	14/04/2022 16:08:23	14/04/2022 16:10:59	00:02	1798
Unload(1)	14/04/2022 16:15:19	14/04/2022 16:21:48	00:06	150
Reload(2_1)	14/04/2022 16:26:35	14/04/2022 16:30:42	00:04	1628
Reload(2_2)	14/04/2022 16:31:34	14/04/2022 16:33:05	00:01	1772
Reload(2_3)	14/04/2022 16:34:23	14/04/2022 16:35:28	00:01	1902
Reload(2_4)	14/04/2022 16:36:45	14/04/2022 16:38:16	00:01	2015
Unload(2)	14/04/2022 16:49:32	14/04/2022 16:55:36	00:06	149
refSLT(2)	14/04/2022 16:56:02	14/04/2022 17:05:47	00:09	28
Reload(3)	14/04/2022 17:08:36	14/04/2022 17:12:17	00:03	1253

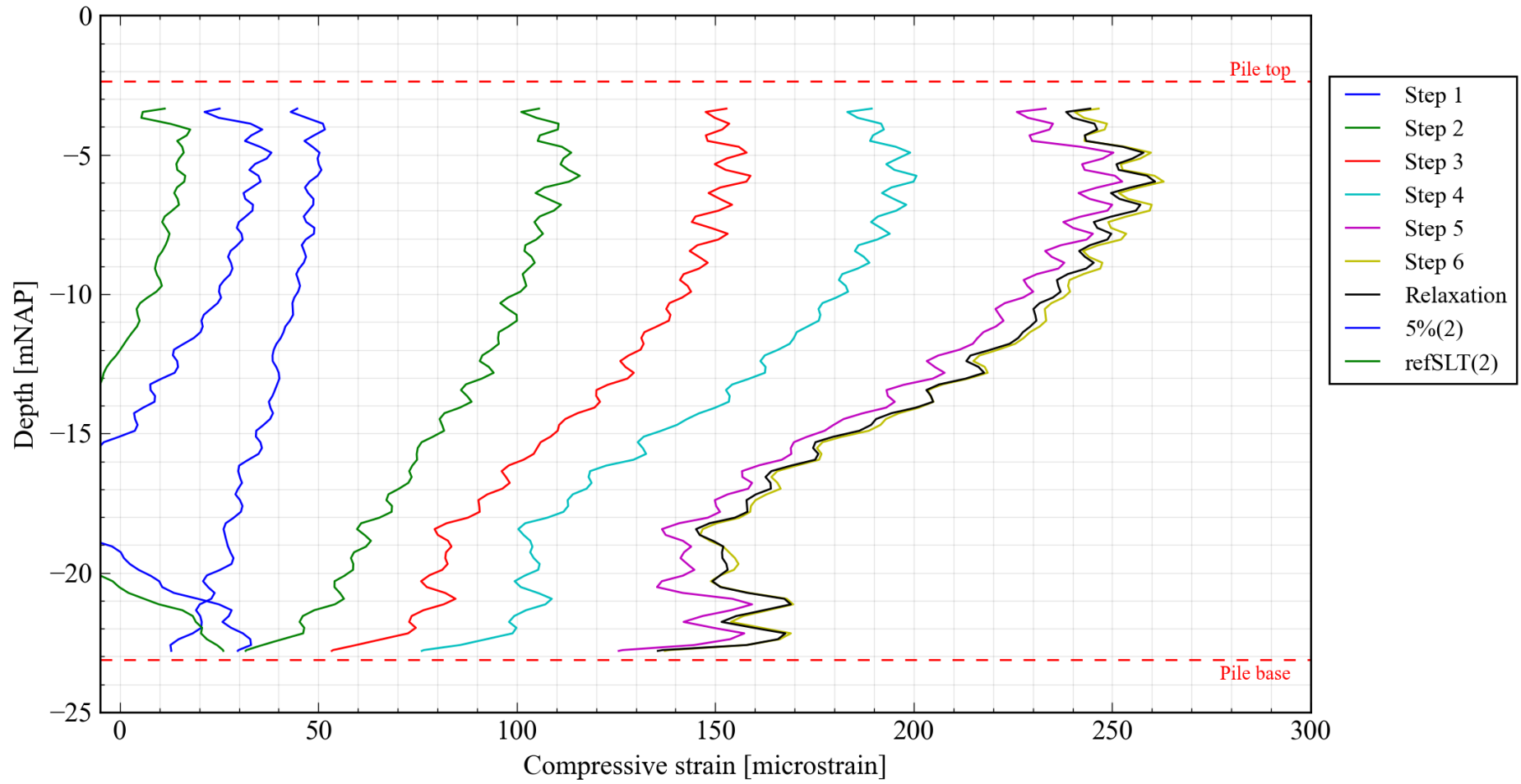


Figure 5.69: Strain measurements in pile T3 over the course of the load test

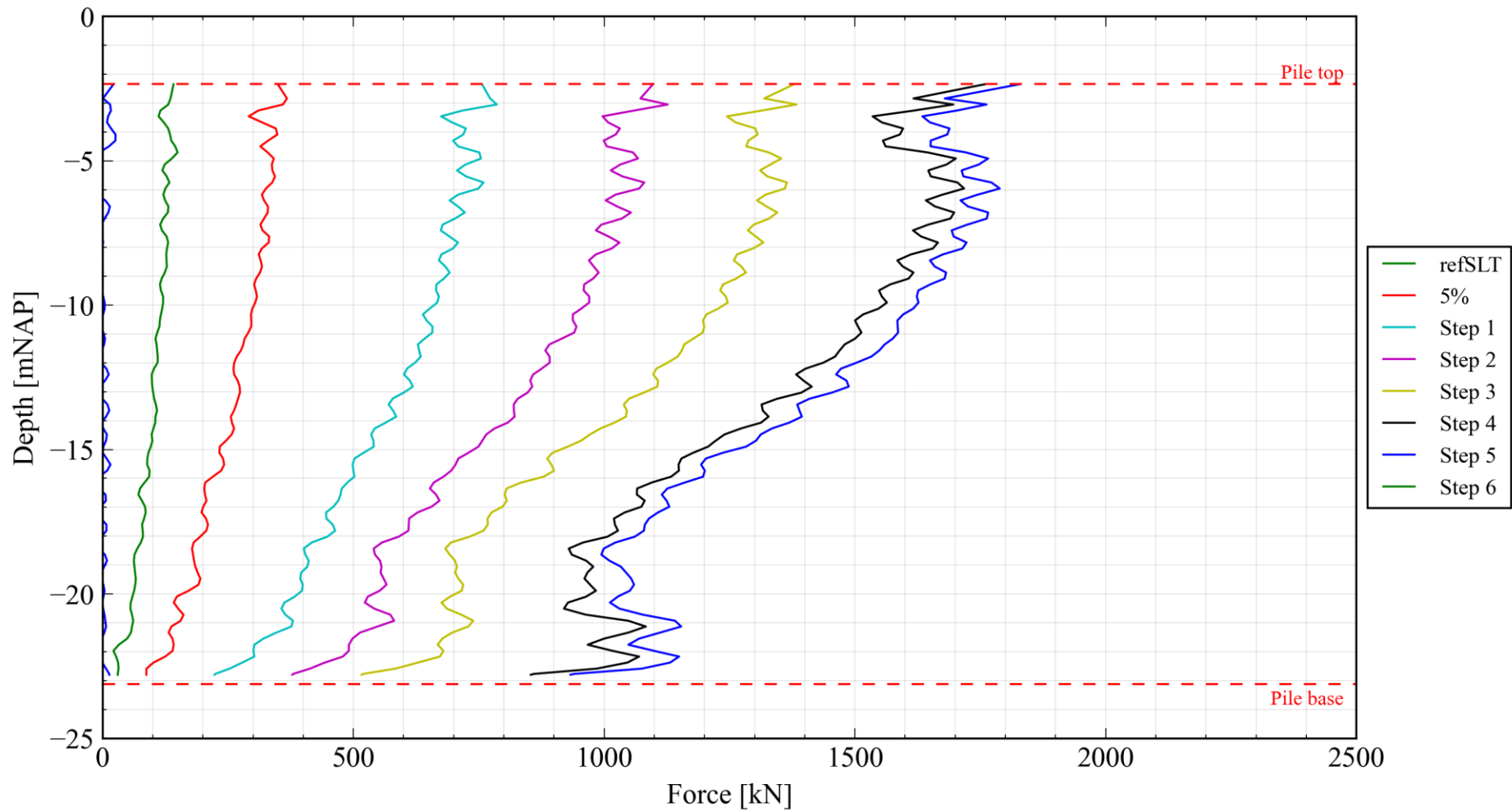


Figure 5.70: Normal force measurements in pile T3 at the end of each load step, including the load measured by the load cell. For more details on strain-to-force conversion, see Section 6.1

5.6. 20th April 2022: Pile F3

Pile F3 was tested on the 20th of April, the last of all piles to be tested. Weather conditions throughout the test were warm and sunny with little to no breeze. Wind picked up slightly towards the evening.

Only two of the three fibre lines were working following installation of pile F3. Furthermore, the removal of the FO cables from the protruding reinforcing also created sharp bending points in the optical fibre, which inevitably affected the measurement quality and noise. The optical losses measured with the OTDR were approximately 5-15dB.

At the end of the main test, during the relaxation period, cracking in the grout at the pile head was observed. This grout was readily removable.

A load of 1000kN was left on the pile over the weekend to minimise settlement of the test frame. Measurements of strain were made for five minutes after reloading and stopped thereafter.

Table 5.11: Particularities associated with the test on pile F3

Relevant period		Remark
Time	Step	
11:17	Step 3	Interruption in FO strain measurements. Not clear as to the cause.
13:10	Step 5	Tape placed over the optical scope of the reference unit to reduce noise caused by the large amount of sunlight. Results in slight deviation in reference measurements.
14:51	Step 6 -> Step 7	Popping sound from around the pile/test frame. No visible evidence of damage and all equipment functioning correctly
19:53	Step 11	Pump cut out whilst trying to follow the failing pile. Resulted in slight drop in load during the starting up of the pump again. Relaxation carried out thereafter



Figure 5.71: Cracked grout at pile head



Figure 5.72: Sharp bending in the FO cable of pile F3, leading to loss in light intensity and reduction in measurement quality

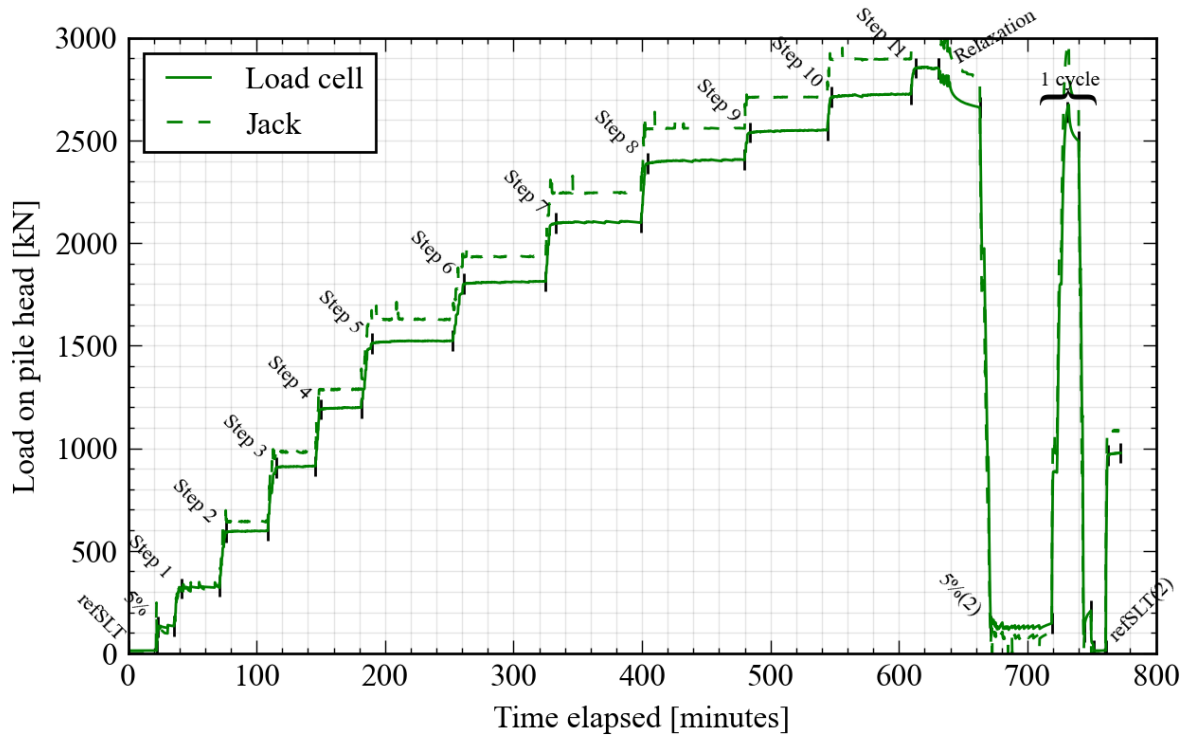


Figure 5.73: Plot of load exerted on pile head against the time elapsed for F3

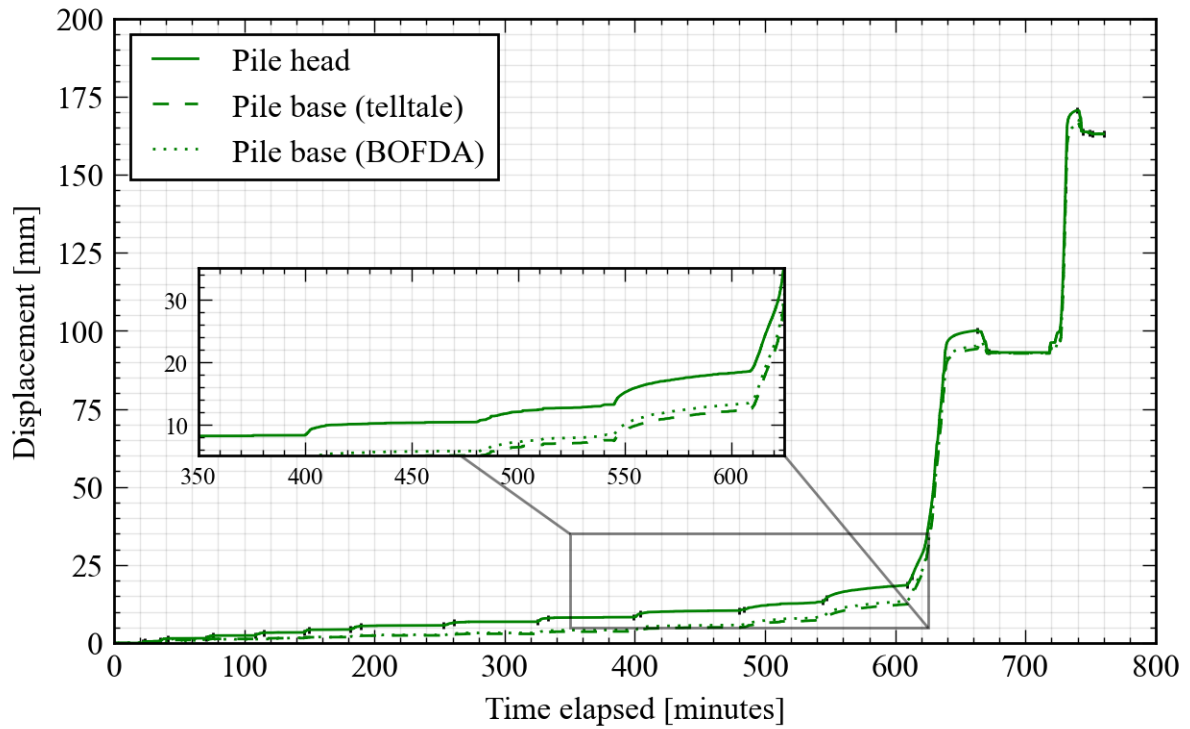


Figure 5.74: Plot of displacement measured at the pile head against the time elapsed for F3

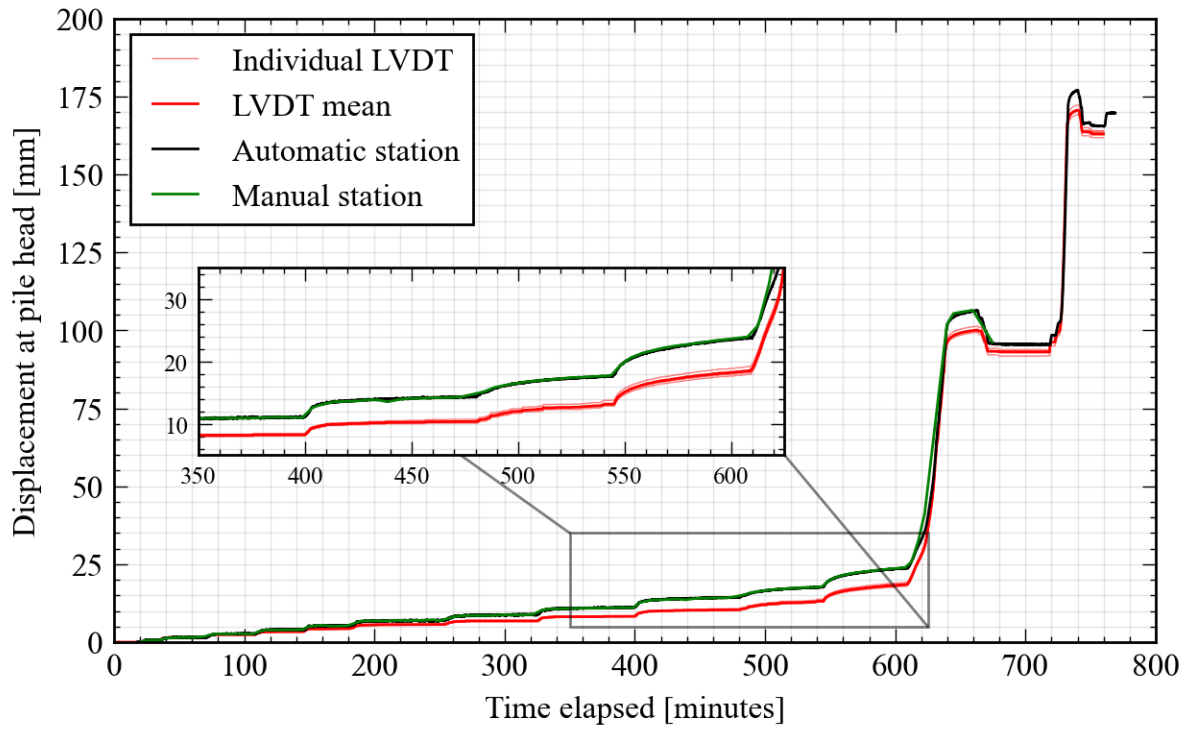


Figure 5.75: All pile head displacement readings for pile F3

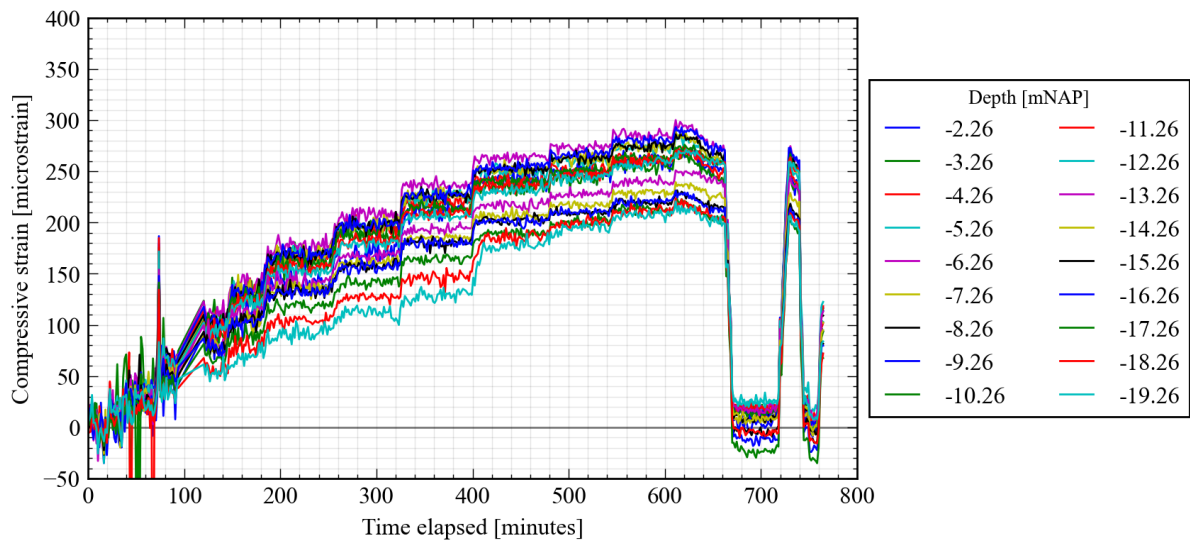


Figure 5.76: Plot of strain versus time for selected BOFDA increments for F3

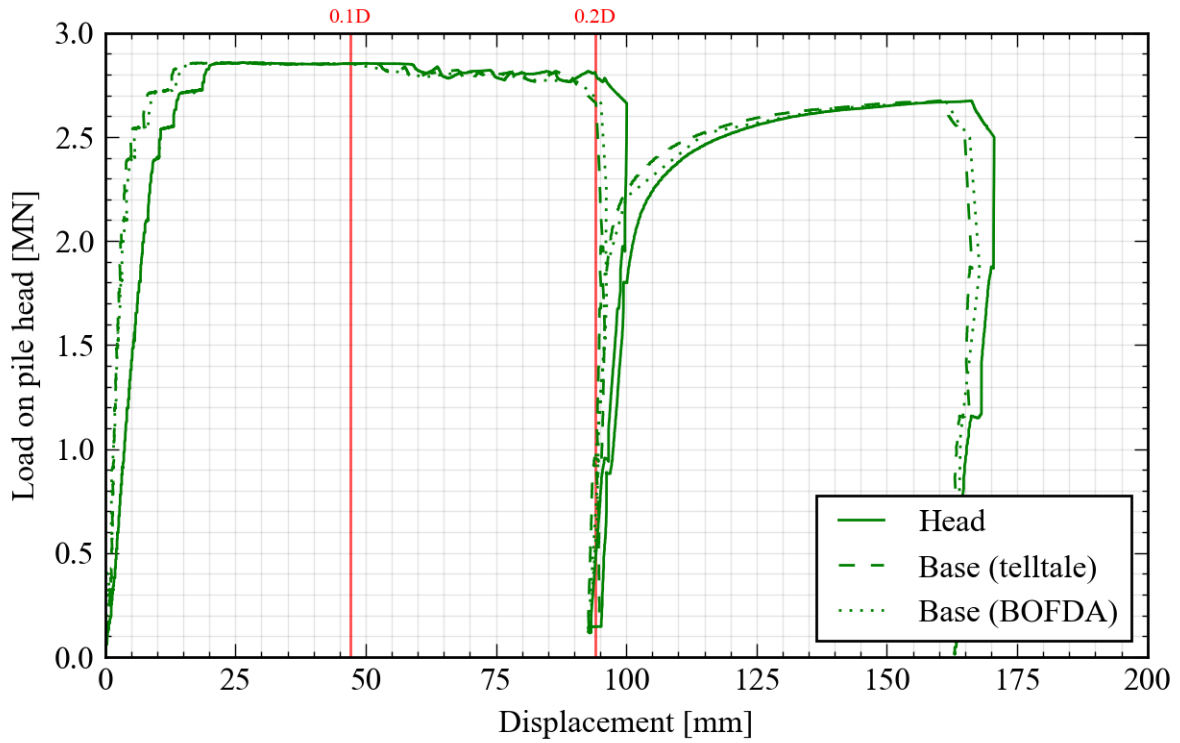


Figure 5.77: Plot of load versus displacement at pile head for F3

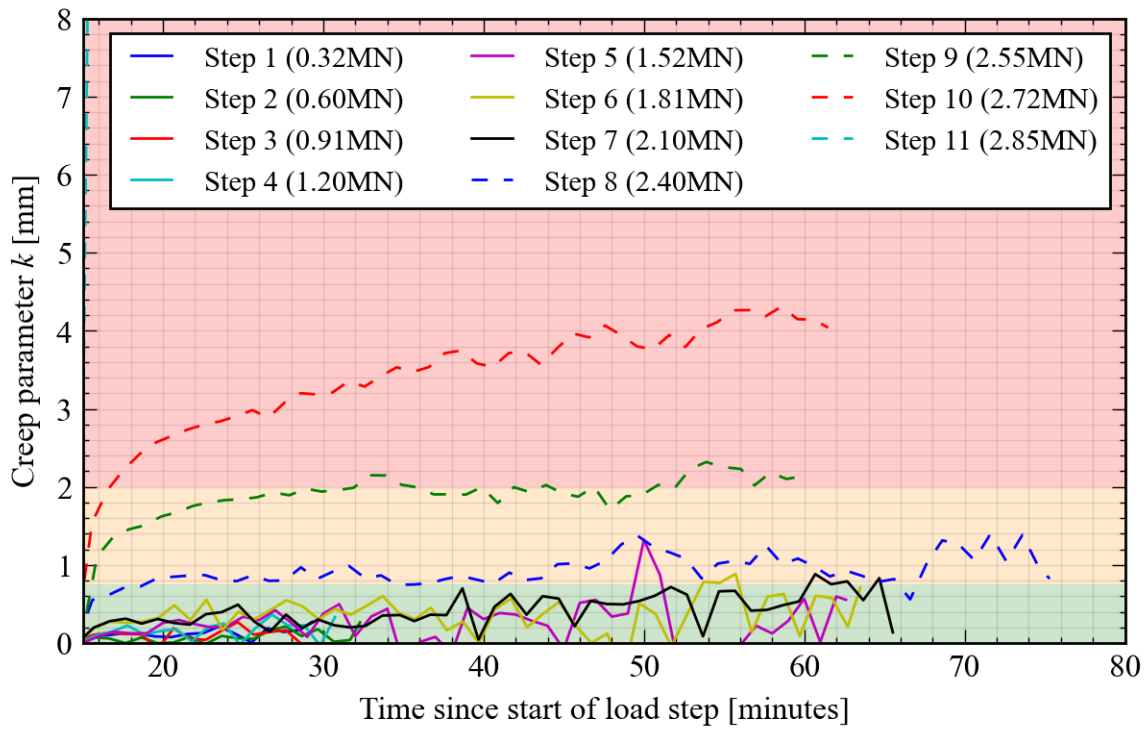


Figure 5.78: Creep parameter versus time across selected load steps for F3. The thresholds for increasing the step size/duration are also indicated

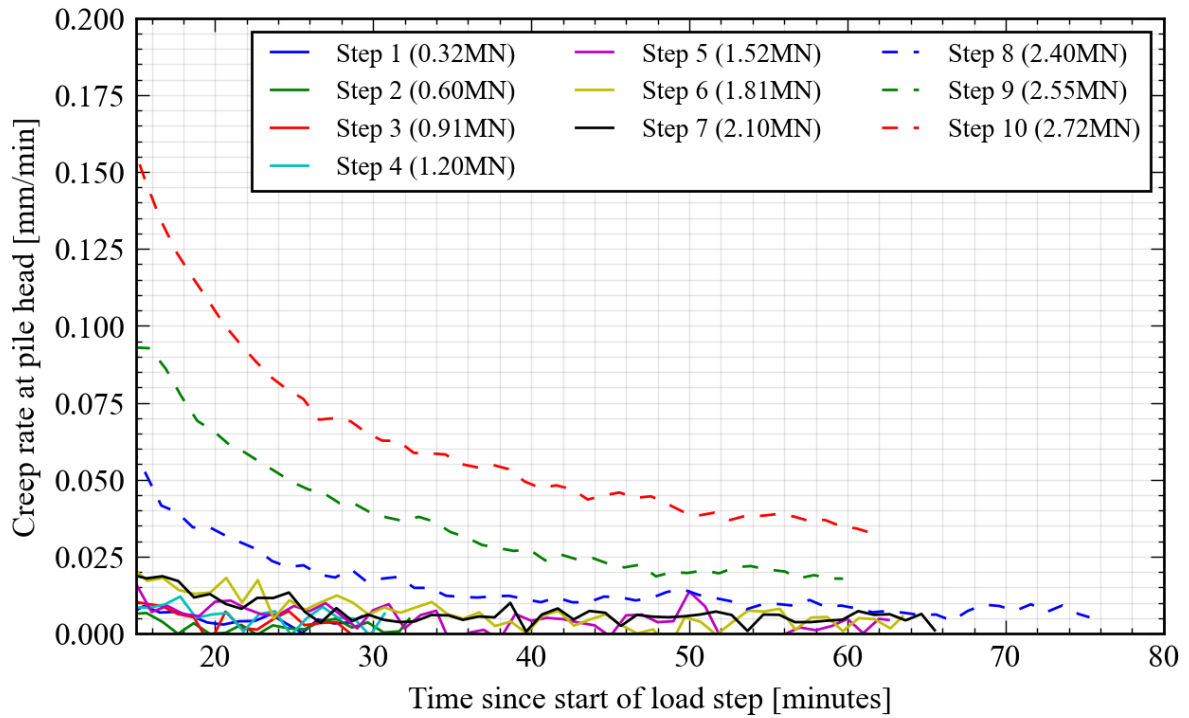


Figure 5.79: Creep rate versus time across selected loading steps for F3. Step 11 is not shown due to high creep rate

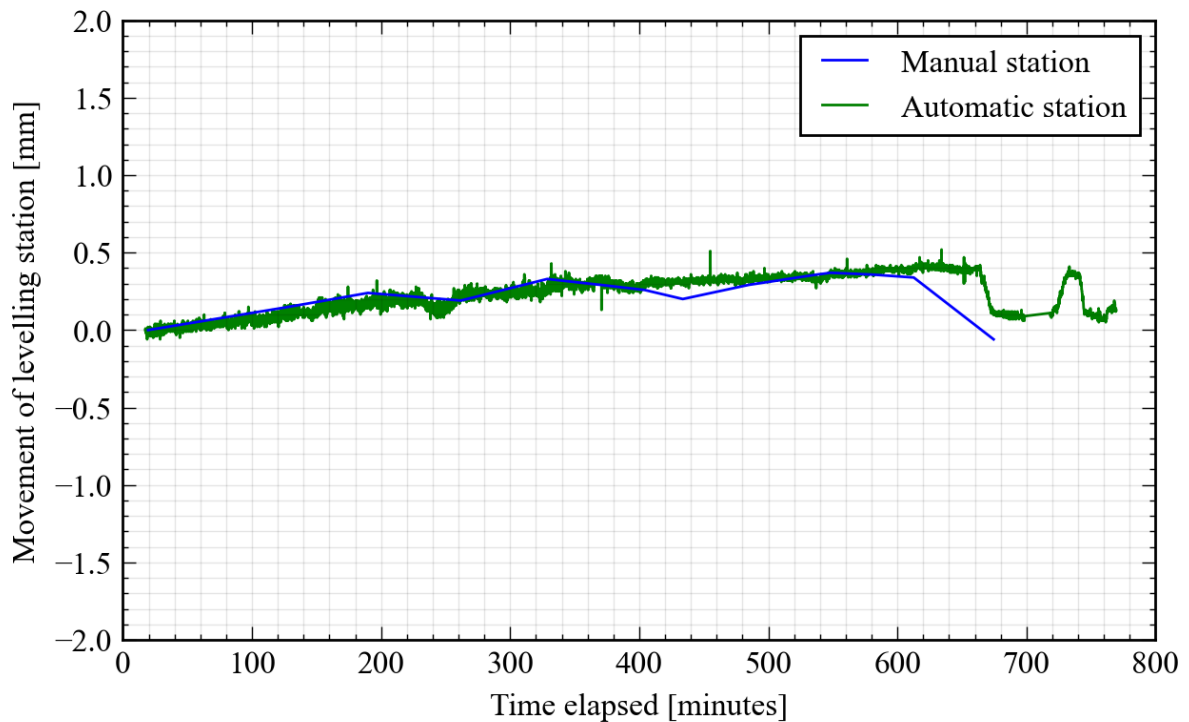


Figure 5.80: Movement of the levelling stations for pile F3, assuming a fixed reference point. Positive sign indicates upward movement

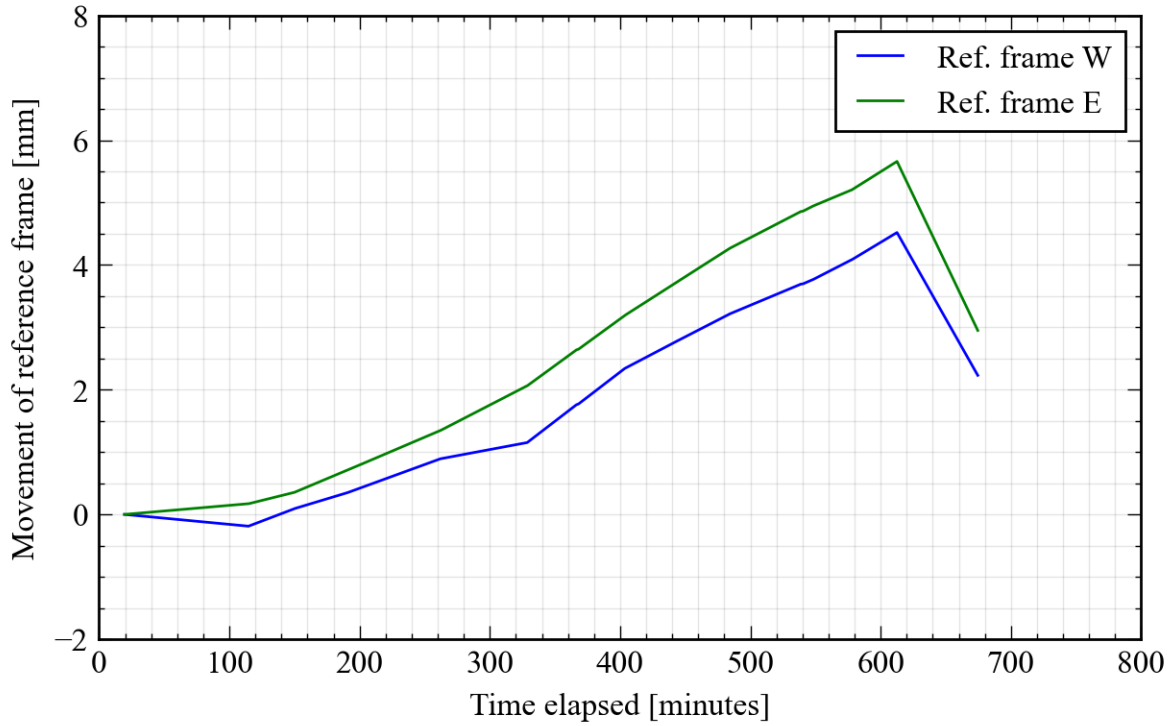


Figure 5.81: Measurements of the reference frame during the test on pile F3

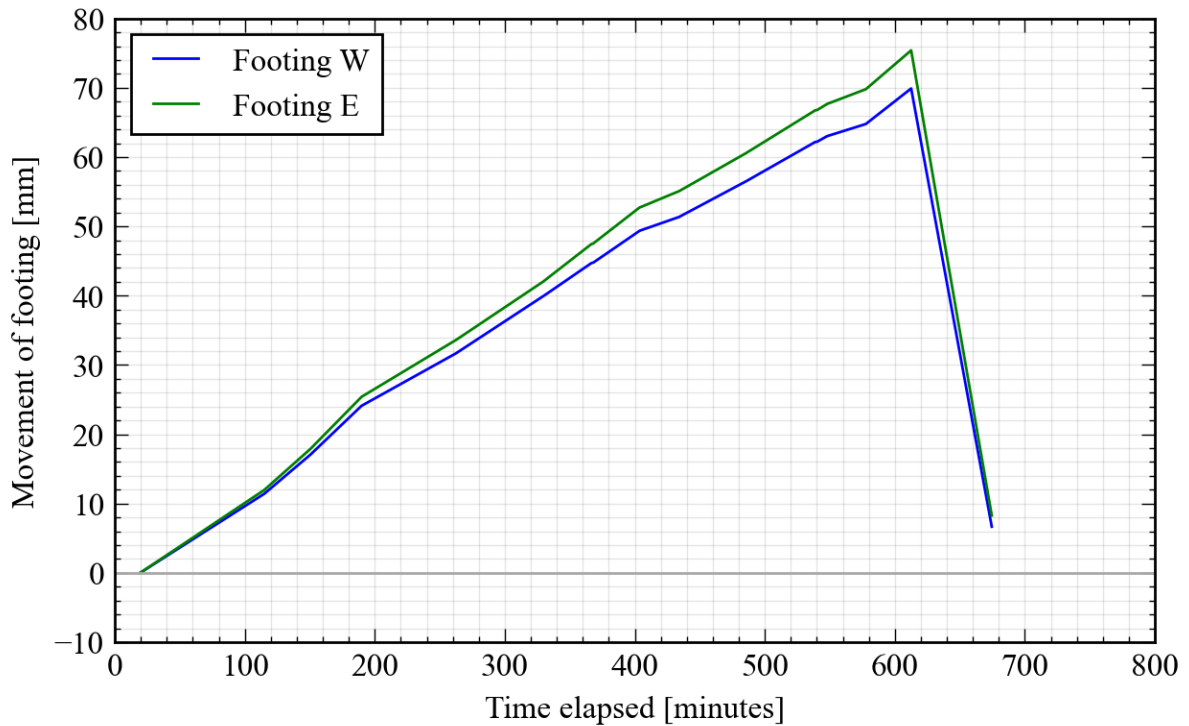


Figure 5.82: Measurements of the test frame footings during the test on pile F3. Positive sign indicates upward movement

Table 5.12: List of load steps and corresponding durations in pile test F3

Step	Start	End	Duration (HH:MM)	Average Load [kN]
refSLT	20/04/2022 09:20:25	20/04/2022 09:42:35	00:22	13
5%	20/04/2022 09:43:53	20/04/2022 09:56:10	00:12	130
Step 1	20/04/2022 10:01:58	20/04/2022 10:31:31	00:29	323
Step 2	20/04/2022 10:36:41	20/04/2022 11:09:14	00:32	596
Step 3	20/04/2022 11:15:41	20/04/2022 11:46:18	00:30	911
Step 4	20/04/2022 11:50:24	20/04/2022 12:21:50	00:31	1196
Step 5	20/04/2022 12:30:01	20/04/2022 13:33:11	01:03	1521
Step 6	20/04/2022 13:41:35	20/04/2022 14:45:32	01:03	1809
Step 7	20/04/2022 14:53:39	20/04/2022 15:59:40	01:06	2102
Step 8	20/04/2022 16:04:48	20/04/2022 17:20:23	01:15	2401
Step 9	20/04/2022 17:24:14	20/04/2022 18:24:39	01:00	2546
Step 10	20/04/2022 18:27:51	20/04/2022 19:29:48	01:01	2721
Step 11	20/04/2022 19:33:15	20/04/2022 19:51:23	00:18	2854
Relaxation	20/04/2022 19:51:23	20/04/2022 20:23:25	00:32	2720
5%(2)	20/04/2022 20:31:57	20/04/2022 21:19:24	00:47	131
Reload(1)	20/04/2022 21:31:09	20/04/2022 21:40:20	00:09	2557
Unload(1)	20/04/2022 21:44:23	20/04/2022 21:49:57	00:05	179
refSLT(2)	20/04/2022 21:51:52	20/04/2022 22:01:28	00:09	14
Reload(2)	20/04/2022 22:02:58	20/04/2022 22:13:02	00:10	923

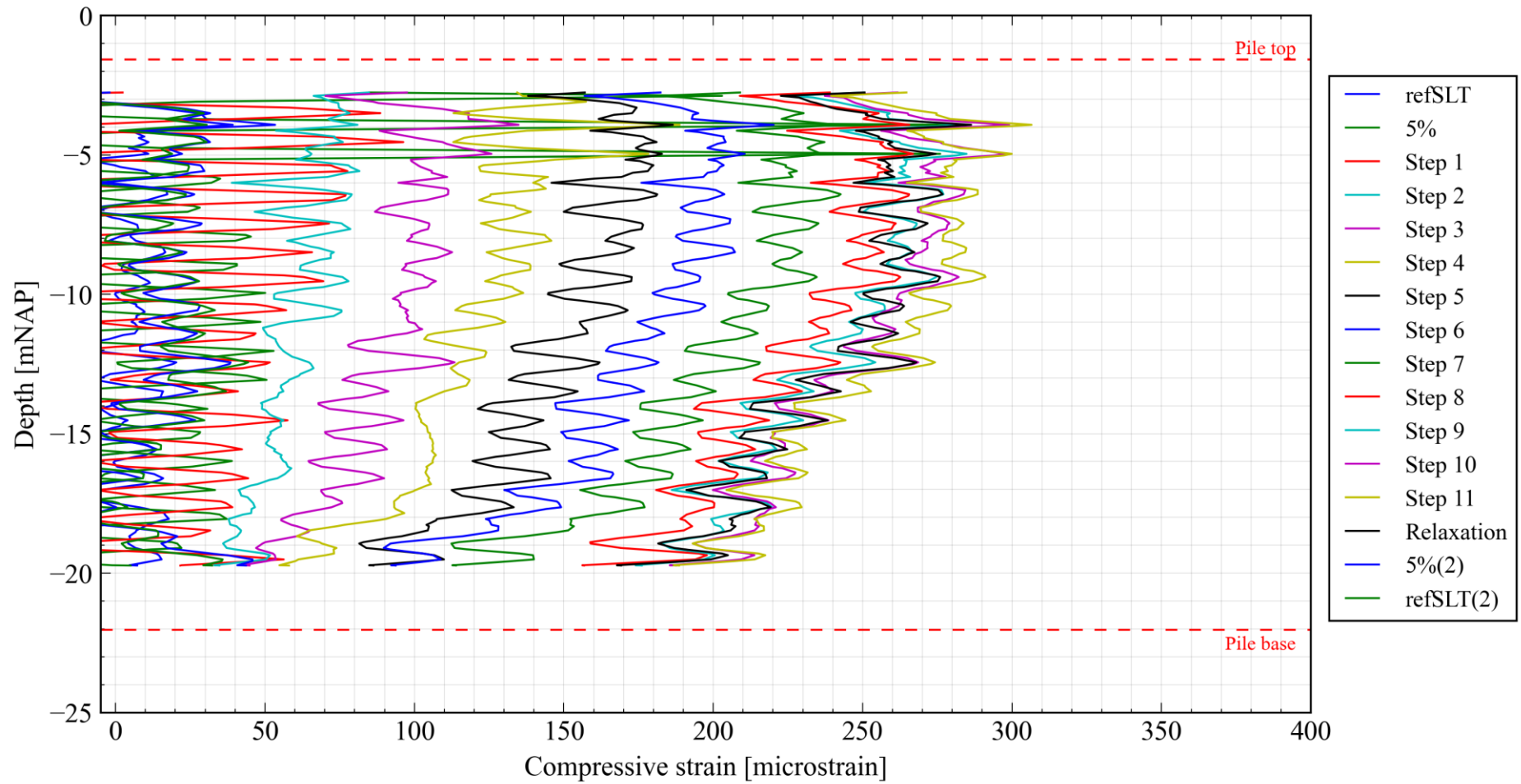


Figure 5.83: Strain measurements in pile F3 over the course of the load test (rolling average applied)

5.7. All Combined

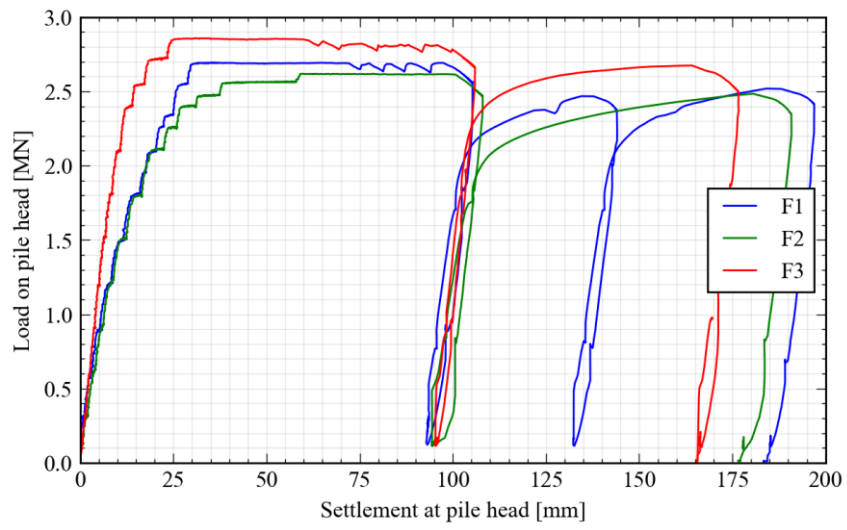


Figure 5.84: Load-displacement curves of the SI piles

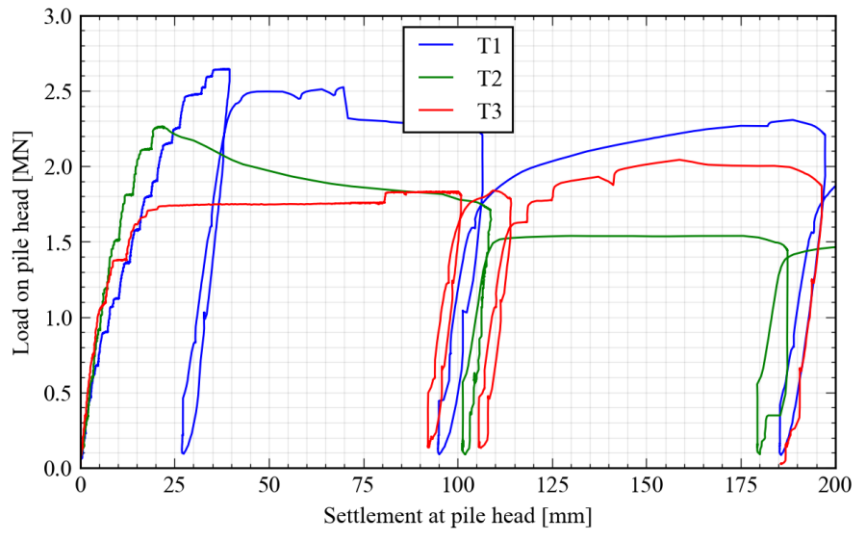


Figure 5.85: Load-displacement curves of the SIc piles

6. Data Interpretation

The full interpretation of the results, particularly in the context of Dutch design code and screw displacement piles overall, is presented in Duffy et al. (2024). This section includes several details not included—or at least just partially included—in the original publication.

Because of the installation problems with pile F3 (Section 0), the pile was deemed unrepresentative for considering the geotechnical capacity of the pile. Consequently, the pile was not considered in a detailed analysis.

6.1. Strain-to-force conversion

Theoretical stiffness

One of the primary difficulties of the strain-to-force conversion is anticipating the degree of influence of the grout shell, which may or may not be present along certain parts of the pile, particularly given the problems with return outflow during installation. As an initial consideration, a theoretical calculation is given in **Table 6.1**. In doing so, the grout shell diameter was assumed to be equal to the maximum pile tip diameter (0.47m), along with a relatively high grout stiffness of 20 GPa. A characteristic stiffness of 36 GPa was assumed for the C45/55 concrete used in both the SI and SIc piles. The calculations show that the grout is expected to contribute 20% at most to the theoretical (composite) stiffness.

Given the less-than-ideal conditions for concrete curing and concrete casting, the total stiffness is expected to be less than theoretical stiffness. Furthermore, the stiffness degradation coefficient m of all three piles is expected to be minimal as the maximum test load (<3 MN) is only one third of the total theoretical capacity (=9.5 MN) and so the response is expected to be relatively linear (Wight and MacGregor, 2012).

Table 6.1: Theoretical initial stiffness of the three piles

Pile	Grout [GN]	Concrete [GN]	Steel [GN]	Total [GN]
SI	1.20 (20%)	3.92 (63%)	1.03 (17%)	6.15
SIc	1.18 (15%)	3.46 (43%)	3.29 (41%)	8.04
F3	1.49 (16%)	2.63 (29%)	5.03 (55%)	9.15

Measured stiffness

Stiffness of the piles was derived using a combined interpretation of the secant stiffness $EA_{secant}(Q_0/\epsilon)$ and tangent stiffness $EA_{tangent}(\Delta Q_0/\Delta \epsilon)$ in the upper part of the pile, correlating the strains measured by the BOFDA sensors to the load measured in the load cell.

Based on experience with previous tests and also of other authors (Fellenius, 2001), the tangent stiffness is generally preferred. However, BOFDA measurements measure at lower frequencies compared to conventional pile test instrumentation (e.g. vibrating wire gauges) and so the derived tangent stiffnesses usually exhibit more noise compared to the secant stiffnesses.

Figure 6.1 and **Table 6.2** show the load-strain curves and the interpreted stiffnesses for each pile. The interpretation is summarised as follows:

- No stiffness degradation (strain-softening) was exhibited for any of the piles, in line with theoretical expectation. However, strain-hardening was exhibited by pile F2 and potentially piles F1 and T2. Two potential causes have been surmised: (1) influence of loading/unloading

of the test frame footings on the made-ground layer, and correspondingly, the pile itself (see Section 7.4) or (2) changes in load-transfer within the pile structure itself, with load being transferred more through the steel as microcracking developed within the concrete. With this in mind, the initial load-strain response was used to derive the stiffness for each pile.

- The SIc exhibited identical initial stiffnesses whereas the SI piles showed more dispersion—perhaps suggestive of the fact that the casing in the SIc piles leads to more consistent cross-sectional areas and corresponding stiffnesses.

For more details on the load-strain curves and derived stiffnesses for each pile, see Appendix F.

Strain was then converted to force assuming a constant stiffness along the entire pile length:

$$F = EA_{meas}\varepsilon$$

In reality, some variation is expected in EA with depth because of differences in the confining stresses provided by different soil layers and the presence/absence of a grout shell, like at the pile head (Section 4.5) where the measurements were made. However, there were no reliable means of deriving alternative stiffness values based on the data collected at the test site.

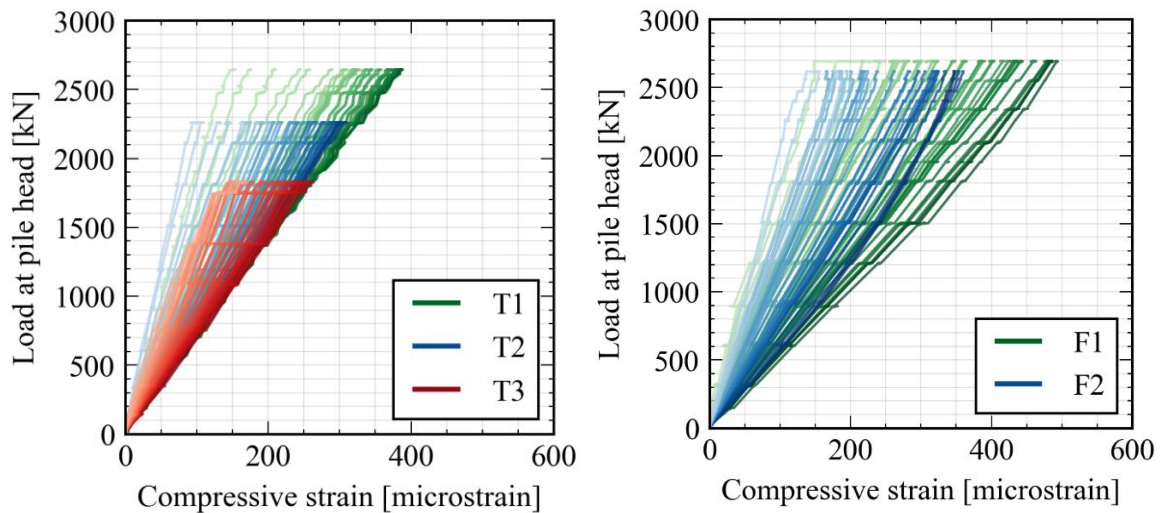


Figure 6.1: Measured load-strain curves across (left) the SIc piles and (right) the SI piles. Measurements closer to the pile base appear more transparent

Table 6.2: Chosen stiffness EA_{meas} (in GN) for each pile

Pile	EA_{meas}	Theoretical
F1	5.2	6.2
F2	6.3	6.2
F3	8.5	9.2
T1	6.8	8.0
T2	6.8	8.0
T3	6.8	8.0

6.2. Load distribution

The complete load distributions for each pile are given at end of each subsection in Section 5. A summary of these distributions is presented below in **Figure 6.2**, from which the following conclusions can be made:

- Pile T1 represents the “characteristic” load distribution of the site, where the load gradually reduces with depth through the soft upper layers. The load reduces at much higher rate through the lower sand layer, unsurprising given the higher strength of the layer.
- Periodic fluctuations with a frequency of 0.5m are seen throughout the load distribution of pile T1 as well as the other piles, likely corresponding to inhomogeneities within the fibre optic cables themselves. These fluctuations may affect the derivation of shaft resistance, particularly when shaft resistances over very small distances is being considered (say <0.5m).
- Sudden displacement at the pile heads of T2 and T3 occurred suddenly during the test, a change which also corresponded with a change in the load distribution in the lower sand layer. The onset of this sudden change in load-transfer is likely caused by structural failure of the grout shell, either at the grout-steel interface or within the grout body itself. The load distribution also appears to indicate that little to load is transferred in shaft resistance across this layer, and instead is transferred directly to the pile base.
- Piles F1 and F2 showed localised deviations in the load distribution across the layer of mixed sand and clay, particularly when compared to the S1c piles. Across the lower sand layer, the reduction in load is also not constant, with an initially slow reduction occurring across the first metre, followed by a reduction in load consistent with that of the S1c piles. It’s likely that the deviations in the load distribution are related the installation method of the SI pile—where the removal of the steel tube is likely to lead to a non-uniform cross-sectional area compared to an S1c pile. Problems with the return grout flow may have also exacerbated variations in cross-sectional stiffness, particularly in soft soil layers or at layer interfaces.

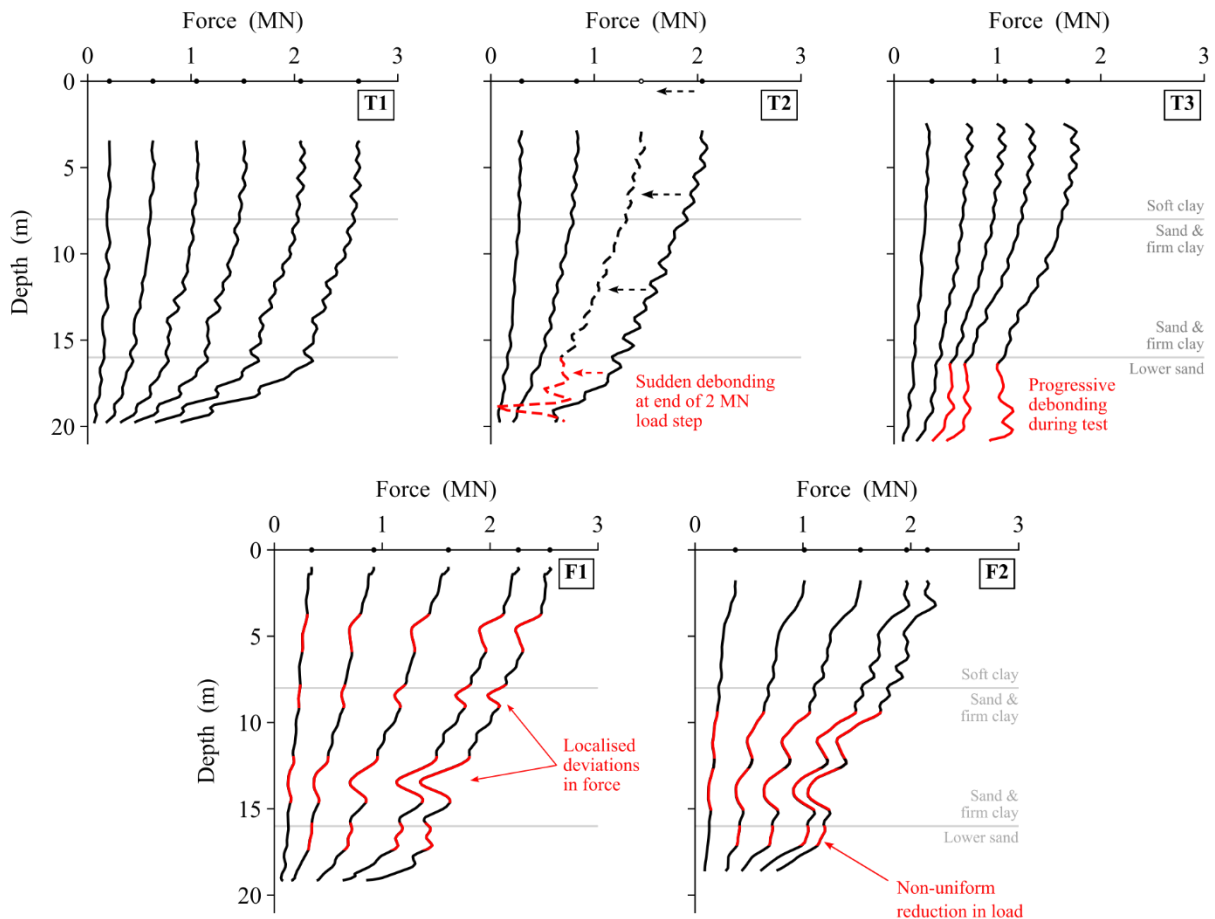


Figure 6.2: Load distribution at selected time steps for each pile. The load measured by the load cell on the pile head is indicated by a discrete point at 0m (NAP -2.2m)

6.3. Mobilisation of base and shaft resistance

To derive the base resistance, the last point of the load distribution was extrapolated to the pile base, a distance which ranged from 0.6D to 1.9D (**Table 7.1**). The area of the pile base was taken at the diameter of the outermost screw flange (=470 mm). For piles T2 and T3, which both failed structurally in the lower sand layer, it was assumed that no load could be transferred to the lower sand layer once structural failure occurred. Instead, the load at the top of the lower sand layer was transferred directly to the pile base.

The average shaft resistance in each layer was determined using the outermost diameter across all parts of the pile. For each layer, the average shaft resistance across the entire load distribution in the layer was calculated, excluding the red zones in **Figure 6.2** to remove the effect of structural discontinuities on the measurements. From this, the mobilisation curves in **Figure 6.3** and **Figure 6.4** were obtained. The sum of each of these mobilisation curves corresponds roughly to the load applied on each pile. To normalise the curves all four CPTs were used to calculate the average cone tip resistance $q_{c,avg}$. For the base resistance, the filter averaging method in De Boorder et al. (2022) was applied to each of the four CPTs, and then each of the four $q_{c,filter}$ values were averaged together.

The behaviour of all piles is comparable across all three layers—with primary exception being the soft upper clay layer where the SI piles mobilised peak resistances of 30–50kPa, compared to the 10–20kPa of the SIc piles (albeit subject to uncertainties regarding the pile stiffness and influence of the load

test frame, Section 7.5). In the Pleistocene peak shaft resistances of 230–250kPa are mobilised. Pile T1 mobilised the highest shaft resistances, however, problems with the test frame (Section 5.1) meant that the pile was unloaded before clear plastic failure was exhibited. Subsequent reloading resulted in a reduced shaft resistance of 180 kPa. By contrast, the SI piles exhibit a clear shear failure once post-peak dilatancy has finished, with post peak resistances of 170–200kPa.

Mobilised base resistances at a base displacement of $0.1D$ range from 2.4 MPa to 4.8 MPa. When normalised by $q_{c,filter}$, four of five piles show comparable α_p values of around 0.25. The only exception is pile T1 which mobilises an α_p of up to 0.5, albeit during the rapid reloading stages following the initial test.

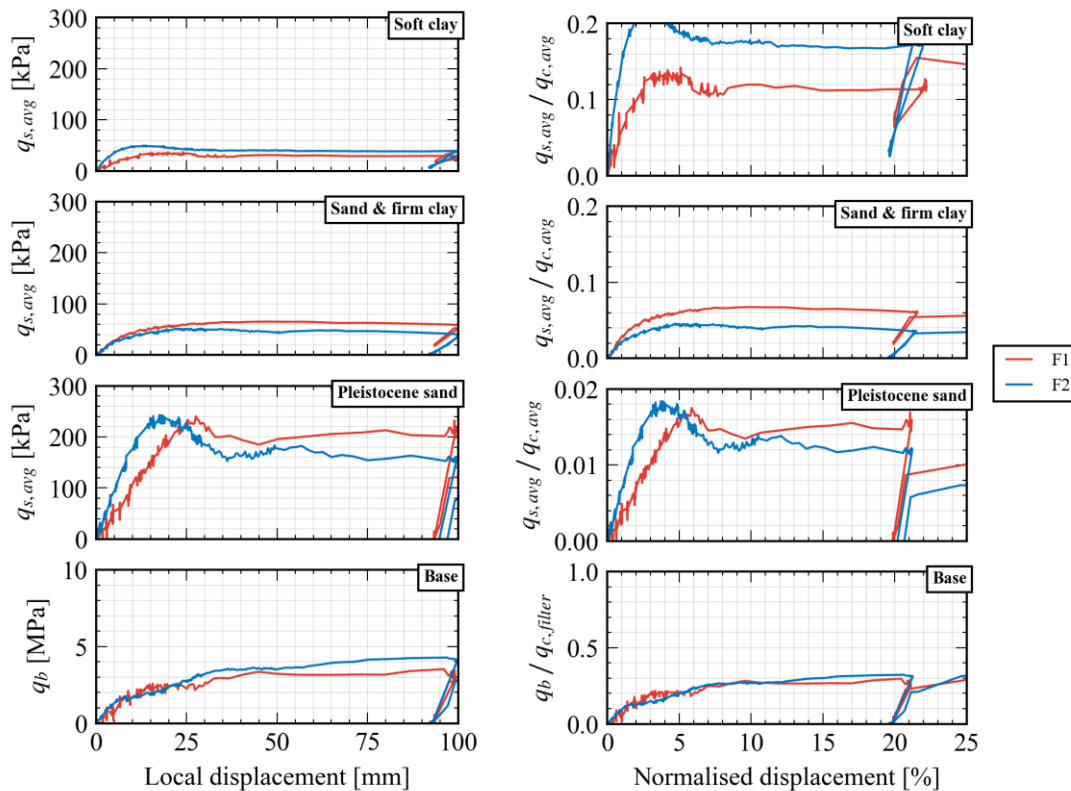


Figure 6.3: Mobilisation curves of the SI piles, both non-normalised (left) and normalised (right). Note: the y-axis scale is different for the normalised resistances in each layer

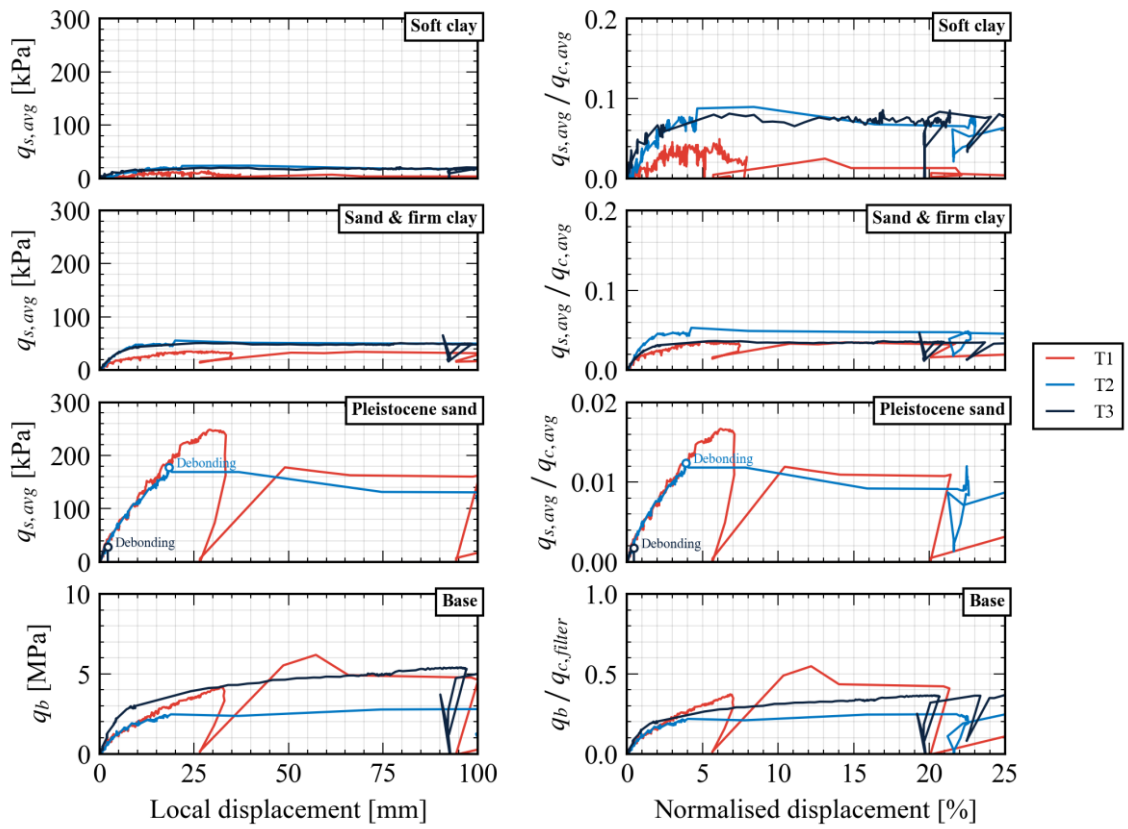


Figure 6.4: Mobilisation curves of the Slc piles, both non-normalised (left) and normalised (right). Note that the y-axis scale is different for the normalised resistances in each layer.

Table 6.3: Interpreted base and shaft resistances from the mobilisation curves

	Unit	F1	F2	T1	T2	T3
Shaft resistance: Soft clay						
$q_{c,avg}$	MPa	0.26	0.23	0.29	0.27	0.25
Peak $q_{s,avg}$	kPa	33	49	9	19	19
Peak α_s	-	0.127	0.213	0.031	0.070	0.076
Shaft resistance: Sand & firm clay						
$q_{c,avg}$	MPa	0.97	1.14	0.99	1.05	1.40
Peak $q_{s,avg}$	kPa	64	50	34	49	50
Peak α_s	-	0.062	0.057	0.034	0.051	0.070
Shaft resistance: Pleistocene sand						
$q_{c,avg}$	MPa	13.73	13.21	14.90	14.30	16.10
Peak $q_{s,avg}$	kPa	233	235	247	176	33
Peak α_s	-	0.017	0.018	0.017	0.012	0.002
Post-peak $q_{s,avg}$	kPa	200	170	n/a	n/a	n/a
Post-peak α_s	-	0.015	0.013	n/a	n/a	n/a
Base resistance						
$q_{c,filter}$	MPa	11.90	13.30	11.30	11.30	14.80
q_b at $s_b = 0.1D$	MPa	3.0	3.5	4.8	2.4	4.7
α_p at $s_b = 0.1D$	-	0.25	0.26	0.42	0.21	0.32
q_b at $s_b = 0.2D$	MPa	3.5	4.3	4.8	2.8	5.3
α_p at $s_b = 0.2D$	-	0.29	0.32	0.42	0.25	0.36

Unit shaft resistance

As an alternative interpretation of the shaft resistance, the unit shaft resistances in the lower sand layer are presented in **Figure 6.5**. For this, 0.5m long increments were taken along the load distribution, from which the unit shaft resistance was deduced. This includes both the maximum unit resistance measured and the resistance after post-peak dilatancy (not applicable for the SIc piles).

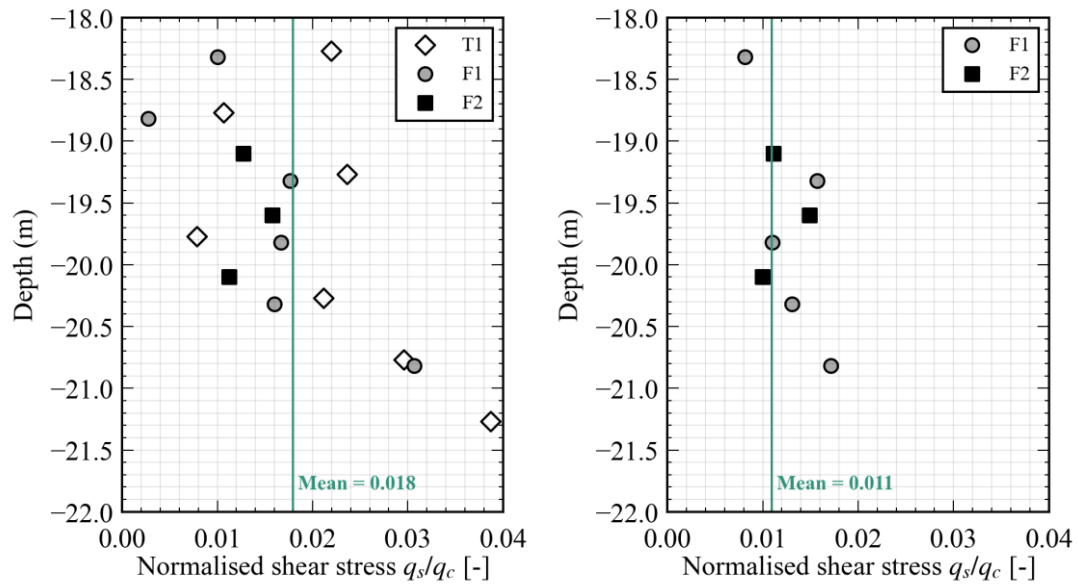


Figure 6.5: Unit shaft resistances across 0.5m increments (left) peak mobilised resistance (right) post-peak mobilised resistances—not applicable for the SIc piles

7. Data Quality & Lessons Learned

This section focusses primarily on the quality of the collected data, highlighting some of the uncertainties and inaccuracy associated with the collected data. Lessons learned are also incorporated into this section for the benefit of future practitioners performing load testing and for those interpreting the test results.

Conclusions with respect to the geotechnical performance of screw injection piles are presented in Duffy et al. (2024).

7.1. The benefits of instrumenting indoors

Both the SI pile reinforcement and SIc piles were instrumented indoors in a temperature-controlled environment on the premises of Deltares. For most test sites, procuring such a site is generally quite difficult or expensive. However the benefit of an indoor environment cannot be understated. Even within the Deltares warehouse, some rusting was observed on the steel when this was left overnight, albeit to a very small degree. In outdoor environments, the extent of steel corrosion will inevitably be much greater and so repeated scouring of the steel will need to be performed to remove this. Morning dew or rain will also significantly reduce the adherence of the glue, so maintaining a dry environment on-site is crucial and at the same time challenging.

Tying in with this, surface preparation in general is vital and well-recognised. To offer an illustrative example, Figure 7.1 shows the amount of dust that has accumulated on the surface of the steel reinforcing. This thin layer can lead to increased risk in debonding occurring between the glue and steel. In the case of this test site, compressed air was used to initially clean the surface although a degreasing agent was also needed to fully remove this thin layer.

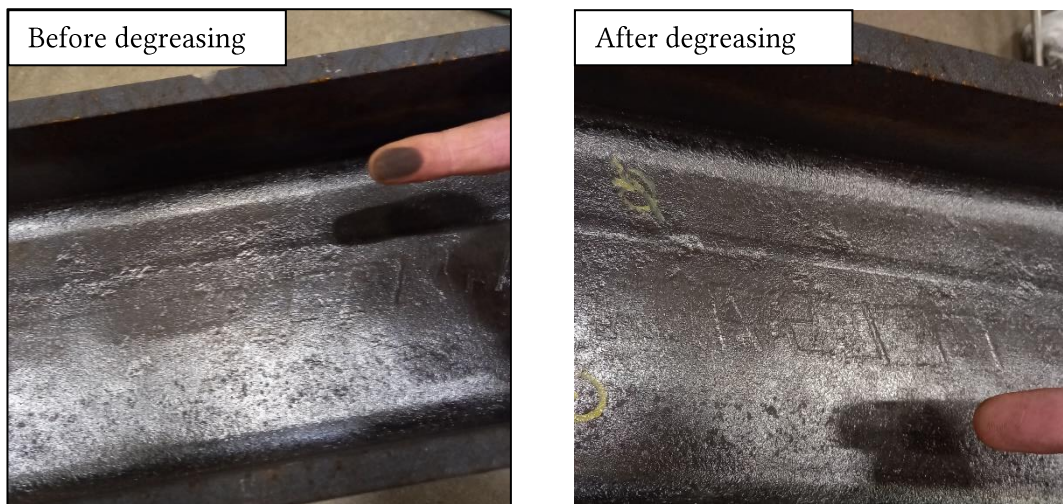


Figure 7.1: Simple finger swab of the steel reinforcing before and after degreasing and cleaning

Furthermore, every part of the fibre optic cable acts as a sensing element in distributed fibre optic sensors, so the surface area that needs to be prepared is also much greater. Instrumentation of all six piles (i.e. fifteen twenty metre long fibre optic lines) took roughly five days with two people.

7.2. Strain distribution at the pile ends

During each load test, the fibre optics measured along the entirety of the fibre optic network, including loops around the pile, within connection boxes, as well as the connection cable between the pile and the data logger. As a result, the actual elevation of the fibre optic readings had to be interpreted relative to the local elevation (mNAP) and the pile itself.

At the test site, the endpoints of the axial deformation measurement within the pile was done using detailed measurements during the instrumentation process (Appendix E.1) and by simple “stress tests” at the pile head prior to load testing, that is, observing changes in the measurements in response to a stress placed on the fibre optic at its entry point into the pile. The fibre optics readings were then sliced accordingly.

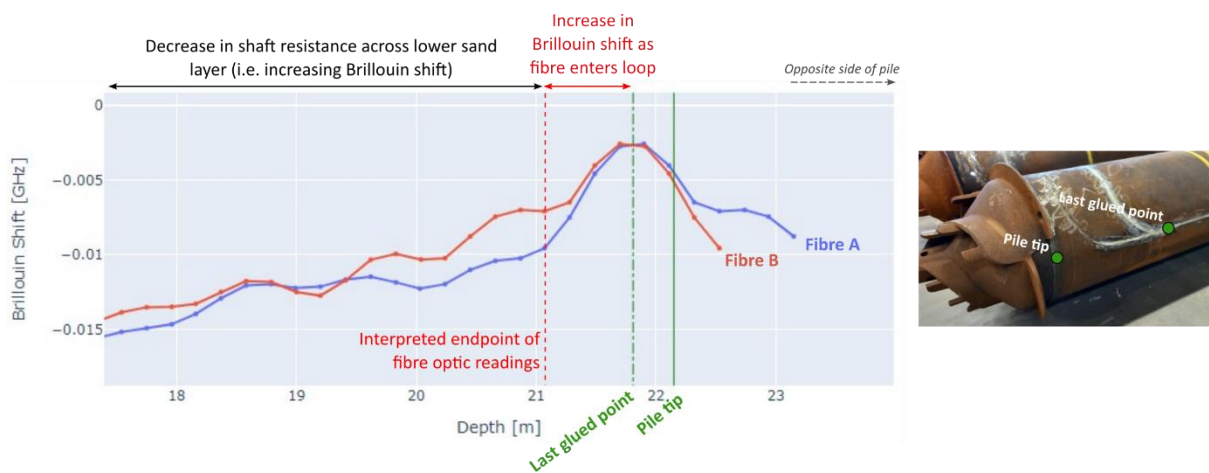


Figure 7.2: Fibre optic readings during a load test at the bottom of an S1c pile, showing how the endpoint of the readings is interpreted

However, for some piles there were larger-than-expected differences between the interpreted endpoint of the measurement and the predicted endpoint based on the measurements made during instrumentation, an effect that was also particularly prominent at the heads of the S1c piles. A similar effect was also encountered in previous tests in the InPAD programme, including the driven closed-ended pile tests and at Amaliahaven.

The spatial resolution of the fibrisTerre data logger (=20cm) inevitably plays a role in this, implying that any significant changes in measurements (e.g. fibre looping around the pile base) over a 20cm long interval will have an effect on the readings at a given point. This is potentially abetted by a non-uniform stress distribution across the entire pile cross-section and on the fibre optic cable itself at the top and bottom of the pile—meaning structural phenomena are affecting what is primarily meant to be a geotechnical measurement. The effect is also most significant the pile head—where bending at the pile head is likely to be another confounding factor.

Table 7.1: Comparison between the expected start and end of the fibre optic measurements (i.e. the last glued point) to what was interpreted from the readings

	Elevation pile head	Expected	Interpreted	Elevation pile base	Expected	Interpreted
F1	-1.68	-2.50	-3.31	-22.02	-21.12	-21.02
F2	-1.58	-1.66	-3.92	-21.28	-20.67	-20.59
F3	-1.58	-2.26	-2.26	-22.04	-20.41	-19.72
T1	-1.66	-1.85	-5.53	-22.15	-21.81	-21.81
T2	-1.82	-2.26	-4.92	-22.56	-22.20	-21.70
T3	-2.35	-2.83	-2.84	-23.13	-22.77	-22.80

7.3. Difficulties in sustaining a constant load

In a couple of instances during load testing, the hydraulic pump (Enerpac ZE5840LW-R; max. flow rate of 1.64 L/min) connected to the jack could not keep up with the pile at high rates of displacement. This most notably occurred towards the end of the test on pile T2 (Section 5.3) where the pile displaced rapidly upon failure however the pump could not react quickly enough to sustain a constant load.

With the exception of the latter stages of pile F1, the load steps have been executed within the 1% margin of error prescribed by NPR 7201 (**Figure 7.3**). This is primarily a concern at load steps close to failure.

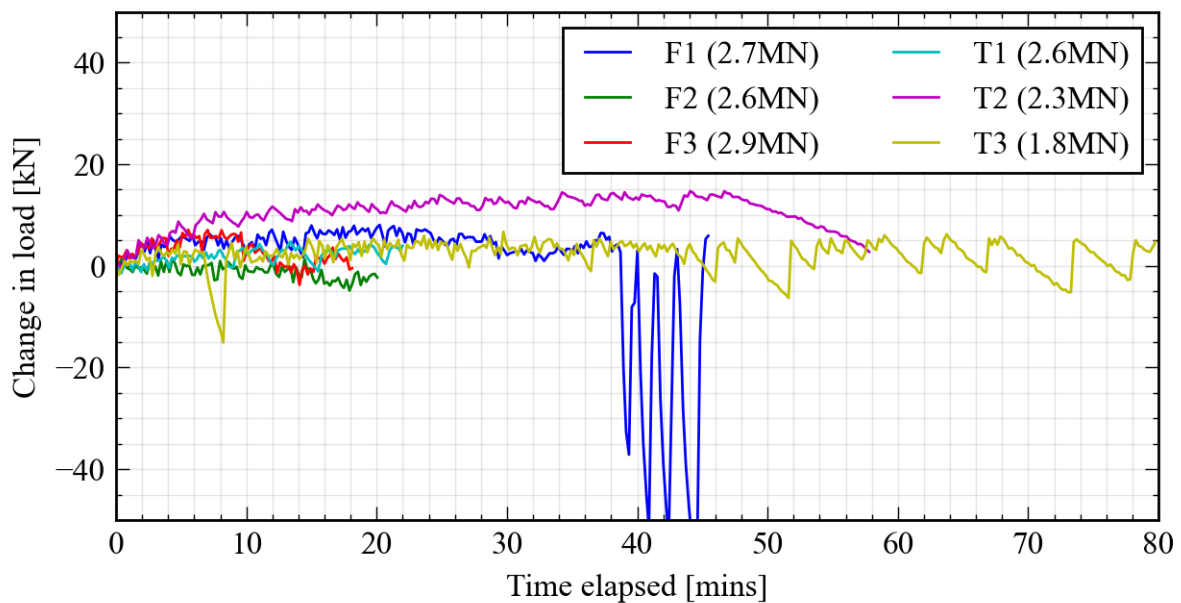


Figure 7.3: Comparison of the change in applied load at the final load step prior to failure

7.4. Impact of loading on levelling stations

The automatic levelling station made measurements of a reference point located at different locations for each test (**Table 7.2**; Appendix E.4), shown in **Figure 7.4**. The top graph of **Figure 7.4** shows the measurements of the levelling station's temperature sensor. The temperature fluctuates by $\pm 10^{\circ}\text{C}$ and as expected, reaches a peak just after midday and reduces over the course of the afternoon and evening.

In the bottom graph, the levelling measurements show clear changes with time, varying by up to 1.5mm. A persistent noise is present in all readings, ranging from $\pm 0.1\text{mm}$ for pile T1 to $\pm 0.3\text{mm}$ for pile T2. Some this noise can be attributed to the accuracy of the levelling station, reported as 0.3 mm. (Appendix D.3). The noise may also correlate with the local weather conditions. For instance, the tests on F3 (in grey) and T3 (in green) were performed on days where the sunlight was relatively consistent throughout with little clouds or rain (**Table 7.2**). Both piles also show little noise in the measurements, measuring less than 0.1 mm.

Table 7.2: Location of the reference station. More details are given in Appendix E.4

Pile	Location	Wind	Clouds?	Sun?
F1	Crane	Strong breeze	Cloudy	Occasional
F2	Pile	Light breeze	Cloudy	Occasional
F3	Pile	Light breeze	None	All day
T1	Tripod	Breeze	Cloudy with showers	None
T2	Pile	Breeze	In the afternoon	In the morning
T3	Tripod	Light breeze	None	All day

Very little thermal expansion of the Invar beacons and levelling station tripods is expected since both are made of aluminium, with a thermal expansion coefficient of $<1.5 \times 10^{-6}$. The levelling measurements verify this, as the peak of the levelling measurements does not correspond with the peak of the temperature measurements. Instead, the measurements correspond with the peak load applied on the piles. The effect of the unload/reload cycles at the end of each load test is also clear, causing movements of up to 0.6 mm. These measurements imply that the levelling station moved upwards when the test load increased because of the relieving effect of the test frame footings on the surrounding soil.

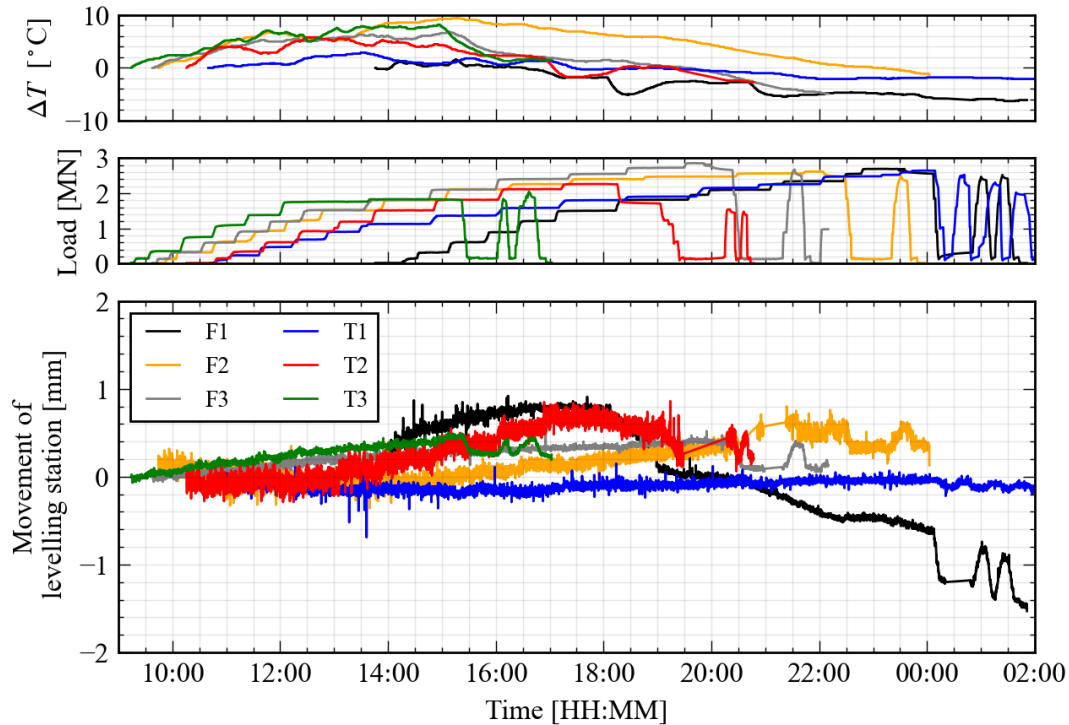


Figure 7.4: Measurements of the levelling station across all piles, assuming the reference point is fixed. Temperature was measured in the levelling station itself

In all cases, the levelling station was placed on the fill layer. Pile T1 was the only pile where the made ground was below surface level and not directly under the footings. Correspondingly, pile T1 exhibits little deviation over the course of load test, with a maximum deviation of ± 0.2 mm.

To summarise, the impact of localised ground movement on the levelling stations is relatively marginal for interpreting the tests, with a maximum error of approximately ± 1 mm expected. The measurements of the pile head displacement have been corrected for based on these reference point readings.

7.5. Impact of loading on reference frame

Ground-induced movements of the reference are also expected. This reference frame was used for the potentiometer readings and consisted of two wooden beams connected to one another. The beams rested on two dragline mats, 11m apart (**Figure 7.5**). The movement of both beams during the load test was recorded using the manual levelling station (**Figure 7.6**). The recorded movement of both beams was very similar so only the measurements of the “western” beam has been presented in **Figure 7.6**.



Figure 7.5: Reference frame, resting on dragline mats, each 5.5m away from the pile

Figure 7.6 shows that there isn't a consistent trend in the movement of the reference frame across all the load tests. For example, loading affects the reference frame of piles F2, F3 and T3 quite similarly, but on the other hand, piles T1, T2 and F1 show little effect of loading. The only exception to this is the sudden displacement at the end of testing pile T2 (at 18:00) and during the loading cycles on pile T1. However, this may have been caused by either the load cycles or when the potentiometers were adjusted to allow for additional stroke, accidentally causing a movement of the frame or beacons.

Some of the movement may have been caused by the unloading of the soft upper clay as the load is transferred from the footings to the pile (Section 7.5). However, it is not clear why two diverging trends were recorded across the piles.

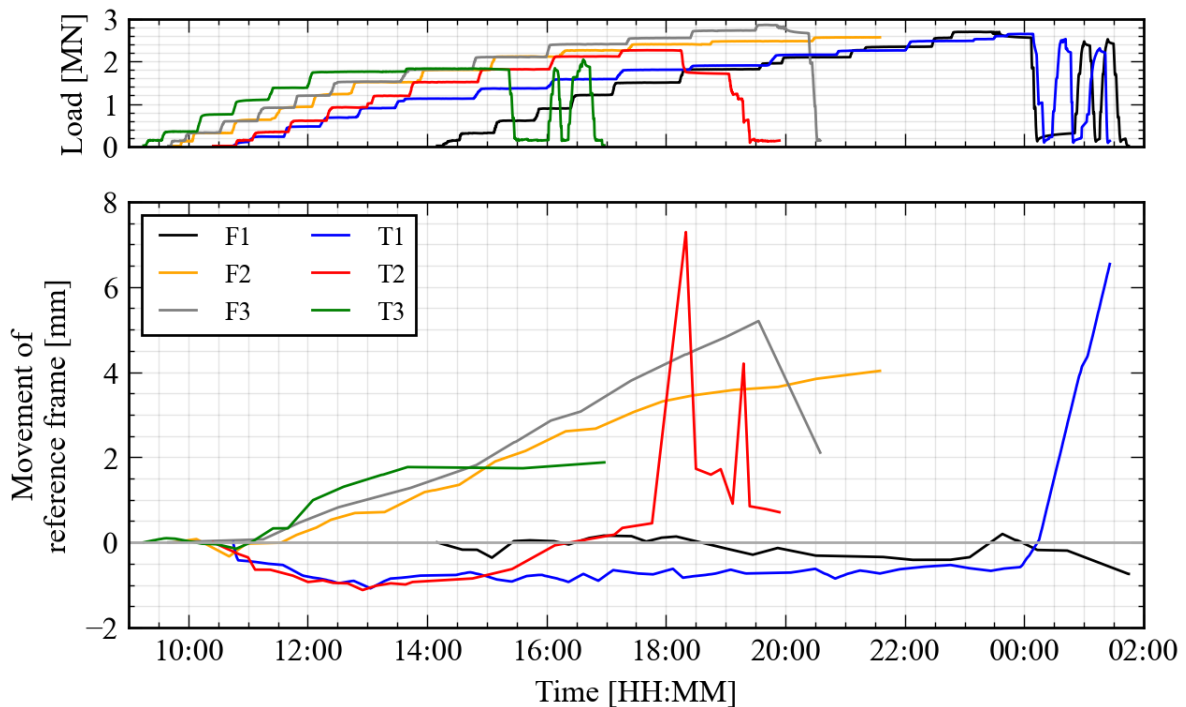


Figure 7.6: Movement of the western reference frame across all piles, compensated by relative movement between the levelling stations and the reference point

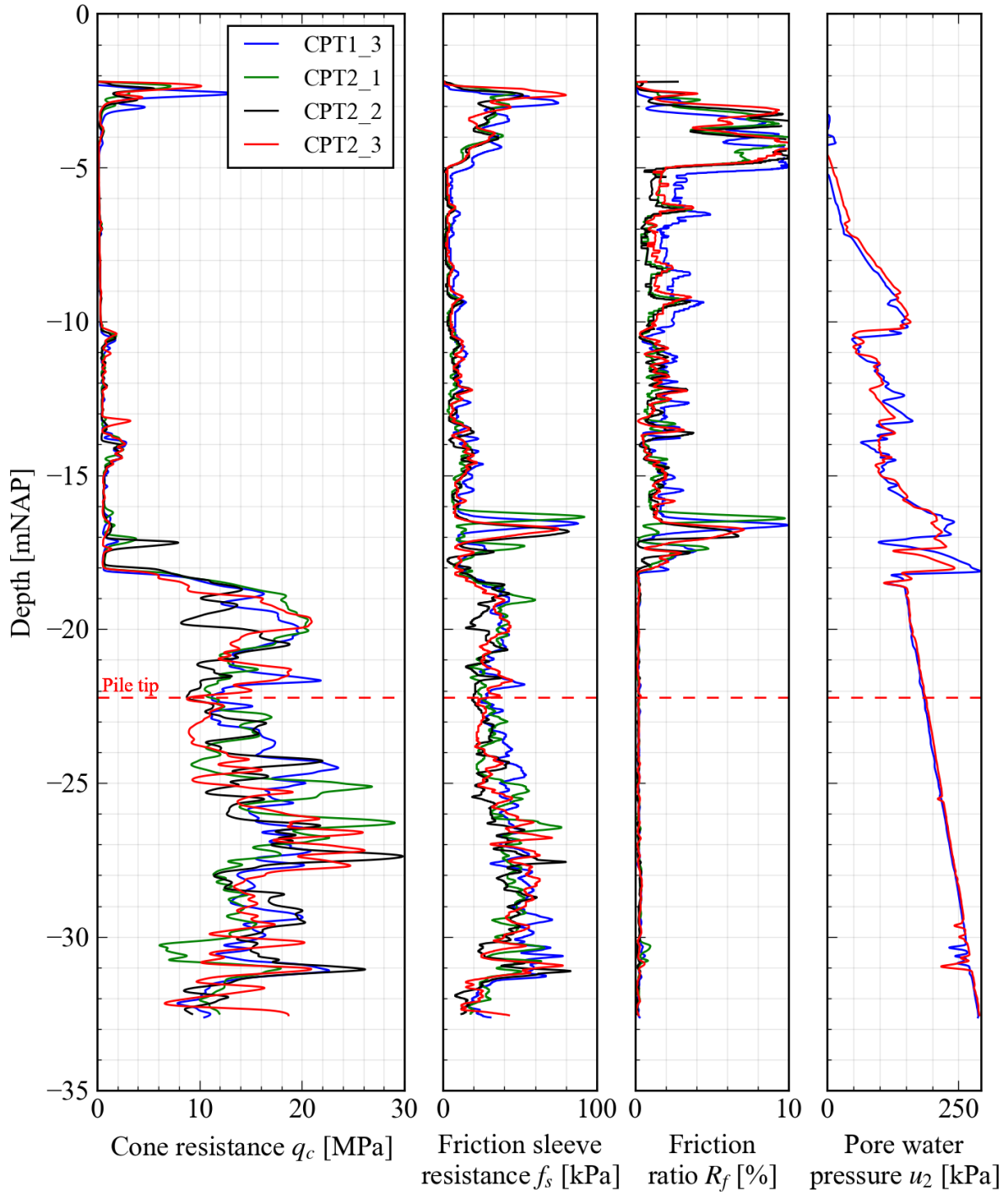
References

- de Boorder, M. (2019) *Development of a new CPT averaging technique and review of existing CPT based methods for the calculation of total pile capacity*. M.Sc. Thesis. TU Delft.
- de Boorder, M., de Lange, D.A. and Gavin, K.G. (2022) 'An alternative CPT averaging procedure to estimate pile base capacity', in *Proceedings from the 11th International Conference on Stress Wave Theory and Design and Testing Methods for Deep Foundations. The 11th International Conference on Stress Wave Theory and Design and Testing Methods for Deep Foundations*, Rotterdam, The Netherlands. Available at: <https://doi.org/10.5281/zenodo.7142197>.
- Duffy, K.J., Gavin, K.G., de Lange, D.A., *et al.* (2024) 'Base resistance of screw displacement piles in sand', *Journal of Geotechnical and Geoenvironmental Engineering*, 150(8), p. 04024070. Available at: <https://doi.org/10.1061/JGGEFK/GTENG-12340>.
- Duffy, K.J., Gavin, K.G., Korff, M., *et al.* (2024) 'Influence of the installation method on the axial capacity of piles in very dense sand', *Journal of Geotechnical and Geoenvironmental Engineering*, 150(6). Available at: <https://doi.org/10.1061/JGGEFK/GTENG-12026>.
- Fellenius, B.H. (2001) 'From strain measurements to load in an instrumented pile', *Geotechnical News Magazine*, pp. 35–38.
- NEN (2017) *NEN 9997-1+C2:2017*. Delft, The Netherlands: Nederlands Normalisatie-Instituut (Geotechnisch ontwerp van constructies - Deel 1: Algemene regels).
- NPR 7201 (2017) *NPR 7201:2017 - Geotechniek - Bepaling van het axiaal draagvermogen van funderingspalen door middel van proefbelastingen*. Delft, The Netherlands.
- Wight, J.K. and MacGregor, J.G. (2012) *Reinforced Concrete: Mechanics and Design*. 6th edn. New Jersey, USA: Pearson. Available at: </content/one-dot-com/one-dot-com/us/en/higher-education/product.html> (Accessed: 23 March 2021).

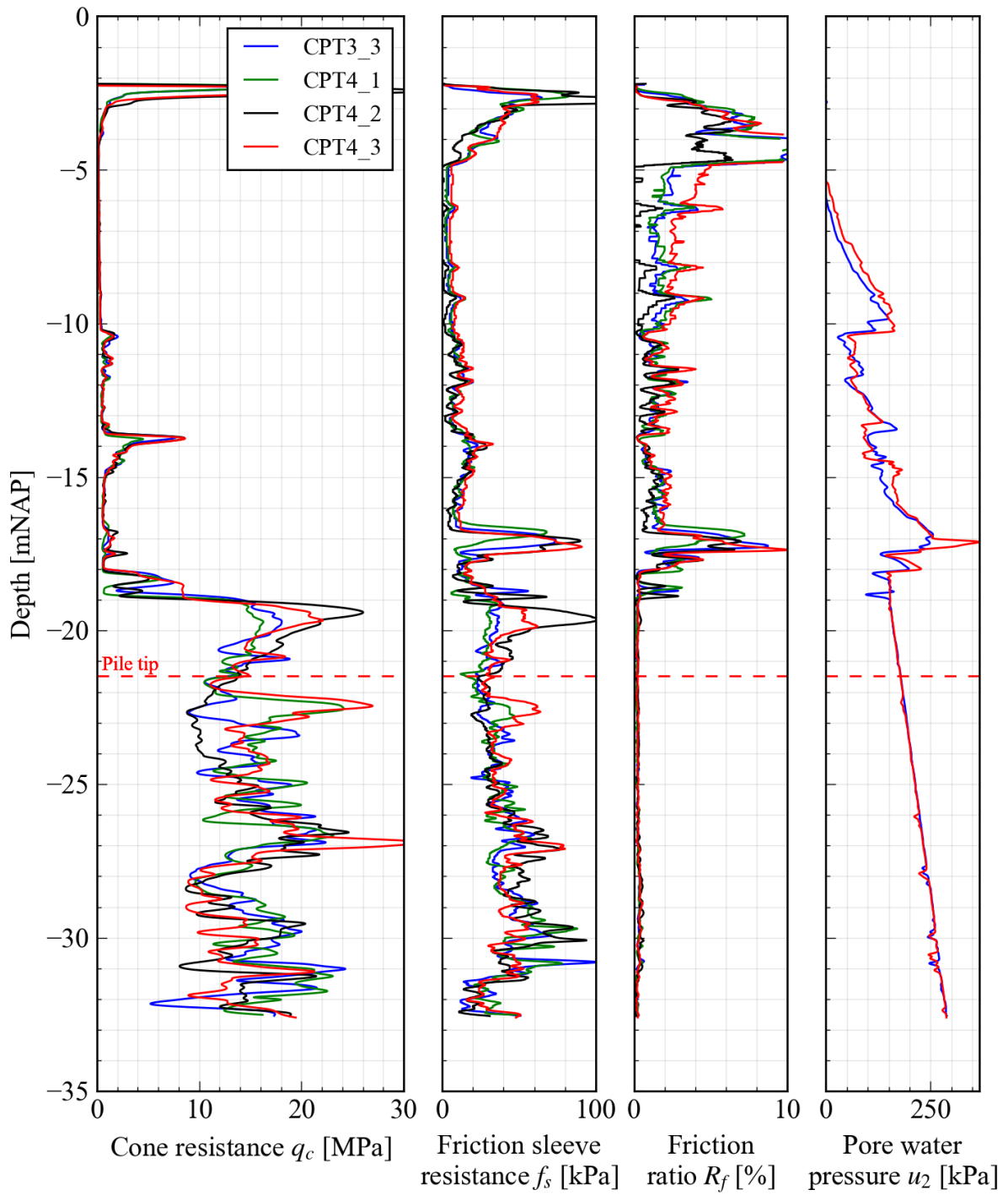
Appendix A Site Investigation: CPTs

The following plots present all CPTs within two metres of each pile. CPTs have not been corrected for inclination and no correction of the cone resistance for excess pore water pressure has been made (i.e. q_t).

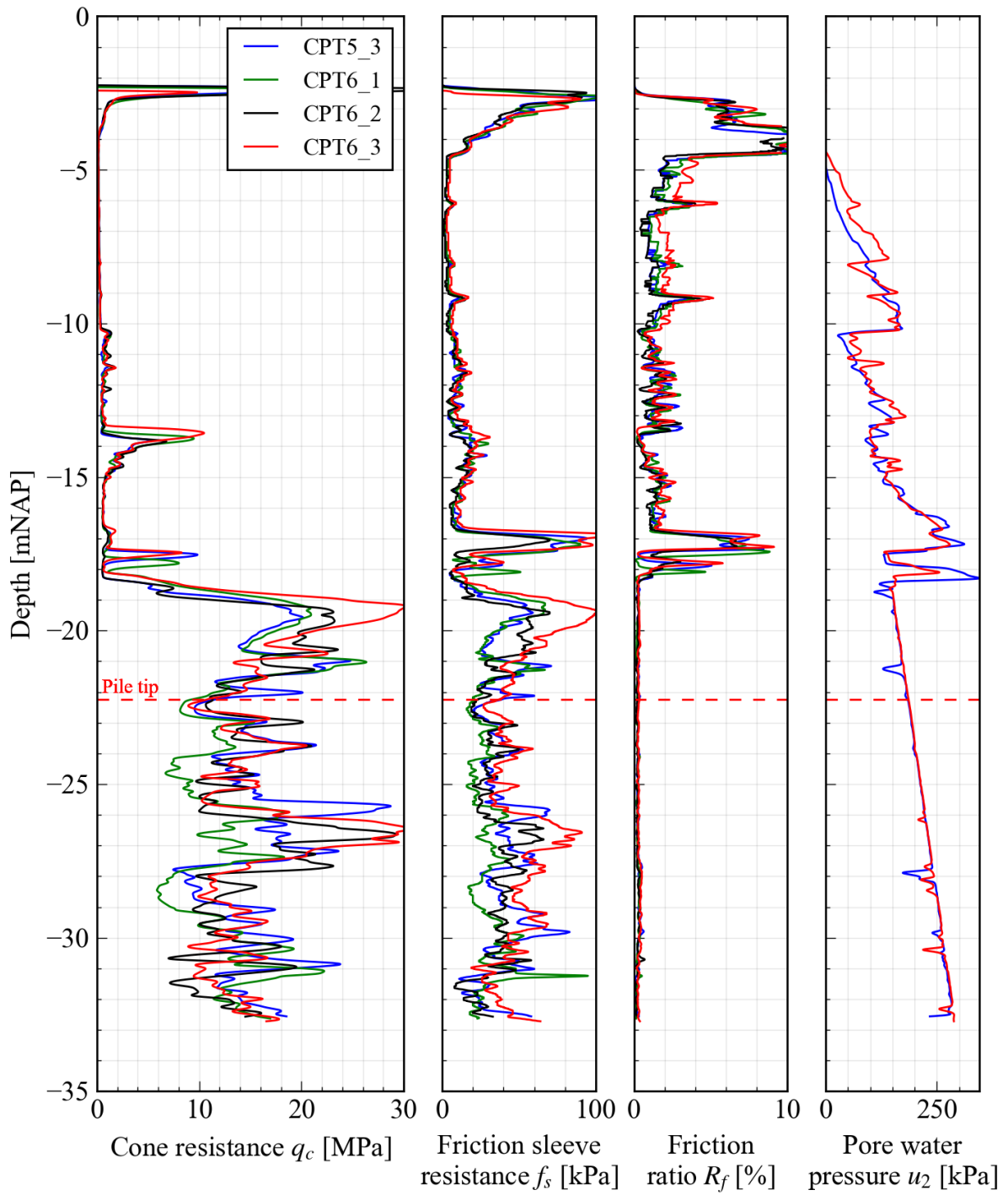
A.1 F1



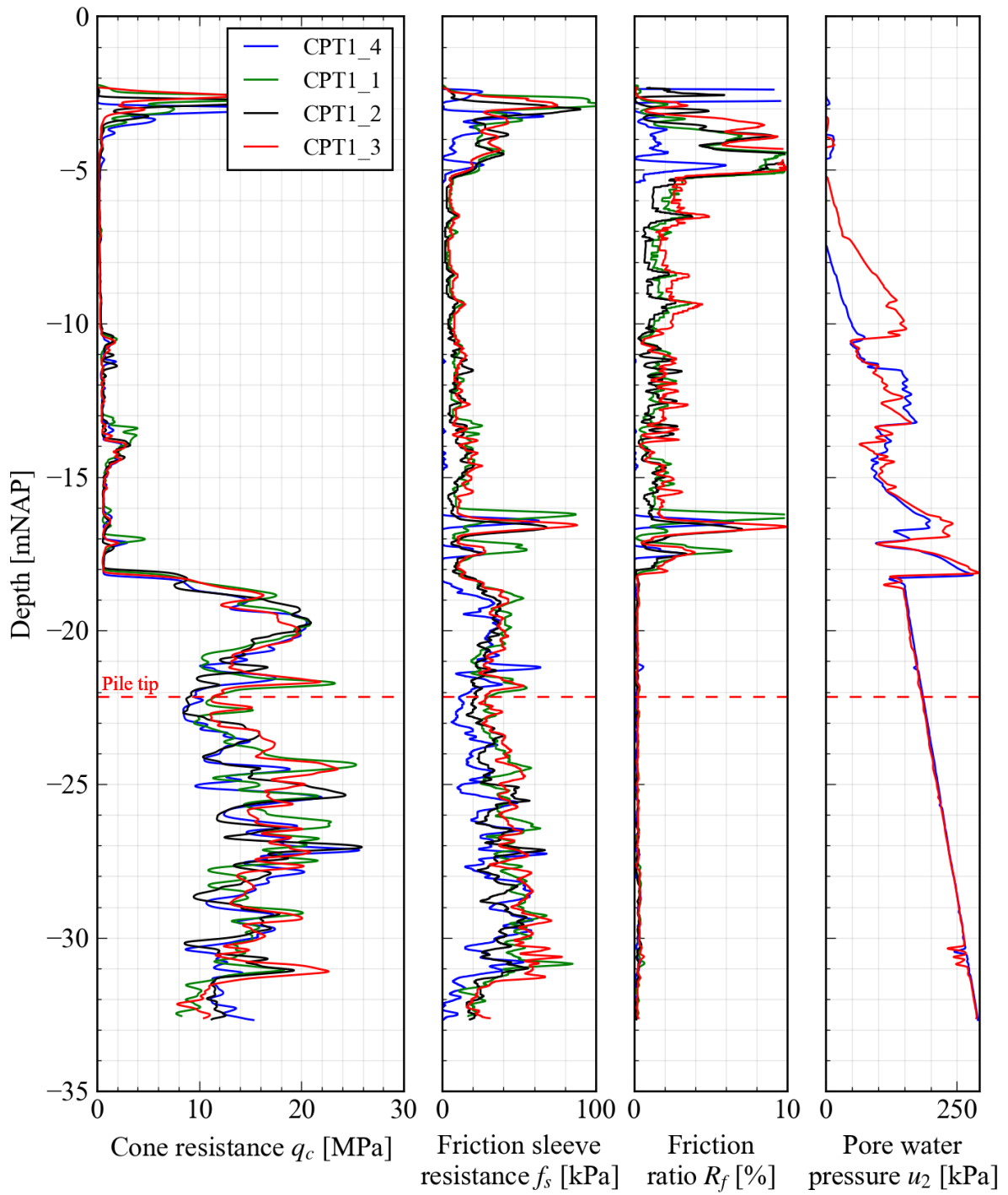
A.2 F2



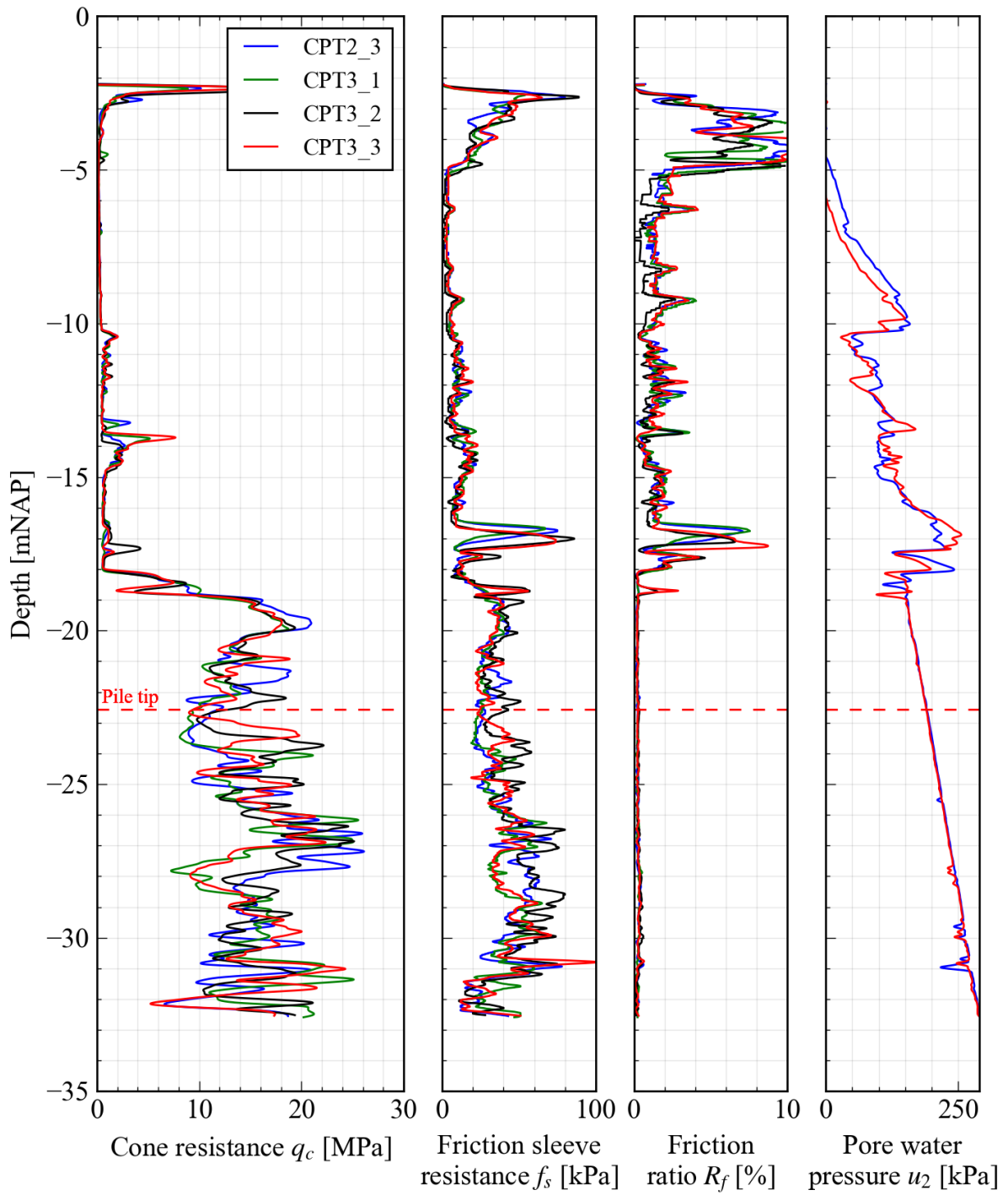
A.3 F3



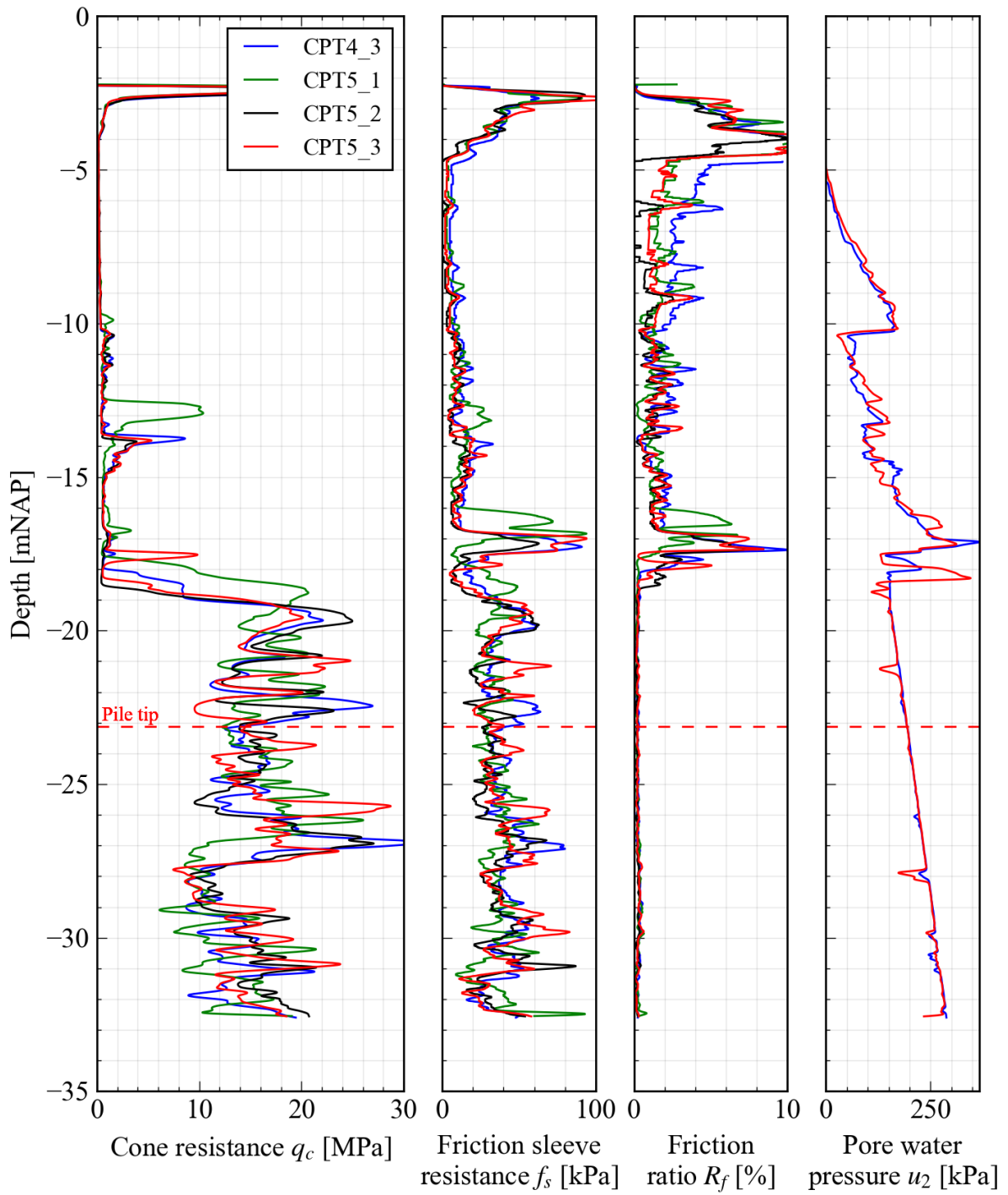
A.4 T1



A.5 T2

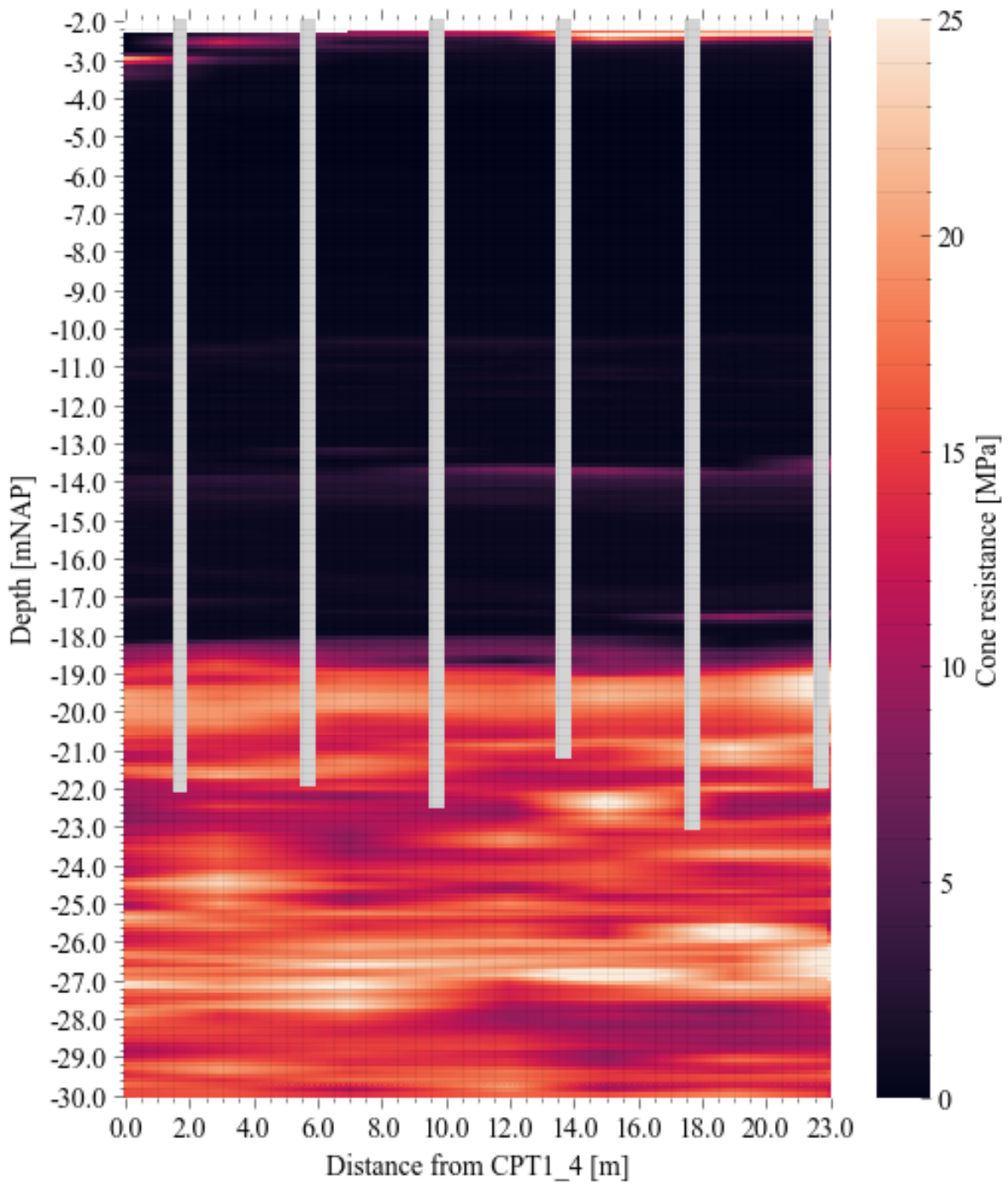


A.6 T3



A.7 Interpolated CPTs

Direct linear interpolation of all CPTs along the centre line of the test site (i.e. CPTs executed between piles).



Appendix B Guidance Document for Pile Installation

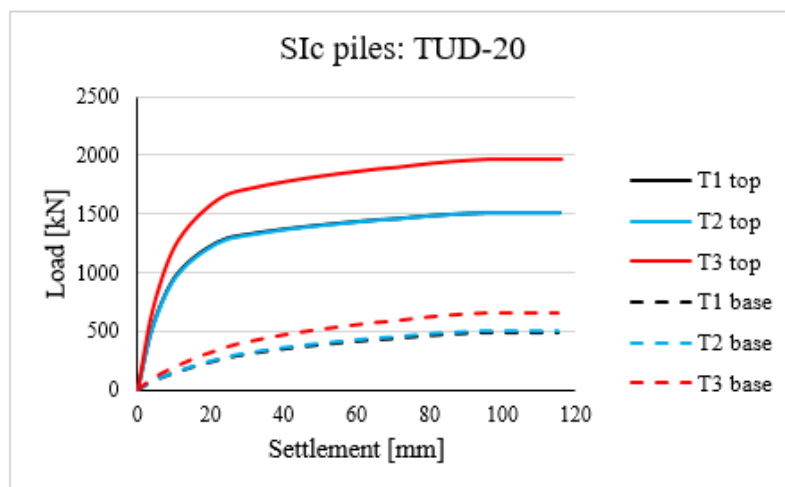
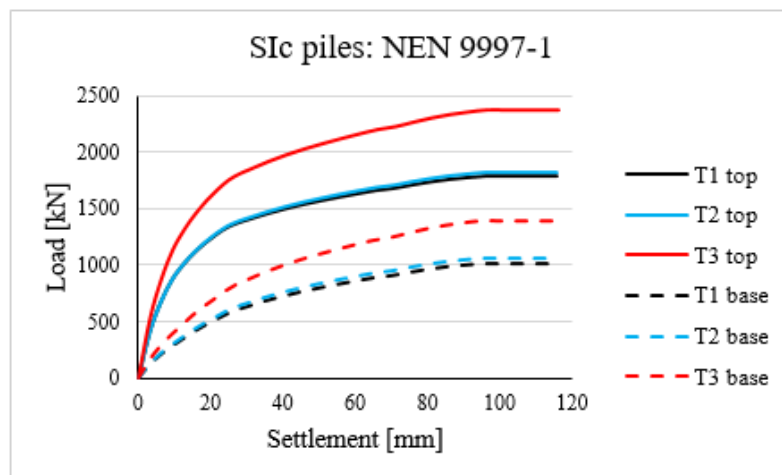
The aim of the test programme was to test screw injection piles representative of piles installed in the industry. For this purpose, the Dutch Association of Piling Contractors (NVAF, *Nederlandse Vereniging Aannemers Funderingswerken*) provided the following guidance document for the test programme, outlining typical installation parameters used in practice.

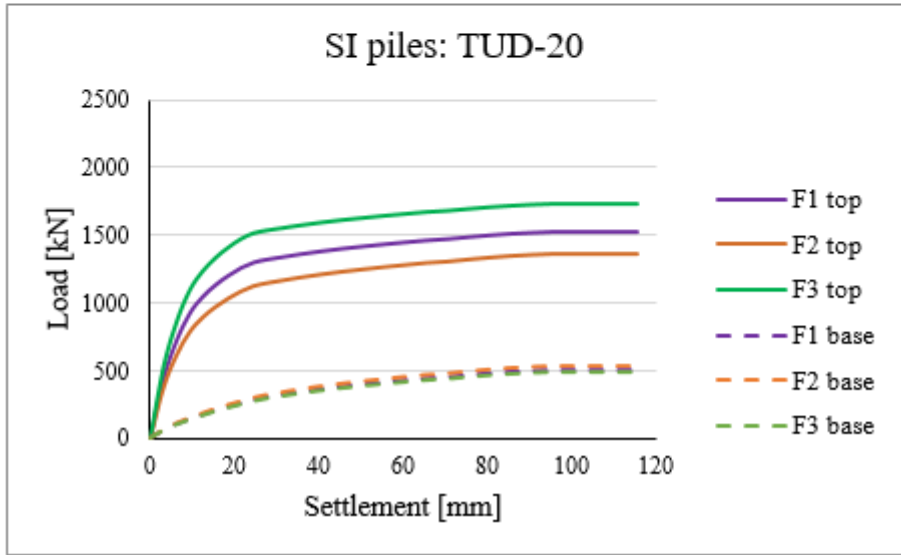
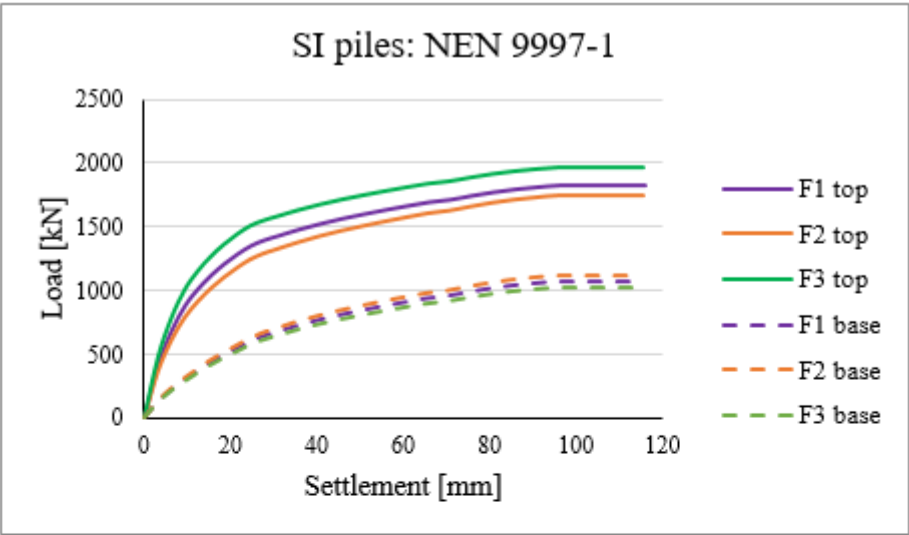
Appendix C Prediction of Pile Behaviour

The calculation has been carried out both with the prescribed NEN 9997-1 α_p and α_s factors (0.63 and 0.011 respectively) along with the factors obtained from Amaliahaven (0.30 and 0.012 respectively). No limiting resistances have been included and for clay soils, the I_{SBT} dependent α_s has been used for both methods.

Table C.1: Predicted capacities at failure according to the NEN 9997-1 and TU Delft method

		F1	F2	F3	T1	T2	T3
NEN	Base	1.1	1.0	1.0	1.0	1.0	
	Shaft	1.0	0.9	1.1	1.1	1.0	1.3
	TOTAL	2.1	1.9	2.1	2.1	2.0	2.6
TUD	Base	0.6	0.7	0.6	0.5	0.6	0.8
	Shaft	1.3	1.1	1.5	1.0	1.3	1.7
	TOTAL	1.9	1.8	2.1	1.5	1.9	2.5





Appendix D General Specifications

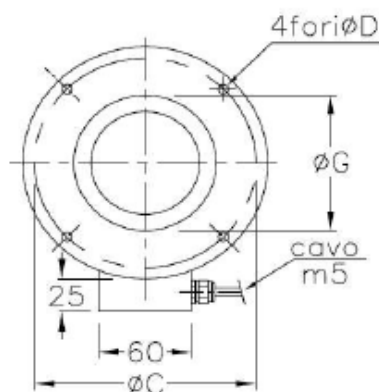
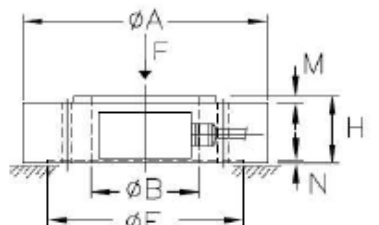
D.1 Calibration Sheet: Load Cell

Belotti
SISTEMI

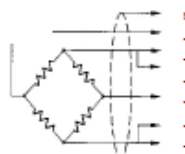


Dati Tecnici	Specifications	
Portate	Capacity	300 + 2500 kN
Sensibilità nominale	Nominal Sensivity	2,0 mV/V +/- 0,1 %
Coeff. Temperatura di zero	Zero temperature coeff.	± 0,005 %F.S /°C
Coeff. Temperatura di F.S.	Span temperature coeff.	± 0,005 %F.S /°C
Errore combinato	Combined error	± 0,10 % F.S.
Ripetibilità	Repeatability	± 0,02 % F.S.
Creep a pieno carico (20')	Nominal load creep (20')	± 0,03 % F.S.
Resistenza di Ingresso	Input resistance	700 ± 20 Ohm
Resistenza di uscita	Output resistance	700 ± 5 Ohm
Isolamento	Insulation	>5000 M Ohm
Alimentazione elettrica	Electrical excitation	2 + 15 Vcc/ca
Compensazione in temp.	Compensated temp. Range	-10 + +50°C
Temp. di funzionamento	Operating temp. Range	-20 + +70°C
Sovraccarico ammesso	Safe overload	150 % F.S.
Sovraccarico di rottura	Ultimate overload	>300 % F.S.
Freccia massima a carico	Deflection at rated capacity	0,4 mm
Grado di Protezione	Protection degree	IP 67
Materiale	Material	Acciaio Inox
Funzionamento	Working	Flessione

Dimensioni / Dimensions (mm)



Schema elettrico
Electrical connections



MODELLO	A	B	C	D	E	G	H	M	N	OUT	POSO
	Ø	Ø	Ø	Ø	Ø	Ø				mv/v	kg.
CRR 50-300 kN	163	50	145	6,5	131	95	45	5	2	2	5
CRR 50-500 kN	163	50	145	6,5	131	95	45	5	2	2	5
CRR 50-750 kN	163	50	145	6,5	131	95	45	5	2	2	5
CRR 75-500 kN	163	75	145	6,5	131	95	45	5	2	2	5
CRR 75-750 kN	163	75	145	6,5	131	95	45	5	2	2	5
CRR 120-750 kN	229	120	207	6,5	186	150	45	5	2	2	9
CRR 120-1000 kN	229	120	207	6,5	186	150	45	5	2	2	9
CRR 120-1250 kN	229	120	207	6,5	186	150	45	5	2	2	9
CRR 165-1250 kN	275	165	252	6,5	231	195	45	5	2	2	14
CRR 165-1500 kN	275	165	252	6,5	231	195	45	5	2	2	14
CRR 165-1800 kN	275	165	252	6,5	231	195	45	5	2	2	14
CRR 225-1800 kN	320	225	302	6,5	285	250	55	5	2	2	20
CRR 225-2500 kN	320	225	302	6,5	285	250	55	5	2	2	20

N.B. Le celle mod CRR 225/2500 kN hanno un sovraccarico di rottura 200 % F.S.

NOTE The max admitted oveange for Load Cells CRR 225/2500 kN is 200 % F.S.

OPZIONE : uscita 4=20 mA a 2 o 3 fili, su richiesta.

OPTION: output 4=20 mA at 2 or 3 wires, on request.

SCHEMMA
- SEGNALE (BIANCO)
- ALIMENTAZIONE (NERO)
- RIF. (MARRONE)
- SEGNALE (VERDE)
- ALIMENTAZIONE (ROSSO)
- RIF. (BLU)

SHIELD
- SIGNAL (WHITE)
- EXCITATION (BLACK)
- SENSE (BROWN)
+ SIGNAL (GREEN)
+ EXCITATION (RED)
+ SENSE (BLUE)

Belotti Sistemi S.a.s
Via F.lli Bandiera, 8
20068 Peschiera Borromeo (MI)

Tel.: +39 02 55.30.82.23
Fax: +39 02 55.30.31.55
belotti.sistemi@belotti-online.it

Cod. Fisc. e P.I. 03666960152
REA Milano n° 964486
www.belotti-online.it



CERTIFICATE OF CALIBRATION

Certificate Number : 12257-2 13.327

Approved Signatory

Date of Issue : 27 januari 2022



G.J. van Delzen
 D. Herremans

Customer /Owner

IFCO Funderingsexpertise B.V.

Instrument/Device	Description	Loadcell Compression
	Manufacturer	Belotti
	Model	CRR 225-2500kN
	Serial Number	LC3029 / 201609814

Comments

Environmental Conditions

Temperature: 22,0°C ±4°C

Supply Voltage: 230V ±23V @ 50Hz ±0Hz

Relative Humidity: 50% RH ±10% RH

Traceability Information

Instrument Description

Serial No

Form+Test Seidner 3000kN Compression

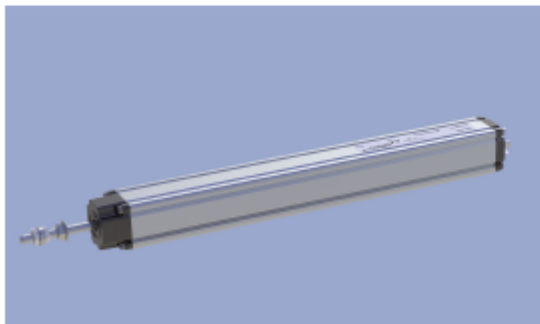
82/6125

D.2 Calibration Sheet: Potentiometers

novotechnik
Siedle Group

Transducer
Potentiometric

LWH



Special Features

- Long life up to 100 Mio. movements, depending on application
- Outstanding linearity up to $\pm 0.04\%$
- High resolution better than 0.01 mm
- Very high operating speed
- Connection via plug and socket to DIN EN 175301-803 (previous DIN 43650, hydraulic connector)
- Protection class IP55

Applications

- Manufacturing Engineering (plastic injection molding, textile, packaging, sheet metal and wood work machinery)
- Automation technology

Position transducers made from conductive plastic for direct, accurate measurement of travel in display- or feedback applications. High resolution combined with a stroke length of up to 900 mm permits the accurate measurement of linear displacement. Rack and pinions or similar devices are not required because the design of the transducers is such that they may be built directly into the mechanical system. Tighter tolerances on the extruded die combined with a special surface treatment permit high operating speeds and reduced wear. A pivoting front bearing over comes „stick-slip“ type of operation even where some angular or out of parallel errors are present. The technique for fixing and making connections to the resistance track ensures the highest degree of reliability even under harsh working conditions.

By mounting overhead on difficult-to-reach spaces it is possible to premount the clamps to the mounting surface and then simply „snap-on“ the transducer. The transducer has mounting grooves on all four housing surfaces. Thus the transducer can always be mounted with the resistance element directed upwards (recognizable by the position of the middle mounting groove directly across from the resistance element), independent of the mounting surface. Erosion particles from inside the transducer will therefore not remain on the resistance element, improving the life of the sensor.

Description

Material	Housing: aluminium, anodized Actuating rod: SS 1.4305 / AISI 303, rotatable, external thread M6
Mounting	Adjustable clamps and cylinder screws M4x20 (included in delivery)
Fastening torque of mounting	max. 200 Nm
Bearing	Slide bearing, pendular fixed
Resistance element	Conductive plastic
Wiper	Precious metal multi-finger wiper, elastomer damped
Electrical connection	Plug socket to DIN EN 175301-803, 4-pin (mating plug connector GDM 3009 for cable $\varnothing 4.5 \dots 7\text{ mm}$ and sealing gasket GDM 3-16 included in delivery)

Mechanical Data

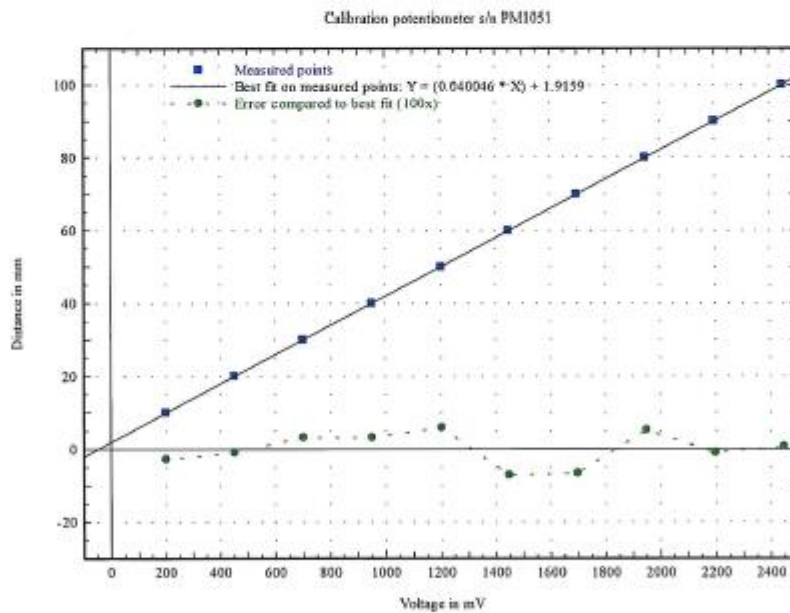
Type	LWH 0060	LWH 0075	LWH 0100	LWH 0110	LWH 0130	LWH 0150	LWH 0175	LWH 0200	LWH 0225	LWH 0250	LWH 0275	LWH 0300	LWH 0325	LWH 0350	LWH 0380	LWH 0400	LWH 0425	LWH 0450	LWH 0500	LWH 0550	LWH 0600	LWH 0650	LWH 0750	LWH 0800	LWH 0900	
Dimensions	See dimension drawing																									
Length of housing [mm] (dim. A $\pm 2\text{ mm}$)	121	148	171	182	201	222	248	273	298	324	349	375	400	425	436	451	476	502	527	578	629	680	730	832	919	984
Mechanical travel [mm] (dim. B $\pm 2\text{ mm}$)	50	85	110	120	140	161	186	212	237	262	288	313	339	362	374	390	415	440	466	518	567	618	669	770	858	923
Weight [g]	200	220	250	265	290	320	350	380	410	440	470	500	530	560	570	590	620	650	680	740	806	870	900	1050	1110	1230
Weight actuating rod with wiper [g]	30	50	55	57	60	65	72	78	85	90	95	100	105	112	115	120	125	130	136	145	160	170	180	210	220	245
Operating force, horizontal	$\leq 10\text{ N}$																									
Operating force, vertical	$\leq 10\text{ N}$																									

Calibration Certificate

Potentiometer

Type : PLS1005KMR
S/n : 902474
IS s/n : PM1051
Equipment used : Mitutoyo slide gauge CD-15B s/n: 313090
Engineer : J.V. Ledderhof

Distance Mitutoyo [mm]	Distance potentiometer [mm]
10	9.97
20	19.99
30	30.03
40	40.03
50	50.06
60	59.93
70	69.93
80	80.05
90	89.99
100	100.01



Date: 15-12-2021

Signature:

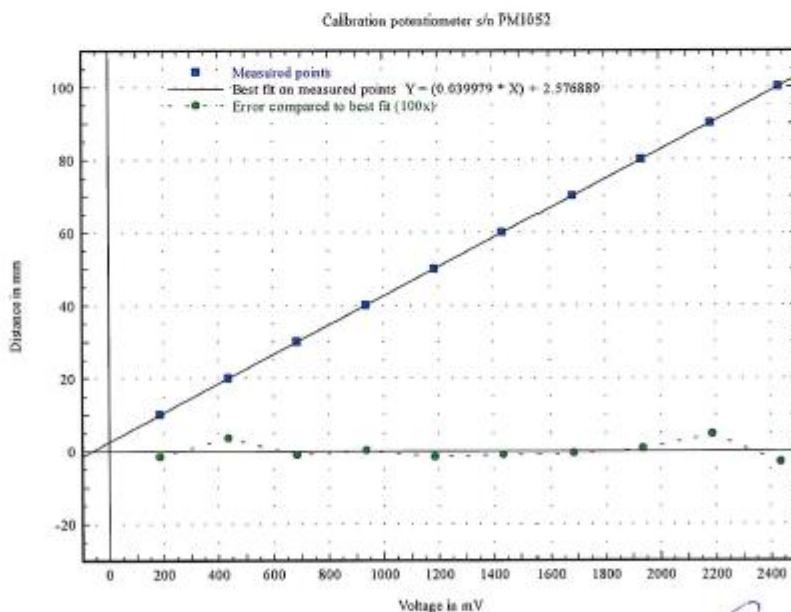


Calibration Certificate

Potentiometer

Type : PLS1005KMR
S/n : 902473
IS s/n : PM1052
Equipment used : Mitutoyo slide gauge CD-15B s/n: 313090
Engineer : J.V. Ledderhof

Distance Mitutoyo [mm]	Distance potentiometer [mm]
10	9.97
20	20.01
30	29.94
40	39.97
50	50.02
60	59.99
70	69.97
80	80.02
90	90.04
100	99.97



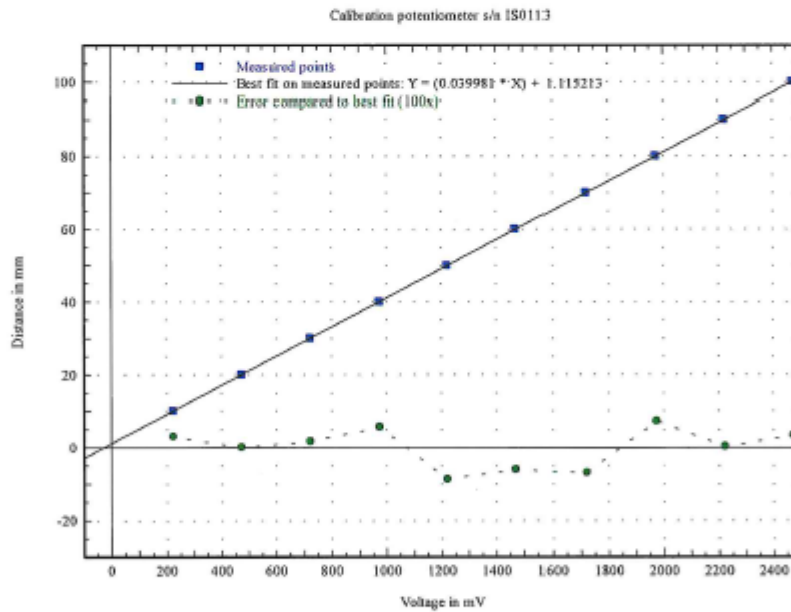
Calibration Date: 15-12-2021

Signature: 

Calibration Certificate Potentiometer

Type : PM1005KMR
S/n : H07035
IS s/n : IS0113
Equipment used : Mitutoyo slide gauge CD-15B s/n: 313090
Engineer : J.V. Ledderhof

Distance Mitutoyo [mm]	Distance potentiometer [mm]
10	10.01
20	19.99
30	30.03
40	40.01
50	49.87
60	59.91
70	69.94
80	80.05
90	89.98
100	100.01



Calibration Date: 14-12-2021

Signature: 

Profound BV
 Mozartlaan 46-A
 NL-2742 BN Waddinxveen
 The Netherlands

ISO 9001:2015 certified
 Tel. +31 (0)182 640 964
 info@profound.nl
www.profound.nl

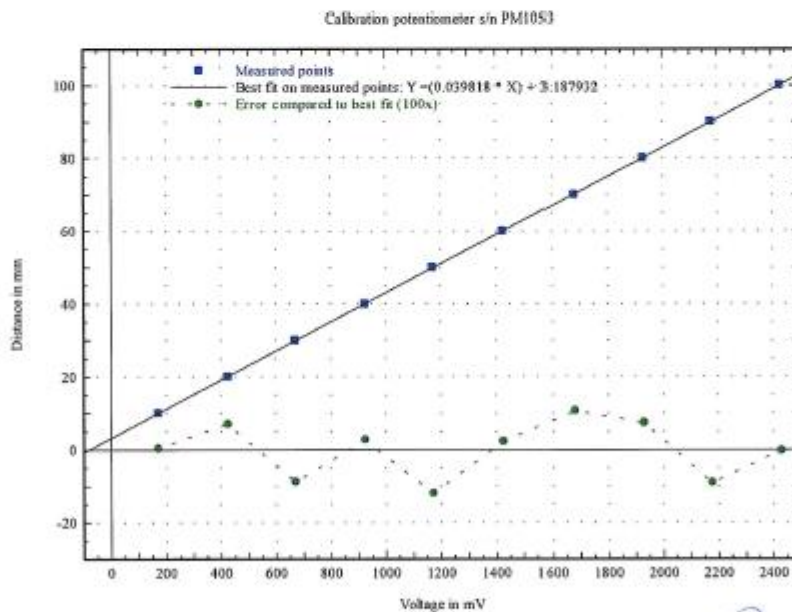
VAT number NL806166800B01
 IBAN NL79 RABO 0116 9166 13
 BIC RABONL2U
 Chamber of Commerce Rotterdam 27242091

Calibration Certificate

Potentiometer

Type : PLS1005KMR
S/n :
IS s/n : PM1053
Equipment used : Mitutoyo slide gauge CD-15B s/n: 313090
Engineer : J.V. Ledderhof

Distance Mitutoyo [mm]	Distance potentiometer [mm]
10	9.97
20	20.12
30	29.93
40	40.02
50	49.89
60	59.99
70	70.01
80	80.02
90	89.93
100	99.99



Calibration Date: 14-12-2021

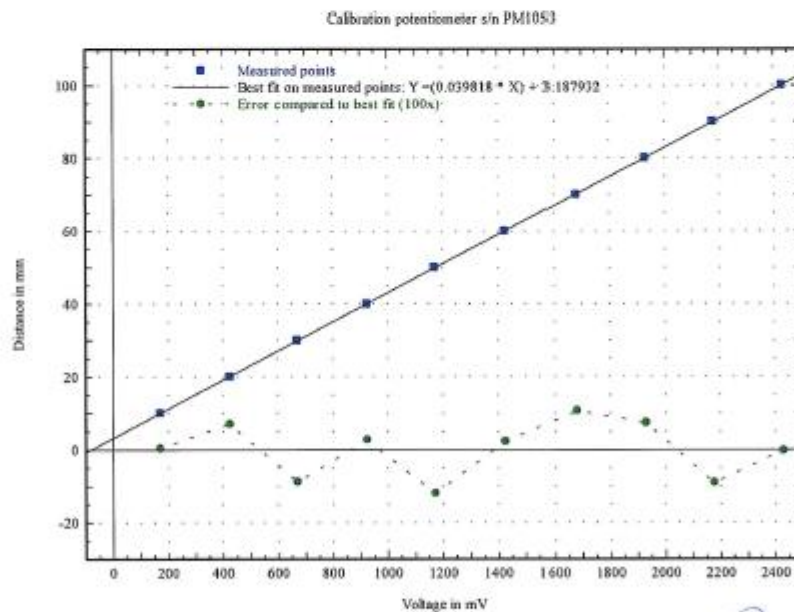
Signature: 

Calibration Certificate

Potentiometer

Type : PLS1005KMR
S/n :
IS s/n : PM1053
Equipment used : Mitutoyo slide gauge CD-15B s/n: 313090
Engineer : J.V. Ledderhof

Distance Mitutoyo [mm]	Distance potentiometer [mm]
10	9.97
20	20.12
30	29.93
40	40.02
50	49.89
60	59.99
70	70.01
80	80.02
90	89.93
100	99.99



Calibration Date: 14-12-2021

Signature: 

Profound BV
 Mozartlaan 46-A
 NL-2742 BN Waddinxveen
 The Netherlands

ISO 9001:2015 certified
 Tel. +31 (0)182 640 964
info@profound.nl
www.profound.nl

VAT number NL806166B00B01
 IBAN NL79 RABO 0116 9166 13
 BIC RABONL2U
 Chamber of Commerce Rotterdam 27242091

D.3 Leica DNA03

Technical data	LEICA DNA03	LEICA DNA10
Area of use	<ul style="list-style-type: none"> - Quick measurements of heights, height differences and stake outs - I. and II. order levelling - High precision measurements 	<ul style="list-style-type: none"> - Quick measurements of heights, height differences and stake outs - Cadastral levelling - Precision measurements
Accuracy	Standard deviation height measurement per 1 km double-run (ISO 17123-2)	
Electronic measurements:		
with Invar staffs	0.3 mm	0.9 mm
with standard staffs	1.0 mm	1.5 mm
Optical measurements	2.0 mm	2.0 mm
Distance measurement (standard deviation)	(electr.) 1 cm/20 m (500 ppm)	
Range		
Electronic measurement	1.8 m – 110 m	
Optical measurement	from 0.6 m	
Electronic measurement		
Resolution height measurement	0.01 mm, 0.0001 ft, 0.0005 inch	0.1 mm, 0.001 ft
Time for single measurement	typically 3 seconds	
Measurement modes	Single, average, median, repeated single measurements	
Measurement programs	Measure & Record, staff height/distance, intermediate BF, aBF, BFFB, aBFFB, onboard adjustment, quick closure, stakeout	
Coding	Remark, Free code, Quick code	
Data storage		
Internal memory	6000 measurements or 1650 station	
Backup	PCMCIA card (ATA-Flash/SRAM/CF)	
Online operations	GSI format via RS232	
Data exchange internal memory	GSI8/GSI16/XML/flexible formats	
Telescope magnification	24x	
Compensator		
Type	Pendulum compensator with magnetic damping	
Slope range	±10'	
Compensator setting accuracy (standard deviation)	0.3"	0.8"
Display	LCD, 8 lines at 24 characters	
Battery operated		
GEB111	12 h operation	
GEB121	24 h operation	
Battery adapter GAD39	Alkaline battery, 6x LR6/AA/AM3, 1.5 V	
Weight	2.8 kg (incl. battery GEB111)	
Environmental conditions		
Working temperature	-20° C to +50° C	
Storage temperature	-40° C to +70° C	
Dust/water (IEC60529)	IP53	
Humidity	95%, non condensing	

D.4 Fujikura JBS-00240D

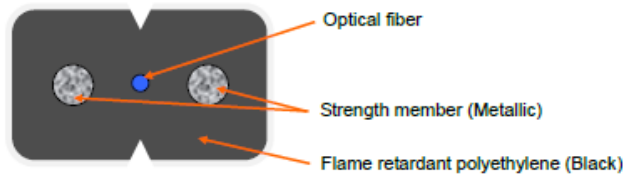
The FutureGuide®-SR15E (ITU-T G.657.A1) model is to be used for the pile test.



JBS-00240D
1/3

Specification for Low Friction Optical Fiber Cable (INO-M Series)

● Cable Construction



* Not to scale. Schematic diagram only.

● Features

- Very low coefficient of friction that makes installation extremely easier
- Installation by pulling/pushing methods

● Application

- Indoor/Outdoor installation
- Suitable for SDU and MDU wiring (Inside ducts, or bundled in cable trays)

● Reference Standards

- Recommendations ITU-T G.657
- IEC 60794-1-2

● Mechanical Characteristics

Product code	Fiber count	Approx. dimension (mm)	Approx. weight (kg/km)	Permissible tensile strength (Newton)	Permissible bending radius (mm)
INO-M-1(t*)	1	1.6×2.0	7	220	15
INO-M-2(t*)	2	1.6×2.3	8	220	15
INO-M-4(t*)	4	1.6×2.8	9	220	15

* t denotes fiber type: FutureGuide®- SR15E = SR15E, FutureGuide®- BIS-B = BIS-B

● Fiber Identification

1	Blue	2	Orange	3	Green	4	Brown
---	------	---	--------	---	-------	---	-------

● Environmental Characteristics

Item		Characteristics
Temperature	Installation	-10°C to +50°C
	Operation	-15°C to +70°C
	Transportation & Storage	-15°C to +70°C
Oxygen index of sheath		≥ 27
Flame retardant test		IEC 60332 - 1
Coefficient of friction		≤ 0.3 for 1 & 2-fiber cable
		≤ 0.4 for 4-fiber cable

● Sheath Marking

FR t*-n**F FUJIKURA <Year of Manufacturing> <Cable ID>*** <Length marking>

Note: * t denotes fiber type (G657A1 or G657A2)

** n denotes fiber count

***Manufacturer's <Cable ID> may be included if necessary.

● Optical Characteristics

Characteristics	Unit	Fiber type	
		FutureGuide®-SR15E (ITU-T G.657.A1)	FutureGuide®-BIS-B (ITU-T G.657.A2)
Geometrical Characteristics			
Mode field diameter at 1310nm	μm	8.6 ± 0.4	8.6 ± 0.4
Cladding diameter	μm	125 ± 0.7	125 ± 0.7
Core concentricity error	μm	≤ 0.5	≤ 0.5
Cladding non-circularity	%	≤ 1.0	≤ 1.0
Primary coating diameter (including color layer)	μm	250 ± 15	250 ± 15
Coating-cladding concentricity error	μm	≤ 12.5	≤ 12.5
Fiber curl radius	m	≥ 4	≥ 4
Transmission Characteristics			
Attenuation at 1310nm	dB/km	≤ 0.40	≤ 0.40
Attenuation at 1383nm*	dB/km	≤ 0.35	≤ 0.35
Attenuation at 1550nm	dB/km	≤ 0.30	≤ 0.30
Macro bending loss ** φ30mm, 10 turns, 1550nm	dB	≤ 0.25	≤ 0.03
Macro bending loss ** φ30mm, 10 turns, 1625nm	dB	≤ 1.0	≤ 0.10
Macro bending loss ** φ20mm, 1 turn, 1550nm	dB	≤ 0.75	≤ 0.10
Macro bending loss ** φ20mm, 1 turn, 1625nm	dB	≤ 1.50	≤ 0.20
Macro bending loss ** φ15mm, 1 turn, 1550nm	dB	-	≤ 0.50
Macro bending loss ** φ15mm, 1 turn, 1625nm	dB	-	≤ 1.0
Cut-off wavelength (λ _{cut})	nm	≤ 1260	≤ 1260
Chromatic dispersion at 1310nm	ps/nm.km	≤ 3.5	≤ 3.5
Chromatic dispersion at 1550nm	ps/nm.km	≤ 18	≤ 18
Zero dispersion wavelength	nm	1300-1324	1300-1324
Zero dispersion slope	ps/nm ² .km	≤ 0.092	≤ 0.092
Mechanical Characteristics			
Proof stress level	%	1.5	1.5

*Attenuation increase due to hydrogen aging at this wavelength in bare optical fiber is tested in accordance with IEC60793-2-50 test procedure.

**This characteristic is measured before coloring process.

● Packing

Cables are packed in standard durable and export quality suitable reels / boxes and suitable protection means are applied to prevent damage of cables during shipment and storage.

Standard length is 1000m or 2000m. Other lengths less than the standard length shall be provided upon mutual agreement.

The impressions on the cable surface at crossover locations will not affect the cable performance as far as the customer handles the cable by following the handling instructions mentioned on the box.

● Precautions to avoid handling trouble

Please follow instructions attached on the reel. For more details, contact our local sales office.

● Ordering information

INO-M-n*(t**) = FR-OGINHE t**× n*C (Black)

* n denotes fiber count: for example: 1, 2, and 4.

** t denotes fiber type: FutureGuide®-SR15E = SR15E, FutureGuide®-BIS-B = BIS-B

● Note

This specification may be subjected to change without notice. Customization is possible for Fiber identification and Sheath marking. In this case Fujikura will prepare new specification.

D.5 Fibre Optic Data Logger: fibrisTerre fTB 5020

Performance, features and technical data

BOFDA technology mode – sensor configuration: fiber loop

Distance range (fiber loop)		50 km ¹⁾	
Spatial resolution	up to 2 km fiber	0.2 m ²⁾	
	up to 25 km fiber	0.5 m	
	up to 50 km fiber ¹⁾	1.0 m	
Spatial accuracy		0.05 m	
Dynamic range ³⁾		> 20 dB	
Accuracy ⁴⁾ and range	strain	Accuracy < 2 µε	Range +/- 3% ⁵⁾
	temperature	< 0.1°C	-200 to +1000°C ⁴⁾
	Brillouin freq. shift	< 100 kHz	9 – 13 GHz
Typical acquisition time ⁶⁾	0.2 km fiber	20 seconds	
	2 km fiber	1 minute	
	10 km fiber	8 minutes	
	25 km fiber	25 minutes	

BOFDR technology mode – sensor configuration: single-ended

Distance range		25 km	
Spatial resolution		1.5 m	
Accuracy ⁴⁾ and range	strain	Accuracy < 20 µε	Range +/- 3% ⁵⁾
	temperature	< 1°C	-200 to +1000°C ⁴⁾
	Brillouin freq. shift	< 1 MHz	9 – 13 GHz

General information

Optical connectors		E-2000 / APC, other options available
Communication interface		Ethernet
Supported platforms		Windows and Linux
Data interfacing / SCADA		File export (binary, text), Telnet, Modbus TCP/IP, SNMP, proprietary API
Measurement modes		Manual measurements and autonomous monitoring schedule; detection of fiber length, attenuation
Operating temperature		0 – 45°C
Relative humidity		5 – 95%, non-condensing
Power consumption		40 W
Physical dimensions	L x W x H	365 x 483 x 88 mm (19" rack case)
		Desktop case (436 mm width) upon request
Weight		7 kg
Laser class		1M

¹⁾ Standard distance range is 25 km. Options: 50 km (loop) and 25/50 km one-direction (with blind return fiber)

²⁾ Optional feature "Enhanced resolution" selectable in user interface

³⁾ High optical losses along the sensing fiber may degrade the strain / temperature accuracy

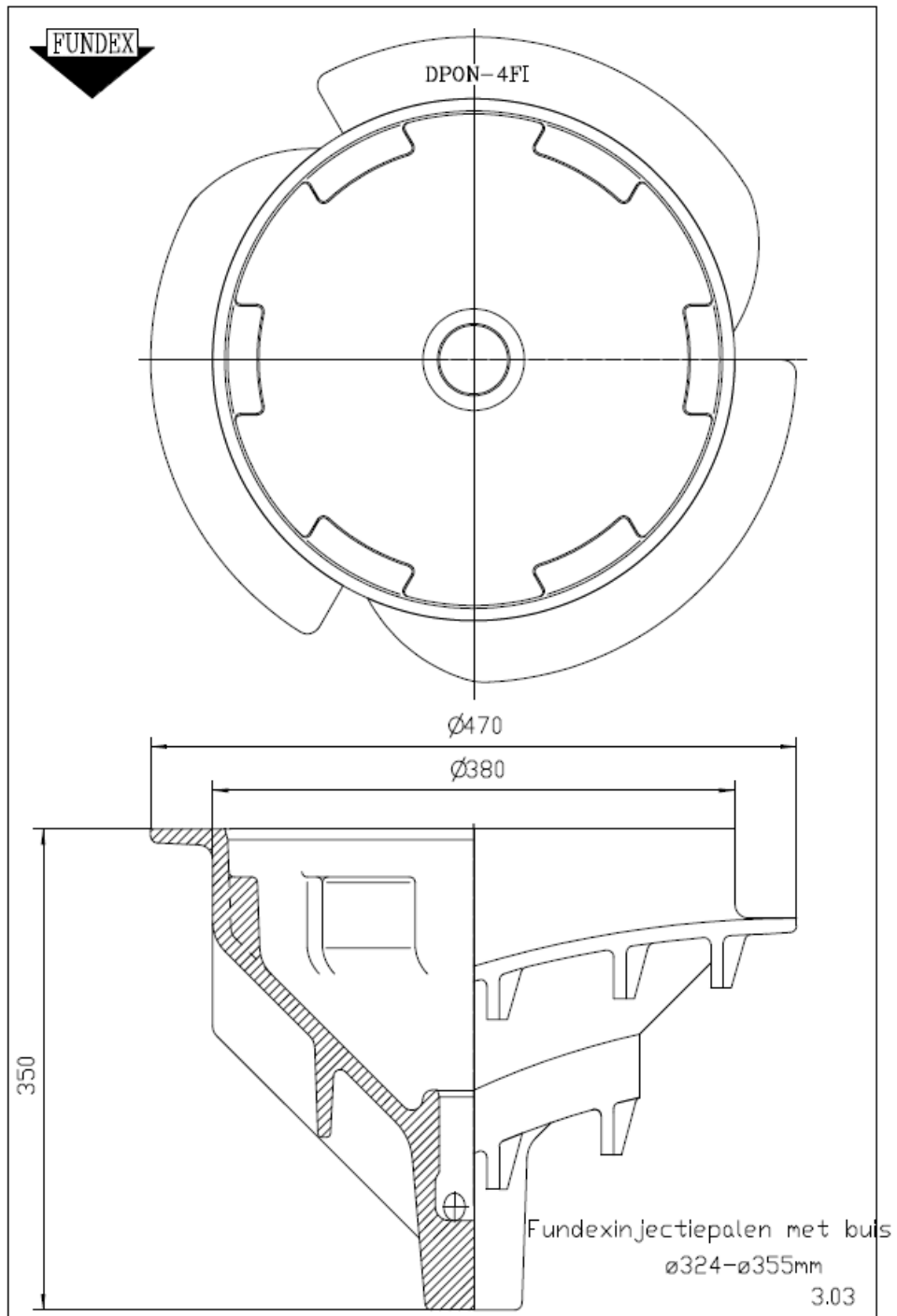
⁴⁾ Accuracy expressed in terms of measurement repeatability (2σ), assuming ideal calibration coefficients

⁵⁾ Limited by optical fiber

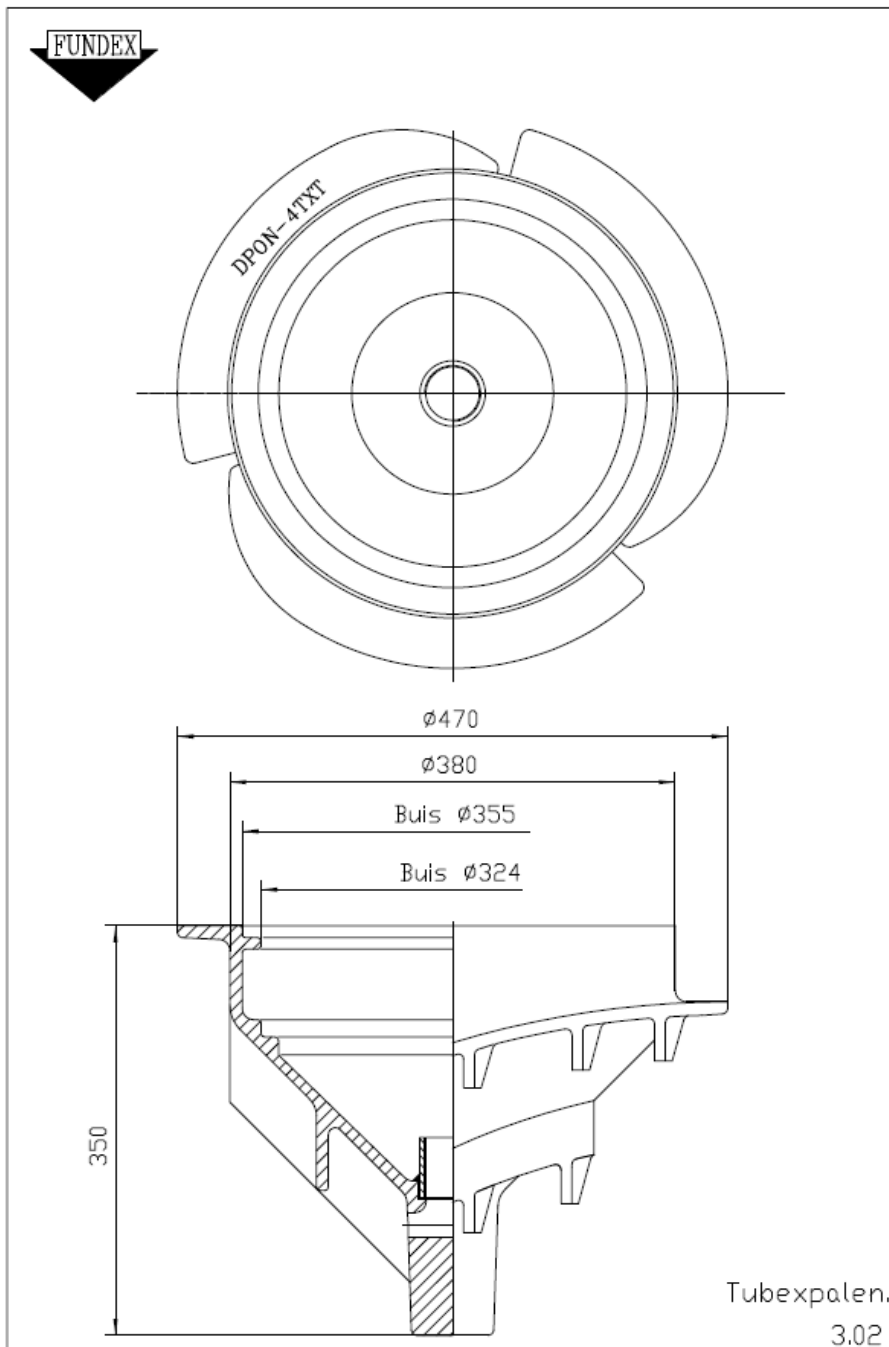
⁶⁾ Typical acquisition time varies with measurement parameters such as resolution, accuracy, strain/temperature range

D.6 Pile Tip

SI piles (Fundex pile)



Slc piles (*Tubex*)



D.7 Concrete Mix & Delivery Tickets (Betonbonnen)

SI piles

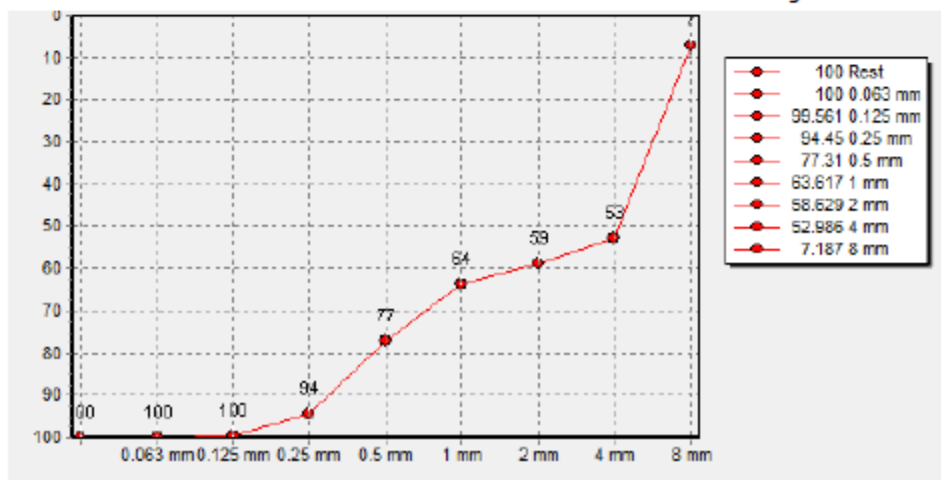
Zeefanalyses en betonsamenstelling



Vestiging	Code	T06	Datum berekend
Delft	8004	CEM III/B	2022-01-28 12:17:46

Zeven volgens NEN 2560 ZAND 0/4 GRIND 2/8 Mengsel				Sterkte klasse	C45/55
Toeleveringscode	65094	64609		Statistische milieu klasse	XA3
8 mm	0,0%	14,4%	7,2%	Milieuklasse	XS3, XF4 (XD3, XS2, XF2)
4 mm	8,3%	97,7%	53,0%	Milieuklasse	XA3
2 mm	17,8%	99,5%	58,6%	Consistentie	Schudmaatklasse F4
1 mm	27,6%	99,7%	63,6%	Maximale korrelgrootte	DMax = 8
0.5 mm	54,6%	100,0%	77,3%	wbf / wcf	0,430 / 0,430
0.25 mm	88,9%	100,0%	94,5%	Zand (t.o.v. toeslag)	50,00% V/V
0.125 mm	99,1%	100,0%	99,6%	Chloridegehalte (tot bindmiddel)	0,08% M/M
0.063 mm	100,0%	100,0%	100,0%	Alkaligehalte	3,40kg
Rest	100,0%	100,0%	100,0%	Luchtgehalte	20,0L
Fijnheidmodulus	2,96	6,11	4,54	Temperatuur:	20°C
Vocht	3,7%	2,0%		waterbehoefte	185,3L
Absorptie	0,0%	0,0%		Aanmaakwater	137,1L
Verhouding toeslag	100,00%	100,00%		Eff. aanmaakwater (zonder slib)	137,1L
Fractie	50,00%	50,00%		Geabsorbeerd water	0,0L
Vol. massa	2,60kg/L	2,60kg/L		Aanhangend vocht	48,2L

Grondstoffen	producent	Te doseren massa	Droge massa	Volume fijn	T.o.v. cement
CEM I 52,5R Dyckerhoff Lengerich	Dyckerhoff Lengerich	172kg	172kg	54,7L	
CEM III/B 42.5 N LH/SR	Dyckerhoff Neuss	259kg	259kg	87,7L	
ZAND 0/4	Dyckerhoff Basal Toeslagstoffen	877kg	846kg	36,1L	
GRIND 2/8	Dyckerhoff Basal Toeslagstoffen	863kg	846kg	1,1L	
Vliegas EFA Füller MR-3 Cat A	Baumineral	0kg	0kg	0,0L	
VC 1550 con. 30%	SIKA	0,991kg	0,991kg	0,0L	0,23% m/m
UCS Pak Colloidaal	SIKA	0,160kg	0,160kg	0,0L	
Harex PM 6/18 [Kunststofvezel]	KrampeHarex	0,360kg	0,360kg	0,0L	
Koud water	Dyckerhoff Basal Betonmortal	137kg	185kg	0,0L	
Lucht		20L	20L	0,0L	
Totaal		2310kg		179,6L	





Dyckerhoff Basal

Betonmortel

KOPIE

ea 1.0m' onderstort
paal + A (1)
19.95 m'

LAADPUNT

LpDelftA (088-6078420)

DATUM / TIJD

01-02-2022 / 12:51 H1431027

ORDERNUMMER

BONNUMMER

H4130509

Klantnummer: 6981
Funderingstechniek Verstraeten BV
Postbus 55
4500 AB OOSTBURG

Afleveradres:
Deltares
Thijsseweg

DELFT
Bouwonderdeel: Onbekend

Besteld: 2.75 m³

Verwarmd
no

Betonmortel NEN EN 206

Certificaatcode 22-ji-BBK

Sterkteklasse Milieuklasse
C45/55 XA3

Cons.klasse
F4

Stortsnelheid Loswijze
6.00 m3/uur Kraan

CEM I 52.5 R 40.00%
Grind 2-8 100.00%
Harex 6/18 0.36kg
Paal storten natte omstandigheden 2/8mm
Min. cementgehalte 430 kg
Colloidale eigenschappen

Deze levering: 2.75 m³

Afgeleverd t/m deze bon: 2.75 m³

RECEPTOMSCHRIJVING (receptnummer 8004)

Uw mengselcode :

CEM I 52,5R Dyckerhoff Lengerich
CEM III/B 42.5 N LH/SR
GRIND 2/8
VC 1550 con. 30%

Kwaliteitsgarantie

Leveringen geschieden conform de BRL1801, NEN EN 206 en NEN 8005, in Chlorideklasse CL0.40, tenzij anders aangegeven. Beton is volgens het Besluit Bodemkwaliteit beoordeeld als een vormgegeven bouwstof.

Indien zonder schriftelijke goedkeuring van leverancier door of namens koper water, hulpstoffen, vezels of anders aan de mixerinhoud worden toegevoegd, vervalt deze kwaliteitsgarantie.

Invullen indien van toepassing:

Door of namens koper is op het werk aan de mixerinhoud het navolgende toegevoegd zonder schriftelijke goedkeuring van de leverancier:

De aankomsttijd op het werk, de starttijd lossen en de vertrektijd van het werk, worden door middel van statusmelding automatisch geregistreerd.

AW..... SL..... VW.....

Truck : Flock02

Chauffeur : uzle

Opmerkingen: - Proef Ron Mulder
- Palen

LET OP HET BOUWWEER !!

Informatie is te vinden op: <https://betonhuis.nl/betonmortel/beton-de-zomer-en-winter>

Handtekening Afnemer :



Paal FB (2)
19.25 m³



Dyckerhoff Basal

Betonmortel

KOPIE

LAADPUNT

LpDelftA (088-6078420)

DATUM / TIJD

01-02-2022 / 14:32 H1431028

ORDERNUMMER

BONNUMMER

H4130524

Klantnummer: 6981

Funderingstechnieken Verstraeten BV
Postbus 55
4500 AB OOSTBURG

Afleveradres:

Deltares
Thijsseweg

DELFT

Bouwonderdeel: Onbekend

Besteld: 3.25 m³

Verwarmd

no

Betonmortel NEN EN 206

Certificaatcode 22-jj-BBK

Sterkteklasse Milieuklasse

C45/55

XA3

Cons.klasse

F4

Stortnelheid

6.00 m³/uur

Loswijze

Kraan

CEM I 52.5 R 40.00%
Grind 2-8 100.00%
Harex 6/18 0.36kg
Paal storten natte omstandigheden 2/8mm
Min. cementgehalte 430 kg
Colloidale eigenschappen

Deze levering: 3.25 m³

Afgeleverd t/m deze bon: 3.25 m³

RECEPTOMSCHRIJVING (receptnummer 8004)

Uw mengselcode :

CEM I 52,5R Dyckerhoff Lengerich
CEM III/B 42.5 N LH/SR
GRIND 2/8
VC 1550 con. 30%

Kwaliteitsgarantie

Leveringen geschieden conform de BRL1801, NEN EN 206 en NEN 8005, in Chlorideklasse CL0.40, tenzij anders aangegeven. Beton is volgens het Besluit Bodemkwaliteit beoordeeld als een vormgegeven bouwstof.

Indien zonder schriftelijke goedkeuring van leverancier door of namens koper water, hulpstoffen, vezels of anders aan de mixerinhoud worden toegevoegd, vervalt deze kwaliteitsgarantie.

Invullen indien van toepassing:

Door of namens koper is op het werk aan de mixerinhoud het navolgende toegevoegd zonder schriftelijke goedkeuring van de leverancier:

De aankomsttijd op het werk, de starttijd lossen en de vertrektijd van het werk, worden door middel van statusmelding automatisch geregistreerd.

AW..... SL..... VW.....

Truck : Flock04

Chauffeur :

Opmerkingen: - Proef Ron Mulder
- Palen

LET OP HET BOUWWEER !!

Informatie is te vinden op: <https://betonhuis.nl/betonmortel/beton-de-zomer-en-winter>

Handtekening Afnemer :



kiwa kiwa
gecertificeerd gecertificeerd



ISO 9001 ISO 14001



Dyckerhoff Basal
Betonmortel

Paal FC (3)
19,95m
Hbint 1m' onhog
gleanen
3e's
kuyl
gebouwd
1990
Afgebrand!

LAADPUNT LpDelftA (088-6078420) **DATUM / TIJD** 01-02-2022 / 15:44 **ORDERNUMMER** H1431026 **BONNUMMER** H4130533

Klantnummer: 6981 Funderingstechnieken Verstraeten BV Postbus 55 4500 AB OOSTBURG	Afleveradres: Deltares Thijssseweg DELFT Bouwonderdeel: Onbekend
---	---

Besteld: 3.25 m³ **Verwarmd** no **Betonmortel** NEN EN 206 **Certificaatcode** 22-jj--BBK
Sterkteklasse C45/55 **Milieuklasse** XA3 **Cons.klasse** F4 **Stortsnelheid** 6.00 m3/uur **Loswijze** Kraan

CEM I 52.5 R 40.00%
Grind 2-8 100.00%
Harex 6/18 0.36kg
Paal storten natte omstandigheden 2/8mm
Min. cementgehalte 430 kg
Colloïdale eigenschappen



Paal met 'casing'

Deze levering: 3.25 m³ **Afgeleverd t/m deze bon:** 3.25 m³

RECEPTOMSCHRIJVING

CEM I 52,5R Dyckerhoff Lengerich
CEM III/B 42.5 N LH/SR
GRIND 2/8
VC 1550 con. 30%

Uw mengselcode :

Kwaliteitsgarantie

Leveringen geschieden conform de BRL1801, NEN EN 206 en NEN 8005, in Chlorideklasse CL0.40, tenzij anders aangegeven. Beton is volgens het Besluit Bodemkwaliteit beoordeeld als een vormgegeven bouwstof.

Indien zonder schriftelijke goedkeuring van leverancier door of namens koper water, hulpstoffen, vezels of anders aan de mixerinhoud worden toegevoegd, vervalt deze kwaliteitsgarantie.

Invullen indien van toepassing:
Door of namens koper is op het werk aan de mixerinhoud het navolgende toegevoegd zonder schriftelijke goedkeuring van de leverancier:

De aankomsttijd op het werk, de starttijd lossen en de vertrektijd van het werk, worden door middel van statusmelding automatisch geregistreerd. AW..... CI..... MW.....

Truck : 5065 **Chauffeur** :

Opmerkingen:

LET OP HET BOUWWEER !!
Informatie is te vinden op: <https://betonhuis.nl/betonmortel/beton-de-zomer-en-winter>

Handtekening Afnemer :



Identifying information (names, signatures) has been redacted.

Zeeanalyses en betonsamenstelling

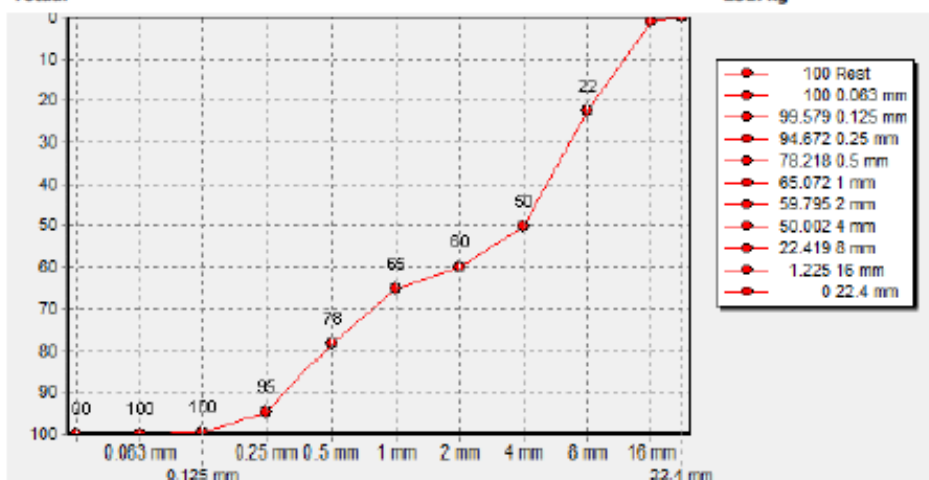
Vestiging	Code	T04	Datum berekend
Delft	8003	CEM III/B	2022-01-28 12:16:23

Zeven volgens NEN 2560 ZAND 0/2 ZAND 0/4 GRIND 4/16 Mengsel

Toeleveringscode	64354	65094	65183	
22.4 mm	0,0%	0,0%	0,0%	0,0%
16 mm	0,0%	0,0%	2,4%	1,2%
8 mm	0,0%	0,0%	43,1%	22,4%
4 mm	0,0%	8,3%	88,5%	50,0%
2 mm	3,4%	17,8%	98,6%	59,8%
1 mm	9,7%	27,6%	99,7%	65,1%
0.5 mm	28,5%	54,6%	100,0%	78,2%
0.25 mm	74,3%	88,9%	100,0%	94,7%
0.125 mm	97,8%	99,1%	100,0%	99,6%
0.063 mm	100,0%	100,0%	100,0%	100,0%
Rest	100,0%	100,0%	100,0%	100,0%
Fijnheidmodulus	2,14	2,96	6,32	4,71
Vocht	4,1%	3,7%	2,2%	
Absorptie	0,0%	0,0%	0,0%	
Verhouding toeslag	0,00%	100,00%	100,00%	
Fractie	0,00%	48,00%	52,00%	
Vol. massa	2,60kg/L	2,60kg/L	2,60kg/L	

Sterkte klasse	C45/55
Statistische milieu klasse	XA3
Milieuklasse	XA2
Milieuklasse	XS3, XF4 (XD3, XS2, XF2)
Milieuklasse	XA3
Milieuklasse	XC4, XD2, XF3, XS1
Consistentie	Schudmaatklasse F4
Maximale korrelgrootte	DMax = 16
wbf / wcf	0,430 / 0,438
Zand (t.o.v. toeslag)	48,00% V/V
Chloridegehalte (tot bindmiddel)	0,10% M/M
Alkaligehalte	3,85kg
Luchtgehalte	20,0L
Temperatuur:	20°C
waterbehoefte	175,2L
Aanmaakwater	125,1L
Eff. aanmaakwater (zonder slib)	125,1L
Geabsorbeerd water	0,0L
Aanhangend vocht	50,0L

Grondstoffen	producent	Te doseren massa	Droge massa	Volume fijn	T.o.v. cement
CEM III/B 42.5 N LH/SR	Dyckerhoff Neuss	240kg	240kg	81,4L	
CEM I 52,5R Dyckerhoff Lengerich	Dyckerhoff Lengerich	160kg	160kg	50,8L	
ZAND 0/2	Dyckerhoff Basal Toeslagstoffen	0kg	0kg	0,0L	
ZAND 0/4	Dyckerhoff Basal Toeslagstoffen	853kg	823kg	35,1L	
GRIND 4/16	Dyckerhoff Basal Toeslagstoffen	911kg	891kg	1,1L	
Vliegas EFA Füller MR-3 Cat A	Baumineral	26kg	26kg	11,7L	
VC 1550 con. 30%	SIKA	0,693kg	0,693kg	0,0L	0,17% m/m
BV-1 M con 36%	SIKA	1,426kg	1,426kg	0,0L	0,36% m/m
Koud water	Dyckerhoff Basal Betonmortel	125kg	175kg	0,0L	
Lucht		20L	20L	0,0L	
Totaal		2317kg		180,0L	



Paal T x, y, z.
φ302/450

Dyckerhoff Basal
Betonmortel

LAADPUNT LpDelftA (088-6078420) **DATUM / TIJD** 31-01-2022 / 15:15 **ORDERNUMMER** H1431229 **BONNUMMER** H4130438

Klantnummer: 6961 Funderingstechnieken Verstraeten BV Postbus 55 4500 AB OOSTBURG	Afleveradres: Deltares Boussinesweg 1 DELFT Bouwonderdeelt: Paal
---	--

Besteld: 7.50 m³ **Verwarmd** no **Betonmortel** NEN EN 206
Sterkteklasse C45/55 **Milieuklasse** XA3 **Cons.klasse** F4 **Certificaatcode** 22-ji--BBK
Stortsnelheid 6,00 m³/uur **Loswijze** Kraan
CEM I 52.5 R 40.00%
Grind 4-16 100.00%
Min. cementgehalte 400 kg
Paal storten natte omstandigheden

Deze levering: 7.50 m³ **Afgeleverd t/m deze bon:** 7.50 m³

RECEPTOMSCHRIJVING

CEM I 52,5R Dyckerhoff Lengerich
CEM III/B 42.5 N LH/SR
Vliegas EFA Füller MR-3 Cat A
GRIND 4/16
BV-1 M con 36%
VC 1550 con. 30%

Uw mengselcode :

Kwaliteitsgarantie

Leveringen geschieden conform de BRL1801, NEN EN 206 en NEN 8005, in Chlorideklasse CL0.40, tenzij anders aangegeven. Beton is volgens het Besluit Bodemkwaliteit beoordeeld als een vormgegeven bouwstof.

Indien zonder schriftelijke goedkeuring van leverancier door of namens koper water, hulpstoffen, vezels of anders aan de mixerinhoud worden toegevoegd, vervalt deze kwaliteitsgarantie.

Invullen indien van toepassing:

Door of namens koper is op het werk aan de mixerinhoud het navolgende toegevoegd zonder schriftelijke goedkeuring van de leverancier:

De aankomsttijd op het werk, de starttijd lossen en de vertrektijd van het werk, worden door middel van statusmelding automatisch geregistreerd.

Truck : 5037

Opmerkingen:

LET OP HET BOUWWEER !!

Informatie is te vinden op: <https://betonhuis.nl/betonmortel/beton-de-zomer-en-winter>

Handtekening Afnemer :



Identifying information (names, signatures) has been redacted.

Appendix E Measurements of Test Set-Up

All measurements are listed in metres unless otherwise stated. Drawings are not to scale.

E.1 Instrumentation

The instrumentation of the SIc piles was considerably more simple compared to the SI piles, given that only one cable was needed and gluing in a groove required less preparation when compared to using the surface of the H-beam reinforcing.

In the examples below the uppermost and lowermost gluing points refer to the last reasonable fibre optic measurements in the context of measuring the axial deformation of the measurand.

Table E.1: Measurements of different points along the SIc casing (prior to cutting of the casing head). The “uppermost” and “lowermost” gluing points refer to the last straight section of cable that has been glued

	T1	T2	T3
Distance from tip shoulder: Apex of bend in cable	0.21	0.21	0.21
Distance from tip shoulder: Lowermost gluing point	0.34	0.36	0.36
Distance from top of casing: Uppermost gluing point	1.70	1.70	1.70



Figure E.1: Base of the H-beam reinforcing of an SI pile. Each fibre optic cable runs to the connection box where a fusion splice connects one optical fibre in the cable to the other optical fibre in the same cable. The Point (a.) is referred to as the “last gluing point” and is last reasonable axial strain measurement before the cable bends into the connection box



Figure E.2: Head of the H-beam reinforcing of an SI pile. The reinforcing of the SI piles had a free length of 1-2m, part of which was cut off after installation. As a result, the highest glued point of the fibre optic cables was set conservatively.

Head	F1	F2	F3
1	1.70	1.70	1.55
2	1.70	1.00	1.55
3	1.48	1.38	1.22
4	n/a	n/a	n/a

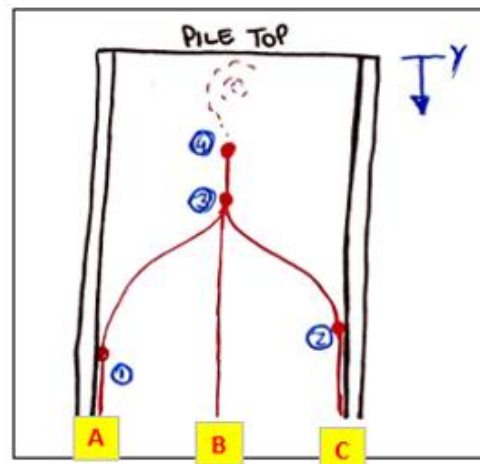


Figure E.3: Measurements to the last gluing points on the reinforcing of the SI piles (note: “pile top” is with reference to the uncut reinforcing).

Pile	F1	F2	F3
A	19.99	20.01	20.01
B	17.99	18.01	18.01
C	15.99	16.01	16.00
D	5.91	8.91	8.91
E	5.03	5.02	5.016
F	3.03	3.02	3.031
G	1.02	1.02	1.033
H	14.51	14.53	14.52
I	20.49	20.51	20.51

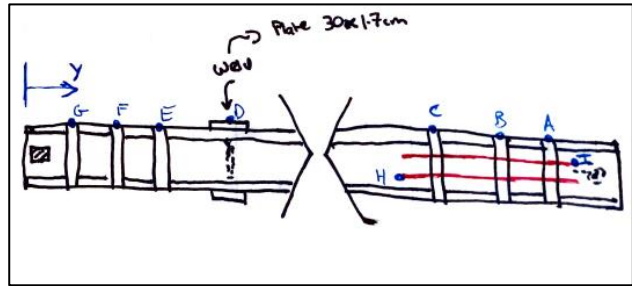
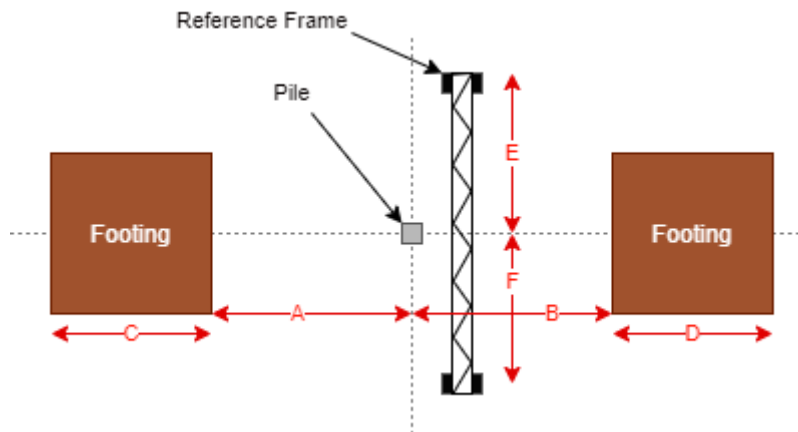


Figure E.4: Measurements of different points along the reinforcing of the SI piles. The points H and I refer to the additional reinforcing bars placed at the head of the reinforcing

E.2 Test frame

Note that the rotation of the reference frame with respect to the test frame may deviate up to 20° from perpendicular. In every test, the footings measured $4 \times 8.2 \text{ m}$. The 12 m long reference frame was placed on two dragline mats, 1 m in size. The centre-centre distance between these supports and the pile is indicated in the table below

Drawing is not to scale and orientated due north.



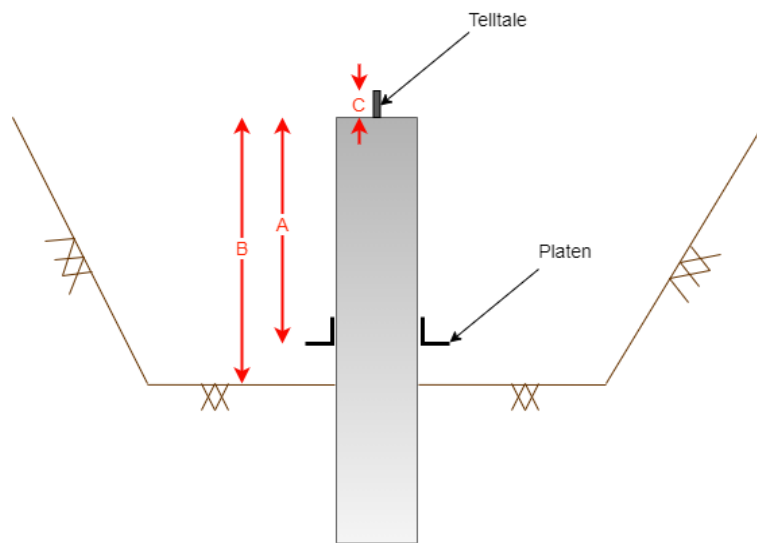
	A [m]	B [m]	C [m]	D [m]	E [m]	F [m]	G
F1	3.5		4.0		6.0	5.0	8.2
F2					5.6	5.4	
F3					6.5	5.7	
T1					5.5	5.5	
T2					5.5	5.7	
T3					6.1	5.8	



Figure E.5: Footing configuration for each test. The number of dragline mats between the concrete block and the frame was changed from test to test to ensure enough height above surface level was provided

E.3 Pile head

The schematic at table below give measurements made at the head of each pile during load testing. The drawing is not to scale.








	A [m]	B _{min} [m]	B _{max} [m]	C [m]
T1	0.16			
F1	0.05	0.90	1.04	0.17
T2	0.19	0.59	0.72	0.23
F2	0.00	0.72/1.03*	0/1.03	0.19
T3	0.22	0.60	0.65	0.195
F3	0.04	0.86	1.00	0.18


**To grout shell"/"to soil"

E.4 Reference point location

The reference point was moved several times during the test to improve the quality of reference readings (e.g. to minimise noise caused by wind loading or impact of the test frame) and also to ensure visibility of the reference point from the location of the levelling stations. These locations are presented in **Table E.2** below.

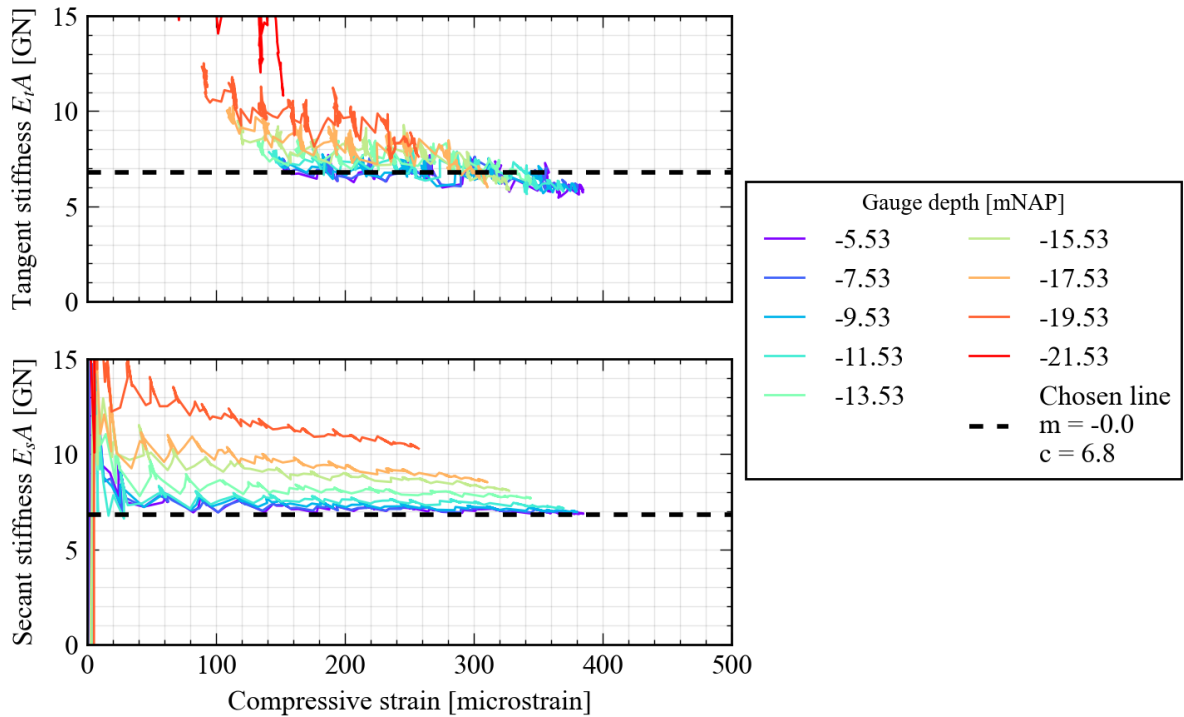
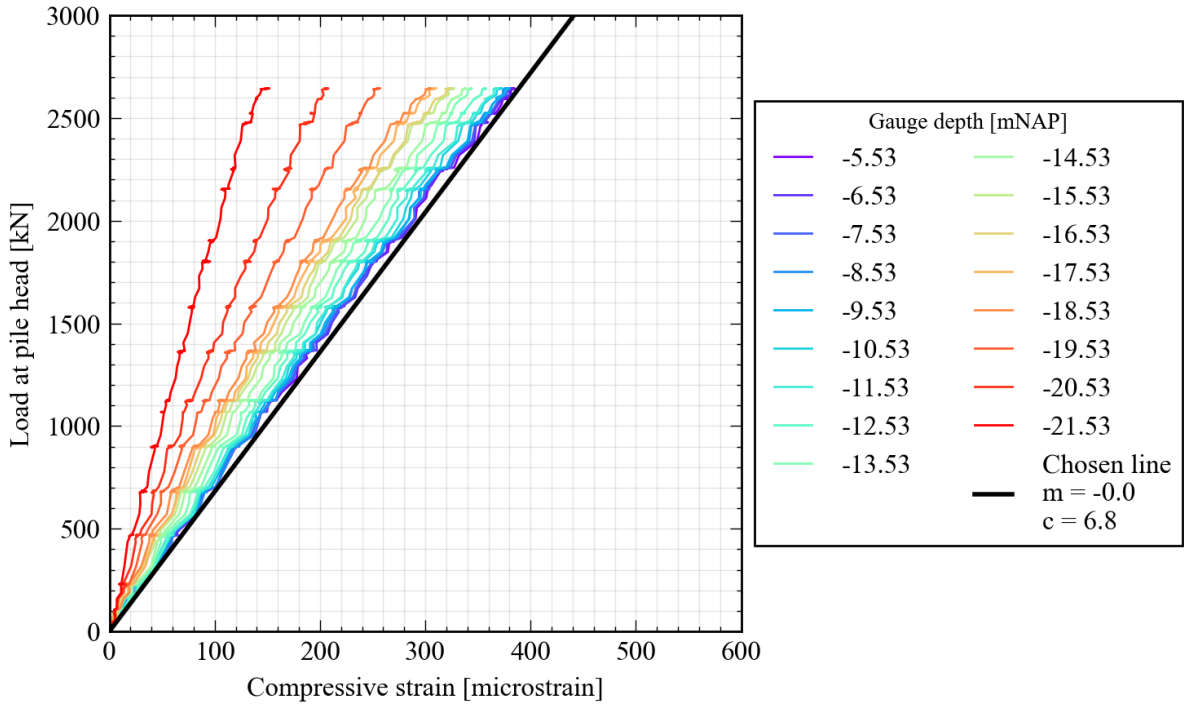
Table E.2: Reference beacon locations, sorted chronologically

File	Location	Photo
T1	Attached to tripod, 22m away from pile. Levelling station 17m away from pile	
F1	Taped onto the foot of a crane, 18m away from pile. Levelling station 16m away	
T2	Fixed to pile T3, 7m away from pile T2. Levelling station 10m away from pile.	
F2	Fixed to pile F3, 8m away from pile F2. Levelling station 15m away from pile	
T3	Attached to tripod adjacent to pile F3, 4m away from pile T3. Levelling station 13m away from pile	

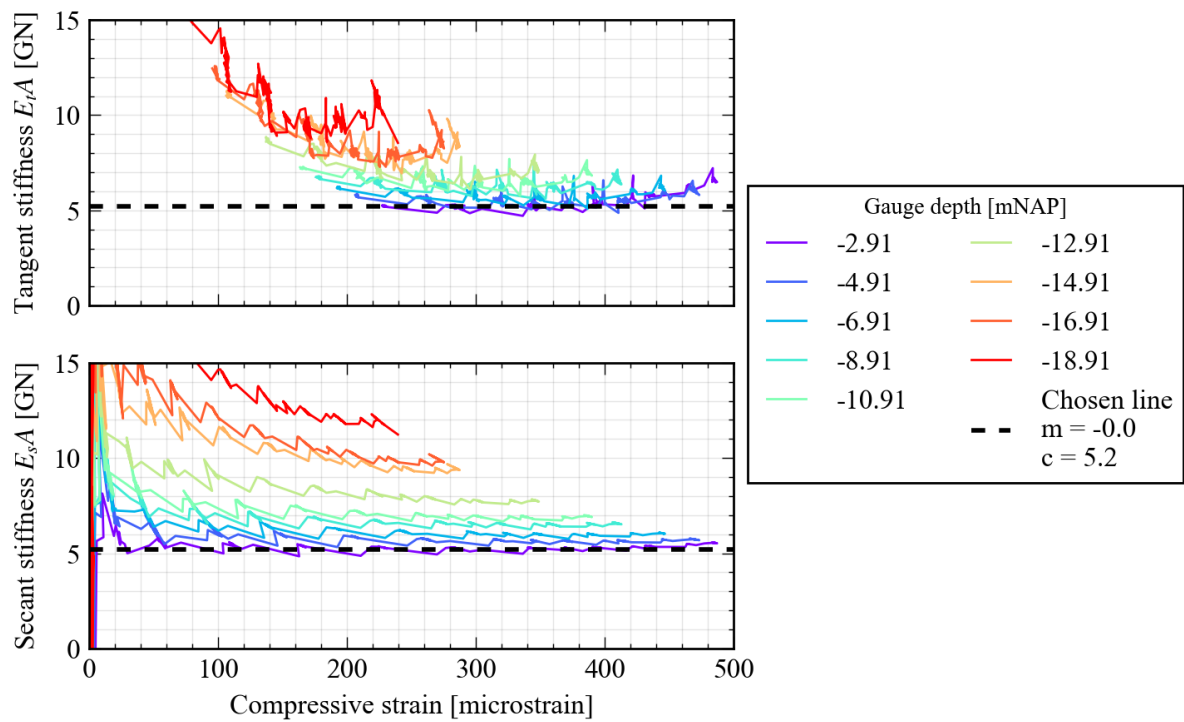
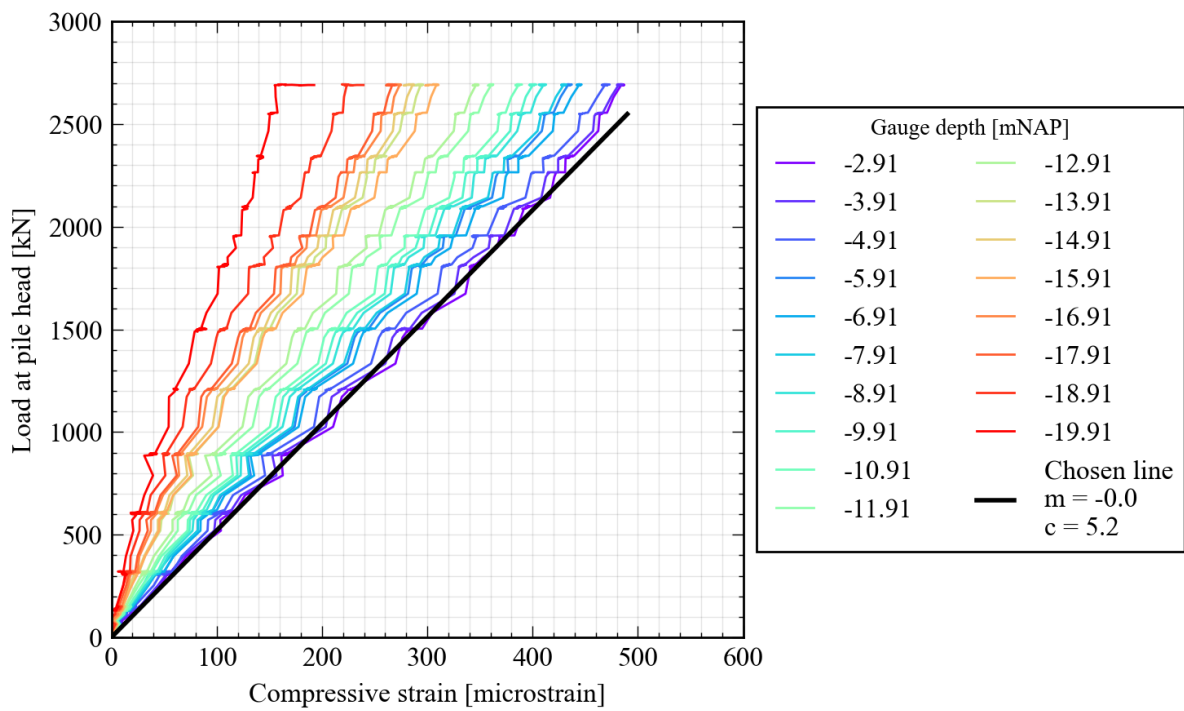
F3	Attached to pile T2, 12m away from pile F3. Levelling station 16m away from pile			
----	--	--	--	--

Appendix F Load-Strain Response

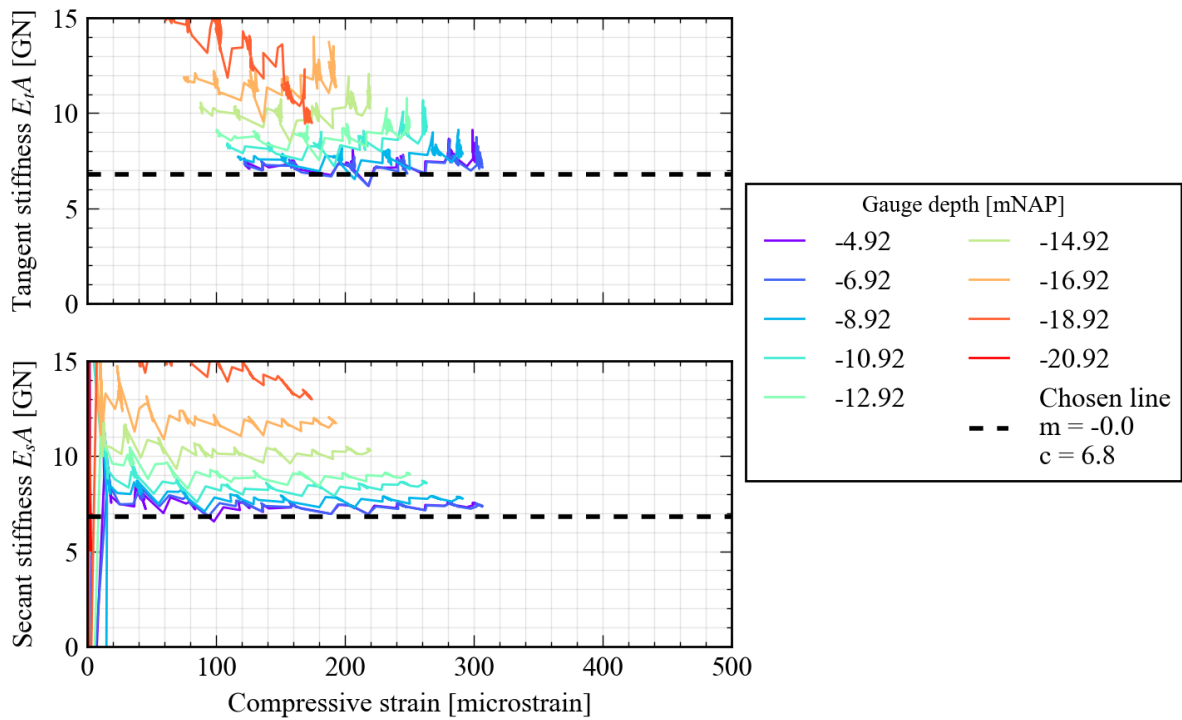
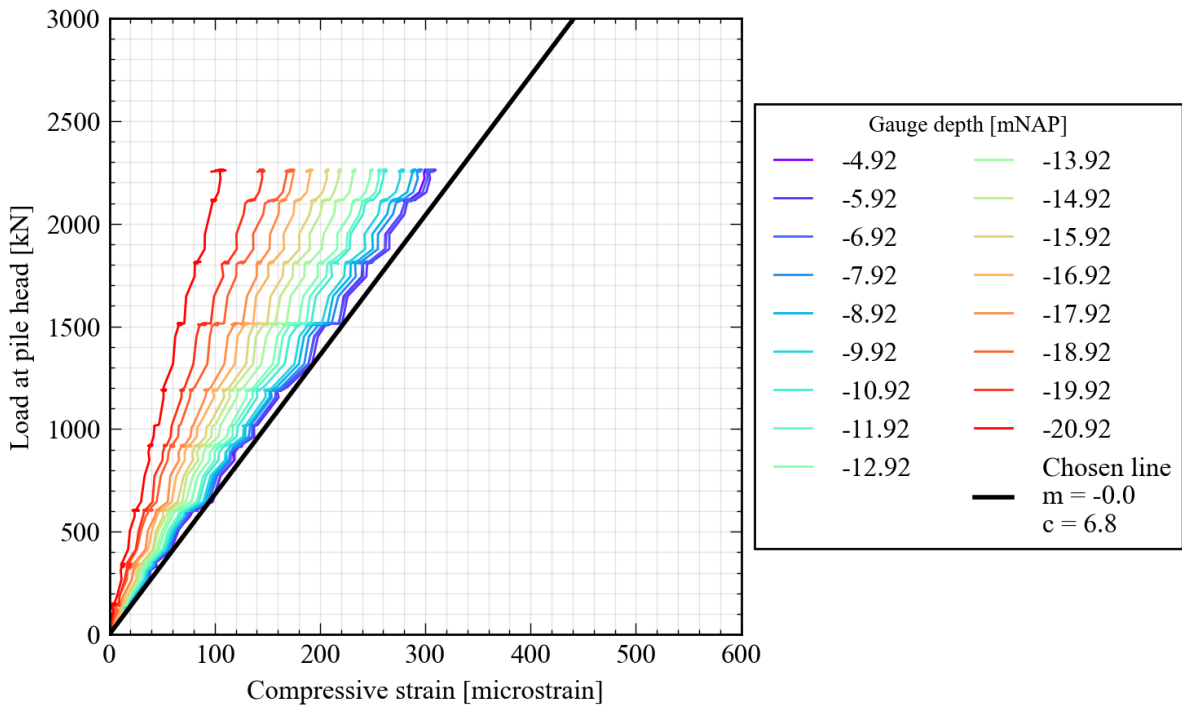
Pile T1



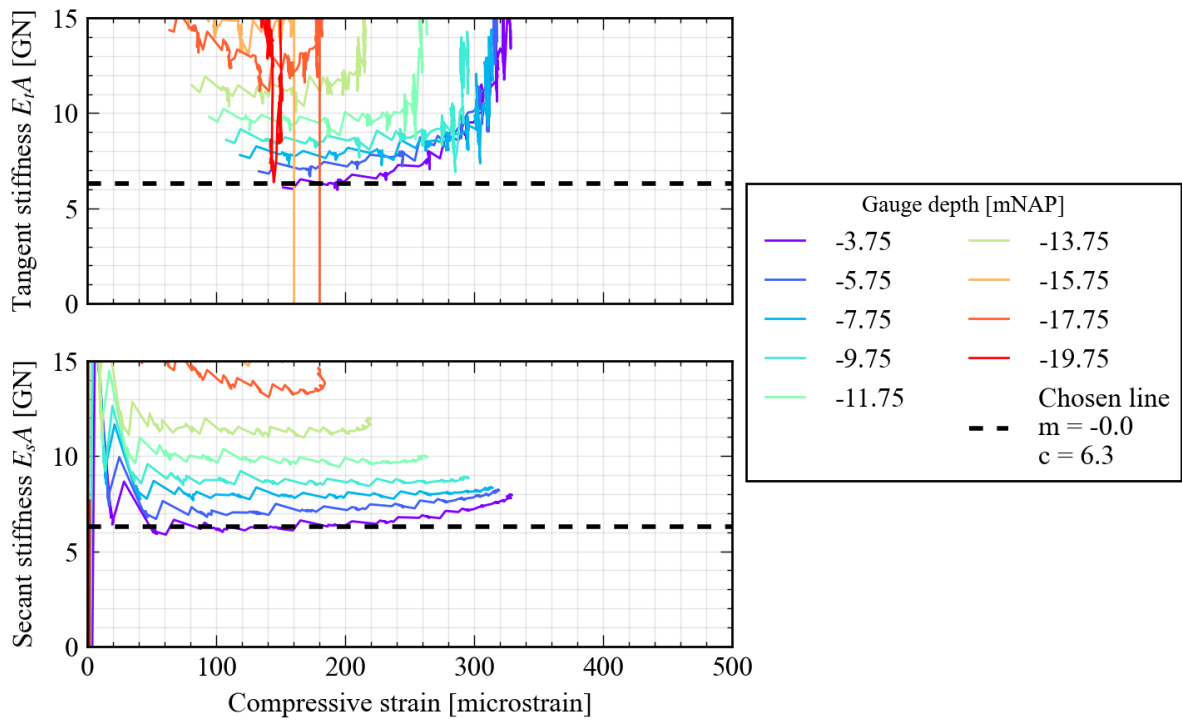
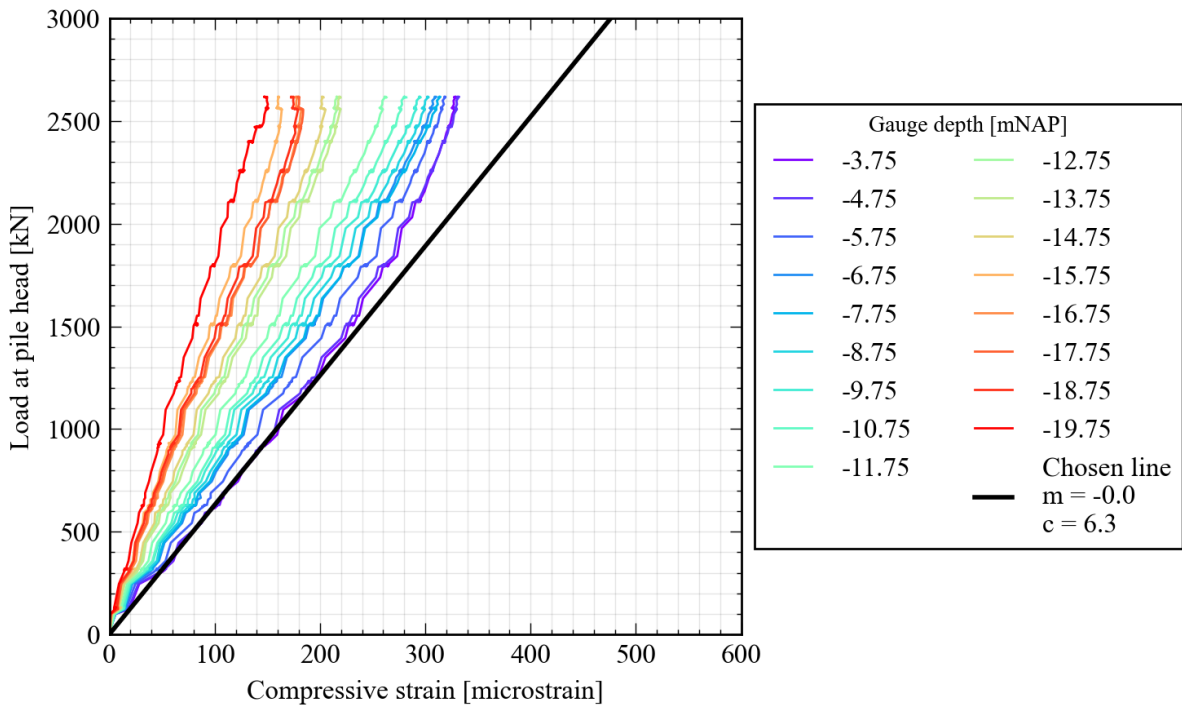
Pile F1



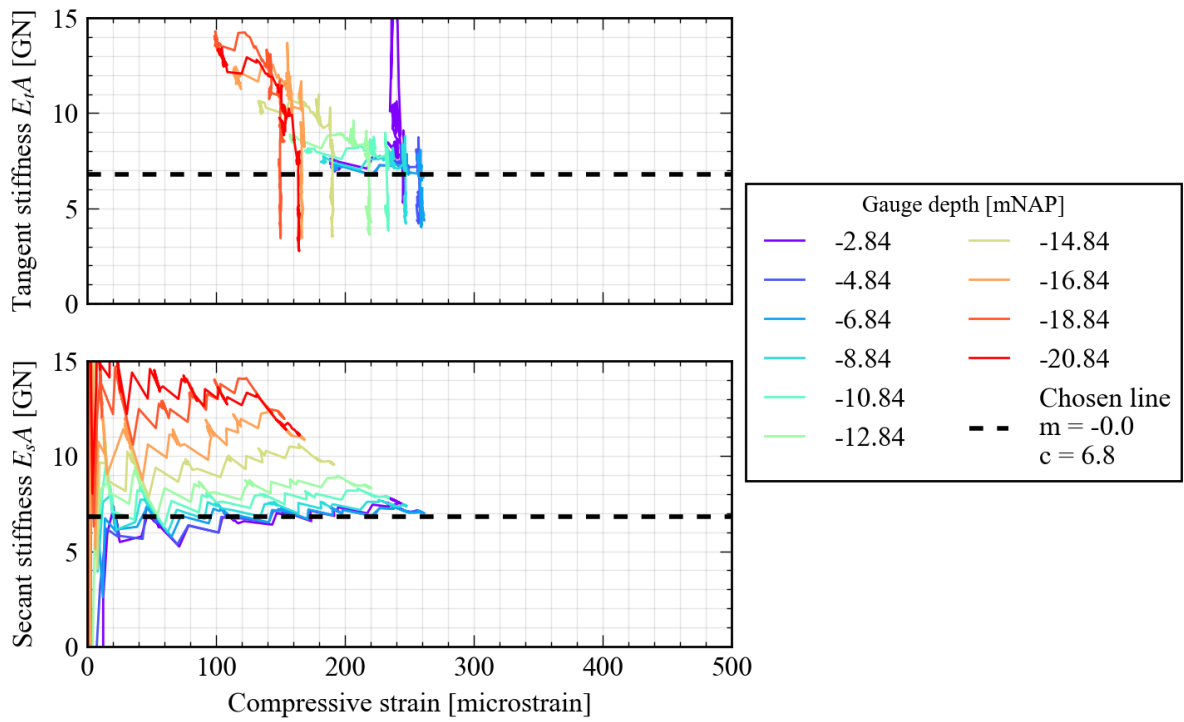
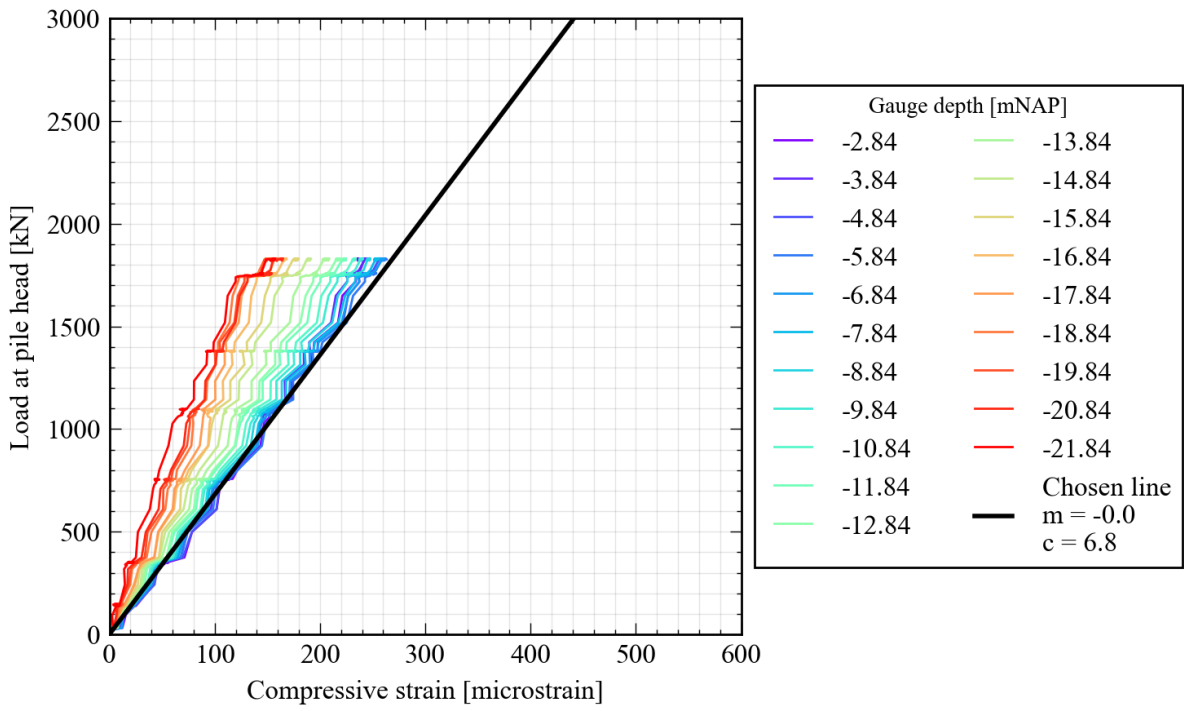
Pile T2



Pile F2



Pile T3



Pile F3

